UNIVERSITÀ
DEGLI STUDI
DI PADOVA

Sede Amministrativa: Università degli Studi di Padova
Dipartimento di Scienze biomediche sperimentali

SCUOLA DI DOTTORATO DI RICERCA IN BIOSCIENZE
INDIRIZZO: BIOLOGIA CELLULARE
CICLO XXII

TWO TOPICS OF PHYSIOPATHOLOGICAL INTEREST IN MITOCHONDRIAL RESEARCH: INNER MEMBRANE CHANNELS AND MITOCHONDRIOTROPIC REDOX-ACTIVE COMPOUNDS

Direttore della Scuola : Ch.mo Prof. Tullio Pozzan
Coordinatore d'indirizzo: Ch.mo Prof. Cesare Montecucco
Supervisore : Dr. Mario Zoratti

Dottorando : Nicola Sassi

Contents

Riassunto dell'attività svolta

Il gruppo presso cui ho svolto il mio corso di dottorato si interessa di vari aspetti della funzionalità mitocondriale. I progetti che ho seguito riguardano due ambiti molto diversi tra loro; tuttavia in entrambi i casi si tratta di studi il cui obiettivo a lungo termine è l'individuazione di composti potenzialmente utili per un'azione antitumorale a livello mitocondriale.

Uno di questi progetti riguarda i canali del potassio presenti nella membrana mitocondriale interna. Negli ultimi anni ne sono stati individuati diversi. Oltre ad aver un ruolo nella regolazione di processi e parametri mitocondriali questi canali son risultati interessanti per il loro coinvolgimento in altri aspetti della fisiologia cellulare. Due di questi sembrano aver un ruolo nella protezione dal danno ischemico (precondizionamento), mentre un recente studio svolto dal nostro gruppo in collaborazione con un gruppo tedesco ha messo in evidenza come un terzo, il mtK_V1.3, svolga un ruolo importante nell'apoptosi mediata da Bax in linfociti. Da qui l'interesse da parte nostra verso quest'ultimo canale.

Ho verificato se il mtK_V1.3 fosse presente nei mitocondri non solo dei linfociti T, dove è stato individuato inizialmente, ma anche in alcune altre linee tumorali. Sono riuscito finora ad individuarlo in due linee umane (PC3 e MCF7) (Gulbins et al., 2010 - Cap. 1). Ho successivamente indagato se l'inibizione del canale potesse indurre morte cellulare in tali linee. Ciò sarebbe di notevole interesse nello sviluppo di nuovi chemioterapici. Tuttavia dai risultati ottenuti l'utilizzo di inibitori specifici del canale nelle differenti linee non ha mostrato effetti rilevanti di induzione di morte cellulare (Cap. 2).

Sempre nell'ambito di questo progetto abbiamo individuato un altro canale mitocondriale: il mtK_{Ca}3.1 che abbiamo osservato nei mitocondri di una linea tumorale del colon umana (HCT116) sia mediante patch-clamp che Western blot. (De Marchi et al., 2009 - Cap. 3). Ho poi verificato se la sua inibizione potesse essere citotossica o almeno citostatica, tuttavia anche in questo caso non abbiamo ottenuto una risposta positiva. Ho verificato la presenza o meno del canale anche in due altre linee tumorali del colon (C26 e Caco2) per comprendere se fosse un canale espresso in modo tumore-specifico procedendo successivamente a

confronti con cellule non tumorali, tuttavia in ambedue i casi il canale è risultato presente solo nella plasma membrana (Sassi et al., 2009 - Cap 4).

L'altro progetto da me intrapreso riguarda lo sfruttamento farmacologico dei polifenoli vegetali presenti in molti cibi e bevande. Una notevole letteratura mostra come tali composti possiedano interessanti proprietà biologiche che potrebbero esser utili in diversi ambiti, come la protezione cardiovascolare o dalla neurodegenerazione, oppure nel prevenire l'insorgere e nell'inibire la crescita di molti tipi di cancro. Questi composti dalle interessanti potenzialità trovano una notevole difficoltà d'utilizzo a causa della loro scarsa biodisponibilità. A priori, un modo per ovviare a questo problema è accumulare tali composti in un'opportuna sede d'azione. Una scelta ovvia è il mitocondrio, dato che i polifenoli sono molecole redox-attive (la cui attività può essere anti- o pro-ossidante in base a differenti condizioni come pH, presenza di $Fe^{2+/3+}$ o $Cu^{+}/^{2+}$ e concentrazione del composto) e che i mitocondri son il principale sito di produzione dei radicali, oltre ad esser coinvolti nei processi di morte cellulare. Questi composti mitocondriotropici potrebbero aver una rilevanza biomedica sia che dimostrino un'attività anti-ossidante/citoprotettiva sia invece che si comportino da pro-ossidanti citotossici.

Il nostro gruppo ha quindi sintetizzato alcuni derivati di quercitina e resveratrolo - due polifenoli particolarmente studiati presi a modello - in grado di accumularsi nei mitocondri. Questo grazie alla funzionalizzazione con un gruppo trifenilfosfonio (TPP^{+}), un catione lipofilico che può diffondere attraverso le membrane biologiche e accumularsi in regioni a potenziale negativo, quali la matrice mitocondriale e il citoplasma. Abbiamo verificato che questi derivati si accumulassero effettivamente nei mitocondri (Mattarei et al, 2008 - Cap. 5; Biasutto et al, 2008 – Cap. 6). Una prima indagine sugli effetti biologici di questi nuovi composti è stata condotta con due derivati della quercetina (Q3BTPI, QTA3BTPI). Abbiamo osservato come questi composti con mitocondri isolati siano potenziali co-induttori della transizione di permeabilità mitocondriale (MPT), nonché inibitori della respirazione e dell'ATP sintasi mitocondriale. Osservazioni a livello cellulare mostrano una depolarizzazione mitocondriale indipendente dalla MPT indotta da entrambi i composti e un modesto aumento

della produzione cellulare di ROS da parte della QTA3BTPI (Biasutto et al., 2010 – Cap. 7).

Ho ampliato lo studio per valutare la possibile azione citotossica/citostatica su linee cellulari tumorali (C26) e non (MEF) dei vari composti mitocondriotropici. Ho anche indagato come tali composti influiscano sull'attività mitocondriale di un'altra linea cellulare tumorale (Jurkat). I risultati di esperimenti di vitalità cellulare mostrano come diversi composti mitocondriotropici, somministrati a concentrazioni in ambito micromolare, possano aver un' attività citotossica/citostatica su cellule a crescita veloce, mentre il loro effetto su cellule non tumorali è molto modesto se esse hanno crescita lenta. I risultati iniziali di uno studio meccanicistico hanno evidenziato come concentrazioni relativamente elevate (nell'ambito di 10^{-5} M) di questi composti possano causare alterazioni morfologiche, depolarizzazione mitocondriale e generazione di specie radicaliche (Cap. 8).

Summary of the research activities

The group I have been part of during my doctorate thesis research is interested in various aspects of mitochondrial function. The projects I have been involved in are concerned with two very different topics; both studies have however as long-term objective the discovery and validation of compounds potentially useful for an anti-cancer action at the mitochondrial level.

The first of these projects concerns the potassium-selective channels of the inner mitochondrial membrane. A few have been discovered over the past several years. Besides participating in the regulation of mitochondrial processes and parameters these channels have attracted attention because of their involvement in other aspects of cellular physiology. Two of them seem to be able to afford protection from ischemic damage (preconditioning), while a recent study by our group in collaboration with German researchers has provided evidence that a third, mtK_V1.3, plays an important role in Bax-mediated apoptosis in lymphocytes. Hence our interest in this channel.

I have verified whether mtK_V1.3 might be present in the mitochondria not only of T lymphocytes, where it has been discovered, but also in those of a few other cancerous cell lines. So far I have succeeded in establishing its presence in two human lines (PC3 and MCF7) (Gulbins et al., 2010 – Chapt. 1). I have then investigated whether inhibition of the channel might cause cell death in these lines, a finding which would have been of considerable interest for the development of new chemotherapeutic drugs. Unfortunately I have not been able to obtain evidence of a death-inducing effect by a specific inhibitor of mtK_V1.3 (Chapt. 2).

Within this project we have also discovered another mitochondrial channel: Ca^{2+}-activated mtK_{Ca}3.1, which we have observed in the mitochondria of a human colon tumor line (HCT116) both by patch-clamping the inner membrane and by Wester blotting (De Marchi et al., 2009 – Chapt. 3). I have then investigated whether its inhibition might be cytotoxic or at least cytostatic, but in this case also the answer has so far been negative. I have checked for the presence of mtK_{Ca}3.1 in two other cell lines of colonic origin (C26 and Caco2) to try and understand whether this channel might be expressed in a cancer-specific manner by

subsequently performing a comparison with non-tumoral cells or tissue. However, in both cases the channel has turned out to be present only in the plasma membrane (Sassi et al., 2010 – Chapt. 4).

The other project I have taken part in concerns the pharmacological exploitation of plant polyphenols, contained in many foods and beverages. A vast literature shows that these compounds have interesting biological properties which could be useful in health care endeavours such as protection from cardiovascular damage or neurodegeneration, or to prevent the onset and inhibit the growth of many types of cancer. Practical applications for these potentially useful compounds are made difficult by their low bioavailability. A priori, one way to circumvent this problem may be to cause their accumulation in an opportune site of action. The mitochondrion is an obvious choice, since polyphenols are redox-active molecules (whose activity may be anti- or pro-oxidant depending on conditions such as pH, presence of $Fe^{2+/3+}$ o $Cu^{+}/^{2+}$ and concentration of the polyphenol itself) and mitochondria are the main cellular site of production of radicals as well as being mechanistically involved in cell death. Mitochondriotropic compounds might turn out to have biomedical relevance regardless of whether their activity may be anti-oxidant/cytoprotective or pro-oxidant/cytotoxic.

Our group has therefore synthesized a few derivatives of quercetin and resveratrol – two much-studied model polyphenols – capable of accumulating into mitochondria. This property is conferred by the triphenylphosphonium group (TPP^{+}), a lipophylic cation which can diffuse through biomembranes and accumulate in regions held at negative electrical potential, such as the mitochondrial matrix and the cytoplasm. We have verified that these derivatives indeed accumulate in mitochondria as expected (Mattarei et al., 2008 – Chapt. 5; Biasutto et al., 2008 – Chapt. 6). A first exploration of the biological properties of these new compounds has been carried out with two quercetin derivatives (Q3BTPI, QTA3BTPI). We have observed that these compounds supplied to isolated mitochondria are potential co-inducers of the mitochondrial permeability transition (MPT), as well as inhibitors of respiration and of the F_0F_1 ATPase. At the cellular level, both compounds induce an MPT-independent depolarization of mitochondria and a modest increase in the cellular production of ROS at least in the case of QTA3BTPI (Biasutto et al., 2010 – Chapt. 7).

I have extended the study to evaluate the possible cytostatic/cytotoxic action of the various mitochondriotropic compounds on tumoral (C26) and non-tumoral (MEF) cell lines. I have furthermore investigated what impact these compounds have on the mitochondria of another tumoral cell line (Jurkat lymphocytes). The results of cell vitality determinations showed that the various mitochondriotropic derivatives, administered at concentrations in the μM range, can have a cytotoxic/cytostatic activity vs. rapidly growing cells, while their effect on slowly dividing non-tumoral ones is much more modest. The initial findings of a mechanistic study have revealed that relatively high (10^{-5} M range) concentrations can elicit structural alterations, mitochondrial depolarization and generation of radical oxygen species (Chapt. 8).

Organization of the thesis

As mentioned in the preceding general introduction, my thesis research work developed along two distinct lines. The thesis therefore comprises two sections. Each begins with an introductory background section, followed by chapters corresponding to individual research projects. This organization has been favoured over a more traditional, monograph-style layout mainly with the intent of facilitating reading. Some of the chapters (Chapt.s 1,3,4,5,6,7) correspond to published papers. In other cases the specific parcel of work was still unfinished as the thesis was due; the corresponding sections report the available data and comments (Chapt.s 2,8). Thus, the chapters are not homogenous in length and relevance. I hope the benefits of such an organization outweigh this disadvantage. The literature references pertaining to the introductions and to Chapts. 2 and 8 are collected together in a single list at the end of the thesis, for ease of consultation and to avoid repetitions.

Mitochondrial potassium channels

Introduction

A remarkable aspect of mitochondrial physiology is the control of ion fluxes through the inner membrane, which has a relatively low permeability to minimize energy dissipation and to maintain the electrochemical driving force necessary for the production of ATP through oxidative phosphorylation. Ion transport on a variety of carriers, exchangers, pumps and ion-conducting channels has roles under both normal and pathological conditions (see below) (Halestrap, 1989; Brierley et al., 1994; Bernardi, 1999; Garlid et al., 2003; O'Rourke, 2005).

K^+ is the major intracellular cation. Its influx into the matrix via leaks and selective K^+ channels is balanced by a K^+/H^+ exchanger (mtKHE) which "pumps" K^+ out of the matrix. The relative activities of the two systems play a key role in the regulation of matrix volume, in the efficiency of the respiratory chain, in ROS production and, as recently demonstrated, in apoptosis. (Szewczyk, 2006; O'Rourke, 2007; Nowikovsky et al., 2008; Szabò et al., 2008, 2010)

The mtKHE is a non-selective antiporter distinct from the Na^+-selective one in that it transports Na^+, K^+, Li^+, Rb^+ as well as Cs^+. It is inhibited by quinine, propanolol or DCCD and it is allosterically regulated by Mg^{2+} (Beavis and Garlid, 1990; Brierley et al., 1994). The existence of the mtKHE has been demonstrated by a number of experimental approaches (e.g. Brierley and Jung, 1988; Li et al., 1990; Bernardi, 1999) but its molecular nature has remained an open question.

The K^+-selective channels know to be present in the IMM so far are five, all of which have counterparts in the plasma membrane: mtK_{ATP}, whose presence in mitochondria is still debated, two types of Ca^{2+}-activated K^+ channels, $K_{Ca}1.1$ (BK_{Ca}) and $K_{Ca}3.1$ (IK_{Ca}), twin-pore TASK-3 and Shaker-type $K_V1.3$.

The plasma membrane K_{ATP} channels are assembled by four inwardly-rectifying Kir family (Kir6.1 or Kir6.2) subunits, which form the pore region, and four sulfonylurea receptor subunits (SUR1 or SUR2), members of the ATP-binding cassette (ABC) protein family, which form the regulatory region (Nichols, 2006). The presence of mtK_{ATP} has been reported in liver, heart, brain, kidney, skeletal muscle and T lymphocyte mitochondria, but it remains a matter of controversy

(rev.: Zoratti et al., 2009). Biochemical approaches have produced both affirmative and negative results for the presence of K_{ATP} subunits in mitochondria. Evidence in favor of a functional mtK_{ATP} channel comes from electrophysiological observations: patch-clamp experiments on mitochondria and planar bilayer recordings of activity after fusion of IMM vesicles or incorporation of isolated protein fractions. The characteristics of the channels identified, on the basis of pharmacological effects, as mtK_{ATP} in these experiments vary considerably, probably at least in part because of a recognized cooperative behavior of these channels, which appear to often occur in clusters (Mironova et al., 2004) and, also, of the redox sensitivity of the channel (Zhang et al., 2001). Its molecular identity is still unknown.

The mtK_{ATP} is probably involved in the control of mitochondrial ionic homeostasis, but the interest for this mitochondrial channel is due mainly to its role in ischemic preconditioning (IP). Briefly, the IP consists of short sub-lethal ischemic periods that are capable of protecting against subsequent massive ischemia (Murry, 1986). A "chemical IP" is induced by K_{ATP} openers (diazoxide) (Grover et al., 1989; Garlid et al., 1996; Garlid et al., 2003), which unfortunately have other effects, so that the involvement of K_{ATP} in preconditioning is actually doubted by part of the researchers (Halestrap et al., 2004). The mechanism of preconditioning has also not been established yet, but it presumably involves different cellular pathways activated via an "hormetic" induction: K_{ATP} activation would result somehow in ROS production, which would start a chain of events leading to long-lasting protection (Zoratti et al., 2009). In any case it may be more appropriate to assign a role in IP not specifically to this channel but to K^+ influx, since BK_{Ca} is also relevant for preconditioning.

The presence in the IMM of $mtBK_{Ca}$ is less controversial. This channel has been found in the mitochondria of glioma, skeletal muscle, heart and brain cells. It has been observed by direct patch-clamp on mitoplasts (Siemen et al., 1999; Xu et al., 2002; Ohya et al., 2005) and by planar lipid bilayer experiments (Skalska et al., 2008). Evidence has also been provided by Western blot, electron microscopy and immunofluorescence microscopy (Xu et al., 2002; Skalska et al 2008; Piwońska et al., 2008). The pharmacological studies confirm also the inhibition of this channel by specific toxins, like ChTx, activation by Ca^{2+} in μM concentrations and a

voltage-dependence (opening with depolarization of IMM). The $mtBK_{Ca}$ has a conductance of 100-300pS and is composed of a tetramer of α-subunits, which form the pore, in association with different possible auxiliary β-subunits which determine the pharmacological properties (Torres et al., 2007).

Plasma membrane BK_{Ca} channels are a very useful negative feedback tool which can counteract depolarization and Ca^{2+} entry via voltage-dependent Ca^{2+} channels by opening and promoting (re)polarization (Wellman 2003). $mtBK_{Ca}$ is believed to carry out a similar feedback regulatory role linking matrix [Ca^{2+}] to IMM K^+ permeability and mitochondrial volume (Xu et al., 2002). As in the case of mtK_{ATP}, the interest for this channel is largely due to its possible role in IP (Sakamoto et al., 2008; Redel et al., 2008). Indeed specific activators of this channel, such as NS1619, produce a preconditioning-like protection in the heart (Park et al., 2007).

As part of my doctorate thesis research, I have participated in the discovery of a second Ca^{2+}-activated K^+ channel of the IMM, namely $K_{Ca}3.1$ (or IK_{Ca}). The Reader is referred to chapts. 3 and 4 for some background information and a description of this work

TASK-3 is a TWIK acid-sensitive K^+ channel. It is sensitive to alterations of extracellular pH (closing with acidification) and it is involved in the regulation of aldosterone secretion, adjustment of neuronal excitability and acid sensitivity of peripheral chemoreceptors. It seems to participate in some other phenomena such as the induction of apoptotic cell death of cerebellar granule cells. The exact connection between the activity of this channel and cell death is still unclear. Its expression is very significant in malignant melanoma cells, and it is particularly present in cell organelles, with a relatively insignificant presence on the plasma membrane. Immunohistochemistry and immunofluorescence microscopy demonstrated the co-localization of mitochondria and TASK-3 channel subunits in melanoma cells and in keratinocytes (a non-malignant cell line), but not in rat neurons. It is reasonable to assume that TASK-3 channel is situated in the IMM (other experiments are necessary to confirm this localization) and is involved in the regulation of matrix volume and in the efficiency of oxidative functions. (Rusznák et al., 2007).

$K_V1.3$ is a member of the voltage-dependent *Shaker*-like family (Cahalan et al., 2001, Sands et al., 2005). This channel is formed by a tetramer of ion-conducting α-subunits, generally associated with a tetramer of one of various possible β-subunits. The main characteristic of PM $K_V1.3$, besides K^+ selectivity, is voltage-dependence, consisting in rapid depolarization-induced opening, followed by inactivation. $K_V1.3$ is expressed in different tissues and is the main potassium channel present in lymphocytes (Lewis et al., 1995), where it has been clearly demonstrated to represent a key factor for proliferation and volume regulation (Chandy et al., 2004; Panyi et al., 2006).

Evidence of the presence of a mitochondrial population of $K_V1.3$ ($mtK_V1.3$) (Szabó et al., 2005) in peripheral human blood lymphocytes and Jurkat T lymphocytes comes from electron microscopy, Western blots, FACS analysis and patch-clamp experiments on isolated mitoplasts. The latter demonstrated its existence in the inner membrane also by showing co-localization with the Mitochondrial Permeability Transition Pore (MPTP) and the "107-pS" anion-selective channel, which are present only in the IMM.

Our interest for $mtK_V1.3$ derives mostly from its recently demonstrated role in apoptosis (Szabó et al., 2008). Various experimental approaches showed how Bax plus t-Bid induce hyperpolarization, followed by depolarization and cytochrome c release, only in isolated $K_V1.3$-positive mitochondria, indicating apoptotic changes in these organelles, while $K_V1.3$-deficient mitochondria did not respond. Furthermore Bax induced a $K_V1.3$-dependent increase in reactive oxygen species (ROS) production. Specific inhibitors of $K_V1.3$, the toxins Margatoxin and ShK, induce the same alterations as Bax.

Immunoprecipitation and patch-clamp data show that Bax interacts directly with the vestibule region of $K_V1.3$. A lysine in position 128 in Bax seems to be particularly important for the interaction of Bax with $mtK_V1.3$, since its mutation to glutamic acid abrogated inhibition of $K_V1.3$ by Bax and the pro-apoptotic activity of Bax.

These results led to a model for the action of $mtK_V1.3$ during apoptosis (see Fig. 1). Bax inhibits $mtK_V1.3$ via interaction of K128 with the channel pore vestibule inducing an hyperpolarization of the IMM. This hyperpolarization results in reduction of respiratory chain activity and in an enhanced production of ROS,

which promote cytochrome c release from the periplasmic space and the activation of the MPTP. The latter is a large pore which opens in the IMM upon exposure to elevated matrix Ca^{2+} and oxidative stress, causing mitochondrial and cellular dysfunction (revs.: Zoratti and Szabò, 1995; Rasola and Bernardi, 2007; Zoratti et al., 2010).

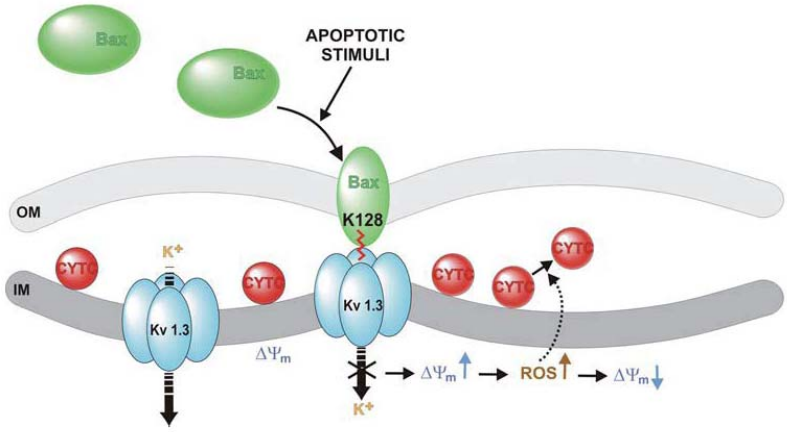

Fig 1: Model for action of mitochondrial Kv1.3 during apoptotis

The project

As understandable given the findings summarized above, the interest in mitochondrial potassium channels is increasing, in particular because of their roles in apoptosis and ischemic preconditioning.

This part of my thesis research developed along two different main themes. One concerned further studies on mtK_V1.3 to confirm its role in apoptosis, to identify by a biochemical screening the presence of mtK_V1.3 in other cell lines (cancerous or not) and to verify whether inhibition of the channel by a pharmacological agent might be sufficient to induce cell death. This work is presented in chapters 1 and 2.

The second aspect of the project had to do with the discovery of a new mitochondrial channel, mtK_{Ca}3.1 (or mtIK), and the search for possible effects of its inhibition on proliferation or apoptosis. Chapters 3 and 4 report on this.

1. Role of Kv1.3 mitochondrial potassium channel in apoptotic signalling in lymphocytes

BBA – Bioenergetics in press

Erich Gulbins[1], Nicola Sassi[2], Heike Grassmè[1], Mario Zoratti[2] and Ildikò Szabò[3]
[1]Department of Molecular Biology, University of Essen, Hufelandstrasse 5., Essen, Germany,
[2]CNR Center for Neurosciences and [3]Department of Biology of University of Padova, viale G. Colombo 3., Padova, 35122 Italy

To whom correspondence should be addressed
ildi@civ.bio.unipd.it, erich.gulbins@uni-due.de
Tel: 00-39-049-8276324; 00-49-201-7233418

Abstract

Mitochondria have been shown to play a pivotal role in apoptotic signalling in various cell types. We have recently reported that in lymphocytes the voltage-gated potassium channel Kv1.3, known to reside in the plasma membrane, is active also in the inner mitochondrial membrane. Upon induction of apoptosis, outer-membrane inserted Bax binds to and inhibits Kv1.3 resulting in hyperpolarization, an increase in reactive oxygen species production and cytochrome c release. In cells lacking Kv1.3 these events do not take place. Here, we present new data which further corroborates an important role of this channel in the sequence of events leading to Bax-induced cytochrome c release. Recombinant Kv1.3, when pre-incubated with Bax, prevents the actions of Bax at the level of mitochondria. Furthermore, we report the presence of Kv1.3 protein in mitochondria from PC3 and MCF-7 cancer cells, suggesting that this channel might play a role in the apoptotic signalling not only in lymphocytes but also in other cells.

Keywords: potassium channel, mitochondria, apoptosis

Abbreviations: CHO: Chinese hamster ovary cell line; CTLL-2: interleukin-2 dependent murine cytotoxic T lymphocyte; FITC: fluorescein isothiocyanate; GST: glutathione S-transferase; IMM: inner mitochondrial membrane; IP3R: inositol triphosphate receptor; MCF-7: human breast adenocarcinoma cell line; MPT: mitochondrial permeability transition; MgTx: margatoxin; OMM: outer mitochondrial membrane; PC3: human prostate cancer cell line; PMCA: plasma membrane calcium ATP-ase; PTP: permeability transition pore; ROS: reactive oxygen species; SERCA: sarcoplamic/endoplasmic reticulum calcium ATP-ase; ShK: *Stichodactyla* toxin; TNF: tumor necrosis factor α; VDAC: voltage-dependent anion channel;

Introduction

Several plasma membrane ion channels play an essential role for cell proliferation. A cell cycle-dependent function has been demonstrated for some voltage-gated potassium channels (e.g. ether à go-go [1]), Ca^{2+}-dependent potassium channels as well as calcium and chloride channels (for reviews see e.g. [2-5]). Along with other membrane conductances, these channels control the membrane voltage and Ca^{2+} signaling as well as intracellular ion concentration, cytosolic pH and cell volume in proliferating cells and thus participate in the regulation of the cell cycle, known to be altered in cancer cells. Ion channels have an impact also on programmed cell death (apoptosis), a process shown to be defective in many cancer types. Various plasma membrane channels have been

shown to be regulated during apoptosis. Voltage-gated potassium channels [6,7,8], IP3R [9], the ATP-gated ion channel P(2X1) [10], an outwardly rectifying swelling-activated chloride channel [11,12] and calcium release-induced calcium channel (I_{CRAC}) [13] were among the first ion channels shown to be regulated upon induction of apoptosis by various stimuli in different cell types. In general, the plasma membrane-located channels can be easily targeted by specific drugs, therefore ion channels are emerging targets for anti-tumor therapy. Several different channel inhibitors have been shown to impair tumor growth both *in vitro and in vivo* (for recent review see [14]).

In addition to plasma membrane-located ion channels, several mitochondrial ion channels, including the permeability transition pore (PTP) and the voltage-dependent anion channel (VDAC) have been implicated in regulation of apoptosis, especially of events taking place at mitochondria (for review see e.g. [15-17]). Mitochondrial potassium fluxes are important for controlling the proton motive force in energized mitochondria [18-20]. Several agents are being developed for possible tumor therapy that act on mitochondrial potassium channels (for review see e.g.[21]). For example, the potassium channel openers diazoxide and cromakalim, known to affect the mitochondrial as well as the plasma membrane K_{ATP} channels [22], have anti-tumor potential in human neuroblastoma and human astrocytoma [23]. Benzothiazine diazoxide have been shown to decrease the division of leukemic cells by causing mitochondrial membrane depolarization [24]. However certain potassium channel openers such as minoxidil have been shown to stimulate the growth of breast cancer cells, while potassium channel blockers like amioradone and dequalinium inhibit it [25]. In accordance, glibenclamide, a K_{ATP} channel blocker acts as an antitumor agent for a human gastric cell line [26]. The lack of specificity of most drugs for mitochondrial versus plasma membrane potassium channels as well as contradictory observations (see above) make it difficult to assign a specific role of mitochondrial potassium channels in the regulation of tumor cell growth and/or apoptosis by using only pharmacological strategies.

We have recently set up a genetic model in order to clarify the role of Kv1.3 in the regulation of apoptosis in lymphocytes [27]. Kv1.3 is the predominant type of voltage-gated Kv channel expressed in the plasma membrane in human lymphocytes. Its activation is a key event in T cell proliferation [28]. In accordance, specific inhibitors of Kv1.3 have a strong immunosuppressive effect [29]. As a genetic model, we used interleukin-2 dependent murine cytotoxic T lymphocytes (CTLL-2), known to be deficient for Kv1.3 [30] (CTLL-2/pJK), and stably transfected these cells with Kv1.3 (CTLL-2/Kv1.3) [27]. Either absence (in CTLL-2/pJK cells), or downregulation of Kv1.3 by siRNA in human peripheral T lymphocytes blunted death induced by various apoptotic stimuli [31]. Multiple evidence was obtained in favour of previously not described mitochondrial inner membrane (IMM) localization of the Kv1.3 (mitoKv1.3) in CTLL-2/Kv1.3 as well as in Jurkat lymphocytes [32,33]. In T cells, mitochondria provide a powerful, generally decisive potentiation of the apoptotic process induced by death receptor engagement (for reviews see e.g. [34,35]). The molecular identification of the potassium conductance in T lymphocyte mitochondria (mitoKv1.3) allowed us to determine a critical role of this channel in the regulation of apoptosis. In a previous work [31] we provided evidence that the pro-apoptotic Bcl-2 family member Bax interacts with and inhibits mitoKv1.3 via a lysine residue in position 128. Events known to take place at mitochondria in various apoptotic models, like reactive oxygen species (ROS) production, membrane potential changes and cytochrome c release were all dependent on the presence of mitoKv1.3.

In the present work we provide further experimental evidence in favour of our model according to which, at least in lymphocytes, Bax interaction with mitoKv1.3 is a crucial step, which precedes cytochrome c release during apoptosis.

Materials and Methods

Mitochondria were isolated, mitochondrial membrane potential and cytochrome c release were determined as described previously [31].

Confocal microscopy.
Cells were washed in phosphate saline buffer (PBS), fixed in PBS-buffered 2% paraformaldehyde (pH 7.3) for 10 min, washed again and permeabilized for 5 min with 0.1% Triton X-100. Cells were washed again and blocked with PBS/1% FCS for 10 min, washed and stained with FITC-labeled rabbit-anti-Bax antibodies (UBI) for 45 min at room temperature. Samples were washed 3-times in PBS and incubated for 45 min with Cy3-labeled murine anti-cytochrome C antibodies (clone 7H8.2C12, BD-Biosciences). After extensive washing, confocal microscopy was performed analysed on a Leica confocal microscope DMIRE 2. Sequential scanning was performed in order to exclude cross-detection of FITC signal in the Cy3 channel and vice versa.

Reactive oxygen species (ROS) formation in intact cells.
To determine the formation of reactive oxygen species cells were stimulated as indicated or left untreated. Cells were lysed in 0.1% SDS, 0.5% deoxycholic acid, 1% Triton X-100, 10 mM EDTA, 25 mM HEPES pH 7.3, 10 mM sodium pyrophosphate, 10 mM sodium fluoride, 125 mM NaCl, and 1 mg/ml cytochrome C (Sigma) as previously described in [36,37]. Samples were immediately transferred to a cuvette, covered with mineral oil and absorbance at 550 nm was determined.

Expression, purification and polyacrylamide gel (PAGE) analysis of recombinant Bax and Kv1.3
Bax (aminoacid aa 1-170) and Kv1.3 (either aa 319-523 (accession number NM 002232 in NCBI) or full length) were cloned into pGEX-3X, expressed in *E.coli* BL21A1 and purified from bacterial lysates using glutathione-sepharose. Bacteria were lysed in 50 ml of 25mM HEPES, pH 7.4, 0.1% SDS, 0.5% sodium deoxycholate, 1% Triton X-100, 125 mM NaCl, 10 mM each NaF, Na_3VO_4, sodium pyrophosphate, 10 µM each aprotinin and leupeptin (A/L), and 1 mg/ml lysozyme. Samples were incubated on ice for 15 min, brought to 30 mM $MgCl_2$, 5 µg/ml DNAaseI was added, and samples were incubated for an additional 30 min. Insoluble material was clarified by a 50-min centrifugation at 11,000 *g* at 4°C. The supernatant was collected and 300 µl of glutathione Sepharose (GE Healthcare) were added to immobilize GST-fusion proteins for 1 h at 4°C. The beads were pelleted by centrifugation at 500 *g* for 2 min, and the supernatant was discarded. The pellet was washed twice with 50 ml of the lysis buffer (minus lysozyme). After the last wash, 49.5 ml of the supernatant were removed, the pellet was resuspended in 5 ml of Hepes/Saline (H/S) supplemented with 20 mM glutathione (pH 7.4) and incubated for 30 min at 4°C to detach the GST-fusion proteins. Samples were centrifuged at 500 *g* for 2 min, the supernatant was collected, diluted with 15 ml of H/S, and concentrated by a 60-min centrifugation through size exclusion columns (cut-off, 10,000 Da; Viva Science, Sartorius) for Bax and Kv1.3 to 1 ml. The samples were again diluted with 20 ml of H/S and purified via size-exclusion columns. This procedure was performed for a total of five times to ensure elimination of the detergents. Finally, Bax was resuspended in H/S, Kv1.3 in H/S supplemented with micellular 0.1% NP40.

GST-Kv1.3 or GST (each 20 µg) were separated on a 5% polyacrylamide gel (PAGE) containing 0.1% SDS. The sample buffer contained 41 mM Tris/HCl pH 6.8, 10 % glycerol and Bromophenol Blue, without dithiothreitol (DTT) and sodium dodecyl sulphate (SDS) and the sample was not boiled before loading for PAGE (Fig. 4). The gel was soaked for one hour before transblotting to polyvinylidenefluoride (PVDF) membrane in a sampling buffer containing 9% SDS. The blots were developed with rabbit anti-Kv1.3 antibodies (provided by O. Pongs) and ECL. A similar method

has previously been shown to allow detection of multimeric forms of a potassium channel from *Streptomyces lividans*, according to Cortes and Perozo [38].

Binding of Margatoxin to GST-Kv1.3
We immobilized approximately 2 nmoles of CHAPS-solubilized, partly tetrameric GST-Kv1.3 on glutathione-agarose, washed the beads, incubated with 0, 0.05, 0.1, 0.25, 0.5, 1, 2 and 4 nmol Biotin-labelled MgTx (volume: 1 ml), washed again and incubated the samples with 1 µg/ml alkaline phosphatase-coupled anti-Biotin antibodies. The samples were washed again and then incubated with AP (alkaline phosphatase) substrate (diaminobenzidine DAB tablets) to convert the colourless substrate into a red dye. The absorption of the samples was determined to measure binding of MgTx-Biotin to GST-Kv1.3.

Immunoprecipitation
Fusion proteins in the soluble form were subjected to co-immunoprecipitation experiments with a rabbit anti-mouse Kv1.3 antibody, kindly gifted by O. Pongs, directed against the external epitope 409-525 of human Kv1.3 (crossreactive with rat and mouse) or a commercial rabbit anti-Kv1.3 antibody (from Alamone Lab.) directed against the epitope aa 471- 523 of human Kv1.3 (cross-reactive with mouse Kv1.3). Both antibodies gave the same results, revealing co–immuno-precipitation of Kv1.3 with Bax. Western blots were done either with the rabbit anti-Kv1.3 antibody from O. Pongs (all data on murine cells) or antibody from Alamone, both antibodies gave the same results.

Results and Discussion

Recombinant Bax as well as full-length Bax have previously been shown to inhibit Kv1.3 channel activity and to physically interact with the mitoKv1.3 protein, only in mitochondria isolated from apoptotic cells [31]. The electrochemical gradient for K^+ in energized mitochondria predicts that K^+ flow through an IMM-located potassium channel should be inward. If an influx of positive charge through mitoKv1.3 is inhibited, a hyperpolarization is expected. Hyperpolarization in turn results in the reduction of respiratory chain components such as Fe/S centers, cytochromes and the ubiquinone pool, and in enhanced production of reactive oxygen species (ROS) (e.g.: [39,40]). In agreement, addition of recombinant Bax or of toxins, known to inhibit Kv1.3 and mitoKv1.3 with high specificity (like MgTx or ShK), to isolated mitochondria in suspension resulted in hyperpolarization and ROS production [31]. ROS production would therefore be expected to be associated with Kv1.3-dependent apoptosis. Figure 1. illustrates that treatment of CTLL-2/Kv1.3 intact cells with the anti-oxidants Tiron and N-acetylcysteine prevents the release of ROS as well as induction of apoptosis after treatment with staurosporine, C_6-ceramide and tumor necrosis factor (TNF) indicating that indeed apoptosis induced by various factors is dependent on ROS in our system.

ROS are able to oxidize thiol groups and thus to elicit mitochondrial depolarization by activation of the PTP [41-43]. PTP opening and consequent $\Delta\psi m$ decrease downstream of transient mitochondrial hyperpolarization and/or increase in ROS production has been reported in several studies employing drugs or Ca^{2+}-overload to induce apoptosis (e.g.: [44-46]). In our case, Bax-induced hyperpolarization was indeed followed by CSA-sensitive depolarization, indicating that PTP opening was induced [31]. Our data are consistent with previous studies showing a transient hyperpolarization and/or increase of ROS followed by a MPT-mediated decrease of mitochondrial membrane potential upon treatment with, e.g., the cytostatic drug BMD188, ceramide, oxygen-glucose-deprivation or staurosporine to name a few [45, 47-49].

ROS have also been shown to oxidize cardiolipin resulting in the release of cytochrome c from the inner mitochondrial membrane [50,51]. In accordance, the presence of the channel has been shown to be crucial for both ROS release and Bax-induced cytochrome c release as previously

assayed by Western blots [31]. Figure 2. shows confocal microscopy studies on CTLL/pJK and CTLL/Kv1.3 that illustrate translocation of Bax into mitochondria in both cell types upon treatment with staurosporine but release of cytochrome c only in Kv1.3-positive cells. These latter cell types express also mitoKv1.3 in their mitochondria, as shown previously [31, 32]. The cells were stained with anti-cytochrome c and anti-Bax antibodies. Confocal microscopy clearly proves that Bax migrated to mitochondria after staurosporine treatment and was not only present in a layer directly above or below the mitochondria. The signal for cytochrome *c* released in the cytoplasm is relatively weak, since confocal microscopy visualizes thin sections. Please note that T cells are characterized by an U-shaped nucleus, causing the observed distribution of fluorescent signal within the cell. Data of Figure 2. together with previously published data indicate a translocation of Bax into mitochondria of CTLL-2/pJK cells without release of cytochrome c, while the CTLL/Kv1.3 cells do release cytochrome c into the cytoplasm upon translocation of Bax.

Our data suggest that inhibition of mitoKv1.3 triggers the release of ROS, which finally mediate release of cytochrome c. If hyperpolarization, triggered by the inhibition of mitoKv1.3 by Bax, was necessary for cytochrome c release to occur, replacing KCl by NaCl in the suspension medium of isolated mitochondria should prevent these events, since K^+-selective mitoKv1.3 does not carry an inward current under these conditions. Our data confirmed this hypothesis, and showed that Bax-induced hyperpolarization and cytochrome c release were prevented by substitution of external potassium with sodium [31]. This result however might seem to be in contradiction with results published by Uren et al. [52] who have shown that NaCl and LiCl (at least 50 mM) worked as well as KCl in permitting the release of cytochrome c upon treatment of mitochondria with t-Bid, a BH3-only pro-apoptotic Bcl-2 family member, which activates endogenous Bax that is attached to mitochondria. In the absence of external salt, cytochrome *c* is not released because of its strong electrostatic interactions with negative lipids in the inner mitochondrial membrane. In the studies by Uren et al. [52] 10 mM potassium was however present in all experiments. In mitochondria from Jurkat cells (Figure 3), 10 mM KCl in the medium is sufficient to allow hyperpolarization of the mitochondrial membrane and ROS production upon addition of Bax. However, cytochrome c release does not take place with 10 mM KCl (and no other salt), while it does occur at high salt, in agreement with the findings by Uren et al [52]. In our experiments on KCl substitution with NaCl the salt concentration was the same (100 mM), therefore the interaction of cytochrome *c* with negatively charged phosphatidylserine is fully expected to be equally weakened in the two cases. However, no KCl was present when the NaCl-based medium was used. Thus, the ion substitution experiment indicate that indeed cytochrome c release requires potassium as well as a high ionic strength of the external medium for complete detachment.

If our model is correct, addition of recombinant Kv1.3 channel protein which competes with endogenous mitoKv1.3 for Bax binding should be able to prevent the effects of Bax on mitochondria. A fusion protein consisting of a GST-tag and aa 319-523 of Kv1.3 was chosen for these experiments. A full length GST-Kv1.3 fusion protein was also produced, although with low expression efficiency. Full-length Kv1.3 has previously been shown to be purified with similarly low efficiency from Kv1.3-expressing CHO cells in the presence of deoxycholate as detergent [53]. In our experiments, the protein was purified from bacterial extracts with glutathione-agarose in the presence of detergents SDS and deoxycholate. In most experiments we used GST-Kv1.3 (aa 319-523), however, critical experiments were confirmed with a GST-fusion protein of full length Kv1.3. Native Kv1.3 is a homotetrameric channel. To address the issue of whether tetrameric protein is present in our preparation, we performed non-denaturing gels (containing 0.1% SDS, according to [38]) that were blotted with polyclonal rabbit anti-Kv1.3 antibodies. The results of 3 independent studies show bands for monomeric, dimeric and tetrameric constructs indicating the presence of tetrameric GST-Kv1.3 (Fig. 4 A).

The tetrameric, functionally active nature of the recombinant GST-Kv1.3 fusion protein was indicated also by the observation that it was able to bind Margatoxin, its specific inhibitor, with high affinity. To determine MgTx binding, we immobilized soluble GST-Kv1.3 on glutathione and

tested the binding of Biotin-labelled MgTx. The data obtained show a half maximal binding upon addition of approximately 1.1 nmol MgTx-Biotin for 2 nmol GST-Kv1.3, and near-saturation at about 2 nmoles of added MgTx-Biotin. While precision is not sufficient to determine an accurate KD, the experiments show that the affinity of GST-Kv1.3 for MgTx-Biotin is very high, in the same range as that of membrane Kv1.3 for MgTx (110 pM, [54]). The data also demonstrate that MgTx competes with MgTx-Biotin for binding to immobilized GST-Kv1.3 with very similar affinity, since half-saturation of MgTx-Biotin binding is observed when equal amounts of MgTx and MgTx-Biotin are added.

Previous studies indicated that binding of the highly specific Kv1.3 inhibitor toxins, which dock in the outer-facing vestibule of Kv1.3 (involving D386 residues), is pH dependent, and that protonation of Histidine 404 of Kv1.3 weakens pore-toxin interaction [55]. H404 and D386 are both present in the GST-Kv1.3 fusion protein used in our experiments. We have previously shown that the IC_{50} of GST-Bax for Kv1.3 binding increased from 4 to 12 nM when in patch clamp experiments on T lymphocytes the bath solution pH was lowered to pH 6.7 and to a value >> 50 nM at pH 6.0. These data indicated a toxin-like interaction of Bax with the external vestibule of Kv1.3 and mitoKv1.3 [31]. Here we show that co-incubation of GST-Bax with GST-Kv1.3 resulted in strong association of the two proteins (Fig. 4B) as revealed by immunoprecipitation experiments. The strength of this interaction significantly decreased when pH was lowered to 6.0, confirming again that Bax binds to Kv1.3 in a manner similar to Margatoxin. To further prove the specificity of the interaction of Bax and Kv1.3 we added MgTx (5 μM) to GST-Kv1.3 (~2 nM) prior to addition of GST-Bax. As MgTx specifically binds to the pore of Kv1.3 with very high affinity (IC_{50}: 110 pM), an excess of MgTx (5 μM) will prevent binding of Bax to Kv1.3, but only if Bax binds in the pore region of Kv1.3. Our results show that Margatoxin indeed prevented the interaction of GST-Kv1.3 with GST-Bax excluding a non-specific interaction of the two proteins (Fig. 4B).

Finally, we tested the effect of the recombinant GST-Kv1.3 on membrane potential changes of isolated mitochondria induced by toxins or Bax, as well as on Bax-induced cytochrome c release. Pre-incubation of Margatoxin or ShK (Fig. 5A) as well as of Bax (Fig. 5B) with recombinant GST-Kv1.3 prevented their effects on changes in mitochondrial membrane potential. Neither early hyperpolarization, nor later depolarization occurred, indicating that the recombinant protein competed with endogenous mitoKv1.3 for Bax and the toxins. The same kind of experiment was performed when assessing cytochrome c release (Fig. 5C), further demonstrating that Bax interacts with mitoKv1.3 and the importance of this interaction for cytochrome c release.

Kv1.3, as plasma membrane channel, is known to be expressed in different tissues and cell types, including brain, lung, thymus, spleen, lymph node, fibroblasts, B lymphocytes, T lymphocytes, tonsils, macrophages, microglia, oligodendrocytes, osteoclasts, platelets, and testis [56]. An altered expression level of Kv1.3 has been found in several types of cancer [14], including prostate and breast cancer [25, 57,58]. Therefore, we checked whether Kv1.3 might be present in the mitochondria not only of lymphocytes but also of other types of cells. Figure 6. shows that a mitochondrial location of Kv1.3 can be identified in prostate cancer PC3 and in breast cancer MCF-7 cell lines. At equal protein quantities loaded, intensity of mitochondrial markers Bak and prohibitin, as well as of Kv1.3 increases in purified mitochondria with respect to whole-cell lysate, whereas intensity of the plasma membrane marker Ca^{2+}-ATP-ase PMCA and of the ER marker Ca^{2+}-ATP-ase SERCA decreases. These data indicate that the presence of mitoKv1.3 in mitochondria is not restricted to lymphocytes. Furthermore, a functional mitoKv1.3 seems to be present also in hippocampal mitochondria [59]. Whether mitoKv1.3 in these cells may represent a possible target for modulating apoptosis remains to be clarified.

Conclusion

The data presented above further confirm the importance of mitoKv1.3 for apoptosis in lymphocytes and points to a direct interaction of mitoKv1.3 with Bax. Inhibition of mitoKv1.3 by outer-membrane inserted Bax leads to early hyperpolarization (within 5 minutes), ROS release, a

later depolarization (15 minutes after treatment) and cytochrome c release. We used low nanomolar concentrations of Bax in our experiments. They do not exclude that Bax may also form oligomeric pores in the membranes or that it interacts with other mitochondrial proteins. Bax-induced cytochrome c release may well be a multi-stage process, inhibition of mitoKv1.3 by presumably monomeric Bax representing only an early step, to be followed by other processes, such as ROS release, detachment of cytochrome c from the surface of the IMM, and PTP activation. Bax has recently been shown to be inserted into the OMM first as monomer and then undergoing oligomerization [60]. Formation of Bax oligomers and pore formation by Bax in the OMM may well occur independently of the presence of Kv1.3. Although our data indicate PTP activation downstream of Bax-Kv1.3 interaction, we should stress that they do not discriminate whether cytochrome c efflux is directly linked to PTP opening – which may induce distension of cristae and increased availability of cytochrome c for efflux – or is triggered independently of PTP – for instance, by oxidation of cardiolipin.

In summary, previous data as well as those described in the present manuscript indicate an important function of mitoKv1.3 in lymphocyte apoptosis. The presence of mitoKv1.3 in other cell types as well suggests that the action of mitoKv1.3 might not be restricted to lymphocytes only.

Acknowledgements

The authors are grateful to M. Soddemann for preparing the fusion proteins. The authors thank Drs. O. Pongs (University of Hamburg, Hamburg, Germany) for important reagents. This work was supported in part by Italian Association for Cancer Research grants (to I.S. and to M.Z.), an European Molecular Biology Organization Young Investigator Program and a Progetti di Rilevante Interesse Nazionale grant (to I.S.) and by DFG-grant Gu 335/13–3 and the International Association for Cancer Research (to E.G.).

FIGURE LEGENDS

Figure 1. ROS release and apoptosis are correlated in intact cells. (A) CTLL-2/Kv1.3 cells were pre-treated for 30 min with Tiron (1 mM) or N-acetylcysteine (1 mM, NAC) and then stimulated with 20 μM C_6-ceramide, 1 μM staurosporine or 100 ng/ml TNFα, respectively. ROS was measured as described in Materials and Methods section. **(B)** Apoptosis was measured by FACS analysis after staining with FITC-Annexin (Roche) for 15 min at 22 °C. Given are the mean ± SD of 3 independent experiments each (*p <0.05, t-test to controls, p>0.05 to untreated samples).

Figure 2. Bax migrates to mitochondria but does not induce the release of cytochrome c in Kv1.3-deficient CTLL-2/pJK cells. CTLL/Kv1.3 or CTLL/pJK cells were stimulated for 1 hr with 1 μM staurosporine, and stained with anti-Bax antibodies and with anti-cytochrome c antibodies. Confocal microscopy images are shown.

Figure 3. Cytochrome c release requires K^+ and a high concentration of salt. The data show hyperpolarization and ROS formation after treatment of isolated mitochondria with 5 nM GST-Bax in the presence of about 10 mM KCl (70 mM sucrose, 210 mM mannitol, 1 mM EDTA, and 10 mM HEPES/KOH, pH 7.5), while no release of cytochrome c from isolated mitochondria was observed

under these conditions. Increasing the concentration of potassium to 100 mM in the experimental medium allowed cytochrome c release. Mitochondrial membrane potential, cytochrome c release and ROS-generation in isolated mitochondria was measured as described in material and methods of [31].

Figure 4. Recombinant GST-Kv1.3 interacts with GST-Bax in vitro. (A) Monomeric, dimeric and tetrameric forms of GST-Kv1.3 are visible on non-denaturing PAGE. **(B)** Co-incubation of GST-Kv1.3 with GST-Bax (~200 ng/ml each) reveals an association of the two proteins, which is blocked by pre-incubation and neutralization of GST-Kv1.3 with Margatoxin (5 µM). The association of the two proteins is strongly decreased by altering the pH from 7.4 to 6.0. Shown are Western blot experiments performed with anti-Bax and anti-Kv1.3 antibodies, respectively, which are representative of 3 very similar results. The lower blots demonstrate that similar amounts of protein were loaded in all lanes.

Figure 5. Pre-incubation of Bax with GST-Kv1.3 abolishes its effects on membrane potential changes in mitochondria and on cytochrome c release from isolated mitochondria. Incubation of purified, Kv1.3-positive mitochondria from Jurkat with 20 nM MgTx or 10 nM ShK **(A)** or 5 nM GST-Bax **(B)** resulted in hyperpolarization, followed by depolarization. The presence of 100 nM recombinant GST-Kv1.3 during the 30-min incubation neutralized the toxins and Bax and blocked their effects. Control GST was without effect. The flow cytometry panels show plots representative of 3 independent experiments reporting $\Delta\Psi m$ in isolated Jurkat mitochondria stained with 10 nM $DioC_6(3)$. Complete depolarization upon application of CCCP served as control for mitochondria integrity. **(C)** Purified Kv1.3-expressing mitochondria responded to incubation with GST-Bax with release of cytochrome c, whereas pre-incubation of Bax with GST-Kv1.3 abolished the effect of Bax. Cytochrome c release was determined by Western blotting. Blots are representative of 5 similar experiments.

Figure 6. Kv1.3 is located to mitochondria also in PC3 and MCF-7 cancer cells. 50 µg of total protein per lane was loaded of whole cell-lysate (1), a membrane-enriched fraction (2) and Percoll-purified mitochondria (3). See description in the text. Kv1.3 was detected with an apparent MW of 64 kDa. Blots with marker proteins were obtained by stripping and re-blotting. Differences in background are due to different exposure time and/or development method.

References

[1] L.A. Pardo, D. del Camino, A. Sánchez, F. Alves, A. Brüggemann, S. Beckh, W. Stühmer, Oncogenic potential of EAG K^+ channels, EMBO J. 18 (1999) 5540-5547.

[2] F. Lang, M. Föller, K.S. Lang, P.A. Lang, M. Ritter, E. Gulbins, A. Vereninov, S.M. Huber, Ion channels in cell proliferation and apoptotic cell death. J Membr. Biol. 205 (2005) 147-157.

[3] W. Stühmer, F. Alves, F. Hartung, M. Zientkowska, L.A. Pardo, Potassium channels as tumour markers. FEBS Lett. 580 (2006) 2850-2852.

[4] K. Kunzelmann, Ion channels and cancer, J Membr Biol. 205 (2005) 159-173.

[5] B. Nilius, Chloride channels go cell cycling, J. Physiol. 532 (2001) 581.

[6] P. Nagy, G. Panyi, A. Jenei, L. Bene, R. Jr. Gáspár, J. Matkó, S. Damjanovich, Ion channel activities regulate transmembrane signaling in thymocyte apoptosis and T-cell activation, Immunol. Lett. 44 (1995) 91-95.

[7] I. Szabò, E. Gulbins, H. Apfel, X. Zhang, P. Barth, A.E. Busch, K. Schlottmann, O. Pongs, F. Lang, Tyrosine phosphorylation-dependent suppression of a voltage-gated K^+ channel in T lymphocytes upon Fas stimulation. J. Biol. Chem. 271 (1996) 20465-20469.

[8] S.P. Yu, C.H. Yeh, S.L. Sensi, B.J Gwag, L.M. Canzoniero, Z.S. Farhangrazi, H.S. Ying, M. Tian, L.L. Dugan, D.W. Choi, Mediation of neuronal apoptosis by enhancement of outward potassium current. Science. 278 (1997) 114-117.

[9] A.A. Khan, M.J. Soloski, A.H. Sharp, G. Schilling, D.M. Sabatini, S.H. Li, C.A. Ross, S.H. Snyder, Lymphocyte apoptosis: mediation by increased type 3 inositol 1,4,5-trisphosphate receptor, Science. 273(1996) 503-507.

[10] Y. Chvatchko, S. Valera, J.P. Aubry, T. Renno, G. Buell, J.Y. Bonnefoy, The involvement of an ATP-gated ion channel, P(2X1), in thymocyte apoptosis. Immunity. 5 (1996) 275-283.

[11] I. Szabò, A. Lepple-Wienhues, K.N. Kaba, M. Zoratti, E. Gulbins, F. Lang, Tyrosine kinase-dependent activation of a chloride channel in CD95-induced apoptosis in T lymphocytes. Proc. Natl. Acad. Sci. U S A. 95 (1998) 6169-6174.

[12] E. Maeno, Y. Ishizaki, T. Kanaseki, A. Hazama, Y. Okada, Normotonic cell shrinkage because of disordered volume regulation is an early prerequisite to apoptosis. Proc. Natl. Acad. Sci. U S A. 97 (2000) 9487-9492.

[13] A. Lepple-Wienhues, C. Belka, T. Laun, A. Jekle, B. Walter, U. Wieland, M. Welz, L. Heil, J. Kun, G. Busch, M. Weller, M. Bamberg, E. Gulbins, F. Lang, Stimulation of CD95 (Fas) blocks T lymphocyte calcium channels through sphingomyelinase and sphingolipids. Proc. Natl. Acad. Sci. U S A. 96 (1999) 13795-13800.

[14] A. Arcangeli, O. Crociani, E. Lastraioli, A. Masi, S. Pillozzi, A. Becchetti, Targeting ion channels in cancer: a novel frontier in antineoplastic therapy. Curr. Med. Chem. 16 (2009) 66-93.

[15] E.A. Jonas, Molecular participants in mitochondrial cell death channel formation during neuronal ischemia. Exp. Neurol. 218 (2009) 203-212.

[16] V. Shoshan-Barmatz, A. Israelson, D. Brdiczka, S.S. Sheu, The voltage-dependent anion channel (VDAC): function in intracellular signalling, cell life and cell death. Curr. Pharm. Des. 12 (2006) 2249-2270.

[17] B. O'Rourke, Evidence for mitochondrial K^+ channels and their role in cardioprotection. Circ. Res. 94 (2004) 420-32.

[18] P. Bernardi, Mitochondrial transport of cations: channels, exchangers, and permeability transition. Physiol. Rev. 79 (1999) 1127-1155.

[19] K.D. Garlid, P. Paucek, Mitochondrial potassium transport: the K^+ cycle, Biochim. Biophys. Acta. 1606 (2003) 23-41.

[20] A. Czyz, A. Szewczyk, M.J. Nalecz, L. Wojtczak, The role of mitochondrial potassium fluxes in controlling the protonmotive force in energized mitochondria, Biochem. Biophys. Res. Commun. 210 (1995) 98–104.

[21] D. Pathania, M. Millard, N. Ne'amati, Opportunities in discovery and delivery of anticancer drugs targeting mitochondria and cancer cell metabolism, Adv. Drug Delivery Rev. 61 (2009) 1250-1275.

[22] K.D. Garlid, P. Paucek, V. Yarov-Yarovoy, X. Sun, P.A. Schindler, The mitochondrial KATP channel as a receptor for potassium channel openers, J. Biol. Chem. 271 (1996) 8796–8799.

[23] Y.S. Lee, M.M. Sayeed, R.D. Wurster, In vitro antitumor activity of cromakalim in human brain tumor cells, Pharmacol. 49 (1994) 69–74.

[24] E. Holmuhamedov, L. Lewis, M. Bienengraeber, M. Holmuhamedova, A. Jahangir, A. Terzic, Suppression of human tumor cell proliferation through mitochondrial targeting, FASEB J. 16 (2002) 1010–1016.

[25] M. Abdul, A. Santo, N. Hoosein, Activity of potassium channel-blockers in breast cancer, Anticancer Res. 23 (2003) 3347–3351.

[26] X. Qian, J. Li, J. Ding, Z.Wang, L. Duan, G. Hu, Glibenclamide exerts an antitumor activity through reactive oxygen species-c-jun NH2-terminal kinase pathway in human gastric cancer cell line MGC-803, Biochem. Pharmacol. 76 (2008) 1705–1715.

[27] J. Bock, I. Szabó, A. Jekle, E. Gulbins, Actinomycin D-induced apoptosis involves the potassium channel Kv1.3. Biochem. Biophys. Res. Commun. 295 (2002) 526-531.

[28] K.G. Chandy, T.E. DeCoursey, M.D. Cahalan, C. McLaughlin, S. Gupta, Voltage-gated potassium channels are required for human T lymphocyte activation. J. Exp. Med. 160 (1984) 369-385.

[29] K.G. Chandy, H.Wulff, C. Beeton, M. Pennington, G.A. Gutman, M.D. Cahalan, K^+ channels as targets for specific immunomodulation, Trends Pharmacol. Sci. 25 (2004) 280–289.

[30] C. Deutsch, L.Q. Chen, Heterologous expression of specific K^+ channels in T lymphocytes: functional consequences for volume regulation, Proc. Natl. Acad. Sci. USA. 90 (1993) 10036–10040.

[31] I. Szabó, J. Bock, H. Grassmé, M. Soddemann, B. Wilker, F. Lang, M. Zoratti, E. Gulbins, Mitochondrial potassium channel Kv1.3 mediates Bax-induced apoptosis in lymphocytes, Proc. Natl. Acad. Sci. USA. 105 (2008) 14861–14866.

[32] I.Szabò, J. Bock, A. Jekle, M. Soddemann, C.Adams, F. Lang, M. Zoratti, E. Gulbins, A novel potassium channel in lymphocyte mitochondria, J.Biol.Chem. 280 (2005) 12790-12798.

[33] M. Zoratti, U. De Marchi, E. Gulbins, I. Szabò, Novel channels of the inner mitochondrial membrane, Biochim. Biophys. Acta, Bioenerg. 1787 (2009) 351-363.

[34] R. Arnold, D. Brenner, M. Becker, C.R. Frey, P.H. Krammer, How T lymphocytes switch between life and death. Eur. J. Immunol. 36 (2006) 1654-1658.

[35] M. Tafani, N.O. Karpinich, A. Serroni, M.A. Russo, J.L. Farber, Re-evaluation of the distinction between type I and type II cells: the necessary role of the mitochondria in both the extrinsic and intrinsic signaling pathways upon Fas receptor activation. J. Cell. Physiol. 208 (2006) 556-565.

[36] E. Gulbins, B. Brenner, K. Schlottmann, J. Welsch, H. Heinle, U. Koppenhoefer, O. Linderkamp, K.M. Coggeshall, F. Lang, Fas-induced programmed cell death is mediated by a Ras-regulated O_2^- synthesis. Immunology. 89 (1996) 205-212.

[37] J.M. McCord, I. Fridovich, Superoxide dismutase. An enzymic function for erythrocuprein (hemocuprein). J. Biol. Chem. 244 (1969) 6049–6055.

[38] D.M. Cortes, E. Perozo, Structural dynamics of the *Streptomyces lividans* K^+ channel (SKC1): oligomeric stoichiometry and stability. Biochemistry 36 (1997) 10343-10352.

[39] B. O'Rourke, S. Cortassa, M.A. Aon, Mitochondrial ion channels: gatekeepers of life and death, Physiol. 20 (2005) 303–315.

[40] M.P. Murphy, How mitochondria produce reactve oxygen species, Biochem. J. 417 (2009) 1–13.

[41] M. Zoratti, I. Szabò, The mitochondrial permeability transition, Biochim. Biophys. Acta 1241 (1995) 139–176.

[42] P. Costantini, B.V. Chernyak, V. Petronilli, P. Bernardi, Modulation of the mitochondrial permeability transition pore by pyridine nucleotides and dithiol oxidation at two separate sites, J. Biol. Chem. 271 (1996) 6746–6751.

[43] M. Giorgio, E. Migliaccio, F. Orsini, D. Paolucci, M. Moroni, C. Contursi, G. Pelliccia, L. Luzi, S. Minucci, M. Marcaccio, P. Pinton, R. Rizzuto, P. Bernardi, F. Paolucci, P.G. Pelicci, Electron transfer between cytochrome c and p66Shc generates reactive oxygen species that trigger mitochondrial apoptosis, Cell. 122 (2005) 221–233.

[44] B. Joshi, L. Li, B.G. Taffe, Z. Zhu, S.Wahl, H. Tian, E. Ben-Josef, J.D. Taylor, A.T. Porter, D.G. Tang, Apoptosis induction by a novel anti-prostate cancer compound, BMD188 (a fatty acid-containing hydroxamic acid), requires the mitochondrial respiratory chain, Cancer Res. 59 (1999) 4343–4355.

[45] A. Quillet-Mary, J.P. Jaffrézou, V. Mansat, C. Bordier, J. Naval, G. Laurent, Implication of mitochondrial hydrogen peroxide generation in ceramide-induced apoptosis, J. Biol. Chem. 272 (1997) 21388–21395.

[46] A.J. Kowaltowski, R.F. Castilho, A.E. Vercesi, Mitochondrial permeability transition and oxidative stress, FEBS Lett. 495 (2001) 12–15.

[47] M. Zhou, Z. Diwu, N. Panchuk-Voloshina, R.P. Haugland, A stable nonfluorescent derivative of resorfin for the fluorimetric determination of hydrogen peroxide: applications in

detecting the activity of phagocyte NADPH oxidase and other oxidases, Anal. Biochem. 253 (1997) 162-168.

[48] T. Iijima, T. Mishima, K. Akagawa, Y. Iwao, Mitochondrial hyperpolarization after transient oxygen-glucose deprivation and subsequent apoptosis in cultured rat hippocampal neurons. Brain Res. 993 (2003) 140-145.

[49] M.G. Vander Heiden, N.S. Chandel, E.K. Williamson, P.T. Schumaker, C.B. Thompson, Bcl-x_L regulates the membrane potential and volume homeostasis of mitochondria, Cell. 91 (1997) 627-637.

[50] S. Orrenius, Reactive oxygen species in mitochondria-mediated cell death, Drug Metab. Rev. 39 (2007) 443–455.

[51] M. Ott, B. Zhivotovsky, S. Orrenius, Role of cardiolipin in cytochrome c release from mitochondria, Cell Death Differ. 14 (2007) 1243–1247.

[52] R.T. Uren, G. Dewson, C. Bonzon, T. Lithgow, D.D. Newmeyer, R.M. Kluck, Mitochondrial release of pro-apoptotic proteins: electrostatic interactions can hold cytochrome c but not Smac/DIABLO to mitochondrial membranes. J. Biol. Chem. 280 (2005) 2266-2274.

[53] R.H. Spencer, Y. Sokolov, H. Li, B. Takenaka, A.J. Milici, J. Aiyar, A. Nguyen, H. Park, B.K. Jap, J.E. Hall, G.A. Gutman, K.G. Chandy, Purification, visualization, and biophysical characterization of Kv1.3 tetramers. J. Biol. Chem. 272(1997) 2389-2395.

[54] K.G. Chandy, H. Wulff, C. Beeton, M. Pennington, G.A. Gutman, M.D. Cahalan, K^+ channels as targets for specific immunomodulation. Trends Pharmacol. Sci. 25 (2004) 280-289.

[55] J. Aiyar, J.M. Withka, J.P. Rizzi, D.H. Singleton, G.C. Andrews, W. Lin, J. Boyd, D.C. Hanson, M. Simon, B. Dethlefs et al, Topology of the pore-region of a K^+ channel revealed by the NMR-derived structures of scorpion toxins. Neuron. 15 (1995) 1169-1181.

[56] G.A. Gutman, K.G. Chandy, S. Grissmer, M. Lazdunski, D. McKinnon, L.A. Pardo, G.A. Robertson, B. Rudy, M.C. Sanguinetti, W. Stühmer, X. Wang, International Union of Pharmacology. LIII. Nomenclature and molecular relationships of voltage-gated potassium channels. Pharmacol. Rev. 57 (2005) 473-508.

[57] M. Brevet, N. Haren, H. Sevestre, P. Merviel, H. Ouadid-Ahidouch, DNA methylation of K(v)1.3 potassium channel gene promoter is associated with poorly differentiated breast adenocarcinoma. Cell Physiol Biochem. 24 (2009) 25-32.

[58] M. Abdul, N. Hoosein, Reduced Kv 1.3 potassium channel expression in human prostate cancer. J. Membr. Biol. 214 (2006) 99-102.

[59] P. Bednarczyk, Potassium channels in brain mitochondria. Acta Biochim. Pol. 56 (2009) 385-392.

[60] M.G. Annis, E.L. Soucie, P.J. Dlugosz, J.A. Cruz-Aguado, L.Z. Penn, B. Leber, D.W. Andrews, Bax forms multispanning monomers that oligomerize to permeabilize membranes during apoptosis. EMBO J. 24 (2005) 2096-2103

Figure1

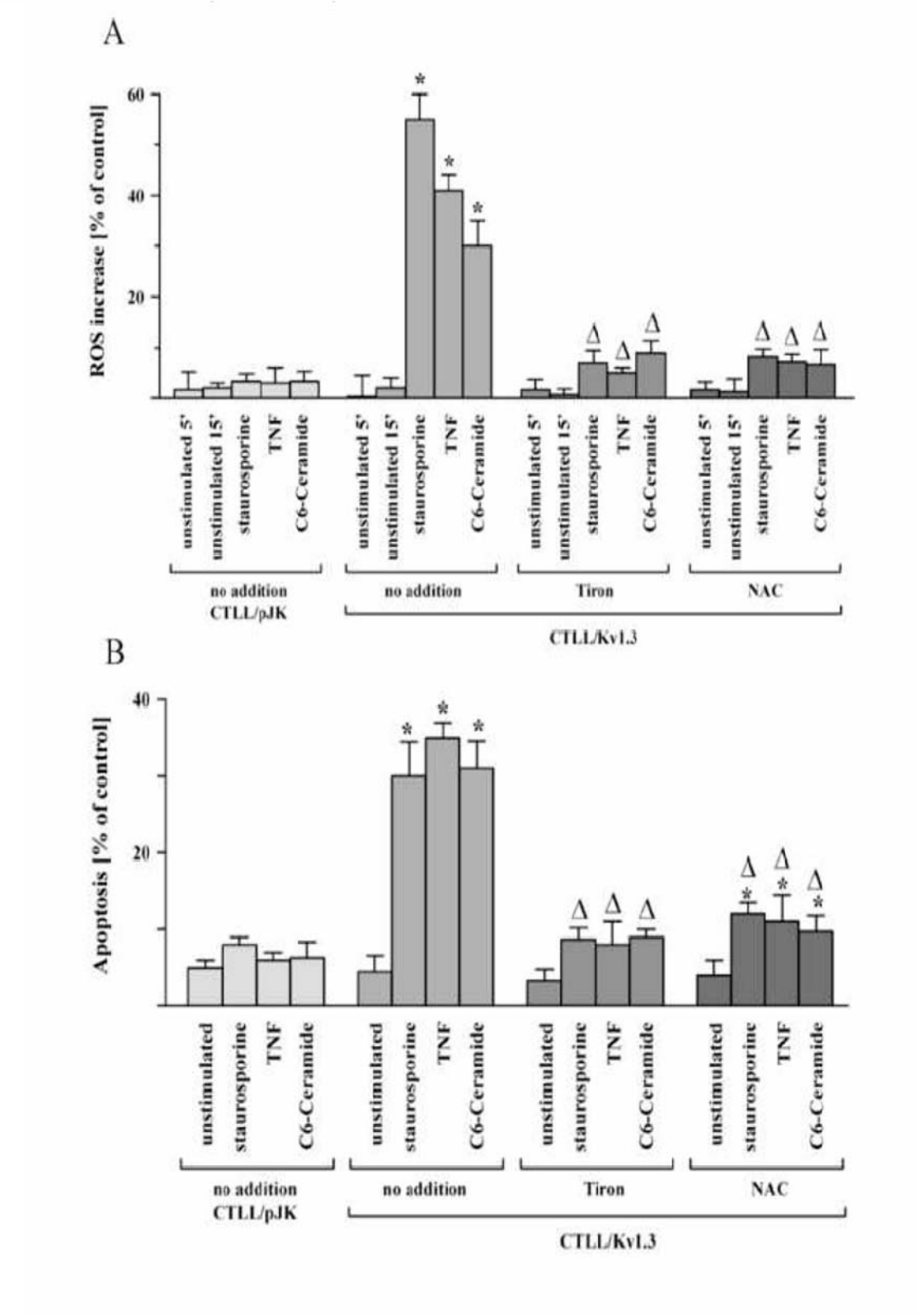
A
ROS increase [% of control]
60
40
20
unstimulated 5'
unstimulated 15'
staurosporine
TNF
C6-Ceramide
no addition
CTLL/pJK
no addition
Tiron
NAC
CTLL/Kv1.3
B
Apoptosis [% of control]
40
20
unstimulated
staurosporine
TNF
C6-Ceramide
no addition
CTLL/pJK
no addition
Tiron
NAC
CTLL/Kv1.3

Figure2

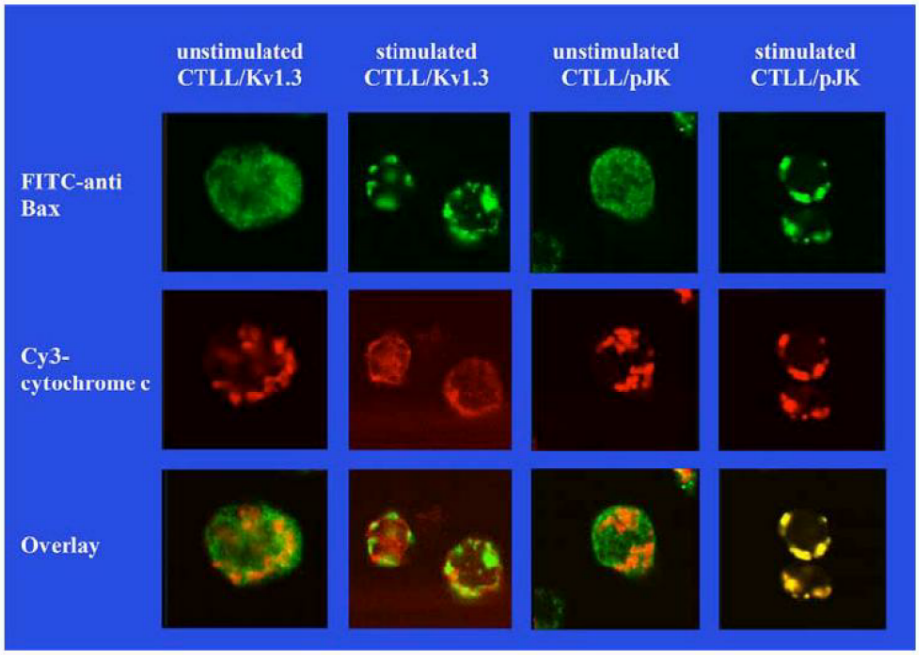
unstimulated CTLL/Kv1.3
stimulated CTLL/Kv1.3
unstimulated CTLL/pJK
stimulated CTLL/pJK
FITC-anti Bax
Cy3-cytochrome c
Overlay

Figure3

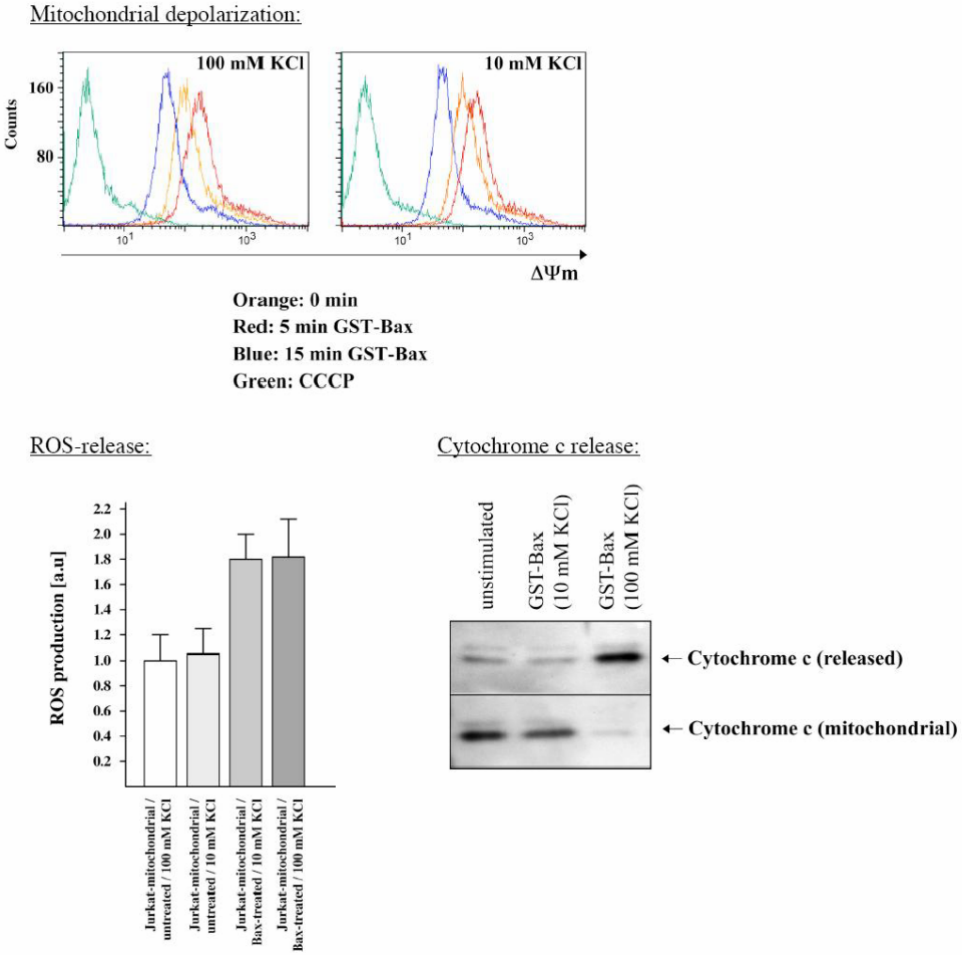
Mitochondrial depolarization:
100 mM KCl
10 mM KCl
Counts
160
80
10^1
10^3
ΔΨm
Orange: 0 min
Red: 5 min GST-Bax
Blue: 15 min GST-Bax
Green: CCCP
ROS-release:
ROS production [a.u]
2.2
2.0
1.8
1.6
1.4
1.2
1.0
0.8
0.6
0.4
0.2
Jurkat-mitochondrial / untreated / 100 mM KCl
Jurkat-mitochondrial / untreated / 10 mM KCl
Jurkat-mitochondrial / Bax-treated / 10 mM KCl
Jurkat-mitochondrial / Bax-treated / 100 mM KCl
Cytochrome c release:
unstimulated
GST-Bax (10 mM KCl)
GST-Bax (100 mM KCl)
← Cytochrome c (released)
← Cytochrome c (mitochondrial)

Figure4

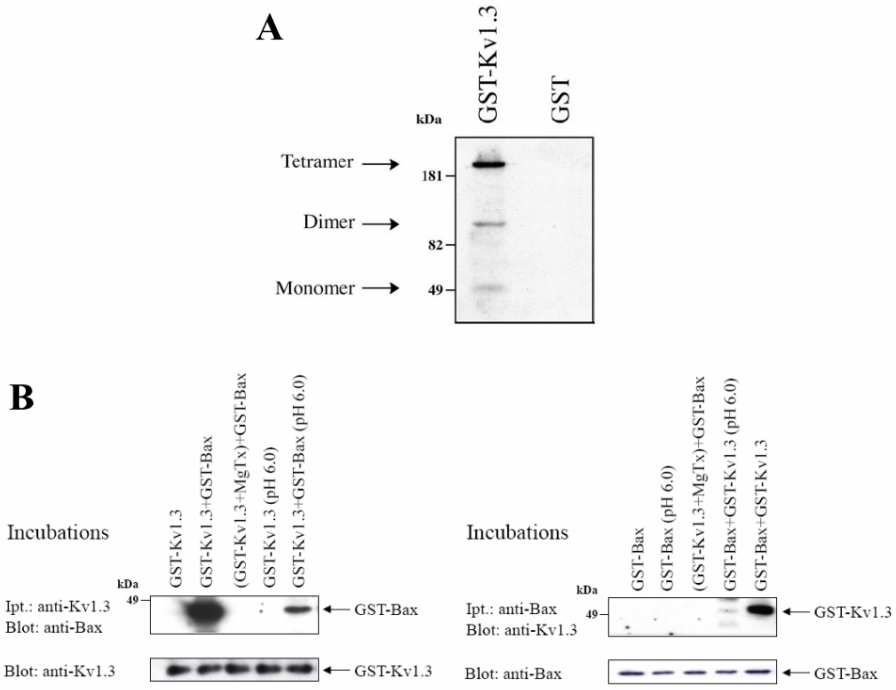
A
GST-Kv1.3
GST
kDa
Tetramer
Dimer
Monomer
181
82
49
B
Incubations
GST-Kv1.3
GST-Kv1.3+GST-Bax
(GST-Kv1.3+MgTx)+GST-Bax
GST-Kv1.3 (pH 6.0)
GST-Kv1.3+GST-Bax (pH6.0)
kDa
49
Ipt.: anti-Kv1.3
Blot: anti-Bax
GST-Bax
Blot: anti-Kv1.3
GST-Kv1.3
Incubations
GST-Bax
GST-Bax (pH 6.0)
(GST-Kv1.3+MgTx)+GST-Bax
GST-Bax+GST-Kv1.3 (pH 6.0)
GST-Bax+GST-Kv1.3
kDa
49
Ipt.: anti-Bax
Blot: anti-Kv1.3
GST-Kv1.3
Blot: anti-Bax
GST-Bax

Figure5

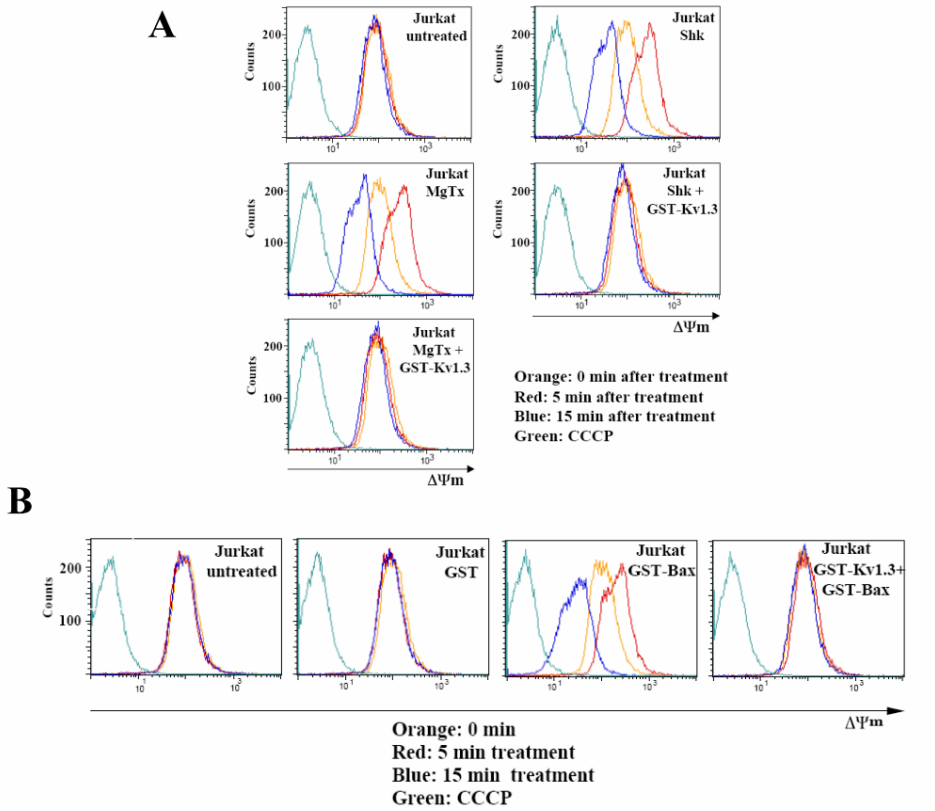
A
Jurkat untreated
Jurkat Shk
Jurkat MgTx
Jurkat Shk + GST-Kv1.3
Jurkat MgTx + GST-Kv1.3
Counts
ΔΨm
Orange: 0 min after treatment
Red: 5 min after treatment
Blue: 15 min after treatment
Green: CCCP
B
Jurkat untreated
Jurkat GST
Jurkat GST-Bax
Jurkat GST-Kv1.3+ GST-Bax
Counts
ΔΨm
Orange: 0 min
Red: 5 min treatment
Blue: 15 min treatment
Green: CCCP
C
Jurkat
unstimulated
GST
GST-Bax
unstimulated + GST-Kv1.3
GST + GST-Kv1.3
GST-Bax + GST-Kv1.3
kDa
19
15
← Cytochrome c (released)
← Cytochrome c (mitochondrial)

Figure6

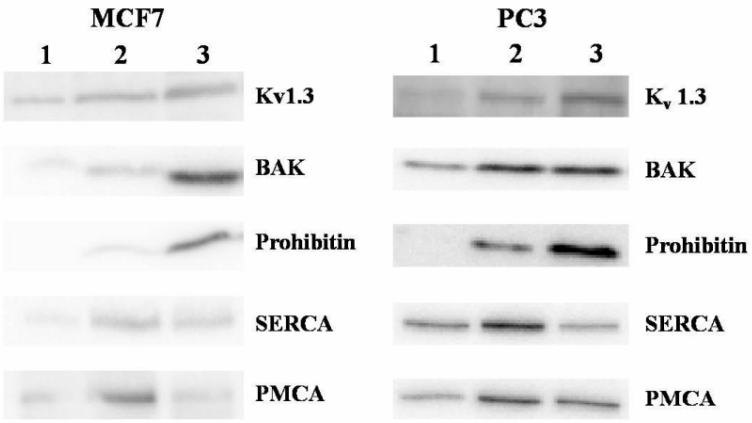
MCF7
1
2
3
Kv1.3
BAK
Prohibitin
SERCA
PMCA
PC3
1
2
3
K_v 1.3
BAK
Prohibitin
SERCA
PMCA

2. Inhibition of mitochondrial Kv1.3 in tumor cell lines

Introduction

Every year new lines of evidence demonstrate that ion channels can be preferential targets for an antitumor action, since channel inhibitors may block tumor growth *in vitro e in vivo*. In particular, plasma membrane potassium channels have been reported to have multiple effects on tumor physiology by their role in regulation of cell volume and calcium fluxes, in the control of membrane potential and of the cell cycle (review: Arcangeli et al., 2009).

In addition to PM channels, also the relevance of their mitochondrial counterparts is growing (see the Introduction to this part of the thesis). Mitochondria, apart from their role in the oxidative phosphorylation, have a key function in the intrinsic apoptotic pathway, mediating cell death in pathological and stress condition via release of pro-apoptotic factors (e.g.: Hengartner, 2000; Green and Kroemer, 2004; Circu and Aw, 2010). The pro-apoptotic Bcl-2 family proteins, in particular Bax and Bak, mediate these apoptotic events, but the exact mechanism is still uncertain. Two recent papers (Szabò et al., 2008, Gulbins et al., 2010 – Chapt. 1) demonstrated that in lymphocytes Bax interacts with and inhibits mtK_V1.3. This interaction strongly facilitates apoptosis in these cell. An essential role is attributed to a Bax lysine residue in position 128. These data have led to a model for the action of mtK_V1.3 during apoptosis (see Fig.1 in the introduction of this section). We have identified this channel in the mitochondria of prostate cancer PC3 and breast cancer MCF7 cell lines (Gulbins et al., 2010 - Chapt. 1) indicating that mtK_V1.3 presence is not limited to lymphocytes. The altered expression level of K_V1.3 found in different cancer cell lines (Arcangeli et al., 2009), the role of mtK_V1.3 in apoptosis and its presence in various cancer cell lines seem a good starting point for the identification of new chemotherapeutic compounds. Here, we performed pharmacological experiments to determine if specific inhibition of mtK_V1.3 may induce apoptosis in the tumor cell lines which express it endogenously.

Materials and methods

Materials and instrumentation. CsH was purchased from Sequoia Research Products while all others compounds were from Sigma unless otherwise specified. All chemicals for buffer preparations were of laboratory grade, obtained from J. T. Baker, Merck, or Sigma.

Cells. Human breast cancer line MCF7 and human prostate cancer line PC3 were grown in Dulbecco's Modified Eagle Medium (DMEM) plus 10 mM HEPES buffer, 10% (v/v) fetal calf serum (Invitrogen), 100 U/mL penicillin G (Sigma), 0.1 mg/mL streptomycin (Sigma), 2 mM glutamine (GIBCO) and 1% nonessential amino acids (100X solution; GIBCO), in a humidified atmosphere of 5% CO_2 at 37 °C. Jurkat T lymphocytes were grown in RPMI-1640 supplemented as above.

Vitality and apoptosis assays. For the evaluation of apoptosis we seeded MCF7 or PC3 cells (both 300.000 cells/well) in 6-well plates. After attachment overnight, cells were treated for 2 or 14 h with the desired drugs (in the example of Fig. 1: Psora-4 10 nM, Margatoxin 20 nM, Tamoxifen 5 μM (as inhibitor of P-glycoprotein (P-gp)) and Staurosporine 1μM in HBSS or DMEM. After treatment, cells were harvested, washed with PBS, resuspended in FACS Buffer (Hepes 10mM; NaCl 135mM, $CaCl_2$ 5mM, pH 7.4) and incubated with Propidium Iodide (1μg/ml) and Annexin V-Fluos (Roche) in the dark at 37°C for 15 min. Samples were then immediately analyzed using a Beckton Dickinson FACScan flow cytometer (BD Biosciences). Data were processed using CellQuest® (BD Biosciences) and WinMDI2.8 (freeware; http://facs.scripps.edu/software.html, by Joe Trotter, the Scripps Institute) software. Essentially the same procedure was followed also for Jurkat cells (300.000 cells/well in 1ml of medium, 6-well plate), except for the overnight attachment period.

For DNA fragmentation assays (Kasibhatla et al., 1998) (treatments of 16 h for Jurkat and 24 h for PC3 cells), after harvesting and washing the cells were resuspended in PBS, an equal volume of 70% ethanol was slowly added under continuous stirring, and the suspension was incubated overnight at 4°C or for 30 min at R.T. After this permeabilization step, during which fragmented DNA is lost, the cells were washed in PBS, resuspended in PBS with RNAse A (20

μg/mL, 1400 units/mL) and incubated for 30 min at R.T. 5 μg/mL of Propidium Iodide were then added and the incubation continued for 20 min on ice in the dark, after which the samples were analyzed as above. Propidium fluorescence intensity is proportional to the amount of (unfragmented) DNA present.

For cell growth/viability tetrazolium reduction (MTT) assays, MCF7 cells (3000 cells/well) were seeded in standard 96-well plates and allowed to grow in DMEM (200 μL) for 24 h. The growth medium was then replaced with medium that contained the desired compounds (from stock solutions in DMSO). The DMSO final concentration was $\leq$ 0.5% in all cases. Four wells were used for each condition. The solution was substituted by a fresh aliquot twice, at intervals of 24 h. At the end of the third 24 h period, the medium was removed, cells were washed with PBS, and 100 μL of PBS containing 10% CellTiter 96® AQUEOUS One solution (Promega) were added into each well. After 1 h of color development at 37°C, absorbance at 490 nm was measured using a Packard Spectra Count 96-well plate reader.

Preparation of mitochondria and cytochrome c release from isolated mitochondria. To isolate mitochondria, $1x10^7$ Jurkat cells or $1x10^6$ MCF7 cells were incubated for 30 min at 4°C in TES buffer (0.3 M sucrose, 10 mM TES at pH 7.4 and 0.5 mM EGTA) and homogenized. Nuclei and unbroken cells were pelleted by centrifugation for 10 min at 600 x g and 4°C. Supernatants were centrifuged for 10 min at 6,000 x g and 4°C. The pellet, which contains mitochondria, was resuspended in incubation buffer (50 mM Pipes-KOH (pH 7.4), 50 mM KCl, 2 mM $MgCl_2$, 2 mM EGTA, 2 mM ATP, 10 mM phosphocreatine, 5 mM succinate, 50 μg/ml creatine kinase and protease inhibitor cocktail (Roche) at the recommended concentration). To assess Cytochrome c release, after a washing step mitochondria were incubated for 30 min on ice in incubation buffer with the desired compounds to allow binding. The temperature was then raised to 37°C to permit release of cytochrome c. The reaction was terminated by addition of 1 vol ice-cold incubation buffer, followed by centrifugation at 14,000 rpm and 4°C for 10 min and separation of the supernatant (cytochrome c released) and pellet (mitochondria). The samples were analyzed by Western blot.

Assessment of cytochrome c release from in situ mitochondria. To evaluate cytochrome c release in cells, Jurkat ($3x10^6$ cells) were treated for 6 or 24 h with the desired drugs (in the example of Fig.5A: probenecid 100μM and CsH 4μM as inhibitors of Pgp, Psora-4 200nM or staurosporine 1μM) in RPMI under standard cell growth conditions. Cells were then pelleted by centrifugation for 10 min at 500 x g. The pellet was resuspended in permeabilization buffer (Mannitol 140mM, Sucrose 46mM, KCl 50mM, KH_2PO_4 1mM, $MgCl_2$ 5mM, Succinate 5mM, EGTA 1mM, Tris pH 7.4 and protease inhibitor cocktail (Roche) at the recommended concentration) and incubated for 10 min on ice with 60ng/μl digitonin. The suspension was then centrifuged for 10 min at 12000 x g and 4°C, and pellet (permeabilized cells) and supernatant (cytochrome C released) were collected and analyzed by Western blot. In other experiments the desired drugs were added together with digitonin (same concentration). In this case incubation was at 22°C for 15min.

Western blotting for Cytochrome c. Samples, dissolved in sample buffer, were allowed to stand for 15 min at R.T., subjected to SDS-PAGE in 10% acrylamide minigels and transferred to a polyvinylidenfluoride (Pall Corporation, Pensacola, FLA, USA) sheet. The primary antibody used was anti-Cytochrome C mouse monoclonal (BD Biosciences cat. n. 556433); the secondary antibody (Calbiochem) was horseradish peroxidase-conjugated and it was used with chemiluminescence detection (Pierce) using film or digital imaging by a Bio-Rad ChemiDoc XRS apparatus.

Results

Cytotoxicity/cytostaticity assays

Using the cell lines in which we had identified the mtKv1.3 (MCF7, PC3 and Jurkat), we verified whether inhibition of the channel induced apoptosis or had a cytostatic effect. Psora-4 (5-(4-Phenylbutoxy)psoralen)) is a membrane permeable specific inhibitor of $K_V1.3$, which it blocks with an EC_{50} of 3 nM (Vennekamp et al., 2004). We used it at 10 or 100 nM by itself or together with inhibitors of MDR efflux pumps (Cyclosporine H between 1 and 4μM or Verapamil 30μM or

Tamoxifen 5μM for P-gp; Probenecid 100μM for MRP1 and MRP2; Chrysin 2.5μM for BCRP). We also used Margatoxin as membrane-impermeable blocker of PM K_V1.3 (Garcia-Calvo et al., 1993) and staurosporine as a positive control for apoptosis induction. Evaluation was carried out using cell counting, annexin/propidium staining, DNA fragmentation assays and MTT assays.

I initially tested for apoptosis induction by the annexin/propidium staining method, using all three cell lines and exposing them to the agents mentioned above for 12 hours (N = 2-3). The results, exemplified for MCF7 cells in Fig.1A, did not provide any evidence supporting an apoptotic effect of the inhibition of mtK_V1.3.

For confirmation, I used also the DNA fragmentation assay. This type of experiment allows one to observe not only apoptosis (an increase of the sub-G1 population), but also variations or blocks in the cell cycle, because it is possible to observe quantitative variations in the portion of cells in the different stages of the cell. Fig 1B shows an experiment with PC3 cells; no effects were visible, except that the positive control (staurosporine) exhibited an increase of the sub-G1 population and variation of cell cycle. Similar results were obtained also with Jurkats (data not shown). For MCF7 cells it was impossible to proceed with this technique, because this cell line has lost caspase-3 and as a consequence apoptotic DNA fragmentation cannot be readily observed (Janicke et al., 1998). For these cells an alternative method to observe cytotoxic/cytostatic effect is the MTT assay. Fig. 2 presents the results of one such experiment. No difference in vitality between the sample with 100 nM Psora-4 plus MDR pumps inhibitors and the one with only the inhibitors was detectable after 72h of treatment.

The results of these various assays were in agreement with those of the microscopic observation of cell cultures, exemplified by the images in Fig. 3 for PC3 cells.

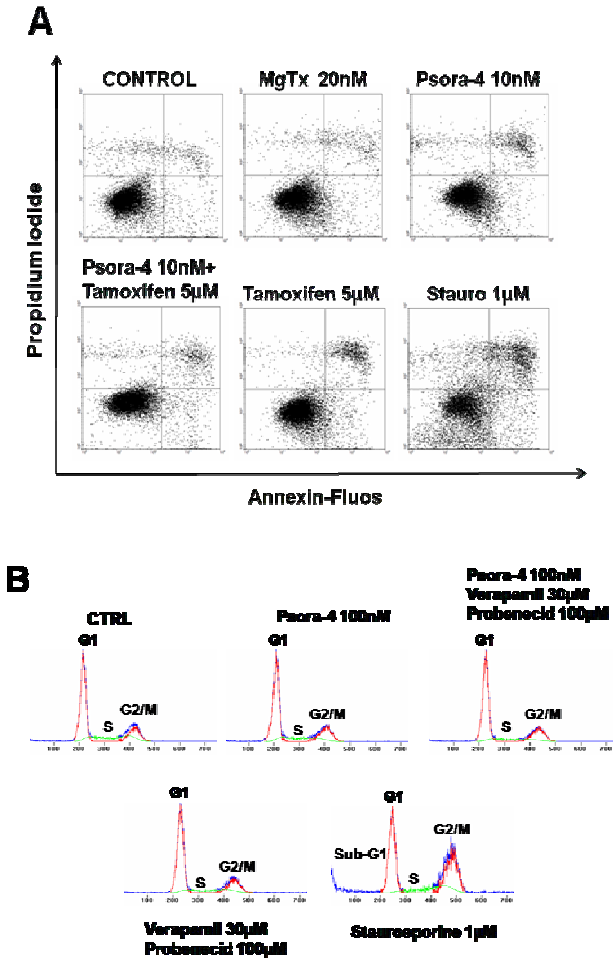

Fig.1 Psora- 4 does not induce cell death or cytostatic effects on MCF7, PC3 and Jurkat cells. A) A representative apoptosis assay using Flow Cytometry (FACS) with MCF7 cells. Cells were incubated in DMEM in the presence of the specified substances for twelve hours, then treated with Propidium and Annexin as described in Materials and Methods. B) A DNA fragmentation assay using FACS with PC3 cells. Cells were incubated in DMEM in the presence of the specified substances for twenty-four hours, then permeabilized and treated with Propidium Iodide as described in Materials and Methods. Peaks labeled G1, S and G2/M correspond to the different phases of the cell cycle. Sub-G1 is fragmented DNA typical of apoptotic cells.

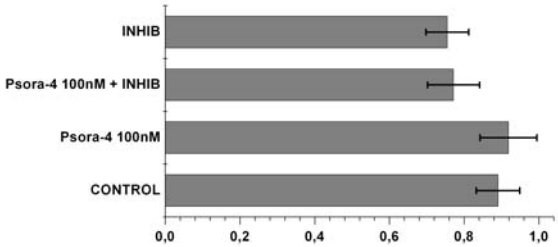

Fig. 2. Effect of Psora-4 and Psora-4 plus MDR pumps inhibitors on the readout of tetrazolium reduction cell proliferation assays. MCF7 cells were allowed to grow for 3 days in the presence of the compounds. The panels show the results of an individual representative experiment. All measurements were performed in quadruplicate. Averages ± s.d. are given. Abbreviations: INHIB: a mix of MDR pump inhibitors: CsH 1µM, Probenecid 100µM and Chrysin 2.5µM.

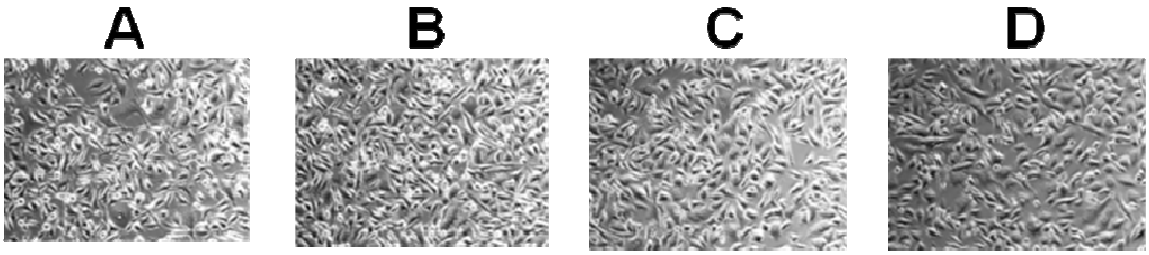

Fig.3. PC3 cell culture images after 48 h incubation with: A: Control; B: Psora-4 100nM; C: Psora-4 100nM + Tamoxifen 5μM + Probenecid 100μM; D: Tamoxifen 5μM + Probenecid 100μM.

Cytochrome c release.

In analogy to what done with CTLL-2/Kv1.3 cells, we tried to observe cytochrome c (cyt c) release upon inhibition of $mtK_V1.3$ in mitochondria isolated from Jurkat and MCF7 cells. Isolated mitochondria were treated with specific channel inhibitors (Psora-4 or Margatoxin) and as positive controls t-Bid 50nM or $CaCl_2$ plus KH_2PO_4 (respectively 3mM (free) and 1mM). Several attempts (N>10 for Jurkat and N=3 for MCF7), did not lead to a demonstration of a release of cyt c caused by the inhibition of $mtK_V1.3$ only. Fig.4 presents an example of these results with Jurkat mitochondria. Please note that t-Bid induces a strong release, absent with Psora-4 or Margatoxin.

We attempted also to observe cyt c release by treating Jurkats with different compounds before or after permeabilization (in both cases N=2, see Materials and Methods for details). As illustrated in Fig.5A-B only the positive controls (staurosporine and t-Bid) produced an evident effect of release.

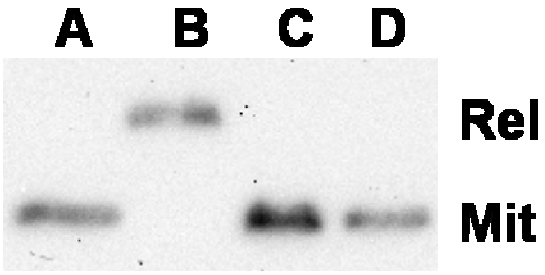

Fig.4. Effects on isolated Jurkat mitochondria. The Kv1.3 inhibitors Psora-4 and Margatoxin did not induce cytochrome c release. Rel: released cytochrome c (supernatant); Mit: mitochondria. A: Control; B: t-Bid 50nM; C: Psora-4 100nM; D: Margatoxin 200nM.

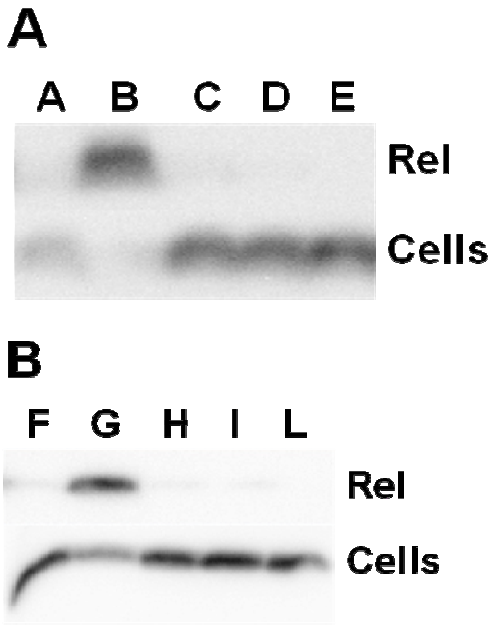

Fig.5. Cytochrome c release in cells. Rel: cytochrome c released; Cells: permeabilized cells. A) Jurkat cells treated for 6 h with compounds and successively permeabilized. A: Control; B: Staurosporine 1μM; C: Psora-4 200nM + Probenecid 100μM + CsH 4μM; D: Psora-4 1μM + Probenecid 100μM + CsH 4μM; E: Probenecid 100μM + CsH 4μM. The presence of MDR pumps inhibitors was meant to prevent the export of Psora-4 from cells. B) Jurkat cell permeabilized and then treated with $K_V1.3$ inhibitors. F: Control; G: t-Bid 250nM; H: Psora-4 10nM; I: Psora-4 100nM; L: Psora-4 200nM.

Discussion

The data presented by Szabò et al. (2008) and Gulbins et al. (2010) (Chapt. 1) show that Bax interacts directly with mt$K_V1.3$ after inserting into the OMM, inhibiting this channel and leading to IMM hyperpolarization, ROS release, a late depolarization and finally to cytochrome c release in Jurkat cells. Our data above, instead, didn't show any release using specific inhibitors of the channel such as Psora-4 or Margatoxin.

This substantial difference can be explained considering the diversity between Bax and the channel inhibitors. The former is widely accepted to form, alone or in cooperation with other components of the OMM, the permeation pathway through which cytochrome c can be discharged to the cytosol. Psora-4 obviously cannot by itself do the same, and we had hypothesised that activation of the MPTP might have the same effect. Several papers have in fact proposed that MPT induction may either be sufficient, or act in a cooperative manner with Bax to allow this phenomenon (recent examples: Kumarswamy and Chandna, 2009; Mullauer et al.,

2009; Petrosillo et al., 2009; Gogvadze et al., 2010). Another possibility was that inhibition of mtK_V1.3 *in situ* might generate ROS in sufficient amounts to initiate a full-fledged apoptotic cascade. So far, neither seems to be the case, but we plan to use, with appropriate controls, higher concentrations. Another possible explanation for the negative results may be the presence of other potassium channels in the inner mitochondrial membrane of our cells. The CTLL2 cells used for most of the experiments by Szabò et al. (2008), do not express endogenous mitochondrial potassium channels. If some, besides mtK_V1.3, were instead present in our cell lines the effect of mtK_V1.3 inhibition may be reduced because of the compensating activity of these other channels. In summary, our study provides no evidence of a possible cytotoxic effect of inhibiting specifically the mtK_V1.3.

3. Intermediate conductance Ca^{2+}-activated potassium channel ($K_{Ca}3.1$) in the inner mitochondrial membrane of human colon cancer cells

Cell Calcium 45 (2009) 509–516

Contents lists available at ScienceDirect

Cell Calcium

journal homepage: www.elsevier.com/locate/ceca

Intermediate conductance Ca^{2+}-activated potassium channel ($K_{Ca}3.1$) in the inner mitochondrial membrane of human colon cancer cells

Umberto De Marchi[a], Nicola Sassi[a], Bernard Fioretti[b], Luigi Catacuzzeno[b], Grazia M. Cereghetti[c], Ildikò Szabò[d], Mario Zoratti[a,e,*]

[a] Department of Biomedical Sciences, University of Padova, Padova, Italy
[b] Department of Cellular and Environmental Biology, University of Perugia, Perugia, Italy
[c] Venetian Institute of Molecular Medicine, Padova, Italy
[d] Department of Biology, University of Padova, Padova, Italy
[e] CNR Institute of Neuroscience, Padova, Italy

ARTICLE INFO

Article history:
Received 19 December 2008
Received in revised form 13 March 2009
Accepted 23 March 2009
Available online 29 April 2009

Keywords:
Mitochondria
Patch–clamp
Inner membrane
IK(Ca)
HCT116

ABSTRACT

Patch–clamping mitoplasts isolated from human colon carcinoma 116 cells has allowed the identification and characterization of the intermediate conductance Ca^{2+}-activated K^+-selective channel $K_{Ca}3.1$, previously studied only in the plasma membrane of various cell types. Its identity has been established by its biophysical and pharmacological properties. Its localisation in the inner membrane of mitochondria is indicated by Western blots of subcellular fractions, by recording of its activity in mitochondria made fluorescent by a mitochondria-targeted fluorescent protein and by the co-presence of channels considered to be markers of the inner membrane. Moderate increases of mitochondrial matrix $[Ca^{2+}]$ will cause mt$K_{Ca}3.1$ opening, thus linking inner membrane K^+ permeability and transmembrane potential to Ca^{2+} signalling.

1. Introduction

The "impermeable" inner mitochondrial membrane of the chemiosmotic hypothesis is now known to be endowed with an array of tightly controlled passive ion diffusion pathways, i.e. channels, several of which remain to be molecularly identified [revs.: 1–5]. The most relevant for this paper are K^+-selective pores. Bioenergetics research has provided evidence for the presence of regulated K^+-permeable channels in the inner mitochondrial membrane (IMM). Garlid's group [6,7] has focused on ATP-inhibited K_{ATP} (whose presence is debated, see, e.g., [8]). Other workers have proposed the presence a H^+ and/or K^+-permeable pore induced by relatively low matrix $[Ca^{2+}]$, possibly representing an early, "narrow" form of the mitochondrial permeability transition (MPT) pore [9–11]. Evidence for K^+-selective transport in plant mitochondria has also been presented [12–14]. Electrophysiological and/or biochemical studies have permitted the observation of K_{ATP} [e.g.: 15,16], *Shaker*-type Kv1.3 [17] and Ca^{2+}-activated big conductance (BK; $K_{Ca}1.1$) [18–20]. Note that these channels are not exclusive to mitochondria. Rather, they are examples of multiple localization of proteins found also in other cellular compartments, chiefly the plasma membrane (PM). Here we report the presence of the intermediate-conductance, Ca^{2+}-activated K^+ channel $K_{Ca}3.1$ (also named IK_{Ca}, KCNN4, SK4, $K_{Ca}4$, Gardos channel) in the inner membrane of mitochondria isolated from the human colon tumor cell line HCT116.

Plasma membrane $K_{Ca}3.1$ [e.g.: 21–26], expressed mainly in blood cells, endothelia and epithelia, forms a K^+-selective channel with a rectifying single channel conductance in the tens-of-pS range. Its activation, mediated by tightly bound calmodulin, takes place at sub-μM cytosolic $[Ca^{2+}]$, and its open probability is not influenced by voltage. Structurally, it adheres to the K_V paradigm, and it consists of a tetramer of subunits with six membrane-spanning helices. It is inhibited by some toxins (charybdotoxin, maurotoxin) and small organic compounds (e.g. clotrimazole,

Abbreviations: BK, big conductance Ca^{2+}-activated K^+-channel ($K_{Ca}1.1$); Clotrimazole, 1-[(2-chlorophenyl)-diphenyl-methyl]imidazole; DC-EBIO, 5,6-dichloro-1-ethyl-1,3-dihydro-2*H*-benzimidazol-2-one; DMEM, Dulbecco's Modified Eagle Medium; ER, endoplasmatic reticulum; HBSS, Hank's Balanced Saline Solution; HCT116, human colon tumor 116; HP, half-PTP; IMM, inner mitochondrial membrane; MPT, mitocondrial permeability transition; PM, plasma membrane; PMCA, plasma membrane Ca^{2+}-ATPase; PTP, permeability transition pore; SK, small conductance Ca^{2+}-activated K^+-channels ($K_{Ca}2.1$-3); TRAM-34, [1-(2-chlorophenyl)diphenyl)methyl]-1*H*-pyrazole; TES, *N*-tris(hydroxymethyl)methyl-2-aminoethanesulfonic acid; SERCA, sarcoplasmic/endoplasmic reticulum Ca^{2+}-ATPase.

* Corresponding author at: CNR Institute of Neuroscience, c/o Department of Biomedical Sciences, Viale Giuseppe Colombo 3, 35121 Padova, Italy.
Tel.: +39 049 8276054; fax: +39 049 8276049.
E-mail address: zoratti@bio.unipd.it (M. Zoratti).

0143-4160/$ – see front matter © 2009 Elsevier Ltd. All rights reserved.
doi:10.1016/j.ceca.2009.03.014

TRAM-34) in the nM range [27,28]. It is the main channel of "naïve" T cells, and it is upregulated during their activation [29]. It is also expressed at high levels and in functionally active form in the plasma membrane of several cancer cell lines, including gliomas [30,31], melanoma [32], prostate [33], pancreas [34], breast [35] and endothelial colon tumor [36] cells. Ca-dependent K^+ channels link cytosolic Ca^{2+} levels to plasma membrane potential, and participate in cellular processes such as progression through the cell cycle, proliferation, differentiation, migration and volume control. $K_{Ca}3.1$ is a component of fluid secretion systems because it acts as the carrier of counterions compensating the charge of excreted chloride [e.g.: 37]. These functions can in turn be regulated: $K_{Ca}3.1$ expression is upregulated by the ERK pathway [30,38] and is repressed by repressor element 1-silencing transcription factor (REST or NRSF) [39]. $K_{Ca}3.1$ knockout mice exhibit however a mild phenotype [40,41], because the lack of $K_{Ca}3.1$ can be compensated by $K_{Ca}2.1$-3 (SK) and $K_{Ca}1.1$ (BK). Defective mast cell activation [42] and intestinal chloride secretion [43] and moderately elevated blood pressure [41] are some reported consequences. On the other hand treatment with clotrimazole or TRAM-34 has been reported to have a cytostatic effect on various cancer lines and to hamper the progression of melanoma [44] or endometrial cancer [45] xenografts. $K_{Ca}3.1$ inhibition may thus coadiuvate chemotherapy approaches.

For none of the cells expressing $K_{Ca}3.1$ the possible existence of an intracellular population of $K_{Ca}3.1$ has been explored. In view of the examples mentioned above, this seemed a possibility worth verifying. We focused on mitochondria because mtKv1.3 has turned out to have an important function in the life cycle of lymphocytes, participating, via interaction with the pro-apoptotic Bax protein, in the apoptotic process [46].

2. Experimental procedures

2.1. Cells and mitochondria

Human colon tumor (HCT116) cells [47] kindly provided by Vogelstein, were grown in Dulbecco's Modified Eagle Medium (DMEM) plus 10 mM HEPES buffer, 10% (v/v) fetal calf serum (Invitrogen), 100 U/mL penicillin G (Sigma), 0.1 mg/mL streptomycin (Sigma), 2 mM glutamine (GIBCO) and 1% nonessential amino acids (100× solution; GIBCO), in a humidified atmosphere of 5% CO_2 at 37 °C. HCT116 mitochondria for patch–clamp experiments were obtained by differential centrifugation as reported in [48]. A further purification was obtained by centrifugation (8500 × *g*, 20 min, 4 °C) on a discontinuous Percoll gradient composed of 60%, 30% and 18% Percoll in TES buffer (300 mM sucrose, 10 mM TES, 0.5 mM EGTA, pH 7.4). The floating material was discarded, and the fraction at the lower interface collected and washed twice by centrifugation at 17,000 × *g* for 5 min. The final pellet was resuspended in TES buffer to form fraction 3 in Fig. 2.

2.2. Western blotting

Samples were dissolved in sample buffer and boiled for 5 min. The same amount of total protein (50 or 100 μg) was loaded into each well and subjected to SDS-PAGE in 12% acrylamide minigels. Proteins were then transferred to a polyvinyidenfluoride (PVDF) (Pall Corporation, Pensacola, FLA) sheet. Primary antibodies used were as follows: anti-hBak NT rabbit polyclonal (Upstate Biotechnology; cat. no. 06-536); anti-prohibitin mouse monoclonal (Lab Vision MS-261-P); anti-SERCA2 ATPase mouse monoclonal (Affinity BioReagents MA3-910); anti-PMCA ATPase mouse monoclonal (Affinity BioReagents MA3-914); anti-$K_{Ca}3.1$ (Alomone Labs APC-064) was raised in rabbit against a peptide comprising amino acids 350–363 of the rat channel. The immunogenic peptide (see Fig. 2) was purchased from Alomone. Secondary antibodies (Calbiochem) were horseradish peroxidase-conjugated and used with chemiluminescence detection (Pierce) using film or digital imaging by a Bio-Rad ChemiDoc XRS apparatus.

2.3. Fluorescent labelling of mitochondria

Twenty-four hour after seeding on 10 cm Petri dishes, HCT116 cells were transfected, using the Lipofectamine 2000 reagent (Invitrogen) following manufacturer instructions, with a plasmid encoding a mitochondrially targeted red fluorescent protein (mtRFP, plasmid pDsRed2-Mito from Clontech, kindly provided by Dr. M. Zaccolo, Padova, Italy; see [49]). Stable transformants were selected using G418 (1 mg/ml) supplemented to the culture medium. After 14-day-selection, single colonies were separated on 96-well plates and colonies expressing mtRFP were detected by the fluorescence signal upon excitation at 568 nm. For microscopy (Fig. 3) cells were sown onto 24 mm round coverslips, allowed to grow for 48 h, and washed with Hank's Balanced Saline Solution (HBSS). The imaging apparatus consisted of a Nikon Eclipse TE300 inverted microscope equipped with a spinning-disk PerkinElmer Ultraview LCI confocal system, a piezoelectric *z*-axis motorized stage (Pifoc, Physik Instrumente, Karlsruhe Germany), and a Orca ER 12-bit CCD camera (Hamamatsu Photonics, Hamamatsu City, Japan).

2.4. Electrophysiology

2.4.1. Patch–clamp on plasma membrane

Perforated whole-cell and cell-attached patch–clamp experiments were performed under voltage-clamp with an EPC-10 amplifier (HEKA), using borosilicate pipettes with a resistance of 3–5 MΩ. Macroscopic and single-channel currents were filtered at 3 and 0.5 kHz and sampled at 100 and 200 μs/point, respectively. Cell capacitance, membrane and access resistance were measured in voltage-clamp configuration using the automatic compensation circuitry of the EPC-10 amplifier. Voltages (*V*) correspond to the difference between the cytoplasmatic and the external side of plasma membrane and currents are positive when flowing from the intracellular to the extracellular side of the membrane. In perforated whole-cell recordings the bathing solution contained (in mM): 106.5 NaCl, 5 KCl, 2 $CaCl_2$, 2 $MgCl_2$, 5 MOPS, 20 glucose, and 30 Na-gluconate at pH 7.25. The pipette solution contained (in mM): 57.5 K_2SO_4, 55 KCl, 5 $MgCl_2$ and 10 MOPS at pH 7.2. Electrical access to the cytoplasm was achieved by adding amphotericin B (200 μM) to the pipette solution. Access resistances in the range of 10–20 MΩ were achieved within 10 min after seal formation. In cell-attached recordings the bathing and pipette solution contained (in mM): 155 KCl, 1 EGTA-K, 2 $CaCl_2$, 1 $MgCl_2$ and 5 MOPS, at pH 7.2 (free Ca^{2+}: 1 mM). All chemicals used were of analytical grade. DMSO, amphotericin B and clotrimazole were from Sigma (St. Louis, MO). Ionomycin and DC-EBIO (5,6-dichloro-1-ethyl-1,3-dihydro-2*H*-benzimidazol-2-one) were from Tocris Cookson (Bristol, UK). TRAM-34, clotrimazole, DC-EBIO, ionomycin and amphotericin B were dissolved in stock solutions with DMSO to concentrations of 20, 20, 100, 1 and 50 mM, respectively. Pharmacological agents were dissolved daily in the appropriate solution at the concentrations stated, and were bath applied by gravity-fed superfusion at a flow rate of 2 ml/min, with complete solution exchange within the recording chamber in ~1 min. The maximal DMSO concentration in the recording solution was always less than 1%.

2.4.2. Patch–clamp on mitoplasts

Experiments were carried out essentially as described in [50]. Mitochondria were added to the experimental medium (150 mM KCl, 0.5 mM $CaCl_2$, 1 mM Pi, 20 mM HEPES, pH 7.4; 1 ml) in the

patch–clamp chamber at R.T. and allowed to swell spontaneously in a Ca^{2+}-dependent process presumably reflecting the occurrence of the mitochondrial permeability transition. Seal configuration was mitochondrion-attached, as confirmed by the polarity of the voltage dependence of the 107 pS channel [51]. Changing the configuration to whole-cell or excised-patch by standard manoeuvres proved unfeasible, leading to loss of the tight seal. Voltage was controlled manually via an Axopatch 200 unit. All data were filtered at 10 kHz and recorded on tape using a VR-10B (Instrutech) adaptor, and recovered later for off-line analysis. Axon pClamp software was used for voltage control and data analysis. For experiments with mitoplasts the voltages reported are those corresponding to the mitochondrial matrix. Inward currents are considered negative and plotted downwards. For selectivity determinations, bath [KCl] was increased by withdrawing an aliquot of the medium and adding back the same volume of a solution having identical composition except for a higher (2 M) [KCl], or the medium was replaced with an identical one containing NaCl instead of KCl. In all cases connection to the Ag/AgCl ground electrode was via a 1 M KCl agar bridge. In pharmacological experiments small volumes of concentrated drug solution in DMSO were added, and the bath contents were thoroughly mixed. DMSO concentration never exceeded 0.5%. In experiments with mitochondria isolated from mtDsRed-expressing cells, the mitochondria were isolated and allowed to deposit and swell in the patch–clamp chamber as above, and washed. The remaining few attached objects were observed with phase contrast optics. After a suitable target (i.e., a round object displaying a "cap" [51]) was selected, optics were switched to fluorescence (excitation wavelength 480–550 nm; emission collected above 590 nm) and the fluorescence of the object was verified (see Fig. 3). In no case ($N = 70$) did a selected object turn out not to be fluorescent. Optics were then turned back to phase contrast in order to establish a tight seal.

3. Results

3.1. Characterization of $K_{Ca}3.1$ in the plasma membrane of HCT116 cells

The expression and properties of plasma membrane $K_{Ca}3.1$ in HCT116 cells had not been previously assessed. Considering its possible oncological relevance [52], we used the perforated whole-cell and cell-attached configurations of the patch–clamp to obtain this information. Because of their voltage independence, stable macroscopic $K_{Ca}3.1$ currents in HCT116 cells were activated by applying the Ca^{2+}-ionophore ionomycin (0.5 μM) plus the $K_{Ca}2/K_{Ca}3$ channel opener DC-EBIO (100 μM) (iono/DC-EBIO). A typical experiment is shown in Fig. 1A. The mean iono/DC-EBIO-activated current density at 0 mV, assessed from five different experiments similar to that shown in Fig. 1A, measured 50 ± 5.4 pA/pF. The reversal potential of the $K_{Ca}3.1$ current, evaluated from voltage ramps from −100 to +100 mV (see inset to Fig. 1A and figure legend for details), was -77.6 ± 0.6 mV ($n = 5$), a value slightly more depolarized than the K^+ equilibrium potential under our recording conditions (−90 mV) in accordance with the significant Na^+ permeability found for $K_{Ca}3.1$ channels [53]. The $K_{Ca}3.1$ current was fully blocked by bath application of 1 μM TRAM-34, and 3 μM clotrimazole (Fig. 1A and inset to Fig. 1B, respectively), both known to be selective inhibitors of the $K_{Ca}3.1$ channel over other Ca^{2+}-activated K^+ channels [28]. The half maximal blocking concentration, IC_{50}, was 49 nM for TRAM-34 ($n = 3$) and 164 nM for clotrimazole ($n = 2$, Fig. 2B), values in agreement with those reported for cloned human $K_{Ca}3.1$ channels [21]. We also recorded unitary $K_{Ca}3.1$ channel activity in cell-attached configuration. In these experiments the membrane potential of HCT116 cells was zeroed by perfusing the cell with a high K^+ solution (see Section 2.4.1). Because of the high density of functional $K_{Ca}3.1$ channels in these cells, we often observed multichannel activity following iono/DC-EBIO perfusion (data not shown). To decrease the multichannel activity, we removed ionomycin from the activating solution. In some instances, under these conditions, we were able to record the activity of a single channel as shown in the inset to Fig. 1C. The *i–V* relationship constructed for this recording displayed a significant inward rectification (typical of IK_{Ca} channels [21]), and a single-channel conductance (assessed by the linear fit of the *i–V* data at negative voltages) of 27 pS. The mean unitary conductance, assessed with the same procedure, from four similar experiments was 24 ± 1 pS ($n = 4$), a value well in agreement with those reported for cloned IK_{Ca} channels [21]. In agreement with previous reports the $K_{Ca}3.1$ channel activity was insensitive to voltage (compare the unitary activity of the channel at −60 and +60 mV in the inset of panel C), and fully blocked by application of 3 μM TRAM-34 (data not shown), a concentration selective for $K_{Ca}3.1$ channels compared to other K^+ channels. All together these data indicate that the $K_{Ca}3.1$ channels are abundantly expressed in the plasma membrane of HCT116 cells, and their biophysical and pharmacological properties agree well with those reported in other studies of cloned and native human $K_{Ca}3.1$ channels.

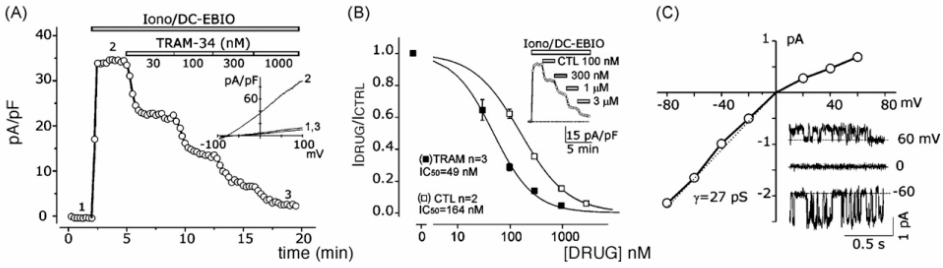

Fig. 1. Functional expression and properties of plasma membrane $K_{Ca}3.1$ currents in HCT116 cells. (A) Time course of the iono/DC-EBIO-activated $K_{Ca}3.1$ current from a HCT116 cell in whole-cell perforated configuration. Each data point represents the $K_{Ca}3.1$ current density assessed at 0 mV from voltage ramp protocols applied every 15 s under the various experimental conditions (control, iono/DC-EBIO application, various TRAM-34 concentrations). *Inset*: Representative current traces in response to voltage ramps from −100 to +100 mV, 800 ms in duration, from a holding potential of 0 mV. Numbers 1, 2, and 3 indicate the corresponding time points in main plot at which the ramps shown were taken. (B) Plot of the fractional residual current vs. TRAM-34 ($n = 3$) and clotrimazole (CTL; $n = 2$) concentration. The solid lines represent the best fit of the experimental data with the Hill relationship: $I_{DRUG}/I_{CTRL} = 1/[1+([DRUG]/IC_{50})^h]$, where I_{DRUG}/I_{CTRL} is the fractional residual current with respect to control at varying drug concentrations, IC_{50} is the half maximal inhibitory concentration of the drug, and h is the Hill coefficient. The best fit parameters for TRAM-34 were: $IC_{50} = 49$ nM, $h = 1.1$, and for clotrimazole were, $IC_{50} = 164$ nM, $h = 0.96$. (C) Unitary *i–V* relationship obtained from a $K_{Ca}3.1$ channel in cell-attached configuration, under symmetrical 155 mM K^+, and in presence of iono/DC-EBIO and 100 nM TRAM-34. The dashed line, representing the linear fit of the data points at negative voltages, gives a slope conductance of 27 pS. *Inset*: Representative unitary $K_{Ca}3.1$ current traces at varying voltages used to construct the *i–V* plot shown in the main panel.

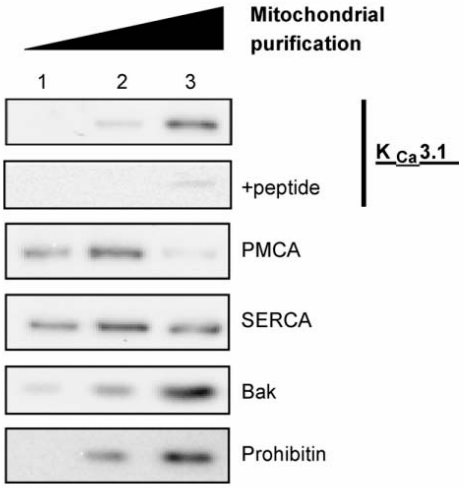

Fig. 2. An anti-$K_{Ca}3.1$ antibody reveals the presence of the channel in HCT116 mitochondria. A representative experiment showing Western blots of the same preparations (1: cell lysate; 2: membrane fraction; 3: Percoll-purified mitochondria). The same amount of proteins (100 μg) was loaded in each lane. Please note that the cell lysate contained also all soluble proteins. The blots presented in the first two rows (control: anti-$K_{Ca}3.1$ Ab; peptide: anti-$K_{Ca}3.1$ Ab preincubated with the immunogenic peptide) were obtained from the same PAGE gel and were blotted and developed together. See text and Section 2 for details. The bands containing mitochondrial markers (29 kDa Bak, 30 kDa Prohibitin) and 55 kDa $K_{Ca}3.1$ are more intense in the Percoll-purified fraction, while those corresponding to contamination markers (110 kDa SERCA, 140 kDa PMCA) decrease. Similar results were obtained in five other experiments.

3.2. Immunochemical detection of $K_{Ca}3.1$ in the mitochondria of HCT116 cells

To investigate the localisation of the channel in mitochondria we used Western blotting of cellular fractions: total cell lysate, a crude membrane fraction isolated by differential centrifugation, and a more highly purified mitochondrial fraction obtained by centrifugation on a discontinuous Percoll gradient (see Section 2). Fig. 2 shows results from one experiment, representative of six similar ones. Compared to the cruder mitochondrial fraction, in the Percoll-purified fraction mitochondrial markers (Bak and Prohibitin) show the expected increase of band intensity, while markers of contamination by ER microsomes (SERCA) and plasma membrane vesicles (PMCA) decrease. The intensity of the 55-kDa band recognized by the anti-$K_{Ca}3.1$ antibody increases, and is nearly abolished by previous exposure of the antibody to the peptide used to raise the antibody itself, thus confirming the specificity of detection.

3.3. Patch–clamp experiments are performed on mitoplasts

Mitoplasts (swollen mitochondria) are easily recognisable and targetable in patch–clamp experiments due to their size, round shape and (often) presence of a "cap", characteristics which distinguish them from the cellular debris also present in the preparation. Nonetheless, to confirm that our electrophysiological experiments were carried out on mitoplasts we transfected HCT116 cells with a plasmid encoding mtDsRed, a mitochondria-targeted red fluorescent protein [49], and isolated mitochondria from these cells. Particles of mitochondrial origin were thus clearly recognizable by fluorescence microscopy (Fig. 3) and could be specifically targeted for patch–clamp recordings in a setup equipped with a fluorescence microscope. Due presumably to photodynamic effects, in these experiments activity by the permeability transition pore (PTP) [54] was prevalent, masking the possible presence of much smaller channels in many experiments. Nonetheless $K_{Ca}3.1$ could be clearly identified and characterized in 7 out of 70 seals established on round fluorescent objects. All the major features of the channel described below, including its pharmacological characteristics and co-localisation with the HP (half-PTP) channel [54], were demonstrated in these experiments (as well as in more numerous experiments performed with only phase-contrast optics, see below), confirming that $K_{Ca}3.1$ is present in HCT116 mitoplasts.

3.4. The mitochondrial $K_{Ca}3.1$ channel

In many experiments mitoplast membrane patches exhibited activity by approx. 0.4 or 1 nS chloride channels, cation-selective channels other than $K_{Ca}3.1$ or no channels at all. $K_{Ca}3.1$ could be confidently identified as such in at least 73 out of a total of 557 seals established on HCT116 mitoplasts. It was always present in one

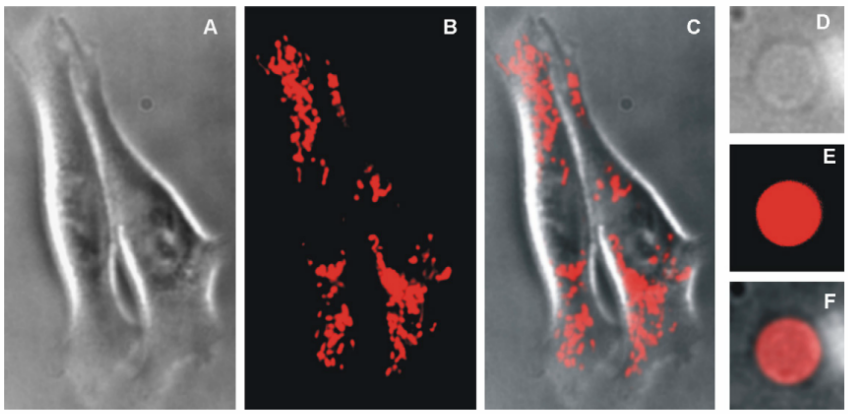

Fig. 3. Red-fluorescent mitochondria in mtDsRed-transfected HCT116 cells. Phase contrast (A and D) and fluorescence microscopy (B and E) images of mtDsRed-transfected HCT116 cells (A and B) and of a mitoplast isolated from such cells deposited on the bottom of a patch–clamp chamber (D and E). Panels C and F show the superposition of the images in A and B and D and E, respectively. The diameter of mitoplasts was 1–3 μm.

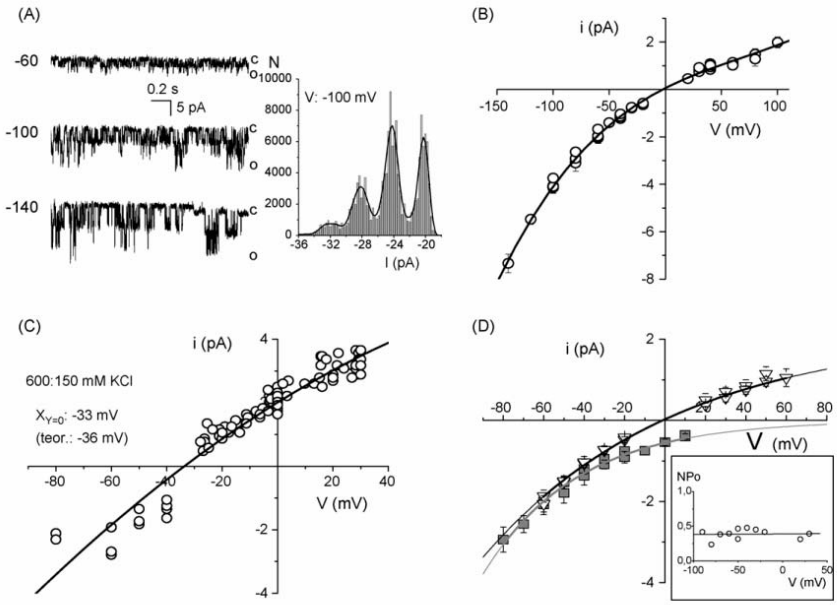

Fig. 4. Biophysical properties of the mtK$_{Ca}$3.1 channel. (A) Single channel activity recorded at the indicated potentials (left) and the corresponding current amplitude histogram (at 100 mV; 30 s.; bin size: 0.244 pA) from a representative experiment in symmetrical 150 mM KCl medium. (B) Single channel conductance. *i–V* plot of mtK$_{Ca}$3.1 single channel amplitude vs. voltage. Symmetrical 150 mM KCl medium. The data are from five independent experiments. (C) K/Cl selectivity. Single channel *i–V* plot from an experiment in a 600 (bath) vs. 150 (pipette) mM KCl gradient. The line drawn is the second-order polynomial best fit of the data points, giving a reversal potential of 33 mV (36 mV calculated by the Goldman equation). (D) K/Na selectivity. *i–V* plots of single-channel current values in symmetrical 150 mM KCl medium (triangles) and in 150 mM KCl (pipette) vs. 150 mM NaCl (bath) (squares). The data points are averages of at least six measurements from two independent experiments (both contributing data under symmetrical and asymmetrical conditions). The curves are the best single-exponential fits of the data. *Inset*: Voltage-dependence. A representative experiment. NPo (*N*: number of active mtK$_{Ca}$3.1 channels; Po: open probability of each channel) was calculated by measuring the average current (leaks subtracted) and dividing the value for the single-channel current amplitude measured in the same experiment. Averages were measured over periods of 10–35 s.

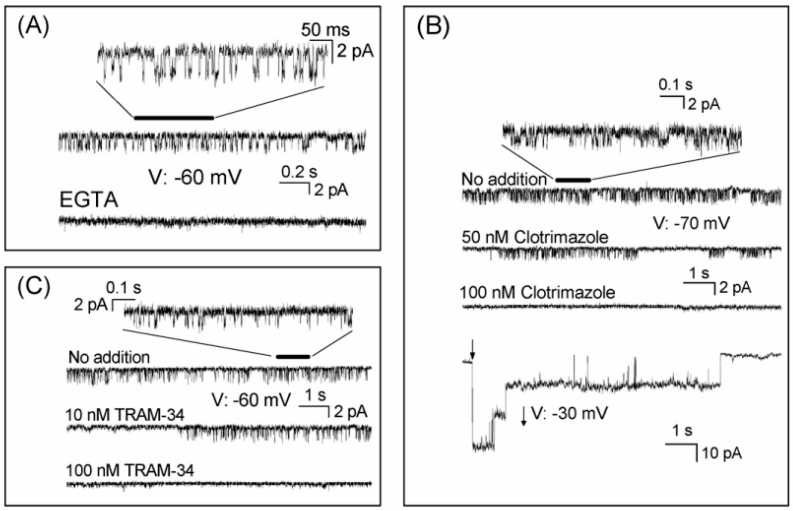

Fig. 5. Pharmacology of mtK$_{Ca}$3.1 and co-localization of mtK$_{Ca}$3.1 and HP channel activity in an mitoplast patch. (A) Channel activity requires Ca^{2+}. The trace showing mtK$_{Ca}$3.1 activity, a segment of which (indicated by the horizontal bar) is amplified at the top, was recorded at the standard [Ca^{2+}] = 0.5 mM on both sides. Addition of 1 mM EGTA to the bath caused the immediate and complete disappearance of the activity (bottom trace). (B) Inhibition by clotrimazole. Exemplary traces recorded under the indicated conditions in standard 150 mM KCl medium. The upmost trace is an expanded segment of the one below it, as indicated. The bottom trace was recorded from the same patch, after K$_{Ca}$3.1 activity had been eliminated and three HP channels had become active. (C) Inhibition by TRAM-34. Exemplary traces recorded under the indicated conditions in standard 150 mM KCl medium. The upmost trace is an expanded segment of the one below it, as indicated.

or a few copies and all recordings were at the single-channel level. Fig. 4 illustrates its biophysical characteristics, which are analogous to those of the plasma membrane $K_{Ca}3.1$: non-ohmic conductance (Fig. 4A and B) ranging from approximately 10 up to 90 pS in the voltage range covered, selectivity for K^+ (Fig. 4C and D) and essentially no dependence of the open probability on voltage (inset in Fig. 4D). Pharmacological properties were also in agreement with those of the plasma membrane channel. Activity was completely abolished by the addition of EGTA or EDTA, indicating Ca^{2+} dependence (Fig. 5A) and by the $K_{Ca}3.1$-specific [26,28, references therein] inhibitors clotrimazole ($n = 4$; Fig. 5B) and TRAM-34 ($n = 8$; Fig. 5C), and inhibition took place in the appropriate tens-of-nM range. Fig. 5B furthermore presents an example of colocalisation of the $K_{Ca}3.1$ channel with the HP channel, a marker of the inner mitochondrial membrane [54]: after $K_{Ca}3.1$ had been inhibited by clotrimazole, three HP channels became active in the same patch. The lowest trace of Fig. 5B shows the characteristic voltage response of the HP channels upon application of voltage (−30 mV, at arrow). $K_{Ca}3.1$-HP colocalisation could be confidently established in at least 13 experiments.

4. Discussion

Our observations lead to the conclusion that the Ca^{2+}-activated, K^+-selective $K_{Ca}3.1$ channel is present in the inner membrane of mitochondria isolated from HCT116 cells. The electrophysiological and pharmacological properties leave no doubt as to the identity of the channel. Both biochemical (Fig. 2) and electrophysiological approaches support the localization in the inner membrane. The biochemical evidence rests on the observed trends, not on absolute values: while even the purest mitochondrial preparations contain small amounts of contaminating membranes, the relevant point is that as this contamination decreases and the relative content of mitochondrial membranes increases, the intensity of the signal produced by the protein of interest ($K_{Ca}3.1$) increases as well.

Concerning the electrophysiological evidence, a first point is that patch–clamp recordings revealing $K_{Ca}3.1$ activity were obtained from mitochondrial membranes, as proven by the experiments with fluorescent mitochondria from transfected cells (Fig. 3). Furthermore, we can confidently conclude that the membrane in question was the inner one. The mitochondria were swollen beyond the point of outer membrane rupture, and activity by inner membrane marker channels, the 107 pS channel first described by Sorgato et al. [51], the PTP and the HP [54], was often observed. It might also be mentioned that while the presence of $K_{Ca}3.1$ in the inner membrane makes good biochemical sense, it is not clear what its role in the outer membrane – freely permeable to ions – would be. A comparison of the *i–V* curves for the plasma membrane (Fig. 1C) and mitochondrial $K_{Ca}3.1$ (Fig. 4) indicates that the latter is inserted into the membrane with its Ca^{2+}-responding domain on the matrix side and its vestibule facing the intermembrane space.

Several membrane proteins are now recognized or proposed to be present in multiple subcellular compartments [e.g. 55–57]. A relevant example, in addition to the K^+ channels already mentioned in the introduction, is provided by the mitochondrial porin VDAC-1, considered to be present also in the ER/SR [e.g. 58,59] and in the PM [60–62]. The mechanisms determining the targeting of multiple-location proteins are known only in part [e.g. 55,57,63–67]; the regulated interaction with partner proteins is probably a major determinant. One other example of particular relevance in this context is that of calmodulin. The Ca^{2+} sensitivity of $K_{Ca}3.1$ is mediated by calmodulin, thus the presence of this channel in the IMM implies the presence of calmodulin in mitochondria. In fact calmodulin has been reported to be present in the matrix as well as in association with the inner membrane and on the cytosolic side of it [68,69], and various mitochondrial CaM-binding proteins have been discovered [70–73].

The $[Ca^{2+}]$ threshold (K_{50}) for half-activation of $K_{Ca}3.1$ is around 300 nM, ideally poised for a prompt response to increases of matrix $[Ca^{2+}]$ above resting levels. By comparison, the open probability of $mtK_{Ca}1.1$, which also depends on voltage, requires at least μM-range Ca^{2+} to be significantly affected in the physiological voltage range [18,74]. The PTP also requires at least μM Ca^{2+} for activation (e.g. [54]). While in the PM Ca^{2+}-activated K^+ channels translate Ca^{2+} rises into PM hyperpolarisation, in mitochondria their opening ought to result in depolarisation, due to K^+ influx driven by the electrochemical gradient of the ion, and in volume increase. $K_{Ca}3.1$ may thus be a component of the mitochondrial system of K^+ "uniporters", involved, together with the counterpart electroneutral exchange system, in the fine regulation of volume, pH and metabolism in these organelles [5,7,75–76]. Indeed, deletion of LETM1, a putative potassium transport pathway, leads to altered mitochondrial morphology [77]. The roles of $mtK_{Ca}3.1$ at the cellular level, if any, may be subtle. Both mitochondrial $K_{Ca}1.1$ [5] and K_{ATP} [e.g.: 5,78–80] have been assigned roles in the protective function elicited by ischemic preconditioning. If indeed $K_{Ca}1.1$ activation protects cardiac muscle from subsequent damage due to MPT onset, there is no evident reason why activation of $K_{Ca}3.1$ (if present in myocytes) should not have the same effect. mtKv1.3 [17] participates in lymphocyte apoptosis via interaction of the vestibule with Bax residue K128, protruding from the outer membrane into the periplasmic space [46]. The vestibule of $K_{Ca}3.1$ is similar to that of Kv1.3 [81,82]. Whether $mtK_{Ca}3.1$ might have a role similar to that of mtKv1.3, perhaps in apoptosis elicited by ER dysfunction and/or mitochondrial Ca^{2+} increase, is currently being investigated.

Acknowledgements

We thank Prof. B. Vogelstein for cells, Dr. M. Zaccolo for the mtDsRed plasmid, Dr. L. Scorrano for access to equipment and Dr. H. Wulff for the generous gift of TRAM-34. This work was financed in part by grants from the Italian Association for Cancer Research (AIRC) to M.Z. and to I.S., by a FIRB grant (Italian Foundation for Basic Research) (M.Z.) and by a grant from the Fondazione Cassa Risparmio Perugia (B.F., L.C.).

References

[1] M. Zoratti, I. Szabó, Electrophysiology of the inner mitochondrial membrane, J. Bioenerg. Biomembr. 26 (1994) 543–553.
[2] H. Ardehali, Cytoprotective channels in mitochondria, J. Bioenerg. Biomembr. 37 (2005) 171–177.
[3] A. Szewczyk, J. Skalska, M. Glab, et al., Mitochondrial potassium channels: from pharmacology to function, Biochim. Biophys. Acta 1757 (2006) 715–720.
[4] B. O'Rourke, Evidence for mitochondrial K^+ channels and their role in cardioprotection, Circ. Res. 94 (2004) 420–432.
[5] B. O'Rourke, Mitochondrial ion channels, Annu. Rev. Physiol. 69 (2007) 19–49.
[6] K.D. Garlid, P. Dos Santos, Z.J. Xie, A.D. Costa, P. Paucek, Mitochondrial potassium transport: the role of the mitochondrial ATP-sensitive K^+-channel in cardiac function and cardioprotection, Biochim. Biophys. Acta 1606 (2003) 1–21.
[7] K.D. Garlid, P. Paucek, Mitochondrial potassium transport: the K^+ cycle, Biochim. Biophys. Acta 1606 (2003) 23–41.
[8] P. Bednarczyk, G.D. Barker, A.P. Halestrap, Determination of the rate of K^+ movement through potassium channels in isolated rat heart and liver mitochondria, Biochim. Biophys. Acta 1777 (2008) 540–548.
[9] K.M. Broekemeier, D.R. Pfeiffer, Inhibition of the mitochondrial permeability transition by cyclosporin A during long time frame experiments: relationship between pore opening and the activity of mitochondrial phospholipases, Biochemistry 34 (1995) 16440–16449.
[10] F. Ichas, J.P. Mazat, From calcium signaling to cell death: two conformations for the mitochondrial permeability transition pore. Switching from low- to high-conductance state, Biochim. Biophys. Acta 1366 (1998) 33–50.
[11] F. Ichas, L.S. Jouaville, J.P. Mazat, Mitochondria are excitable organelles capable of generating and conveying electrical and calcium signals, Cell 89 (1997) 1145–1153.
[12] D. Pastore, M.C. Stoppelli, N. Di Fonzo, S. Passarella, The existence of the K^+ channel in plant mitochondria, J. Biol. Chem. 274 (1999) 26683–26690.

[13] F. Ruy, A.E. Vercesi, P.B. Andrade, M.L. Bianconi, H. Chaimovich, A.J. Kowaltowski, A highly active ATP-insensitive K^+ import pathway in plant mitochondria, J. Bioenerg. Biomembr. 36 (2004) 195–202.
[14] E. Petrussa, V. Casolo, C. Peresson, E. Braidot, A. Vianello, F. Macrì, The K_{ATP}^+ channel is involved in a low-amplitude permeability transition in plant mitochondria, Mitochondrion 3 (2004) 297–307.
[15] I. Inoue, H. Nagase, K. Kishi, T. Higuti, ATP-sensitive K^+ channel in the mitochondrial inner membrane, Nature 352 (1991) 244–247.
[16] Y.A. Dahlem, T.F. Horn, L. Buntinas, T. Gonoi, G. Wolf, D. Siemen, The human mitochondrial KATP channel is modulated by calcium and nitric oxide: a patch–clamp approach, Biochim. Biophys. Acta 1656 (2004) 46–56.
[17] I. Szabò, J. Bock, A. Jekle, et al., A novel potassium channel in lymphocyte mitochondria, J. Biol. Chem. 280 (2005) 12790–12798.
[18] D. Siemen, C. Loupatatzis, J. Borecky, E. Gulbins, F. Lang, Ca^{2+}-activated K^+ channel of the BK-type in the inner mitochondrial membrane of a human glioma cell line, Biochem. Biophys. Res. Commun. 257 (1999) 549–554.
[19] W. Xu, Y. Liu, S. Wang, et al., Cytoprotective role of Ca^{2+}-activated K^+ channels in the cardiac inner mitochondrial membrane, Science 298 (2002) 1029–1033.
[20] J. Skalska, M. Piwońska, E. Wyroba, et al., A novel potassium channel in skeletal muscle mitochondria, Biochim. Biophys. Acta 1777 (2008) 651–659.
[21] T.M. Ishii, C. Silvia, B. Hirschberg, C.T. Bond, J.P. Adelman, J. Maylie, A human intermediate conductance calcium-activated potassium channel, Proc. Natl. Acad. Sci. U.S.A. 94 (1997) 11651–11656.
[22] W.J. Joiner, L.Y. Wang, M.D. Tang, L.K. Kaczmarek, hSK4, a member of a novel subfamily of calcium-activated potassium channels, Proc. Natl. Acad. Sci. U.S.A. 94 (1997) 11013–11018.
[23] N.J. Logsdon, J. Kang, J.A. Togo, E.P. Christian, J. Aiyar, A novel gene, hKCa4, encodes the calcium-activated potassium channel in human T lymphocytes, J. Biol. Chem. 272 (1997) 32723–32726.
[24] M. Stocker, Ca^{2+}-activated K^+ channels: molecular determinants and function of the SK family, Nat. Rev. Neurosci. 5 (2004) 758–770.
[25] P. Pedarzani, M. Stocker, Molecular and cellular basis of small- and intermediate-conductance, calcium-activated potassium channel function in the brain, Cell. Mol. Life Sci. 65 (2008) 3196–3217.
[26] H. Wulff, B.S. Zhorov, K^+-channel modulators for the treatment of neurological disorders and autoimmune diseases, Chem. Rev. 108 (2008) 1744–1773.
[27] K.G. Chandy, H. Wulff, C. Beeton, M. Pennington, G.A. Gutman, M.D. Cahalan, K^+ channels as targets for specific immunomodulation, Trends Pharmacol. Sci. 25 (2004) 280–289.
[28] H. Wulff, A. Kolski-Andreaco, A. Sankaranarayanan, J.M. Sabatier, V. Shakkottai, Modulators of small- and intermediate-conductance calcium-activated potassium channels and their therapeutic indications, Curr. Med. Chem. 14 (2007) 1437–1457.
[29] S. Ghanshani, H. Wulff, M.J. Miller, et al., Up-regulation of the IKCa1 potassium channel during T-cell activation. Molecular mechanism and functional consequences, J. Biol. Chem. 275 (2000) 37137–37149.
[30] B. Fioretti, E. Castigli, M.R. Micheli, et al., Expression and modulation of the intermediate- conductance Ca^{2+}-activated K^+ channel in glioblastoma GL-15 cells, Cell. Physiol. Biochem. 18 (2006) 47–56.
[31] A.K. Weaver, V.C. Bomben, H. Sontheimer, Expression and function of calcium-activated potassium channels in human glioma cells, Glia 54 (2006) 223–233.
[32] R. Meyer, R. Schonherr, O. Gavrilova-Ruch, W. Wohlrab, S.H. Heinemann, Identification of ether a go–go and calcium-activated potassium channels in human melanoma cells, J. Membr. Biol. 171 (1999) 107–115.
[33] A.S. Parihar, M.J. Coghlan, M. Gopalakrishnan, C.C. Shieh, Effects of intermediate-conductance Ca^{2+}-activated K^+ channel modulators on human prostate cancer cell proliferation, Eur. J. Pharmacol. 471 (2003) 157–164.
[34] H. Jäger, T. Dreker, A. Buck, K. Giehl, T. Gress, S. Grissmer, Blockage of intermediate conductance Ca^{2+}-activated channels inhibit human pancreatic cancer cell growth in vitro, Mol. Pharmacol. 65 (2004) 630–638.
[35] H. Ouadid-Ahidouch, A. Ahidouch, K^+-channel expression in human breast cancer cells: involvement in cell cycle regulation and carcinogenesis, J. Membr. Biol. 221 (2007) 1–6.
[36] I. Grgic, I. Eichler, P. Heinau, et al., Selective blockage of the intermediate-conductance Ca^{2+}-activated channel suppresses proliferation of microvascular and macrovascular endothelial cells and angiogenesis in vivo, Arterioscler. Thromb. Vasc. Biol. 25 (2005) 704–709.
[37] M. Albaqumi, S. Srivastava, Z. Li, et al., $K_{Ca}3.1$ potassium channels are critical for cAMP-dependent chloride secretion and cyst growth in autosomal-dominant polycystic kidney disease, Kidney Int. 74 (2008) 740–749.
[38] H. Si, I. Grgic, W.T. Heyken, et al., Mitogenic modulation of Ca^{2+}-activated K^+ channels in proliferating A7r5 vascular smooth muscle cells, Br. J. Pharmacol. 148 (2006) 909–917.
[39] A. Cheong, A.J. Bingham, J. Li, et al., Downregulated REST transcription factor is a switch enabling critical potassium channel expression and cell proliferation, Mol. Cell. 20 (2005) 45–52.
[40] T. Begenisich, T. Nakamoto, C.E. Ovitt, et al., Physiological roles of the intermediate conductance, Ca^{2+}-activated potassium channel Kcnn4, J. Biol. Chem. 279 (2004) 47681–47687.
[41] H. Si, W.T. Heyken, S.E. Wölfle, et al., Impaired endothelium-derived hyperpolarizing factor-mediated dilations and increased blood pressure in mice deficient of the intermediate-conductance Ca^{2+}-activated K^+ channel, Circ. Res. 99 (2006) 537–544.
[42] E. Shumilina, R.S. Lam, F. Wölbing, et al., Blunted IgE-mediated activation of mast cells in mice lacking the Ca^{2+}-activated K^+-channel K(Ca)3.1, J. Immunol. 180 (2008) 8040–8047.
[43] C.A. Flores, J.E. Melvin, C.D. Figueroa, F.V. Sepúlveda, Abolition of Ca^{2+}-mediated intestinal anion secretion and increased stool dehydration in mice lacking the intermediate conductance Ca^{2+}-dependent K^+ channel Kcnn4, J. Physiol. 583 (2007) 705–717.
[44] L.R. Benzaquen, C. Brugnara, H.R. Byers, S. Gatton-Celli, J.A. Halperin, Clotrimazole inhibits cell proliferation in vitro and in vivo, Nat. Med. 1 (1995) 534–540.
[45] Z.H. Wang, B. Shen, H.L. Yao, et al., Blockage of intermediate-conductance-Ca^{2+}-activated K^+-channels inhibits progression of human endometrial cancer, Oncogene 26 (2007) 5107–5114.
[46] I. Szabò, J. Bock, H. Grassmè, et al., Mitochondrial potassium channel Kv1.3 mediates Bax-induced apoptosis in lymphocytes, Proc. Natl. Acad. Sci. U.S.A. 105 (2008) 14861–14866.
[47] L. Zhang, J. Yu, B.H. Park, K.W. Kinzler, B. Vogelstein, Role of BAX in the apoptotic response to anticancer agents, Science 290 (2000) 989–992.
[48] U. De Marchi, S. Campello, I. Szabò, F. Tombola, J.C. Martinou, M. Zoratti, Bax does not directly participate in the Ca^{2+}-induced permeability transition of isolated mitochondria, J. Biol. Chem. 279 (2004) 37415–37422.
[49] R.E. Campbell, O. Tour, A.E. Palmer, P.A. Steinbach, G.S. Baird, D.A. Zacharias, R.Y. Tsien, A monomeric red fluorescent protein, Proc. Natl. Acad. Sci. U.S.A. 99 (2002) 7877–7882.
[50] U. De Marchi, E. Basso, I. Szabò, M. Zoratti, Electrophysiological characterization of the Cyclophilin D-deleted mitochondrial permeability transition pore, Mol. Membr. Biol. 23 (2006) 521–530.
[51] M.C. Sorgato, B.U. Keller, W. Stühmer, Patch–clamping of the inner mitochondrial membrane reveals a voltage-dependent ion channel, Nature 330 (1987) 498–500.
[52] E.L. Lee, Y. Hasegawa, T. Shimizu, Y. Okada, IK1 channel activity contributes to cisplatin sensitivity of human epidermoid cancer cells, Am. J. Physiol. Cell Physiol. 294 (2008) C1398–C1406.
[53] N. Shin, H. Soh, S. Chang, D.H. Kim, C.S. Park, Sodium permeability of a cloned small-conductance calcium-activated potassium channel, Biophys. J. 89 (2005) 3111–3119.
[54] U. De Marchi, I. Szabò, G.M. Cereghetti, P. Hoxha, W.J. Craigen, M. Zoratti, A maxi-chloride channel in the inner membrane of mammalian mitochondria, Biochim. Biophys. Acta 1777 (2008) 1438–1448.
[55] S. Karniely, O. Pines, Single translation-dual destination: mechanisms of dual protein targeting in eukaryotes, EMBO Rep. 6 (2005) 420–425.
[56] N. Regev-Rudzki, O. Pines, Eclipsed distribution: a phenomenon of dual targeting of protein and its significance, Bioessays 29 (2007) 772–782.
[57] M. Dinur-Mills, M. Tal, O. Pines, Dual targeted mitochondrial proteins are characterized by lower MTS parameters and total net charge, PLoS ONE 3 (2008) e2161.
[58] L. Jürgens, J. Kleineke, D. Brdiczka, F.P. Thinnes, N. Hilschmann, Localization of type-1 porin channel (VDAC) in the sarcoplasmatic reticulum, Biol. Chem. 376 (1995) 685–689.
[59] V. Shoshan-Barmatz, A. Israelson, The voltage-dependent anion channel in endoplasmic/sarcoplasmic reticulum: characterization, modulation and possible function, J. Membr. Biol. 204 (2005) 57–66.
[60] R. Dermietzel, T.K. Hwang, R. Buettner, et al., Cloning and in situ localization of a brain-derived porin that constitutes a large-conductance anion channel in astrocytic plasma membranes, Proc. Natl. Acad. Sci. U.S.A. 91 (1994) 499–503.
[61] G. Bàthori, I. Parolini, F. Tombola, et al., Porin is present in the plasma membrane where it is concentrated in caveolae and caveolae-related domains, J. Biol. Chem. 274 (1999) 29607–29612.
[62] M.A. Baker, D.J. Lane, J.D. Ly, V. De Pinto, A. Lawen, VDAC1 is a transplasma membrane NADH-ferricyanide reductase, J. Biol. Chem. 279 (2003) 4811–4819.
[63] E. Sass, S. Karniely, O. Pines, Folding of fumarase during mitochondrial import determines its dual targeting in yeast, J. Biol. Chem. 278 (2003) 45109–45116.
[64] M. Köttgen, T. Benzing, T. Simmen, et al., Trafficking of TRPP2 by PACS proteins represents a novel mechanism of ion channel regulation, EMBO J. 24 (2005) 705–716.
[65] M. Köttgen, G. Walz, Subcellular localization and trafficking of polycystins, Pflugers Arch. 451 (2005) 286–293.
[66] L. Shlevin, N. Regev-Rudzki, S. Karniely, O. Pines, Location-specific depletion of a dual-localized protein, Traffic 8 (2007) 169–176.
[67] N. Regev-Rudzki, O. Yogev, O. Pines, The mitochondrial targeting sequence tilts the balance between mitochondrial and cytosolic dual localization, J. Cell Sci. 121 (2008) 2423–2431.
[68] O. Hatase, M. Tokuda, T. Itano, H. Matsui, A. Doi, Purification and characterization of calmodulin from rat liver mitochondria, Biochem. Biophys. Res. Commun. 104 (1982) 673–679.
[69] O. Hatase, A. Doi, T. Itano, H. Matsui, Y. Ohmura, A direct evidence of the localization of mitochondrial calmodulin, Biochem. Biophys. Res. Commun. 132 (1985) 63–66.
[70] R.L. Pardue, M.A. Kaetzel, S.H. Hahn, B.R. Brinkley, J.R. Dedman, The identification of calmodulin-binding sites on mitochondria in cultured 3T3 cells, Cell 23 (1981) 533–542.
[71] O. Hatase, M. Tokuda, R.K. Sharma, J.H. Wang, D.E. Green, Purification and characterization of the heat-stable calmodulin-binding protein from the matrix of bovine heart mitochondria, Biochem. Biophys. Res. Commun. 113 (1983) 633–637.
[72] P. Gazzotti, M. Gloor, E. Carafoli, Calmodulin binding proteins in rat liver mitochondria, Biochem. Biophys. Res. Commun. 119 (1984) 343–351.
[73] B. Moreau, C. Nelson, A.B. Parekh, Biphasic regulation of mitochondrial Ca^{2+} uptake by cytosolic Ca^{2+} concentration, Curr. Biol. 16 (2006) 1672–1677.

[74] X.P. Gu, D. Siemen, S. Parvez, Y. Cheng, J. Xue, D. Zhou, X. Sun, E.A. Jonas, G.G. Haddad, Hypoxia increases BK channel activity in the inner mitochondrial membrane, Biochem. Biophys. Res. Commun. 358 (2007) 311–316.
[75] A.P. Halestrap, The regulation of the matrix volume of mammalian mitochondria in vivo and in vitro and its role in the control of mitochondrial metabolism, Biochim. Biophys. Acta 973 (1989) 355–382.
[76] P. Bernardi, Mitochondrial transport of cations: channels, exchangers, and permeability transition, Physiol. Rev. 79 (1999) 1127–1155.
[77] K.S. Dimmer, F. Navoni, A. Casarin, et al., LETM1, deleted in Wolf-Hirschhorn syndrome is required for normal mitochondrial morphology and cellular viability, Hum. Mol. Genet. 17 (2008) 201–214.
[78] H. Ardehali, B. O'Rourke, Mitochondrial K(ATP) channels in cell survival and death, J. Mol. Cell. Cardiol. 39 (2005) 7–16.
[79] A.D. Costa, K.D. Garlid, Intramitochondrial signaling - interactions among mitoKATP, PKCε, ROS, and MPT, Am. J. Physiol. Heart Circ. Physiol. 295 (2008) H874–H882.
[80] C.L. Quinlan, A.D. Costa, C.L. Costa, S.V. Pierre, P. Dos Santos, K.D. Garlid, Conditioning the heart induces formation of signalosomes that interact with mitochondria to open MitoKATP, Am. J. Physiol. Heart Circ. Physiol. 295 (2008) H953–H961.
[81] H. Rauer, M. Pennington, M. Cahalan, K.G. Chandy, Structural conservation of the pores of calcium-activated and voltage-gated potassium channels determined by a sea anemone toxin, J. Biol. Chem. 274 (1999) 21885–21892.
[82] H. Rauer, M.D. Lanigan, M.W. Pennington, et al., Structure-guided transformation of charybdotoxin yields an analog that selectively targets Ca^{2+}-activated over voltage-gated K^+ channels, J. Biol. Chem. 275 (2000) 1201–1208.

4. An investigation of the occurrence and properties of the mitochondrial intermediate-conductance Ca^{2+}-activated K^+ channel $mtK_{Ca}3.1$

ARTICLE IN PRESS

BBABIO-46379; No. of pages: 8; 4C: 3, 4, 5

Biochimica et Biophysica Acta xxx (2010) xxx–xxx

Contents lists available at ScienceDirect

Biochimica et Biophysica Acta

journal homepage: www.elsevier.com/locate/bbabio

An investigation of the occurrence and properties of the mitochondrial intermediate-conductance Ca^{2+}-activated K^+ channel $mtK_{Ca}3.1$

Nicola Sassi [a], Umberto De Marchi [a], Bernard Fioretti [b], Lucia Biasutto [a], Erich Gulbins [c], Fabio Franciolini [b], Ildikò Szabò [d], Mario Zoratti [a,e,*]

[a] Department of Experimental Biomedical Sciences, University of Padova, Italy
[b] Department of Cellular and Environmental Biology, University of Perugia, Italy
[c] Department of Molecular Biology, University of Duisburg-Essen, Germany
[d] Department of Biology, University of Padova, Italy
[e] CNR Institute of Neuroscience, Padova, Italy

ARTICLE INFO

Article history:
Received 11 November 2009
Received in revised form 15 December 2009
Accepted 19 December 2009
Available online xxxx

Keywords:
Inner mitochondrial membrane
IK(Ca)
HeLa cells
Patch-clamp
Calcium
TRAM-34

ABSTRACT

The mitochondrial intermediate-conductance Ca^{2+}-activated K^+ channel $mtK_{Ca}3.1$ has recently been discovered in the HCT116 colon tumor-derived cell line, which expresses relatively high levels of this protein also in the plasma membrane. Electrophysiological recordings revealed that the channel can exhibit different conductance states and kinetic modes, which we tentatively ascribe to post-translational modifications. To verify whether the localization of this channel in mitochondria might be a peculiarity of these cells or a more widespread feature we have checked for the presence of $mtK_{Ca}3.1$ in a few other cell lines using biochemical and electrophysiological approaches. It turned out to be present at least in some of the cells investigated. Functional assays explored the possibility that $mtK_{Ca}3.1$ might be involved in cell proliferation or play a role similar to that of the *Shaker*-type $K_V1.3$ channel in lymphocytes, which interacts with outer mitochondrial membrane-inserted Bax thereby promoting apoptosis (Szabò, I. et al., Proc. Natl. Acad Sci. USA 105 (2008) 14861–14866). A specific $K_{Ca}3.1$ inhibitor however did not have any detectable effect on cell proliferation or death.

1. Introduction

Over the past fifteen years or so the operational concept of monovalent ion "leaks" through the inner mitochondrial membrane (IMM) has been replaced by firm evidence for the presence of a multi-component, regulated transport machinery for both cations and anions [1–6]. K^+ is the major intracellular cation, and a relevant mitochondrial K^+ cycle consisting of electrophoretic, channel- and "leak"-mediated influx, and electroneutral efflux via K^+/H^+ exchange is in place. The K^+-selective pores reported to be present in the IMM so far are five, all of them mitochondrial counterparts of channels known to be present in the cellular membrane: mtK_{ATP} [3,7–9], whose presence in mitochondria is still debated (for a recent discussion see [5]), *Shaker*-type $K_V1.3$ [10–12], twin-pore TASK-3 [13], and two (out of the three known) types of Ca^{2+}-activated K^+ channels: $K_{Ca}1.1$ (BK_{Ca}) and $K_{Ca}3.1$ (IK_{Ca}) [14–20].

The Ca^{2+}-activated, high-conductance $mtBK_{Ca}$ ($K_{Ca}1.1$) was first observed in mitoplasts from a glioma cell line [14], and it has been found also in the IMM of cardiomyocytes [15] and in skeletal muscle [16], liver [17] and brain [18] mitochondria. Its activity has furthermore recently been observed in bilayer experiments with IMM preparations from potato mitochondria [19]. Recently, our group has characterised the intermediate-conductance $K_{Ca}3.1$ in the IMM of HCT116 cells [20]. This paper reports further progress in the study of this latter channel.

Abbreviations: BK_{Ca}, big conductance Ca^{2+}-activated K^+-channel ($K_{Ca}1.1$); Clotrimazole, 1-[(2-chlorophenyl)-diphenyl-methyl]imidazole; CsA, Cyclosporin A; DC-EBIO, 5,6-dichloro-1-ethyl-1,3-dihydro-2*H*-benzimidazol-2-one; DMEM, Dulbecco's modified Eagle medium; ER, endoplasmatic reticulum; GST, glutathione-S-transferase; HBSS, Hank's balanced saline solution; HCT116, human colon tumor 116; Hepes, 4-(2-hydroxyethyl)-1-piperazineethanesulfonic acid; IK_{Ca}, intermediate-conductance Ca^{2+}-activated K^+ channel ($K_{Ca}3.1$); IMM, inner mitochondrial membrane; I/R, ischemia/reperfusion; K_{ATP}, ATP-sensitive K^+ channel; MAM, mitochondria-associated membranes; MDR, multiple drug resistance; MEF, mouse embryonic fibroblast; MgTx, margatoxin; MPTP, mitochondrial permeability transition pore; MTT, 3-(4,5-Dimethylthiazol-2-yl)-2,5-diphenyltetrazolium bromide; OMM, outer mitochondrial membrane; PACS, phosphofurin acidic cluster sorting; PBS, phosphate buffered saline; PKA, protein kinase A; PKC, protein kinase C; PM, plasma membrane; PMCA, plasma membrane Ca^{2+}-ATPase; RISK, reperfusion injury salvage kinases; RLM, rat liver mitochondria; ROS, reactive oxygen species; SERCA, sarcoplasmic/endoplasmic reticulum Ca^{2+}-ATPase; ShK, stichodactyla toxin; TASK-3, TWIK-related acid-sensitive K^+ channel ($K_{2P}9.1$); TRAM-34, [1-(2-chlorophenyl)diphenyl]methyl]-1*H*-pyrazole; TES, *N*-tris(hydroxymethyl)methyl-2-aminoethanesulfonic acid

* Corresponding author. CNR Institute of Neuroscience, c/o Dept. of Biomedical Sciences, Viale G. Colombo 3, 35121 Padova, Italy. Tel.: +39 0498276054; fax: +39 0498276049.
E-mail address: zoratti@bio.unipd.it (M. Zoratti).

0005-2728/$ – see front matter © 2009 Elsevier B.V. All rights reserved.
doi:10.1016/j.bbabio.2009.12.015

Please cite this article as: N. Sassi, et al., An investigation of the occurrence and properties of the mitochondrial intermediate-conductance Ca^{2+}-activated K^+ channel $mtK_{Ca}3.1$, Biochim. Biophys. Acta (2010), doi:10.1016/j.bbabio.2009.12.015

Given the important and nearly ubiquitous role of Ca^{2+} in cellular signalling, it is not surprising that cells should have a variety of Ca^{2+}-activated K^+ channels. Besides $K_{Ca}1.1$ (reviews: [21,22]) and $K_{Ca}3.1$ (rev.: [22–24]), these include the $K_{Ca}2$ family of three members, also known as SK_{Ca} because of their lower conductance (rev.: [25]). Two major functions of these channels are to link cytoplasmic Ca^{2+} levels and PM potential – a negative feedback mechanism in excitable cells – and to provide a Ca^{2+}-dependent K^+ permeation pathway, important in secretory epithelia.

$K_{Ca}1.1$ (also called Slo, Slo1, and BK or maxi K channel due to its large conductance of about 260 pS) forms tetrameric complexes composed of four ion-conducting α subunits, each with 7 transmembrane segments and an intracellular domain which acts as Ca^{2+} sensor, and four regulatory β subunits (four variants of which exist). Besides Ca^{2+}, it is modulated by voltage and mechanical stress. It is expressed by a wide variety of cells, including neurons and myocytes, and has pleiotropic functions. It can respond to transient Ca^{2+} increases ("sparks") originated by opening of PM Ca^{2+} channels or sarcoplasmic reticulum ryanodine receptors, and it has been observed to form clusters optimally positioned for such local responses, for which it seems to have been particularly designed by evolution since it responds to $[Ca^{2+}]$ in the μM range.

$K_{Ca}2.1/2/3$ (SK) differs in most respects, exhibiting low single-channel conductances (2–10 pS), insensitivity to voltage, cooperative activation by Ca^{2+} in the 0.3–0.7 μM range through tightly associated calmodulin, and voltage-dependent block by intracellular cations resulting in inward rectification [26]. These channels are subject to regulation by phosphorylation/dephosphorylation events [27], and heterotetramers can form. They are expressed in the nervous system (where they can regulate the firing pattern of neurons) and in various other organs, including heart, liver and muscle, and cell types – such as endothelial cells and lymphocytes – where they often share their functions with $K_{Ca}3.1$. Like the other members of the family, they can co-localize with specific Ca^{2+} sources in a cell type-specific manner.

$K_{Ca}3.1$ (SK4, Gardos channel, IK1, $IK_{Ca}1$, Kcnn4) is closely related to $K_{Ca}2$ and is not as ubiquitous as $K_{Ca}1.1$, but it is nonetheless widespread, being present in, e.g., erythrocytes, lymphocytes, liver and pancreas, but not in excitable cells. Thus, the presence of $K_{Ca}3.1$ in cardiomyocytes has not been reported, although the channel is expressed by vascular smooth muscle, endothelial and blood cells [22] and cardiac fibroblasts [28] and is therefore definitely present in the heart as a whole. It is highly expressed in a variety of cancer cell lines, including prostate PC-3 [29], breast MCF-7 [30] and glial GL-15 [31] lines, and it is thus considered a possible target for anti-cancer intervention [24]. Like the other Ca^{2+}-dependent K^+ channels, it functions in several physiological processes. It has been shown, for example, that $K_{Ca}2$ and $K_{Ca}3.1$ are important for agonist-evoked NO synthesis in vascular endothelial cells, vasorelaxation, and vascular smooth muscle cell (VSMC) proliferation and migration (and thus in atherosclerosis) [32–34]. $K_{Ca}3.1$ plays a major role in colonic salt secretion [35,36]. The channel has a non-ohmic single-channel conductance of 10–90 pS, is voltage-insensitive and responds to $[Ca^{2+}]$ in the sub-μM range, again due to a calmodulin molecule tightly associated to each monomeric unit.

The functions of the mitochondrial K^+ cycle have been identified as the control of matrix volume and the regulation of ROS production [2,3,37–39]. The former, a widely accepted notion, is in turn important for the regulation of metabolic processes and the optimisation of bioenergetic performance [40–42]. The latter, a more controversial issue [4,6,43–48], is considered to impact on cell-wide signalling and cell fate, and to explain the protection afforded by administration of K^+ channel openers against I/R damage, thought to involve activation of the RISK salvage pathway and downstream inhibition of the mitochondrial permeability transition [49–52]. Enhanced ROS generation appears to depend on the development of an inward K^+ current across the mitochondrial membrane, since it is also induced by the ionophore valinomycin [53,54] and by the viral protein p13, which causes K^+ influx [55]. In fact, similar effects are reportedly produced by activation of either mtK_{ATP} or $mtBK_{Ca}$, and Ca^{2+}-sensitive K^+ channels may constitute one of the links between mitochondrial Ca^{2+} handling and ROS generation [56].

Contrary to the cell protecting role assigned to mtK_{ATP} and $mtBK_{Ca}$, $mtK_V1.3$ promotes apoptosis [11]. As recapitulated in the paper by Gulbins et al. in this issue [12], in lymphocytes the pro-apoptotic BH3-only protein Bax, after incorporating into the OMM, interacts with the vestibule of IMM $K_V1.3$ channels, in a manner reminiscent of the mode of action of channel-blocking peptide toxins such as MgTx and ShK. This leads, again, to the production of ROS which in this case favour the detachment and release of cytochrome c. In principle, $mtK_{Ca}3.1$ may act either way: it is expected to open (before $K_{Ca}1.1$ because of its higher affinity for Ca^{2+}) as matrix Ca^{2+} increases, thus perhaps contributing to ROS production and eventually to MPTP inhibition, but an interaction of its periplasmic domain with Bax imbedded in the OMM was also a possibility, which we have verified.

2. Materials and methods

2.1. Materials, cells and mitochondria

Ionomycin and DC-EBIO (5,6-dichloro-1-ethyl-1,3-dihydro-2*H*-benzimidazol-2-one) were from Tocris Cookson (Bristol, UK). Cyclosporin A was from LD Labs (Woburn, MA, USA), Annexin V-Fluos was from Roche (Milan), charybdotoxin was from Alomone Labs (Jerusalem, Israel). All other reagents and materials were from Sigma (Milan) unless specified.

Cells were grown in Dulbecco's modified Eagle medium (DMEM) plus 10 mM HEPES buffer, 10% (v/v) fetal calf serum (Invitrogen), 100 U/mL penicillin G, 0.1 mg/mL streptomycin, 2 mM glutamine (GIBCO) and 1% nonessential amino acids (100× solution; GIBCO), in a humidified atmosphere of 5% CO_2 at 37 °C. mtDsRed-transfected HeLa cells were obtained as already described for HCT116 cells [20]. Mitochondria for patch-clamp experiments were obtained by differential centrifugation [57]. For Western blotting a further purification was obtained by centrifugation (8500 *g*, 10 min, 4 °C) on a discontinuous Percoll gradient composed of 60, 30 and 18% Percoll in TES buffer (300 mM sucrose, 10 mM TES, 0.5 mM EGTA, pH 7.4). The floating material was discarded, and the fraction at the lower interface collected and washed three times by centrifugation at 17,000 *g* for 5 min. The final pellet was resuspended in TES buffer to form fraction 3 in Fig. 1.

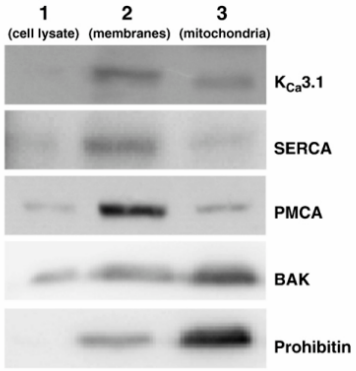

Fig. 1. $K_{Ca}3.1$ is not abundant in C-26 mitochondria. A representative experiment showing Western blots of the same preparations (1: cell lysate; 2: membrane-enriched fraction; 3: Percoll-purified mitochondria). The same amount of proteins (50 μg) was loaded in each lane. The blots on each horizontal line were obtained from the same PAGE gel and were blotted and developed together. The bands containing mitochondrial markers (29 kDa Bak, 30 kDa prohibitin) are more intense in the Percoll-purified fraction, while those corresponding to contamination markers (110 kDa SERCA, 140 kDa PMCA) and to $K_{Ca}3.1$ (55 kDa) decrease. Similar results were obtained in 2 other experiments.

Please cite this article as: N. Sassi, et al., An investigation of the occurrence and properties of the mitochondrial intermediate-conductance Ca^{2+}-activated K^+ channel $mtK_{Ca}3.1$, Biochim. Biophys. Acta (2010), doi:10.1016/j.bbabio.2009.12.015

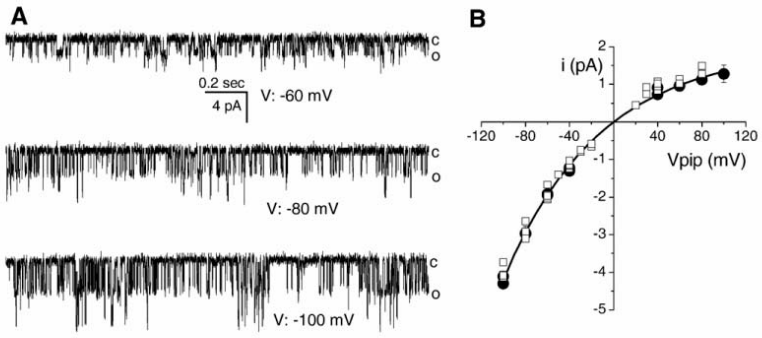

Fig. 2. mtK$_{Ca}$3.1 in HeLa mitochondria. A) Exemplary current records at the indicated voltages, in standard symmetrical 150 mM KCl medium. B) i–V plot. ●: averaged single-channel amplitude data ($N = 6$ to 13) from the experiment in A), fitted with an exponential. Error bars indicate standard deviations. □: analogous data from 5 separate experiments on HCT116 mitoplasts, under the same conditions (error bars have been omitted for clarity).

2.2. Western blotting

Samples, dissolved in sample buffer, allowed to stand for 15 min at R.T. and boiled for 5 min, were subjected to SDS-PAGE in 10% acrylamide minigels and transferred to a polyvinyldifluoride (Pall Corporation, Pensacola, FLA, USA) sheet. Primary antibodies used were: anti-Bak NT rabbit polyclonal (Upstate Biotechnology; cat. n. 06-536); anti-prohibitin mouse monoclonal (Lab Vision MS-261-P); anti-SERCA-2 ATPase mouse monoclonal (Affinity BioReagents MA3-910); anti-PMCA ATPase mouse monoclonal (Affinity BioReagents MA3-914); polyclonal anti-K$_{Ca}$3.1 (Alomone Labs APC-064) was raised in rabbit against a peptide comprising aa 350–363 of the rat channel. The immunogenic peptide was purchased from Alomone. Secondary antibodies (Calbiochem) were horseradish peroxidase-conjugated and used with chemiluminescence detection (Pierce) using film or digital imaging by a Bio-Rad ChemiDoc XRS apparatus.

2.3. Recombinant proteins

hBax(ΔC) (amino acids 1–170) and hBclxL were cloned into pGEX-3X as GST fusion proteins, expressed in BL21A1 and purified from bacterial lysates using glutathione-Sepharose [11,12].

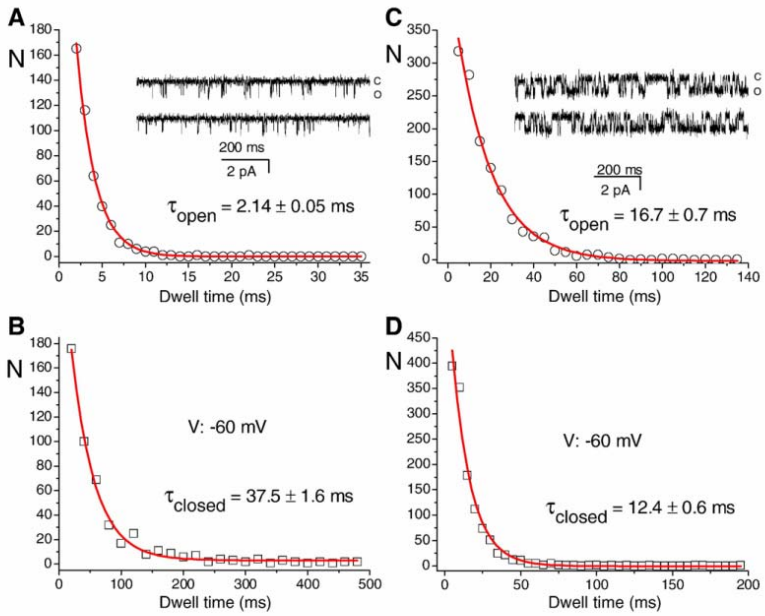

Fig. 3. mtK$_{Ca}$3.1 exhibits distinct kinetic behaviours. Distributions of channel open (panels A and C) and closed (B and D) times fitted with a single exponential. Panels A and B and C and D report data from two different experiments on HCT116 mitoplasts. Bin width: A: 1 ms; B: 20 ms; C and D: 5 ms. Insets in A) and C) show exemplary current records. The experiments were conducted in symmetrical 150 mM KCl medium, at $V = -60$ mV.

Please cite this article as: N. Sassi, et al., An investigation of the occurrence and properties of the mitochondrial intermediate-conductance Ca^{2+}-activated K^+ channel mtK$_{Ca}$3.1, Biochim. Biophys. Acta (2010), doi:10.1016/j.bbabio.2009.12.015

2.4. Vitality and apoptosis assays

For cell growth/viability tetrazolium reduction (MTT) assays, HCT116 cells were seeded in standard 96-well plates and allowed to grow in DMEM (200 µL) for 24 h. The growth medium was then replaced with medium that contained the desired compounds (from stock solutions in DMSO). The DMSO final concentration was ≤0.5% in all cases. Four wells were used for each condition. The solution was substituted by a fresh aliquot twice, at intervals of 24 h. At the end of the third 24 h period, the medium was removed, cells were washed with PBS, and 100 µL of PBS containing 10% CellTiter 96® AQ_{UEOUS} One solution (Promega) were added into each well. After 1 h of colour development at 37 °C, absorbance at 490 nm was measured using a Packard Spectra Count 96-well plate reader.

For the evaluation of apoptosis we plated HCT116 cells (300,000 cells/well) in a 6-well plate. After attachment overnight, cells were treated for 2, 6 and 12 h with the desired drugs (in the example of Fig. 6B: Tram 1 µM, Verapamil 30 µM (as inhibitor of MDR pumps), arachidonic acid 250 µM, as indicated) in DMEM or HBSS. After treatment, cells were harvested, washed with PBS, resuspended in FACS Buffer (Hepes 10 mM; NaCl 135 mM, $CaCl_2$ 5 mM, pH 7.4) and incubated with propidium iodide and Annexin V-Fluos in the dark at 37 °C for 15 min. Samples were then immediately analyzed by using a Beckton Dickinson FACScan flow cytometer (BD Biosciences). Data were processed using CellQuest® (BD Biosciences) and WinMDI2.8 (freeware; http://facs.scripps.edu/software.html, by Joe Trotter, the Scripps Institute) software. For DNA fragmentation assays, after washing the cells were resuspended in PBS, an equal volume of 70% ethanol was slowly added under continuous stirring, and the suspension was incubated overnight at 4 °C or for 30 min at R.T. After this permeabilization step, during which fragmented DNA is lost, the cells were washed in PBS, resuspended in PBS with RNAse A (20 µg/mL, 1400 units/mL) and incubated for 30 min at R.T. 5 µg/mL of propidium iodide were then added and the incubation continued for 20 min on ice in the dark, after which the samples were analyzed as above. Propidium fluorescence intensity is proportional to the amount of (unfragmented) DNA present.

2.5. Electrophysiology

Patch-clamp experiments on swollen mitochondria (mitoplasts) and perforated-patch whole-cell experiments were conducted as described in [20]. Axon pClamp software was used for voltage control and data analysis. For experiments with mitoplasts the voltages reported are those corresponding to the mitochondrial matrix. Inward currents are considered negative and plotted downwards. In the perforated-patch experiments illustrated in Fig. 5 all agents were bath-applied with a superfusion system (Rapid Solution Changer RSC-200; BioLogic Science Instruments, Claix, France). The time for solution exchange was about 500 ms; the solution was perfused via a glass pipette positioned at 300–500 µm from the cell. The maximal DMSO concentration in the recording solution was always less than 1%.

3. Results

A point of obvious relevance for an understanding of the physiological role of $mtK_{Ca}3.1$ is whether its localization in mitochondria is a peculiarity of the HCT116 cell line (human colorectal carcinoma), in which it was discovered, or is instead a common occurrence in cells expressing the channel. We therefore verified whether we could obtain evidence of its presence in mitochondria isolated from a few cell lines. Somewhat to our surprise, we could not reliably detect $mtK_{Ca}3.1$ in either of two colorectal adenocarcinoma cell lines: Caco-2, a human line (not shown), or C-26, a murine one (Fig. 1). In both cases the channel is present at the cell level, but in Western blots on progressively purer mitochondrial fractions the intensity of its band decreases as those of PM and ER markers likewise decrease and those of mitochondrial markers increase. Such a trend does not completely rule out the presence of the protein in mitochondria, but it does indicate that, if present at all, it has a low abundance.

$mtK_{Ca}3.1$ turned out instead to be present in HeLa, of human cervix adenocarcinoma origin (Fig. 2), and in mouse embryonic fibroblasts, non-cancerous cells (not shown). $K_{Ca}3.1$ is known to be expressed both by HeLa [58] and by fibroblasts [59]. In the experiment of Fig. 2, the recordings were obtained from a red-fluorescing mitoplast, isolated from HeLa cells expressing the mitochondria-targeted mtDsRed [20]. The data plotting the averaged single-channel current amplitudes vs. voltage (panel B, full circles) are shown to fall on the same curve as analogous data obtained from HCT116 mitochondria (squares), indicating that the same channel is involved. Our attempts to establish the presence of $mtK_{Ca}3.1$ in rat heart mitochondria have failed so far to provide a reliable answer.

Observation of the activity of $mtK_{Ca}3.1$ at the single-channel level allowed us to identify previously undescribed electrophysiological characteristics. The channel exhibits at least two well-defined rapid kinetic modes: a more frequently encountered one with a short mean open dwell time (time constant (τ) ~2 ms), a longer closed dwell time (τ ~40 ms) and a correspondingly low (voltage-independent) open probability (Fig. 3A and B), and one with longer-lasting (τ ~17 ms) openings and shorter closures (τ ~12 ms) (Fig. 3C and D). "Bursting" behaviour, conductance and voltage dependence of the unitary conductance and of the open probability were similar for the two forms; channels operating in either mode appeared to be equally sensitive to inhibition by TRAM-34 or clotrimazole, two specific inhibitors of intermediate-conductance Ca^{2+}-activated K^+ channels (not shown).

Rarely, the channel also operated in a lower-than-usual conductance state. In the example shown in Fig. 4, a channel with a chord conductance of about 22 pS at −70 mV gave way to the usual activity with a chord conductance of about 36 pS. Since the two types of activity were never observed together, and a subsequent addition of clotrimazole abolished all activity (not shown), we attribute both conductances to one $mtK_{Ca}3.1$ channel.

$mtK_V1.3$ interacts with the pro-apoptotic protein Bax, as shown, among other evidence, by patch-clamp experiments in which whole-cell current conducted by PM $K_V1.3$ was inhibited by externally applied recombinant GST-Bax(ΔC) [11]. We therefore checked whether a similar interaction might take place between $K_{Ca}3.1$ in the plasma membrane of HCT116 cells and this pro-apoptotic protein. Stable macroscopic K_{Ca} currents, recorded in the perforated-patch mode, were activated by applying the Ca^{2+} ionophore ionomycin (0.5 µM) plus the small/intermediate K_{Ca} channel opener DC-EBIO (100 µM). Time courses of the current in response to the various agents were built by plotting the outward current assessed at 0 mV from voltage ramps from −100 to 100 mV ($V_{holding}$ = 0 mV), applied every 5 s (Fig. 5). After stabilization of the current, GST-Bax(ΔC) was applied at 8.25 or 13.2 nM. This had no effect on the amplitude of the ionomycin + DC-EBIO-elicited current, which was instead fully blocked by the $K_{Ca}3.1$ channel antagonist TRAM-34 (3 µM) (N = 3). This observation indicates that there is no $K_{Ca}3.1$ block by GST-Bax(ΔC) at any voltage, and no modification of the permeation properties of the channel. Using the same experimental protocol, we also verified the effects of GST-BclxL (30 nM) on the $K_{Ca}3.1$ currents. GST-BclxL was, as expected, similarly ineffective (not shown).

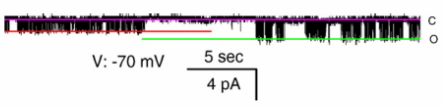

Fig. 4. $mtK_{Ca}3.1$ can adopt a lower-conductance state. A continuous current record showing the activity of a $mtK_{Ca}3.1$ channel in an HCT116 mitoplast. The red and green horizontal lines highlight the difference in current amplitude, the purple line indicates the background current level. See text for details.

Please cite this article as: N. Sassi, et al., An investigation of the occurrence and properties of the mitochondrial intermediate-conductance Ca^{2+}-activated K^+ channel $mtK_{Ca}3.1$, Biochim. Biophys. Acta (2010), doi:10.1016/j.bbabio.2009.12.015

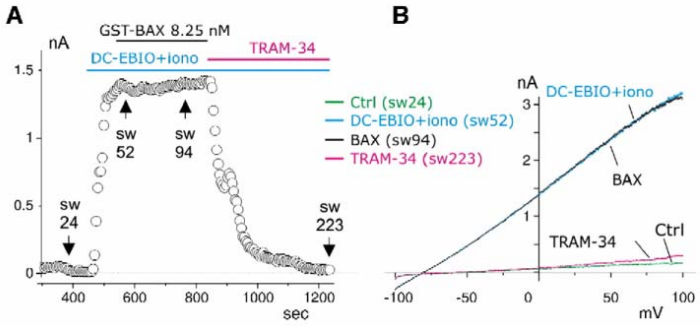

Fig. 5. Bax has no effect on $K_{Ca}3.1$ currents in HCT116 cells. A) Time course of the iono + DC-EBIO-activated $K_{Ca}3.1$ current from a HCT116 cell in whole-cell perforated configuration. Each data point represents the $K_{Ca}3.1$ current assessed at 0 mV from voltage ramp pulses delivered every 5 s under varying experimental conditions: i) control, ii) ionomycin + DC-EBIO (500 nM + 100 μM) alone, iii) iono + DC-EBIO (500 nM + 100 μM) plus GST-Bax(ΔC) (8.25 nM), and iv) ionomycin + DC-EBIO (500 nM + 100 μM) plus TRAM-34 (3 μM). B) Representative current traces in response to voltage ramps from − 100 to + 100 mV (1 s duration, $V_{holding}$: 0 mV), under the various pharmacological conditions shown in panel A. Numbers indicate the corresponding sweep in the time course display in panel A.

Using HCT116 cells, we verified whether the $K_{Ca}3.1$-specific, membrane-permeable inhibitor TRAM-34, by itself or in combination with inhibitors of MDR efflux pumps (Cyclosporin A, Probenecid, Verapamil, and Tamoxifen), had any effect on cell vitality or could induce apoptosis or enhance apoptosis induction by staurosporin. Assessment was carried out using cell counting, the MTT assay ($N = 3$), Annexin/propidium staining ($N = 8$) and DNA fragmentation assays ($N = 3$) (see Materials and methods for details), using staurosporin, indometacin and arachidonic acid as control apoptosis inducers. We could not detect an effect on either cell growth or cell death. Fig. 6 shows two representative experiments. The same result was obtained using the impermeable and less selective blocker charybdotoxin (not shown).

4. Discussion

The data presented above prove that the presence of the intermediate-conductance Ca^{2+}-activated K^+ channel is not a peculiarity of HCT116 cells (nor of cancerous cells, since it is present in the mitochondria of MEF). The mitochondrial subpopulation of $K_{Ca}3.1$ seems to be regulated case by case. Thus, in cell lines of colonic origin it may be detectable (HCT116) or undetectable (Caco-2, C-26). This in turn suggests (although it does not prove) that this population does not originate from an insufficiently selective targeting, i.e., $K_{Ca}3.1$ does not appear in mitochondria "by mistake", but presumably as a consequence of physiological events peculiar to each cell type. Other cases of cell type-specific localization of a protein in mitochondria as well as in another cellular compartment have been identified. For example, COX-2 is present in the mitochondria of several cancer cell lines, but not in those of fibroblasts or endothelial cells, whereas calcium-independent phospholipase A2 was found in the mitochondria of fibroblasts as well as in some cancerous cell lines [60].

One way a regulation of $K_{Ca}3.1$ localization might take place is via modulation of membrane/protein traffic, a signalling-controlled process (e.g.: [61,62]). One possibility is caveolae/lipid rafts-mediated traffic. A traffic route between caveolae, the endosomal system, the ER and Golgi has been identified [63–66], and a functional interaction of caveolae with mitochondria as well is suggested by proteomics profiling of the caveolae [67,68]. Caveolin-1 is targeted to various cellular compartments, including mitochondria, depending on cell type [69]. Garlid and coworkers have proposed that vesicular signalosomes originating from caveolae migrate to mitochondria, bind to OMM receptors and activate mtK_{ATP} via phosphorylations [70,71]. An interaction of the endosomal endocytosis pathway with mitochondria is also suggested by some observations [72]. Delivery of membrane proteins to mitochondria may also conceivably take place at ER-mitochondrion contact sites. These involve a differentiated ER membrane, MAM [73,74], are mediated by proteins such as PACS [75,76] and mitofusin 2 [77] and are sites of intermembrane transfer of phospholipids [78]. Regulation at the membrane-traffic level might result in the protein being present in mitochondria at different levels depending on cellular factors. Hypothetically, this might also explain the contradictory results in the literature on the presence or lack of K_{ATP} and $K_{Ca}1.1$ mitochondrial subpopulations.

IMM channels are furthermore subject to regulation at the molecular level. In the case of mtK_{ATP}, evidence has been presented for an

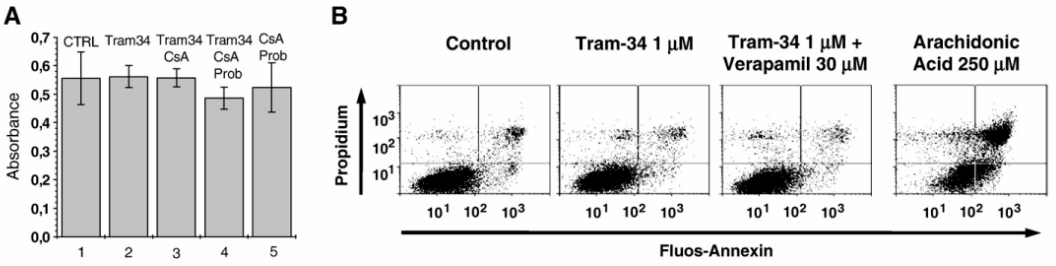

Fig. 6. TRAM-34 has no effect on HCT116 cell proliferation and does not induce cell death. A) Representative results of a tetrazolium salt (MTT) reduction assay. Cells were sowed and assayed after three days of growth (see Materials and methods for details). Conditions: 1: control (no addition); 2: TRAM-34, 2 μM; 3: TRAM-34, 2 μM, and Cyclosporin A, 2 μM; 4: TRAM-34, 2 μM, Cyclosporin A, 2 μM, and Probenecid, 100 μM; 5: Cyclosporin A, 2 μM, and Probenecid, 100 μM. B) A representative apoptosis assay using flow cytometry (FACS). Cells were incubated in DMEM in the presence of the specified substances for 6 h, then treated with propidium and Annexin as described in Materials and methods.

Please cite this article as: N. Sassi, et al., An investigation of the occurrence and properties of the mitochondrial intermediate-conductance Ca^{2+}-activated K^+ channel $mtK_{Ca}3.1$, Biochim. Biophys. Acta (2010), doi:10.1016/j.bbabio.2009.12.015

interaction with and activation by PKCε [79]. Interestingly, PKCε activation can cause caveolin-1- and cholesterol-dependent internalization of PM K_{ATP} channels in vascular smooth muscle cells [80]. PKG has also been proposed to be involved in signalling targeting mtK_{ATP} [81]. $mtK_{Ca}1.1$ is regulated by PKA [82–84]. Whether analogous processes impact on $mtK_{Ca}3.1$ is unknown, but it seems plausible to associate different kinetic and conductance properties (Figs. 3 and 4) with differences in post-translational modifications.

Roles have been assigned to $K_{Ca}3.1$ in a variety of cellular processes (see the Introduction and [20]), but its function can apparently be largely taken over by its smaller- and larger-conductance relatives, so that knock-out animals exhibit relatively mild phenotypes [85,86]. At the cell-culture level we also found it hard to identify clear short-term consequences of its inhibition at the plasma membrane (with charybdotoxin, not shown) or throughout the cell (with TRAM-34) (Fig. 6). In principle $mtK_{Ca}3.1$ ought to be able to mimic, at least to an extent, $mtK_{Ca}1.1$ functions, with the possibly relevant difference of activating at lower matrix Ca^{2+} levels (sub-μM vs. μM range). It is interesting in this context that the two channels have been recently found to interact, with $K_{Ca}3.1$ inhibiting $K_{Ca}1.1$ [87,88]. We had hypothesized [20] that $mtK_{Ca}3.1$ might act similarly to $mtK_V1.3$ [11] and interact with Bax. Experimental verification however has failed to support this hypothesis (Fig. 5). It seems therefore that the interaction of Bax with K^+ channels does not require simply a set of negative charges in the channel vestibule, but depends on more specific features. On the basis of computational simulations and of previous mutagenesis studies [89], Yu et al. [90] have identified 5 channel residues, Tyr-400, Asp-402, His-404, Asp-386 and Gly-380, as being of major relevance for $K_V1.3$-toxin interactions. His-404 is absent in $K_{Ca}3.1$ (Gly-380 corresponds to an Ala residue in $K_{Ca}3.1$). His-404 accounts for the pH-dependence of the interaction between the channel and some toxins, as well as with Bax [12]. Aspartates at positions 375 and 376 in the turret region of Kv1.3 do not have an equivalent in $K_{Ca}3.1$ [89], so that the formal negative charge in this region, presumably important for the interaction with Bax Lys128, is 1/monomer in $K_{Ca}3.1$ vs. 3 in $K_V1.3$.

In summary, the roles of $mtK_{Ca}3.1$ in mitochondrial and cellular physiology may be at least in part redundant, in analogy to what seems to be the case at the cellular level, since fully functional mitochondria exist without it (in cells not expressing the channel but apparently also in cells which do express it). The possibility remains that the channel may play a major role in some specific, yet to be discovered, process, but the data presented here do not support a key role in the control of cell proliferation or drug-induced apoptosis. Where present, $mtK_{Ca}3.1$ is fully expected to contribute to the IMM K^+ conductance following an increase in matrix $[Ca^{2+}]$; the relevance of this contribution in comparison with other K^+ permeation pathways remains to be explored. The mechanisms accounting for its presence in mitochondria need to be investigated, and may well apply to other proteins with multiple localisations.

Acknowledgements

We thank Prof. B. Vogelstein for HCT116 cells, Dr. M. Zaccolo for the mtDsRed plasmid, Prof. H. Wulff for generous gifts of TRAM-34, and Dr. Andrea Rasola for instruction with FACS. This work was supported in part by grants from the Italian Association for Cancer Research (AIRC), the Italian Foundation for Basic Research (FIRB), and the Fondazione Cassa di Risparmio di Padova e Rovigo (Fondazione CARIPARO). L.B. was the beneficiary of a University of Padova post-doctoral fellowship; B.F. was supported by a fellowship of the Umbria Region.

References

[1] P. Bernardi, Mitochondrial transport of cations: channels, exchangers, and permeability transition, Physiol. Rev. 79 (1999) 1127–1155.
[2] K.D. Garlid, P. Paucek, Mitochondrial potassium transport: the K^+ cycle, Biochim. Biophys. Acta 1606 (2003) 23–41.
[3] B. O'Rourke, Mitochondrial ion channels, Annu. Rev. Physiol. 69 (2007) 19–49.
[4] K. Nowikowsky, R.J. Schweyen, P. Bernardi, Pathophysiology of mitochondrial volume homeostasis: potassium transport and permeability transition, Biochim. Biophys. Acta Bioenerg. 1787 (2009) 345–350.
[5] M. Zoratti, U. De Marchi, E. Gulbins, I. Szabò, Novel channels of the inner mitochondrial membrane, Biochim. Biophys. Acta Bioenerg. 1787 (2009) 351–363.
[6] A. Szewczyk, W. Jarmuszkiewicz, W.S. Kunz, Mitochondrial potassium channels, IUBMB Life 61 (2009) 134–143.
[7] I. Inoue, H. Nagase, K. Kishi, T. Higuti, ATP-sensitive K^+-channel in the mitochondrial inner membrane, Nature 352 (1991) 244–247.
[8] Y.A. Dahlem, T.F. Horn, L. Buntinas, T. Gonoi, G. Wolf, D. Siemen, The human mitochondrial K_{ATP} channel is modulated by calcium and nitric oxide: a patch-clamp approach, Biochim. Biophys. Acta 1656 (2004) 46–56.
[9] K. Choma, P. Bednarczyk, I. Koszela-Piotrowska, B. Kulawiak, A. Kudin, W.S. Kunz, K. Dołowy, A. Szewczyk, Single channel studies of the ATP-regulated potassium channel in brain mitochondria, J. Bioenerg. Biomembr. 41 (2009) 323–334.
[10] I. Szabò, J. Bock, A. Jekle, M. Soddemann, C. Adams, F. Lang, M. Zoratti, E. Gulbins, A novel potassium channel in lymphocyte mitochondria, J. Biol. Chem. 280 (2005) 12790–12798.
[11] I. Szabò, J. Bock, H. Grassmè, M. Soddemann, B. Wilker, F. Lang, M. Zoratti, E. Gulbins, Mitochondrial potassium channel $K_V1.3$ mediates Bax-induced apoptosis in lymphocytes, Proc. Natl. Acad. Sci. U. S. A. 105 (2008) 14861–14866.
[12] Erich Gulbins, Nicola Sassi, Heike Grassmè, Mario Zoratti, Ildikò Szabò, Role of Kv1.3 mitochondrial potassium channel in apoptotic signalling in lymphocytes, Biochim. Biophys. Acta, this issue.
[13] Z. Rusznák, G. Bakondi, L. Kosztka, K. Pocsai, B. Dienes, J. Fodor, A. Telek, M. Gönczi, G. Szucs, L. Csernoch, Mitochondrial expression of the two-pore domain TASK-3 channels in malignantly transformed and non-malignant human cells, Virchows Arch. 452 (2008) 415–426.
[14] D. Siemen, C. Loupatatzis, J. Borecky, E. Gulbins, F. Lang, Ca^{2+}-activated K channel of the BK-type in the inner mitochondrial membrane of a human glioma cell line, Biochem. Biophys. Res. Commun. 257 (1999) 549–554.
[15] W. Xu, Y. Liu, S. Wang, T. McDonald, J.E. Van Eyk, A. Sidor, B. O'Rourke, Cytoprotective role of Ca^{2+}-activated K^+ channels in the cardiac inner mitochondrial membrane, Science 298 (2002) 1029–1033.
[16] J. Skalska, M. Piwonska, E. Wyroba, L. Surmacz, R. Wieczorek, I. Koszela-Piotrowska, J. Zielinska, P. Bednarczyk, K. Dolowy, G.M. Wilczynski, A. Szewczyk, W.S. Kunz, A novel potassium channel in skeletal muscle mitochondria, Biochim. Biophys. Acta 1777 (2008) 651–659.
[17] Y. Cheng, X.Q. Gu, P. Bednarczyk, F.R. Wiedemann, G.G. Haddad, D. Siemen, Hypoxia increases activity of the BK-channel in the inner mitochondrial membrane and reduces activity of the permeability transition pore, Cell. Physiol. Biochem. 22 (2008) 127–136.
[18] J. Skalska, P. Bednarczyk, M. Piwonska, B. Kulawiak, G. Wilczynski, K. Dolowy, A.P. Kudin, W.S. Kunz, A. Szewczyk, Calcium ions regulate K uptake into brain mitochondria: the evidence for a novel potassium channel, Int. J. Mol. Sci. 10 (2009) 1104–1120.
[19] I. Koszela-Piotrowska, K. Matkovic, A. Szewczyk, W. Jarmuszkiewicz, A large-conductance calcium-activated potassium channel in potato tuber mitochondria, Biochem. J. 424 (2009) 307–316.
[20] U. De Marchi, N. Sassi, B. Fioretti, L. Catacuzzeno, G.M. Cereghetti, I. Szabò, M. Zoratti, Intermediate conductance Ca^{2+}-activated potassium channel ($K_{Ca}3.1$) in the inner mitochondrial membrane of human colon cancer cells, Cell Calcium 45 (2009) 509–516.
[21] S.N. Wu, Large-conductance Ca^{2+}-activated K^+ channels: physiological roles and pharmacology, Curr. Med. Chem. 10 (2003) 649–661.
[22] A.D. Wei, G.A. Gutman, R. Aldrich, K.G. Chandy, S. Grissmer, H. Wulff, International Union of Pharmacology. LII. Nomenclature and molecular relationships of calcium-activated potassium channels, Pharmacol. Rev. 57 (2005) 463–472.
[23] B.S. Jensen, M. Hertz, P. Christophersen, L.S. Madsen, The Ca^{2+}-activated K^+ channel of intermediate conductance: a possible target for immune suppression, Expert Opin. Ther. Targets 6 (2002) 623–636.
[24] C.C. Chou, C.A. Lunn, N.J. Murgolo, $K_{Ca}3.1$: target and marker for cancer, autoimmune disorder and vascular inflammation? Expert Rev. Mol. Diagn. 8 (2008) 179–187.
[25] M. Stocker, Ca^{2+}-activated K^+ channels: molecular identity determinants and function of the SK family, Nat. Rev. Neurosci. 5 (2004) 758–770.
[26] J. Ledoux, A.D. Bonev, M.T. Nelson, Ca^{2+}-activated K^+ channels in murine endothelial cells: block by intracellular calcium and magnesium, J. Gen. Physiol. 131 (2008) 125–135.
[27] W. Bildl, T. Strassmaier, H. Thurm, J. Andersen, S. Eble, D. Oliver, M. Knipper, M. Mann, U. Schulte, J.P. Adelman, B. Fakler, Protein kinase CK2 is coassembled with small conductance Ca^{2+}-activated K^+ channels and regulates channel gating, Neuron 43 (2004) 847–858.
[28] Y.J. Wang, R.J. Sung, M.W. Lin, S.N. Wu, Contribution of BK_{Ca}-channel activity in human cardiac fibroblasts to electrical coupling of cardiomyocytes-fibroblasts, J. Membr. Biol. 213 (2006) 175–185.
[29] A.S. Parihar, M.J. Coghlan, M. Gopalakrishnan, C.C. Shieh, Effects of intermediate-conductance Ca^{2+}-activated K^+ channel modulators on human prostate cancer cell proliferation, Eur. J. Pharmacol. 471 (2003) 157–164.
[30] H. Ouadid-Ahidouch, A. Ahidouch, K^+ channel expression in human breast cancer cells: involvement in cell cycle regulation and carcinogenesis, J. Membr. Biol. 221 (2008) 1–6.

Please cite this article as: N. Sassi, et al., An investigation of the occurrence and properties of the mitochondrial intermediate-conductance Ca^{2+}-activated K^+ channel $mtK_{Ca}3.1$, Biochim. Biophys. Acta (2010), doi:10.1016/j.bbabio.2009.12.015

[31] B. Fioretti, E. Castigli, M.R. Micheli, R. Bova, M. Sciaccaluga, A. Harper, F. Franciolini, L. Catacuzzeno, Expression and modulation of the intermediate-conductance Ca^{2+}-activated K^+ channel in glioblastoma CL-15 cells, Cell. Physiol. Biochem. 18 (2006) 47–56.
[32] J.Z. Sheng, S. Ella, M.J. Davis, M.A. Hill, A.P. Braun, Openers of SK_{Ca} and IK_{Ca} channels enhance agonist-evoked endothelial nitric oxide synthesis and arteriolar vasodilation, FASEB J. 23 (2009) 1138–1145.
[33] K. Toyama, H. Wulff, K.G. Chandy, P. Azam, G. Raman, T. Saito, Y. Fujiwara, D.L. Mattson, S. Das, J.E. Melvin, P.F. Pratt, O.A. Hatoum, D.D. Gutterman, D.R. Harder, H. Miura, The intermediate-conductance calcium-activated potassium channel $K_{Ca}3.1$ contributes to atherogenesis in mice and humans, J. Clin. Invest. 118 (2008) 3025–3037.
[34] M. Félétou, Calcium-activated potassium channels and endothelial dysfunction: therapeutic options? Br. J. Pharmacol. 156 (2009) 545–562.
[35] W.J. Joiner, S. Basavappa, S. Vidyasagar, K. Nehrke, S. Krishnan, H.J. Binder, E.L. Boulpaep, V.M. Rajendran, Active K^+ secretion through multiple K_{Ca}-type channels and regulation by IK_{Ca} channels in rat proximal colon, Am. J. Physiol. Gastrointest. Liver Physiol. 285 (2003) G185–G196.
[36] C.A. Flores, J.E. Melvin, C.D. Figueroa, F.V. Sepúlveda, Abolition of Ca^{2+}-mediated intestinal anion secretion and increased stool dehydration in mice lacking the intermediate conductance Ca^{2+}-dependent K^+ channel Kcnn4, J. Physiol. 583 (Pt 2) (2007) 705–717.
[37] A.D. Costa, C.L. Quinlan, A. Andrukhiv, I.C. West, M. Jaburek, K.D. Garlid, The direct physiological effects of mitoK(ATP) opening on heart mitochondria, Am. J. Physiol. Heart Circ. Physiol. 290 (2006) H406–H415.
[38] A. Kaasik, D. Safiulina, A. Zharkovsky, V. Veksler, Regulation of mitochondrial volume, Am. J. Physiol. Cell. Physiol. 292 (2007) C157–C163.
[39] A.D. Costa, K.D. Garlid, Mito K_{ATP} activity in healthy and ischemic hearts, J. Bioenerg. Biomembr. 41 (2009) 123–126.
[40] A.P. Halestrap, The regulation of the matrix volume of mammalian mitochondria in vivo and in vitro and its role in the control of mitochondrial metabolism, Biochim. Biophys. Acta 973 (1989) 355–382.
[41] K.D. Garlid, P.E. Puddu, P. Pasdois, A.D. Costa, B. Beauvoit, A. Criniti, L. Tariosse, P. Diolez, P. Dos Santos, Inhibition of cardiac contractility by 5-hydroxydecanoate and tetraphenylphosphonium ion: a possible role of mitoK_{ATP} in response to inotropic stress, Am. J. Physiol. Heart Circ. Physiol. 291 (2006) H152–H160.
[42] M.A. Aon, S. Cortassa, A.C. Wei, M. Grunnet, B. O'Rourke, Energetic performance is improved by specific activation of K^+ fluxes through K_{Ca} channels in heart mitochondria, Biochim. Biophys. Acta 1797 (2010) 71–80.
[43] H.T. Facundo, J.G. de Paula, A.J. Kowaltowski, Mitochondrial ATP-sensitive K^+ channels prevent oxidative stress, permeability transition and cell death, J. Bioenerg. Biomembr. 37 (2005) 75–82.
[44] A.P. Halestrap, S.J. Clarke, I. Khaliulin, The role of mitochondria in protection of the heart by preconditioning, Biochim. Biophys. Acta 1767 (2007) 1007–1031.
[45] S.J. Clarke, I. Khaliulin, M. Das, J.E. Parker, K.J. Heesom, A.P. Halestrap, Inhibition of mitochondrial permeability transition pore opening by ischemic preconditioning is probably mediated by reduction of oxidative stress rather than mitochondrial protein phosphorylation, Circ. Res. 102 (2008) 1082–1090.
[46] B. Kulawiak, A.P. Kudin, A. Szewczyk, W.S. Kunz, BK channel openers inhibit ROS production of isolated rat brain mitochondria, Exp. Neurol. 212 (2008) 543–547.
[47] A.J. Kowaltowski, N.C. de Souza-Pinto, R.F. Castilho, A.E. Vercesi, Mitochondria and reactive oxygen species, Free Rad. Biol. Med. 47 (2009) 333–343.
[48] E.B. Tahara, F.D. Navarete, A.J. Kowaltowsi, Tissue-, substrate-, and site-specific characteristics of mitochondrial reactive oxygen species generation, Free Rad. Biol. Med. 46 (2009) 1283–1297.
[49] D.J. Hausenloy, A. Tsang, D.M. Yellon, The reperfusion injury salvage kinase pathway: a common target for both ischemic preconditioning and postconditioning, Trends Cardiovasc. Med. 15 (2005) 69–75.
[50] F. Di Lisa, M. Canton, R. Menabò, N. Kaludercic, P. Bernardi, Mitochondria and cardioprotection, Heart Fail. Rev. 12 (2007) 249–260.
[51] A.D. Costa, K.D. Garlid, Intramitochondrial signaling: interactions among mitoK_{ATP}, PKCε, ROS and MPT, Am. J. Physiol. Heart Circ. Physiol. 295 (2008) H874–H882.
[52] D.J. Hausenloy, D.M. Yellon, Preconditioning and postconditioning: underlying mechanisms and clinical application, Atherosclerosis 204 (2009) 334–341.
[53] M. Krenz, O. Oldenburg, H. Wimpee, M.V. Cohen, K.D. Garlid, S.D. Critz, J.M. Downey, J.N. Benoit, Opening of ATP-sensitive potassium channels causes generation of free radicals in vascular smooth cells, Basic Res. Cardiol. 97 (2002) 365–373.
[54] A.D. Costa, R. Jakob, C.L. Costa, K. Andrukhiv, I.C. West, K.D. Garlid, The mechanism by which the mitochondrial ATP-sensitive K^+ channel opening and H_2O_2 inhibit the mitochondrial permeability transition, J. Biol. Chem. 281 (2006) 20801–20808.
[55] M. Silic-Benussi, E. Cannizzaro, A. Venerando, I. Cavallari, V. Petronilli, N. La Rocca, O. Marin, L. Chieco-Bianchi, F. Di Lisa, D.M. D'Agostino, P. Bernardi, V. Ciminale, Modulation of mitochondrial K^+ permeability and reactive oxygen species production by the p13 protein of human T-cell leukemia virus type 1, Biochim. Biophys Acta Bioenerg. 1787 (2009) 947–954.
[56] R.F. Feissner, J. Skalska, W.E. Gaum, S.S. Sheu, Crosstalk signaling between mitochondrial Ca^{2+} and ROS, Front. Biosci. 14 (2009) 1197–1218.
[57] U. De Marchi, S. Campello, I. Szabò, F. Tombola, J.C. Martinou, M. Zoratti, Bax does not directly participate in the Ca^{2+}-induced permeability transition of isolated mitochondria, J. Biol. Chem. 279 (2004) 37415–37422.
[58] C. Hougaard, B.L. Eriksen, S. Jørgensen, T.H. Johansen, T. Dyhring, L.S. Madsen, D. Strøbaek, P. Christophersen, Selective positive modulation of the SK3 and SK2 subtypes of small conductance Ca^{2+}-activated K^+ channels, Br. J. Pharmacol. 151 (2007) 655–665.
[59] I. Grgic, E. Kiss, B.P. Kaistha, C. Busch, M. Kloss, J. Sautter, A. Müller, A. Kaistha, C. Schmidt, G. Raman, H. Wulff, F. Strutz, H.J. Gröne, R. Köhler, J. Hoyer, Renal fibrosis is attenuated by targeted disruption of $K_{Ca}3.1$ potassium channels, Proc. Natl. Acad. Sci. U. S. A. 106 (2009) 14518–14523.
[60] J.Y. Liou, N. Aleksic, S.F. Chen, T.J. Han, S.K. Shyue, K.K. Wu, Mitochondrial localization of cyclooxygenase-2 and calcium-independent phospholipase A2 in human cancer cells: implication in apoptosis resistance, Exp. Cell Res. 306 (2005) 75–84.
[61] L. Pelkmans, E. Fava, H. Grabner, M. Hannus, B. Habermann, E. Krausz, M. Zerial, Genome-wide analysis of human kinases in clathrin- and caveolae/raft-mediated endocytosis, Nature 436 (2005) 78–86.
[62] L. Pelkmans, M. Zerial, Kinase-regulated quantal assemblies and kiss-and-run recycling of caveolae, Nature 436 (2005) 128–133.
[63] E.J. Smart, Y.S. Ying, P.A. Conrad, R.G. Anderson, Caveolin moves from caveolae to the Golgi apparatus in response to cholesterol oxidation, J. Cell Biol. 127 (1994) 1185–1197.
[64] P.A. Conrad, E.J. Smart, Y.S. Ying, R.G. Anderson, G.S. Bloom, Caveolin cycles between plasma membrane caveolae and the Golgi complex by microtubule-dependent and microtubule-independent steps, J. Cell Biol. 131 (1995) 1421–1433.
[65] L. Pelkmans, T. Bürli, M. Zerial, A. Helenius, Caveolin-stabilized membrane domains as multifunctional transport and sorting devices in endocytic membrane traffic, Cell 118 (2004) 767–780.
[66] L. Pelkmans, Secrets of caveolae- and lipid raft-mediated endocytosis revealed by mammalian viruses, Biochim. Biophys. Acta 1746 (2005) 295–304.
[67] K.A. McMahon, M. Zhu, S.W. Kwon, P. Liu, Y. Zhao, R.G. Anderson, Detergent-free caveolae proteome suggests an interaction with ER and mitochondria, Proteomics 6 (2006) 143–152.
[68] G. Båthori, I. Parolini, F. Tombola, I. Szabò, A. Messina, M. Oliva, V. De Pinto, M. Lisanti, M. Sargiacomo, M. Zoratti, Porin is present in the plasma membrane where it is concentrated in caveolae and caveolae-related domains, J. Biol. Chem. 274 (1999) 29607–29612.
[69] W.P. Li, P. Liu, B.K. Pilcher, R.G. Anderson, Cell-specific targeting of caveolin-1 to caveolae, secretory vesicles, cytoplasm or mitochondria, J. Cell Sci. 114 (2001) 1397–1408.
[70] C.L. Quinlan, A.D. Costa, C.L. Costa, S.V. Pierre, P. Dos Santos, K.D. Garlid, Conditioning the heart induces formation of signalosomes that interact with mitochondria to open mitoK_{ATP} channels, Am. J. Physiol. Heart Circ. Physiol. 295 (2008) H953–H961.
[71] K.D. Garlid, A.D. Costa, C.L. Quinlan, S.V. Pierre, P. Dos Santos, Cardioprotective signaling to mitochondria, J. Mol. Cell. Cardiol. 46 (2009) 858–866.
[72] C. García-Ruiz, A. Colell, A. Morales, M. Calvo, C. Enrich, J.C. Fernandez-Checa, Trafficking of ganglioside GD3 to mitochondria by tumor necrosis factor-alpha, J. Biol. Chem. 277 (2002) 36443–36448.
[73] J.E. Vance, Phospholipid synthesis in a membrane fraction associated with mitochondria, J. Biol. Chem. 265 (1990) 7248–7256.
[74] R. Rizzuto, P. Pinton, W. Carrington, F.S. Fay, K.E. Fogarty, L.M. Lifshitz, R.A. Tuft, T. Pozzan, Close contacts with the endoplasmic reticulum as determinants of mitochondrial Ca^{2+} responses, Science 280 (1998) 1763–1766.
[75] T. Simmen, J.E. Aslan, A.D. Blagoveshchenskaya, L. Thomas, L. Wan, Y. Xiang, S.F. Feliciangeli, C.H. Hung, C.M. Crump, G. Thomas, PACS-2 controls endoplasmic reticulum-mitochondria communication and Bid-mediated apoptosis, EMBO J. 24 (2005) 717–729.
[76] R.T. Youker, U. Shinde, R. Day, G. Thomas, At the crossroads of homoeostasis and disease: roles of the PACS proteins in membrane traffic and apoptosis, Biochem. J. 421 (2009) 1–15.
[77] O.M. de Brito, L. Scorrano, Mitofusin 2 tethers endoplasmic reticulum to mitochondria, Nature 456 (2008) 605–610.
[78] B. Gaigg, R. Simbeni, C. Hrastnik, F. Paltauf, G. Daum, Characterization of a microsomal subfraction associated with mitochondria of the yeast, *Saccharomyces cerevisiae*. Involvement in synthesis and import of phospholipids into mitochondria, Biochim. Biophys. Acta 1234 (1995) 214–220.
[79] M. Jaburek, A.D. Costa, J.R. Burton, C.L. Costa, K.D. Garlid, Mitochondrial PKCε and mitochondrial ATP-sensitive K^+ channel copurify and coreconstitute to form a functioning signaling module in proteoliposomes, Circ. Res. 99 (2006) 878–883.
[80] J. Jiao, V. Garg, B. Yang, T.S. Elton, K. Hu, Protein kinase C-epsilon induces caveolin-dependent internalization of vascular adenosine 5′-triphosphate-sensitive K^+ channels, Hypertension 52 (2008) 499–506.
[81] A.D. Costa, S.V. Pierre, M.V. Cohen, J.M. Downey, K.D. Garlid, cGMP signalling in pre- and post-conditioning: the role of mitochondria, Cardiovasc. Res. 77 (2008) 344–352.
[82] T. Sato, T. Saito, N. Saegusa, H. Nakaya, Mitochondrial Ca^{2+}- activated K^+ channels in cardiac myocytes: a mechanism of the cardioprotective effect and modulation by protein kinase A, Circulation 111 (2005) 198–203.
[83] H. Nishida, T. Sato, M. Miyazaki, H. Nakaya, Infarct size limitation by adrenomedullin: protein kinase A but not PI3-kinase is linked to mitochondrial K_{Ca} channels, Cardiovasc. Res. 77 (2008) 398–405.
[84] H. Nishida, T. Sato, T. Ogura, H. Nakaya, New aspects for the treatment of cardiac diseases based on the diversity of functional controls in cardiac muscles: mitochondrial ion channels and cardioprotection, J. Pharmacol. Sci. 109 (2009) 341–347.
[85] T. Begenisich, T. Nakamoto, C.E. Ovitt, K. Nehrke, C. Brugnara, S.L. Alper, J.E. Melvin, Physiological roles of the intermediate conductance, Ca^{2+}-activated potassium channel Kcnn4, J. Biol. Chem. 279 (2004) 47681–47687.
[86] H. Si, W.T. Heyken, S.E. Wölfle, M. Tysiac, R. Schubert, I. Grgic, L. Vilianovich, G. Giebing, T. Maier, V. Gross, M. Bader, C. de Wit, J. Hoyer, R. Köhler, Impaired endothelium-derived hyperpolarizing factor-mediated dilations and increased

Please cite this article as: N. Sassi, et al., An investigation of the occurrence and properties of the mitochondrial intermediate-conductance Ca^{2+}-activated K^+ channel mt$K_{Ca}3.1$, Biochim. Biophys. Acta (2010), doi:10.1016/j.bbabio.2009.12.015

blood pressure in mice deficient of the intermediate-conductance Ca^{2+}-activated K^+ channel, Circ. Res. 99 (2006) 537–544.
[87] J. Thompson, T. Begenisich, Membrane-delimited inhibition of maxi-K channel activity by the intermediate conductance Ca^{2+}-activated K channel, J. Gen. Physiol. 127 (2006) 159–169.
[88] J. Thompson, T. Begenisich, Mechanistic details of BK channel inhibition by the intermediate conductance, Ca^{2+}-activated K channel, Channels 3 (2009) 194–204.
[89] H. Rauer, M.D. Lanigan, M.W. Pennington, J. Aiyar, S. Ghanshani, M.D. Cahalan, R.S. Norton, K.G. Chandy, Structure-guided transformation of charybdotoxin yields an analog that selectively targets Ca^{2+}-activated over voltage-gated K^+ channels, J. Biol. Chem. 275 (2000) 1201–1208.
[90] K. Yu, W. Fu, H. Liu, X. Luo, K.X. Chen, J. Ding, J. Shen, H. Jiang, Computational simulations of interactions of scorpion toxins with the voltage-gated potassium ion channel, Biophys. J. 86 (2004) 3542–3555.

Please cite this article as: N. Sassi, et al., An investigation of the occurrence and properties of the mitochondrial intermediate-conductance Ca^{2+}-activated K^+ channel $mtK_{Ca}3.1$, Biochim. Biophys. Acta (2010), doi:10.1016/j.bbabio.2009.12.015

Mitochondriotropic Polyphenols

Introduction

ROS

Treatments that selectively reach cancer cells, avoiding damage to normal cells, are the cornerstone of the fight against cancer. Understanding the molecular basis of alterations that distinguish cancerous from normal cells allows one to accurately identify sensitive targets and may lead to effective therapies to selectively eliminate tumors.

Over the last several years, mitochondria have emerged as the target of various chemotherapeutic compounds, because of differences in properties of mitochondria between cancer and normal cells. Indeed cancer cells generally exhibit metabolic alterations: increased aerobic glycolysis and oxidative stress, while respiration is reduced. These diversities result in metabolic modifications that include changes in signaling pathways and in the activity of transcription factors that lead to significant alterations in gene expression (Ralph et al., 2009).

One aspect of these alterations concerns the dysregulation in the supply of oxygen available to a tumor. This phenomenon occurs during the emergence of cancer, shifting cells from a normal state with sufficient nutrients and oxygen to a condition of starvation and hypoxia (Knowles et al., 2001). In response to hypoxic stress, cancer cells activate the transcription factor HIF-1 (hypoxia-inducible factor-1). This complex induces expression of vascular endothelial growth factor (VEGF), which in turn provokes the formation of new blood vessels within the tumor, and of various genes including key enzymes that increase the glycolytic pathway (Brahimi-Horn et al., 2007).

Among the genes activated by HIF-1, some are particularly important for the altered metabolic state of cancer cells. One is hexokinase II (HK), which is overexpressed and, binding to the porin-like voltage-dependent anion channel (VDAC) of the mitochondrial outer membrane, stabilizes tumor cells mitochondria, suppressing apoptosis and promoting cell survival (Mathupala et al., 2006). Two others are a lactate dehydrogenase isoform (LDH-M) and pyruvate dehydrogenase kinase (PDK-1). After activation of HIF-1, their

expression and activity become elevated, which modifies pyruvate metabolism, promoting pyruvate conversion to lactic acid in the cytosol, and reduces the production and availability of substrates required for the respiratory pathway, such as NADH and succinate (Koukourakis et al., 2005; Roche et al., 2007).

Another observed and interesting difference concerns the mitochondrial inner transmembrane potential ($\Delta\Psi_{m,i}$) which is higher in cancer cells (Modica-Napolitano et al., 2001). The possible reasons for this difference may be variations in the activity of mitochondrial respiratory complexes, electron carriers, ATP synthase, Adenine Nucleotide Translocase and/or changes in membrane lipids.

A difference of major interest concerns the production of reactive oxygen species (ROS) (Pelicano et al., 2004; Trachootham et al., 2008). ROS are defined as highly reactive oxygen-containing chemical species including free radicals, such as superoxide and hydroxyl radicals, and non-radical molecules such hydrogen peroxide. In biological systems, ROS are constantly generated through a variety of pathways, including both enzyme-catalyzed and non-enzymatic reactions. An important biochemical event associated with oxidative phosphorylation is the production of superoxide. Single electrons may escape from the mitochondrial electron transport chain, particularly when coping with overloads or blockages, and can react with molecular oxygen producing superoxide (Murphy, 2009). Superoxide radicals are constantly generated during respiration, and are mostly converted to H_2O_2 and O_2 by mitochondrial SuperOxide Dismutase (SOD). Mitochondria are considered to be the major source of cellular ROS (Halliwell and Gutteridge, 1999).

Much evidence indicates that many types of cancer cells have increased levels of ROS. The higher production of ROS may play an important role in the initiation and progress of cancer because of its relevant role for various aspects of cancer such as: immortalization and transformation; cell proliferation; survival; disruption of cell death signaling; metastasis; angiogenesis and chemoresistance.

Several potential mechanisms are thought to contribute to the increased ROS in cancer cells. Oncogenic signals have been shown to cause amplified ROS generation. For example the expression of genes associated with tumorigenic transformation, such as Ras, Bcr-Abl and c-Myc, was found to induce ROS

production, generate DNA damage, and repress p53 function (Vafa et al., 2002; Behrend et al., 2003). Another possible mechanism of ROS production enhancement may involve malfunction of the mitochondrial respiratory chain. Mitochondrial DNA mutations have been shown to be correlated with increased ROS levels in certain types of cancer cells. Because the mitochondrial respiratory chain is the major site of ROS generation, its malfunction is likely to result in more free radical production due to increased "leakage" of electrons. P53 also regulates the expression of many pro-oxidant and antioxidant genes (Sablina et al., 2005). Loss of function of p53 provokes redox imbalance, ROS stress, high mutagenesis and aggressive tumor growth. In addition extrinsic factors, such as inflammatory cytokines, imbalance of nutrients and hypoxic stress, may influence intracellular redox homeostasis as well (Cook et al., 2004; Azad et al., 2008).

An excessive level of ROS stress can on the other hand be toxic, because this overload can cause oxidative damage to lipids, protein and DNA or activate the cell apoptotic signaling pathway (Perry et al., 2000). Thus cancer cells have acquired mechanisms to avoid the potential toxic effects of elevated ROS and to promote cell-survival pathways. This redox adaptation may consist in the activation of redox-sensitive transcription factors which increase the expression of ROS-scavenging systems such as superoxide dismutase, glutathione peroxidase and catalase (Hileman et al., 2003), and may promote the expression of cell-survival molecules, such as Bcl-2 family proteins. Alterations of the function of cell death factors, such as caspases, may also be involved in redox adaptation (Chen et al., 2007).

Since cancer cells have elevated generation of ROS, which means an increased intrinsic oxidative stress, and are dependent on antioxidants for cell survival, they are more vulnerable to damage by further ROS insults induced by exogenous agents (Pelicano et al., 2004). However the redox adaptation of cancer cells may also be fundamental for drug resistance, in particular conferring an enhanced capacity to tolerate exogenous stress and insults, decreasing apoptosis and elevating the DNA repair capability (Tilgada 2006).

A noteworthy aspect of ROS is their role in the induction of apoptosis. The general mechanism whereby ROS stimulate the mitochondrial apoptotic pathway has not yet been resolved, but probably consists of effects on mobilization of

cytochrome c, activation of MPTP and, still in discussion, the translocation of Bax to mitochondria. In healthy cell, monomeric Bax is located predominantly in the cytoplasm. When an apoptotic stimulus arrives, Bax changes conformation, exposing the mitochondrial-docking motif, and migrates to the mitochondrial outer membrane where it aggregates into oligomers and stimulates apoptosis. Various lines of evidence have indicated that ROS are inducers of Bax migration (Tomiyama et al., 2006; Nie et al., 2008). A report suggests that an excess in ROS production causes dimerization of Bax in the cytosol by generating disulphide bridges between critical Cys residues and changing its conformation as a preliminary step to translocation to the OMM (D'Alessio et al., 2005). However other research (e.g. Annis et al., 2005) suggests the Bax traslocates and inserts as a monomer.

Another very important player of apoptosis is cytochrome c. This mitochondrial protein is present in the inter-membrane space where it is anchored to the inner membrane due to its affinity for the mitochondria-specific phospholipid cardiolipin. Various studies have shown that an elevated production of ROS can oxidize cardiolipin and disrupt its interaction with cytochrome c (Kagan et al., 2009). Subsequently cytochrome c can be relocalized to the cytosol via Bax oligomers and/or activation of the mitochondrial permeability transition pore (MPTP) channel.

The MPTP is a nonspecific pore, permeable to all molecules of less than approx. 1.5 kDa, which opens in the inner mitochondrial membrane in the presence of elevated Ca^{2+} concentrations and co-inducers such as phosphate, and plays an important role in cell death. Its molecular identity remains uncertain and it is modulated by a variety of pathophysiological effectors. Oxidative stress is the most relevant co-inducer, greatly sensitizing the MPTP to Ca^{2+} concentration (Halestrap, 2009).

In summary, mitochondria and mitochondrial ROS production have important roles both in carcinogenesis and in the elimination of cancerous cells by apoptosis. Furthermore, the mitochondria of cancer cells differ in some respects from those of normal cells, which in principle at least makes them possible specific therapeutic targets.

The production of ROS by mitochondria is also considered a factor in aging and in a variety of pathological situations implying that they may be counteracted by anti-oxidant compounds (Murphy, 2009; Koopman et al., 2009; Indran and Parvaiz, 2009). Given the role of ROS in cell life and death, acting on mitochondrial redox status is an attractive possibility. Considerable attention has been devoted over the past several years to the development of mitochondria-targeted antioxidants (revs.: Subramanian et al., 2009; Kagan et al., 2009; Skulachev et al., 2009; Hoye et al., 2008; Murphy, 2008; Murphy and Smith, 2007). To permit preferential accumulation into mitochondria a few strategies were developed, including conversion of a pro-drug to an active specie by specifically mitochondrial enzymes, binding to a mitochondria-specific component (e.g. cardiolipin), irreversible import via the mitochondrial protein import machinery, accumulation in response to the pH difference across the mitochondrial inner membrane. The most popular approach has been the conjugation to the membrane-permeant triphenylphosphonium cation, TPP. TPP can pass directly through phospholipid bilayers without requiring a specific uptake mechanism and accumulate substantially within mitochondria owing to the large membrane potential (Liberman et al., 1969; Ross et al., 2008). The best example of this approach is probably Mito-Q (Murphy and Smith, 2007), a ubiquinone derivative bearing the TPP moiety at the end of an aliphatic chain.

Polyphenols

Plant polyphenols are a huge and diversified family of natural compounds characterized by the presence of a few phenolic hydroxyls. They are present in a great variety of foods and, on the basis of mostly *in vitro* studies, many of them display a variety of activities of biomedical relevance. Scheme 1 shows the structures of some of the most important polyphenol subfamilies.

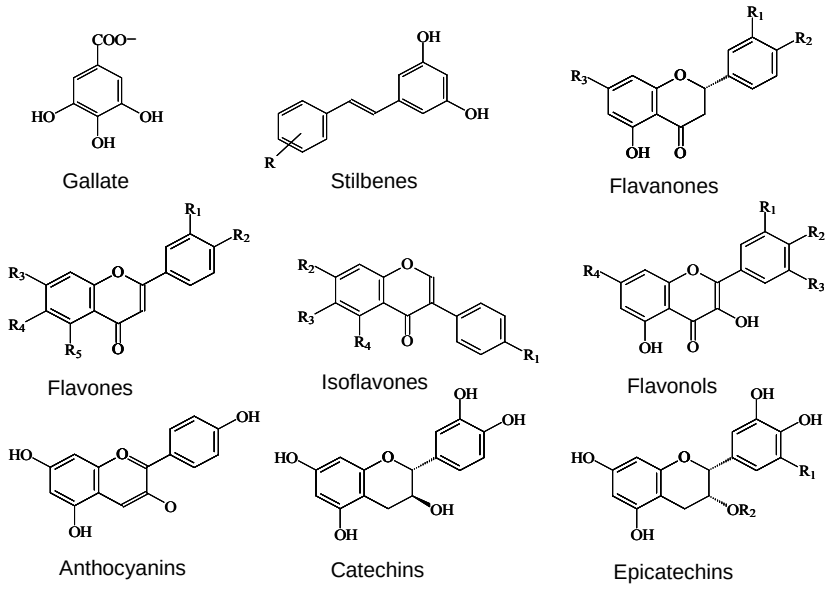

Scheme 1. Some of the most important polyphenol subfamilies

A vast scientific literature assigns them possible functions in the protection of the cardiovascular system and against neurodegeneration, in contrasting chronic inflammation and senescence in the prevention and therapy of cancers by modulation of cellular proliferation, differentiation, apoptosis and metastasis (Ramos, 2007). These biological effects are attributed to their interaction with proteins and to redox properties.

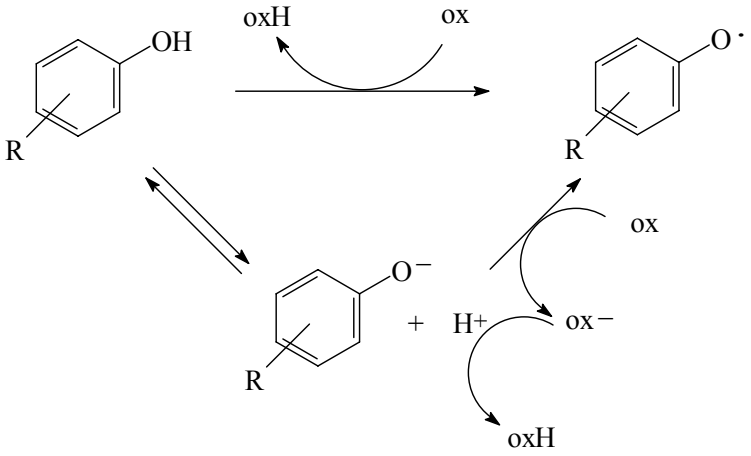

$ox = O_2^{\cdot -}$, ROO·, Cu^{2+}, Fe^{3+}, ...

Scheme 2

Polyphenols are redox active compounds, which can act as anti-oxidants or pro-oxidants depending on circumstances (Halliwell, 2008; Perron and Brumaghin, 2009). Their possible anti-oxidant role is due to the property of their aromatic structure to allow delocalization of charges or unpaired electrons, making polyphenols more acid than alcohols and good radical scavengers. This latter property may results from donation to ROS of $H^{\cdot}$ or, more probably, of an electron after deprotonation (Scheme 2). This anti-oxidant character could contrast ROS-inflicted damages and/or radical-mediated signaling, such as is believed to be involved in aging and neurodegeneration.

The ability of polyphenols to act as pro-oxidants depends on factors such as their concentration, pH, and presence of metallic ions. Indeed they can easily oxidized by Fe^{3+} or Cu^{2+} ions or by redox enzymes such as tyrosinases (which contain copper) and peroxidases (which contain iron). The oxidation of polyphenols by these ions has been studied in detail. Scheme 3 illustrates the reactions which generate $^{\cdot}OH$ with the intermediacy of Cu^{2+} (taken from Sakihama et al., 2002). Most easily oxidizable polyphenols contain a catecholic structure which can be oxidized by Cu^{2+} generating a semiquinone (reaction 1) that can react with O_2 to form $O_2^{\cdot-}$ (reaction 2). $O_2^{\cdot-}$ can oxidize the parent compound to generate another semiquinone and H_2O_2 (reaction 3). H_2O_2 can also form by the disproportionation of $O_2^{\cdot-}$ catalyzed by SOD (reaction 4). H_2O_2 is rapidly converted to the $^{\cdot}OH$ by Cu^{2+} in a Fenton-type reaction (reaction 5).

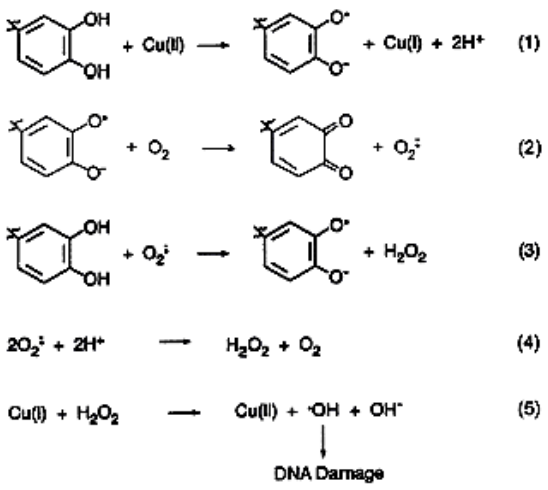

Scheme 3

The formation of $O_2^{\cdot-}$ may involve as an intermediated step the oxidation of NADH to NAD$^{\cdot}$. NAD$^{\cdot}$ cedes an electron to O_2 generating NAD^+ and $O_2^{\cdot-}$, as shown in scheme 4 (Chan et al., 1999).

$$PhO^{\cdot} + NADH \rightarrow PhOH + NAD^{\cdot}$$
$$NAD^{\cdot} + O_2 \rightarrow NAD^+ + O_2^{\cdot-}$$

Scheme 4

Another possibility (scheme 5) is glutathione (GSH) oxidation. In these cases a catalytic redox cycle may intervene, leading to a massive oxidation of GSH and NADH together with oxygen reduction (Galati et al., 1999).

$$PhO^{\bullet} + GSH \rightarrow GS^{\bullet} + PhOH$$
$$GS^{\bullet} + GS^- \rightleftharpoons GSSG^{\bullet-}$$
$$GSSG^{\bullet-} + O_2 \rightleftharpoons GSSG + O_2^{\bullet-}$$

Scheme 5

$O_2^{\cdot-}$ can be transformed to H_2O_2 by SOD or by a polyphenol or by extraction of a H· from glutathione. H_2O_2 can in turn react with Cu^+ or $Fe2^+$, oxidizing them and forming $^{\cdot}OH$ and HO^-, a Fenton reaction (scheme 6)

$$Fe^{2+} + H_2O_2 \rightarrow Fe^{3+} + {}^{\cdot}OH + HO^-$$
$$Fe^{3+} + H_2O_2 \rightarrow Fe^{2+} + {}^{\cdot}OOH + H^+$$

Scheme 6

The cytotoxic pro-oxidant mode of action is as potentially useful as the anti-oxidant one, since it might be exploited to induce death of cancerous cells.

The ambivalent redox characteristic of polyphenols has been recently demonstrated by the interaction of polyphenols (in particular quercetin) with the MPTP (De Marchi et al., 2009). Two *in vitro* experimental approaches led to apparently contradictory results. In patch clamp experiments, conducted with only a few mitoplasts bathed in a medium without metal ions, oxidizable polyphenols

induced MPT channel closure. In swelling experiments with suspension of mitochondria, high concentrations of quercetin, the best inhibitor of the channel in the previous type of experiments, promoted MPTP activation. The presence of $Fe^{2+/3+}$ and $Cu^{+/2+}$ chelators counteracted this activation demonstrating that these ions, released by the dense suspension of mitochondria, were involved in the generation of ROS and in the activation of MPTP.

Aside from their redox activity the interactions of polyphenols with proteins are of major importance. Various polyphenols are known to modulate directly numerous proteins, including metalloproteinases, membrane receptors, channels (e.g. CFTR), cyclooxygenases, transcription factors, deacetylases (sirtuins), cytoskeleton components (tubulin) and many kinases (e.g. Cdk1 and Cdk4) as well as proteins of the blood (albumin, haemoglobin), some toxins (anthrax toxin, VacA) and pro- or anti-apoptotic proteins. However, the necessary concentration levels are often not reached in a physiological setting.

Indeed, a major obstacle for the biomedical/pharmacological exploitation of polyphenols is their low bioavailability. They are rapidly sulfated, glucuronidated and methylated by enterocytes, then mostly re-exported to the intestinal lumen. The fraction entering circulation is rapidly metabolized by liver enzymes and subsequently eliminated by the urinary and biliary systems. Only low concentration of polyphenols are present in plasma even after a polyphenol-rich meal and mostly in the form of conjugates (Manach et al., 2005; Iyanagi 2007).

The project

Since ROS are mostly produced in mitochondria, this organelle is the most appropriate target subcellular location for exerting the redox effect of polyphenols. Part of my thesis work has therefore dealt with the development of derivatives of quercetin and resveratrol incorporating the popular mitochondria-targeting TPP group. We have verified that these compounds accumulate, as expected, into isolated or in situ mitochondria (Mattarei et al., 2008; Biasutto et al., 2008; chapts. 5 and 6). The effects of the quercetin-based mitochondriotropic derivatives on isolated mitochondria have been assessed as a first logical step in understanding/predicting their action in vivo (Biasutto et al., 2010; chapt 7). Their impact on cultured cells has been assessed in cytotoxicity tests (chapt. 8).

5. A Mitochondriotropic Derivative of Quercetin: A Strategy to Increase the Effectiveness of Polyphenols

DOI: 10.1002/cbic.200800162

A Mitochondriotropic Derivative of Quercetin: A Strategy to Increase the Effectiveness of Polyphenols

Andrea Mattarei,[a] Lucia Biasutto,[a, b] Ester Marotta,[a] Umberto De Marchi,[b] Nicola Sassi,[b] Spiridione Garbisa,[b] Mario Zoratti,*[b, c] and Cristina Paradisi[a]

Mitochondria-targeted compounds are needed to act on a variety of processes that take place in these subcellular organelles and that have great pathophysiological relevance. In particular, redox-active molecules that are capable of homing in on mitochondria provide a tool to intervene on a major cellular source of reactive oxygen species and on the processes they induce, notably the mitochondrial permeability transition and cell death. We have linked the 3-OH of quercetin (3,3′,4′,5,7-pentahydroxy flavone), a model polyphenol, and the triphenylphosphonium moiety, a membrane-permeant cationic group, to produce proof-of-principle mitochondriotropic quercetin derivatives. The remaining hydroxyls were sometimes acetylated to hinder metabolism and improve solubility. The new compounds accumulate in mitochondria in a transmembrane potential-driven process and are only slowly metabolised by cultured human colon cells. They inhibit mitochondrial ATPase activity much as quercetin does, and are toxic for fast-growing cells.

Introduction

Polyphenols are a large family of natural compounds exhibiting, at least in vitro, a variety of biomedically important activities. A vast literature documents their potential relevance for such major healthcare endeavours as protection of the cardiovascular[1] and nervous[2] systems, the prevention and therapy of cancer,[1,3] counteracting senescence,[2,4] reducing chronic inflammation[4,5] and lengthening the lifespan of model organisms.[6–8]

These effects are attributed in part to direct interactions of polyphenols with proteins, and in part to their redox properties as reducing agents and ROS (reactive oxygen species) scavengers, that is, antioxidants.[9,10] This antioxidant character has been proposed to underlie the alleged antagonistic effects of polyphenols on ROS-inflicted damage and/or radical-mediated signalling, such as aging and neurodegeneration.[11,12] The level of reactive polyphenol attainable at the site of action is of obvious importance: cells normally maintain redox homeostasis with a mM-range pool of molecules such as glutathione. To have a measurable effect as general reducing agents, polyphenols should therefore reach concentrations that are on the same order of magnitude.

Mitochondria are the subcellular compartment in which most ROS are produced, and are the site of key events in both apoptosis and necrosis. Oxidative processes are of major importance in both cases.[13–15] In apoptosis, for example, oxidation of cardiolipin is needed for the release of cytochrome c.[15] The ROS-induced mitochondrial permeability transition (MPT)[16,17] is now believed to have a fundamental role in necrotic death, such as occurs upon reoxygenation following ischemia.[18,19] Enhanced ROS production is the common theme of mitochondrial dysfunction.[20,21]

A new sector of pharmacology targets mitochondria to prevent or induce, as the case may be, cell death.[22–25] The control of mitochondrial redox processes is an attractive perspective in this context, and the development of drugs capable of accumulating specifically in mitochondria—"mitochondriotropic" compounds—is of obvious importance for such an effort. Important progress in this direction has been made by exploiting the matrix-negative voltage difference of about 180 mV that is maintained by energised mitochondria across their inner membrane. Compounds formed by a redox-active part, which is linked to a membrane-permeant permanent cation (usually triphenylphosphonium, TPP), accumulate in regions that are held at negative potential, that is, the cytoplasm and the mitochondrial matrix.[25,26] Importantly, no significant toxic effects of these compounds have been observed in vivo.[25]

We reasoned that polyphenol–TPP conjugates might act as antioxidants in vivo and be useful for counteracting "basal" ROS production and long-term effects such as chronic inflammation and neurodegeneration. Furthermore, they might find application against acute pathologies, for example those caused by ischemia. Antioxidants (and MPT inhibitors) would be expected to counteract this process, and indeed this seems

[a] *A. Mattarei,[+] L. Biasutto,[+] Dr. E. Marotta, Prof. C. Paradisi*
Department of Chemical Sciences, Università di Padova
via Marzolo 1, 35131 Padova (Italy)

[b] *L. Biasutto,[+] Dr. U. De Marchi, N. Sassi, Prof. S. Garbisa, Dr. M. Zoratti*
Department of Biomedical Sciences, Università di Padova
viale G. Colombo 3, 35121 Padova (Italy)

[c] *Dr. M. Zoratti*
CNR Institute of Neuroscience, c/o Department of Biomedical Sciences
Università di Padova, viale G. Colombo 3, 35121 Padova, (Italy)
Fax: (+39) 049-8276049
E-mail: zoratti@bio.unipd.it

[+] *These authors contributed equally to this work.*

Supporting information for this article is available on the WWW under http://www.chembiochem.org or from the author.

to be the case.[14,24,27] In a relevant piece of work, the mitochondriotropic antioxidant decylquinone–TPP ($MitoQ_{10}$) was administered to rats before explanting the hearts and subjecting them to ischemia and reperfusion (I/R).[28] Treatment resulted in a significant reduction of the necrotic area. A similar protective effect was afforded by high doses of intravenous resveratrol in models of cerebral[29] and cardiac[30] ischemia.

Polyphenols can also induce a potentiation, rather than a reduction, of oxidative and radical chain processes, that is, they might act as "pro-oxidants".[31–33] Which behaviour predominates depends on the abundance of metal ions capable of maintaining a redox cycle and/or of redox-active enzymes, such as tyrosinases ("polyphenol oxidases") and peroxidases, on the ion-chelating properties of the polyphenols themselves, and on pH. Additional factors could include the concentration of the polyphenol[33] and even the subcellular compartment involved.[34] Depending on such factors and on the particular polyphenol involved, polyphenol–TPP conjugates might act as cytotoxic, apoptosis or necrosis-inducing pro-oxidants.

The pro-oxidant mode of action is as potentially useful as the antioxidant one, because it can be exploited to induce the death of unwanted, that is, cancerous, cells. Cancer cells live under oxidative stress,[35] which, in principle, makes them more vulnerable to ROS-mediated damage. Cell death and/or MPT induction by "redox-cycling" compounds, such as menadione or adriamycin, are well known, and antitumour, mitochondrion-targeted, pro-oxidant-based chemotherapeutic approaches have been proposed.[36,37] In vivo it might be possible to focus the action on cancerous cells because in many tumour types, the mitochondria maintain a higher transmembrane potential than in normal tissue.[22,38,39] This approach has already been used in pioneering pharmacological work.[22,40,41] Mitochondriotropic polyphenols might provide significant oncological benefits also if they turn out to act as antioxidants. Recent studies have shown that mitochondrial ROS production is an important determinant of the metastatic potential of cancerous cells,[42] and that polyphenols are capable of reducing cell shedding from tumour masses.[43]

The sheer number and variety of properties of natural polyphenols, their varied reactivity and the relevance of the pathophysiological processes for which they offer promise, suggest that mitochondriotropic polyphenol derivatives could find clinically relevant applications that are not necessarily limited to circumstances that involve redox processes.

Here we report the proof-of-principle synthesis, characterisation and initial biological assessment of triphenylphosphonium-comprising derivatives of quercetin, a widely used model polyphenol.

Results

Quercetin (**1**) and the potentially useful target mitocondriotropic derivatives considered in this work are shown in Scheme 1.

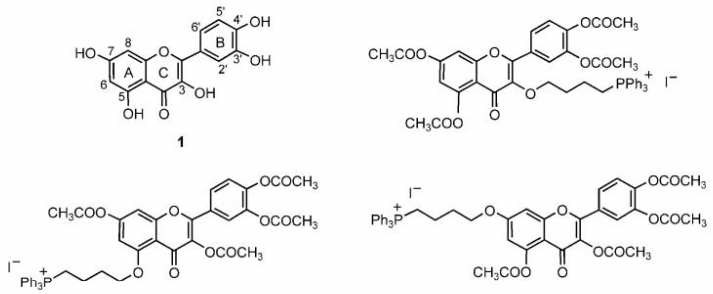

Scheme 1. Quercetin (**1**) and potentially useful target mitocondriotropic derivatives.

Such derivatives were identified on the basis of the following considerations: 1) the hydroxyls of quercetin provide convenient sites to connect—through an ether bond—with a linker that bears the TPP group; 2) because the catecholic hydroxyls determine to a large extent the redox properties of quercetin, they should be maintained as such in the target derivative. The connection to the TPP group ought therefore to involve one of the hydroxyls on the A or C rings; 3) to hinder metabolism and limit the formation of negative charges due to conjugation or ionisation, it was desirable to protect the remaining hydroxyls with groups expected to be rapidly removed by cellular enzymes, such as acetyl moieties. Moreover, hydroxyl groups are also in part responsible for the well-known tendency of polyphenols to form colloidal particles, and for unspecific interactions with proteins. The introduction of the TPP group and the protection of the hydroxyls were thus also expected to increase the low solubility of quercetin and possibly to counteract its notorious tendency to bind to proteins such as haemoglobin and albumin.[44,45] In conclusion, any of the three isomeric derivatives shown in Scheme 1, or even any mixture of them, were in principle useful candidates.

Synthesis

Following the strategy outlined in Scheme 2, we succeeded in synthesising the target derivative **7** with the TPP-bearing linker on the C ring of quercetin. Briefly, the sequence involves protection of the catecholic hydroxyls, selective O-alkylation to introduce a chloroalkyl group, unblocking of the catecholic hydroxyls, acetylation and introduction of the TPP group by nucleophilic substitution on the chloroalkyl linker. The nonacetylated derivative **9** was prepared in a similar manner from **4**.

Ketal **2** was readily obtained by following the procedure of Bouktaib et al.[46] with only small modifications. The reaction of **2** with 1.2 equiv of 1-bromo-4-chlorobutane in the presence of

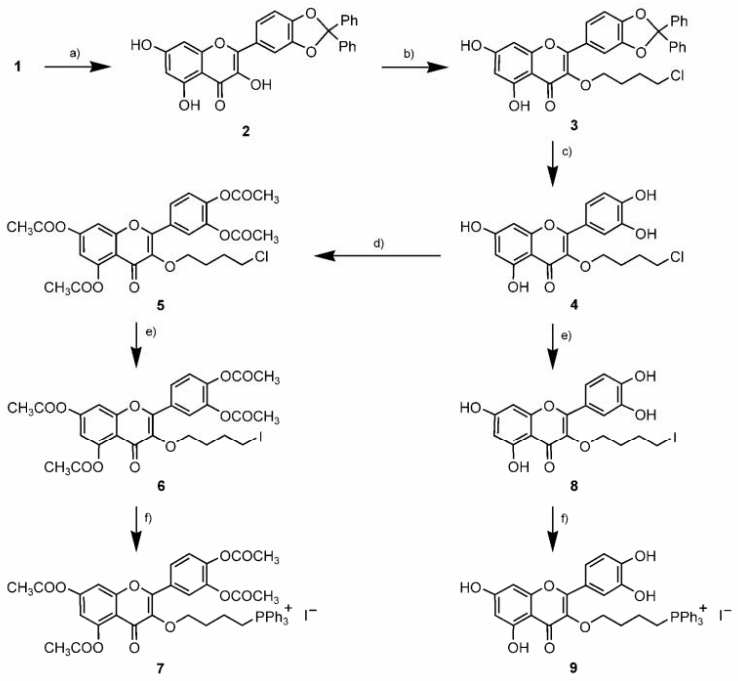

Scheme 2. Synthesis of mitochondriotropic derivatives **7** and **9**. a) Ph_2CCl_2 (3 equiv), 180 °C, 10 min; b) 1-bromo-4-chlorobutane (1.2 equiv), K_2CO_3 (1.3 equiv), DMF, Ar, room temperature, 20 h; c) AcOH/H_2O 8:2, reflux, 2 h; d) $CH_3C(=O)Cl$, pyridine, room temperature, 24 h; e) NaI, acetone, reflux, 20 h; f) PPh_3, 95 °C, 6 h.

K_2CO_3 yielded **3** in reasonably good yield (45% after purification). The assignment of the site of O-alkylation in **3** was based on NMR spectroscopic data. Specifically, the presence of a characteristically narrow NMR peak at approximately 12 ppm indicates the presence of the slowly exchanging proton of the hydroxyl at C5.[47,48] To distinguish the two remaining possibilities, that is, alkylation at C3 or at C7, either of which would have been a useful outcome in this study, we went on to unblock **3** and to compare the NMR chemical shifts of the ring protons of the resulting product, **4**, with those of **1**. We found that the presence of a $-O(CH_2)_4Cl$ group in place of an –OH group does not affect the chemical shifts of H6 and H8, whereas a considerable difference is observed for H2′ and H6′; this indicates that the substitution is at C3 (see Table S1 in the Supporting Information).

Deprotection of the catecholic hydroxyls (Scheme 2, step c) according to a literature procedure[46] gave the desired product **4** in 80% yield after purification. Careful control of the progress of the reaction was required to avoid hydrolysis of the ether linkage. Acetylation of the free hydroxyls in **4** (Scheme 2, step d), gave the chloro derivative **5**. NMR spectroscopic analysis of this intermediate provided additional support for the attribution of the O-alkylation site to C3: comparison of the NMR spectra of **5** and of penta-acetylquercetin showed significant differences in the chemical shifts of ring protons H2′ and H6′; this confirms that C3 was the site of O-alkylation (Table S2). A similar analysis was not possible for the final product **7** due to heavy spectral interferences by the TPP group.

Compound **5** was converted to **7** via the iodo derivative **6**. This indirect route avoided the high temperature necessary for direct reaction of triphenylphosphine with the primary chloro derivative, which caused some decomposition. Compound **4** was converted to **9** in a similar manner.

Solubility in water

The solubility of **7** in water was $(4.96 \pm 0.21) \times 10^{-4}$ mol L^{-1} as determined by spectrophotometric measurements (see the Experimental Section). This solubility is at least 200-fold higher than that of quercetin.[49] This derivative thus satisfies the requirement of increased solubility in aqueous media. The solubility of **9** turned out to be less than 2 μM, presumably because the free hydroxyls facilitate the formation of large aggregates. Because this concentration is too low for recording fluorescence spectra and performing metabolism studies, solutions for those experiments were prepared in HBSS (Hank's balanced saline solution) that contained 0.1% DMSO.

Stability in aqueous solution

Both **7** and **9** are stable for at least 24 h in deionised H_2O, as determined by spectrophotometric and HPLC analysis. Compound **9** is also stable in 90% HBSS, 10% CH_3CN (added to ensure solubility of the reaction products), while in this medium **7** undergoes very slow hydrolysis of the protective acetyl groups (Figure 1).

Metabolism

We assayed metabolism of **1**, **7** and **9** by HCT116 cells, that is, the cells that were used in the experiments concerning mitochondriotropic behaviour (see below). HPLC and LC–MS analysis of the culture medium and cell extracts (see the Experimental section) showed that **1** and **9** were metabolised only to a very limited extent by these cells over a period of 8 h. Modification consisted in the introduction of a methyl group. In anal-

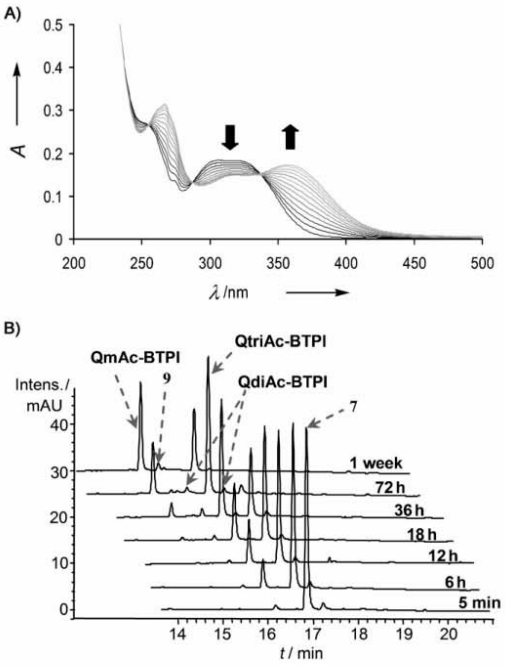

Figure 1. Hydrolysis of **7** in HBSS/CH_3CN (9:1). A) UV/Vis spectra were recorded every 6 h for 72 h. B) HPLC traces were recorded at 300 nm at different reaction times. Abbreviations: QmAc-BTPI: acetyl-3-(4-*O*-triphenylphosphoniumbutyl) quercetin iodide; QdiAc-BTPI: diacetyl-3-(4-*O*-triphenylphosphoniumbutyl) quercetin iodide; QtriAc-BTPI: triacetyl-3-(4-*O*-triphenylphosphoniumbutyl) quercetin iodide.

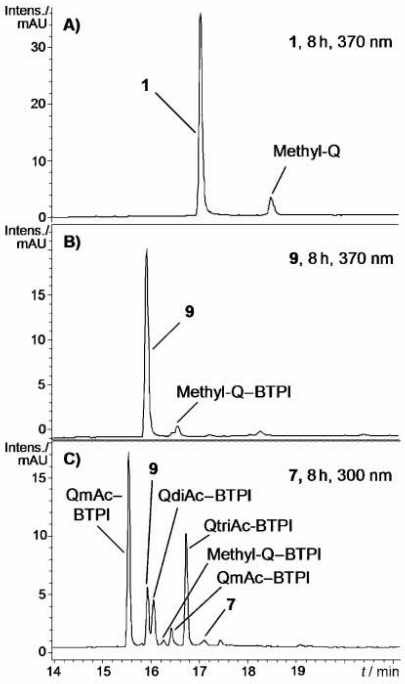

Figure 2. HPLC chromatograms that were recorded at 300 or 370 nm, as indicated, for the extracts obtained after 8 h of incubation of: A) **1**, B) **9** and C) **7** with HCT116 cells. See the Experimental Section for details. Abbreviations as in Figure 1; methyl-Q: methylquercetin; methyl-Q-BTPI: methyl-3-(4-*O*-triphenylphosphoniumbutyl) quercetin iodide.

ogous experiments, **7** was progressively deacylated with the eventual transformation of most of it into the monoacylated compound, but it also underwent little conjugation. Figure 2 shows representative HPLC chromatograms.

Mitochondriotropic behaviour

We verified that compounds **7** and **9** indeed accumulate in mitochondria by two methods. In the first approach we monitored their uptake by isolated, respiring rat liver mitochondria using a TPP-sensitive electrode (Experimental Section).[50] A representative experiment with **7** is shown in Figure 3. The introduction of mitochondria causes a decrease (upward deflection of the trace) of the concentration of our compounds in the incubation medium because they become partly sequestered in the mitochondrial matrix. The subsequent addition of excess Ca^{2+} induces the mitochondrial permeability transition, with loss of mitochondrial transmembrane potential ($\Delta\psi_m$) and release of the TPP derivatives. Release is also induced by the addition of a $\Delta\psi_m$-dissipating protonophore (carbonyl cyanide *p*-trifluoromethoxyphenylhydrazone, FCCP; Figure S1). The accumulation ratio, that is, the fraction of compound that is

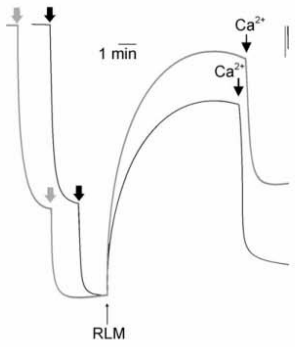

Figure 3. Accumulation of tetraphenylphosphonium (Ph_4P^+; black trace) and **7** (grey trace) by rat liver mitochondria (RLM). Thick arrows indicate the addition of 0.16 μM $Ph_4P^+I^-$ or **7** to the medium (200 mM sucrose, 10 mM HEPES/K^+, 5 mM succinate/K^+, 1 mM NaH_2PO_4, (1.25×10^{-3}) mM rotenone, pH 7.4). Addition of RLM (1 mg protein mL^{-1}) and of $CaCl_2$ (40 μM) are also shown. The traces have been normalised to take into account the different response of the electrode in the two cases, which is quantified by the bars in the upper right corner.

taken up by the organelles, differs somewhat from one compound to the other. This can be attributed to different extents of binding to mitochondrial constituents (lipids, proteins, nucleic acids), which is well known to cause apparent deviations from Nernst's law. This interpretation is supported by the observation that "excess" **7** taken up is retained also after depolarisation. Analogous results were obtained with compound **9** (not shown).

In the second approach we exploited the fluorescence of **7** (Figure S5) to follow its accumulation in the mitochondria of cultured cells (Figure 4). The spectral properties of the compound, which are similar to those of quercetin itself (Figures S2–S5), allowed its fluorescence to be monitored upon excitation in the near-UV (380 nm; Experimental Section). Mitochondria can be easily recognised by their characteristic granulated/filamentous morphology and perinuclear distribution. After the addition of **7** to the medium, their weak autofluorescence due to pyridine nucleotides is progressively overwhelmed by the much more intense signal that is due to accumulation of the quercetin derivative (panels B–D). Addition of FCCP causes the rapid release of **7** (and partially deacylated derivatives) from the mitochondrial matrix (panels E–F). Some of it remains in the cytoplasm of the cells due to the presence of a cytoplasm-negative voltage difference, which is maintained by K^+ diffusion, across the plasma membrane. Complete series of images showing the uptake and release of the compound in an analogous experiment are available as Supporting Information. Compound **9** is expected to behave in the same manner, but its low fluorescence quantum yield (Figure S5) hindered the observation of its accumulation in mitochondria in situ.

We compared the inhibition by quercetin, **7** and **9** of the activity of the mitochondrial ATPase. The results were in good agreement with previous reports of an inhibition by quercetin with an IC_{50} in the 50 μM range,[51] and showed that the introduction of the linker and TPP groups did not have a major effect on its activity (Figure 5).

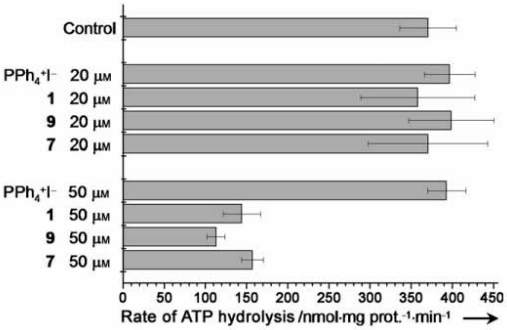

Figure 5. Effects of **7**, **9**, quercetin and tetraphenylphosphonium on the rate of ATP hydrolysis by permeabilised rat liver mitochondria. See the Experimental Section for details. Determinations were carried out in triplicate and averages ± s.d. are reported.

As a preliminary test of possible anticancer activity, we also verified the effects of these compounds, and, as controls, of the parent polyphenol quercetin, of two phosphonium salts and of quercetin plus these latter compounds on cultured cells. We used the murine colon cancer cell line C-26 and, as controls, fast- and slow-growing nontumour mouse embryonic fibroblast cell lines (MEF). Cell growth and viability was quantified by using the tetrazolium salt reduction (MTT) assay. As illustrated by Figure 6A, the various compounds had little effect on C-26 cell proliferation at 1 μM. At 5 μM, quercetin, with or without $Ph_4P^+I^-$ or TPMP (triphenylmethylphosphonium chloride), significantly hindered cell growth, whereas the phosphonium salts by themselves remained innocuous. The mitochondriotropic quercetin derivatives displayed marked cytotoxicity. A similar pattern was followed with a rapidly growing line of cells of nontumour origin, that is, SV-40 immortalised mouse embryo fibroblasts (MEF; Figure 6B); none of the compounds tested had a significant effect, either at 1 or 5 μM, on a distinct, slower-growing MEF line (Figure 6C, and data not shown). Alternative protocols—in which the various compounds were provided only once at the beginning of the three-day period or were added every day (thus reaching formal final concentrations of 3 or 15 μM)—gave results that were in line with those of the substitution protocol (not reported).

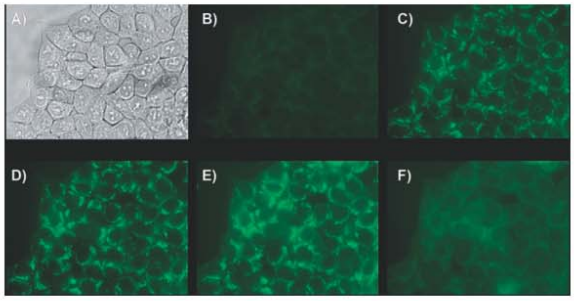

Figure 4. $\Delta\psi_m$-dependent accumulation of compound **7** in the mitochondria of cultured HCT116 cells. A) Phase contrast image taken shortly before the start of the sequential automatic acquisition of 20 fluorescence images that were taken 1 min apart. About 20 s after the first image was recorded, **7** was added to give a final concentration of 4 μM. B–D) Fluorescence images of the same field, taken approximately 0.7, 10 and 20 min, respectively, after the addition of **7**. The compound accumulates in perinuclear organelles that have mitochondrial morphology. E–F) Images recorded approximately 1 and 10 min, respectively, after the subsequent addition of 2 μM FCCP—a classic $\Delta\psi_m$-dissipating protonophore (uncoupler). The fluorescence is released from the mitochondria and diffuses into the cytoplasm. Video clips showing the complete image sequences of fluorescence uptake and release in a similar experiment are available as Supporting Information.

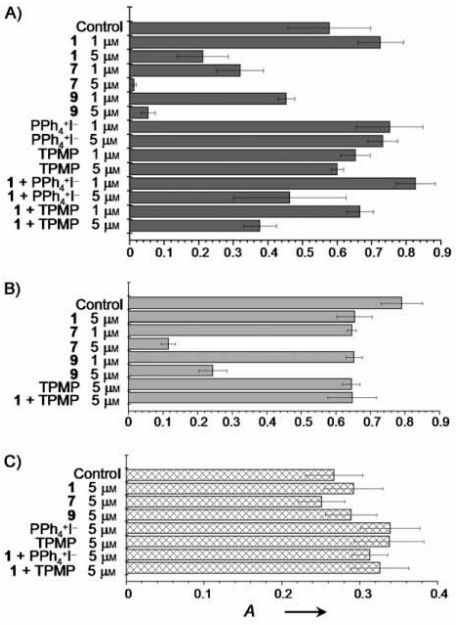

Figure 6. Effect of the mitochondriotropic quercetin derivatives and control compounds on the readout of tetrazolium reduction cell proliferation assays. Cells were allowed to grow for three days in the presence of the specified compounds (see the Experimental Section for details). The panels show the results of individual experiments that are representative of four (A, C) or three (B) similar ones. All measurements were performed in quadruplicate; averages ± s.d. are given. A) C-26 mouse colon tumour cells. B) Fast-growing mouse embryonic fibroblasts (MEF). C) Slow-growing MEF (note different scale).

Discussion

We have synthesised the target compound **7** as well as its non-acylated analogue **9** from the natural polyphenol quercetin (**1**). Both carry a TPP group at the end of a four-carbon, saturated linker connected through an ether bond at C3 of the quercetin skeleton. Both **7** and **9** exhibit the expected mitochondriotropic behaviour. Because a cytoplasm-negative voltage difference also exists across the plasma membrane, the charged compounds are also more concentrated in the cytoplasm than in the surrounding medium. This is best appreciated in fluorescence images taken after protonophore-induced release from the mitochondria, for example, in Figures 4 E and F.

As an initial verification of whether the modifications introduced had altered the pharmacological properties of the quercetin ring system, we compared their activity as mitochondrial F_0F_1 ATPase inhibitors to that of quercetin. The latter is known to inhibit the enzyme,[51] presumably as a consequence of its binding to a site in the F_1 portion, which has been characterised by X-ray crystallography of the enzyme–polyphenol complex.[52] In our assays the mitochondrial membranes had been permeabilised with alamethicin. Therefore, no transmembrane electrical potential could be maintained, no accumulation of mitochondriotropic compounds could occur, and inhibition was expected to take place with similar dose dependence unless the substituent(s) interfered. No such major interference was revealed (Figure 5). Compounds **7** and **9** behave similarly; this suggests that interactions with the aromatic core of the molecule are most relevant for binding and inhibition. ATP synthase inhibition is thus expected to take place upon accumulation of mitochondriotropic polyphenols in mitochondria, and it might well contribute to their overall effects on cells and organisms.

Compounds **7** and **9** behave as cytostatic/cytotoxic agents against fast-growing, but not against slow-growing cells in culture (Figure 6). This mode of action is characteristic of many chemotherapeutic agents. Inhibition of ATP synthesis might obviously be a component of this cytotoxic action. Another tentative mechanism might be that a fraction of the positively charged derivatives associates with mitochondrial DNA due to charge interactions. Quercetin itself is known to form covalent bonds to DNA.[53,54] This might result in a cytotoxic or cytostatic effect that may be more relevant in the case of fast-dividing cells, such as cancerous cells. It should at any rate be emphasised that the parent compound, quercetin, and phosphonium cations ($PPh_4^+I^-$ and TPMP), alone or in combination, have much weaker toxic effects. Clearly the activity of quercetin–TPP conjugates in this case is not simply the sum of the activities of quercetin and $PPh_4^+I^-$.

These and related new compounds will be available for specific tests of their properties in vivo. Their production opens interesting perspectives because, in principle, they can either quench or promote radical oxidative processes. Thus, a class of natural compounds with useful properties can now be targeted to subcellular compartments where they ought to realise their biomedical potential in full.

Experimental Section

Materials and instrumentation: Starting materials and reagents were purchased from Aldrich, Fluka, Merck–Novabiochem, Riedel de Haen (Seelze, Germany), J. T. Baker (Deventer, The Netherlands), Cambridge Isotope Laboratories Inc. (Andover, MA, USA), Acros Organics (New Jersey, USA), Carlo Erba (Milano, Italy) and Prolabo (Fontenay sous Bois, France), and were used as received. The ^1H and ^{13}C NMR spectra were recorded with a Bruker AC 250F spectrometer operating at 250 MHz for ^1H NMR and 62.9 MHz for ^{13}C NMR. Chemical shifts (δ) are given in ppm, and the residual solvent signal was used as an internal standard. LC–MS analyses and mass spectra were performed with a 1100 Series Agilent Technologies system equipped with binary pump (G1312A) and MSD SL Trap mass spectrometer (G2445D SL) with ion trap detector and ESI source. Accurate mass measurements were obtained by using a Mariner ESI-TOF mass spectrometer (PerSeptive Biosystems). TLCs were run on silica gel that was supported on plastic (Macherey–Nagel Polygram®SIL G/UV_{254}, silica thickness 0.2 mm), or on silica gel that was supported on glass (Fluka; silica thickness 0.25 mm, granulometry 60 Å, medium porosity) and were visualised by UV detection. Flash chromatography was performed on silica gel (Macherey–Nagel 60, 230–400 mesh granulometry (0.063–0.040 mm)) under air pressure. The solvents were of analytical or synthetic

grade and were used without further purification. HPLC–UV analyses for assessing the purity of the compounds synthesised were performed by a Thermo Separation Products Inc. system with a P2000 Spectra System pump and a UV6000 LP diode array detector (190–500 nm). UV/Vis spectra were recorded at 25 °C with a Perkin–Elmer Lambda 5 spectrophotometer equipped with water-thermostated cell holders. Fluorescence spectra were recorded at 25 °C with a Perkin–Elmer LS-55 spectrofluorimeter equipped with a Hamamatsu R928 photomultiplier and thermostated cell holder. Quartz cells with an optical pathlength of 1 cm were used for measurements of both absorption and fluorescence spectra.

Synthesis procedures

*3′,4′-O-Diphenylmethane quercetin (**2**)*: The protection of quercetin catechol ring was carried out by a slight modification of the procedure by Bouktaib et al.[46] Briefly, compound **1** (3.0 g, 8.9 mmol, 1 equiv) and dichlorodiphenylmethane (5.1 mL, 27 mmol, 3 equiv) were mixed and heated at 180 °C for 10 min. The residue was diluted in minimal CH_2Cl_2, sonicated and purified by flash chromatography by using CH_2Cl_2/EtOAc (95:5) as eluent to afford **2** in 67% yield. ^{1}H NMR (250 MHz, [D$_6$]DMSO): δ = 6.22 (d, J = 2.0 Hz, 1H; Ar), 6.49 (d, J = 2.0 Hz, 1H; Ar), 7.20 (d, J = 8.0 Hz, 1H; H5′), 7.39–7.60 (m, 10H; Ar), 7.78–7.86 (m, 2H; H2′, H6′), 9.68 (brs, 1H; OH), 10.87 (brs, 1H; OH), 12.41 ppm (s, 5-OH); ESI-MS (ion trap): *m/z*: 466 $[M+H]^+$.

*3′,4′-O-Diphenylmethane-3-(4-O-chlorobutyl) quercetin (**3**)*: K_2CO_3 (0.75 g, 5.4 mmol, 1.3 equiv) and 1-bromo-4-chlorobutane (0.86 g, 5.0 mmol, 1.2 equiv) were added under argon to a solution of **2** (1.94 g, 4.16 mmol) in DMF (10 mL). After stirring overnight, the mixture was diluted in CH_2Cl_2 (30 mL) and washed with distilled H_2O (3×50 mL). The organic layer was dried over $MgSO_4$ and filtered. The solvent was evaporated under reduced pressure, and the residue was purified by flash chromatography by using EtOAc/petroleum ether (3:7) as eluent to afford **3** in 45% yield. ^{1}H NMR (250 MHz, $CDCl_3$): δ = 1.84 (m, 4H; CH_2), 3.46 (t, 2H; CH_2), 3.94 (t, 2H; CH_2), 6.32 (d, J = 2.0 Hz, 1H; Ar), 6.42 (d, J = 2.0 Hz, 1H; Ar), 6.98 (d, J = 8.25 Hz, 1H; H5′), 7.34–7.44 (m, 5H; Ar), 7.55–7.69 (m, 7H; Ar), 12.60 ppm (s, 5-OH); ^{13}C NMR (62.9 MHz, [D$_6$]DMSO): δ = 27.0 (CH_2), 28.9 (CH_2), 45.2 (CH_2Cl), 71.5 (OCH_2), 94.1, 98.9, 104.5, 108.8, 109.1, 117.5, 124.2, 124.3, 126.0, 128.8, 129.8, 137.4, 139.4, 146.8, 148.7, 155.4, 156.6, 161.4, 164.5, 178.2 ppm (C4); ESI-MS (ion trap): *m/z*: 557, $[M+H]^+$; HRMS (ESI-TOF): *m/z*: calcd for $C_{32}H_{26}O_7Cl$: 557.1362 $[M+H]^+$; found: 557.1329.

*3-(4-O-Chlorobutyl) quercetin (**4**)*: The catechol ring protection was removed according to the procedure employed by Bouktaib et al. for analogous quercetin derivatives.[46] Briefly: compound **3** (1.0 g, 1.80 mmol) was dissolved in a mixture of acetic acid/H_2O (4:1; 50 mL) and the solution was heated at reflux for 2 h. Then H_2O (100 mL) and EtOAc (50 mL) were added and the organic layer was collected, washed with sat. aq $NaHCO_3$ solution (100 mL) and dried over $MgSO_4$. After filtration, the solvent was evaporated under reduced pressure, and the residue was purified by flash chromatography by using $CHCl_3$/acetone (8:2) as solvent to afford **4** in 80% yield. ^{1}H NMR (250 MHz, [D$_6$]DMSO): δ = 1.82 (m, 4H; CH_2), 3.66 (t, 2H; CH_2), 3.94 (t, 2H; CH_2), 6.19 (d, J = 1.75 Hz, 1H; Ar), 6.40 (d, J = 1.75 Hz, 1H; Ar), 6.89 (d, J = 8.25 Hz, 1H; H5′), 7.44 (dd, J = 8.25, 2.0 Hz, 1H; H6′), 7.51 (d, J = 2.0 Hz, 1H; H2′,), 12.72 ppm (s, 5-OH); ^{13}C NMR (62.9 MHz, [D$_6$]DMSO): δ = 27.0 (CH_2), 28.9 (CH_2), 45.3 (CH_2Cl), 71.3 (OCH_2), 93.8, 98.7, 104.4, 115.7, 115.8, 120.9, 121.1, 136.8, 145.4, 148.8, 156.2, 156.6, 161.5, 164.3, 178.2 ppm (C4); ESI-MS (ion trap): *m/z*: 393, $[M+H]^+$; HRMS (ESI-TOF): *m/z*: calcd for $C_{19}H_{18}O_7Cl$: 393.0736 $[M+H]^+$; found: 393.0736.

*3′,4′,5,7-Tetra-acetyl-3-(4-O-chlorobutyl) quercetin (**5**)*: Acetyl chloride (1.1 mL, 15 mmol, 20 equiv) was added dropwise and under continuous stirring to a mixture of **4** (300 mg, 0.76 mmol, 1 equiv) and anhydrous pyridine (0.85 mL, 7.6 mmol, 10 equiv), which was cooled in a bath of dry ice/acetone (−78 °C). A white precipitate (pyridinium chloride) formed immediately. The mixture was subsequently allowed to warm to room temperature and stirred overnight. Then CH_2Cl_2 (50 mL) was added, and the organic layer was washed with 0.5 N HCl (3×50 mL) and H_2O (2×30 mL). The organic solution was dried over $MgSO_4$ and filtered. The solvent was evaporated under reduced pressure and the residue was purified by flash chromatography by using CH_2Cl_2/petroleum ether/EtOAc (6:3:1) as eluent to afford the acetylated product **5** in 78% yield. ^{1}H NMR (250 MHz, $CDCl_3$): δ = 1.85 (m, 4H; CH_2), 2.33 (m, 9H; OAc), 2.45 (s, 3H; OAc), 3.56 (t, 2H; CH_2), 3.99 (t, 2H; CH_2), 6.82 (d, J = 2.25 Hz, 1H; Ar), 7.30 (d, J = 2.25 Hz, 1H; Ar), 7.35 (d, J = 8.5 Hz, 1H; H5′), 7.92 (d, J = 2.0 Hz, 1H; H2′), 7.96 ppm (dd, J = 8.5, 2.0 Hz, 1H; H6′); ^{13}C NMR (62.9 MHz, [D$_6$]DMSO): δ = 20.5 (CH_3), 20.6 (CH_3), 21.1 (CH_3), 26.9 (CH_2), 28.8 (CH_2), 45.3 (CH_2Cl), 71.5 (OCH_2), 110.0, 114.2, 114.9, 124.0, 124.3, 127.1, 128.6, 140.4, 142.2, 144.1, 149.6, 153.1, 154.1, 156.3, 168.3 (C=O), 168.4 (C=O), 168.6 (C=O), 169.1 (C=O), 172.5 ppm (C4); ESI-MS (ion trap): *m/z*: 561, $[M+H]^+$; HRMS (ESI-TOF): *m/z*: calcd for $C_{27}H_{26}O_{11}Cl$: 561.1158 $[M+H]^+$; found: 561.1120.

*3′,4′,5,7-Tetra-acetyl-3-(4-O-iodobutyl) quercetin (**6**)*: Compound **5** (100 mg, 0.18 mmol, 1 equiv) was added to a sat. solution of NaI in anhydrous acetone (10 mL) and heated at reflux for 20 h. After cooling, the resulting mixture was diluted in $CHCl_3$ (30 mL), filtered and washed with H_2O (3×30 mL). The organic layer was dried over $MgSO_4$ and filtered. The solvent was evaporated under reduced pressure to afford **6** in 86% yield. ^{1}H NMR (250 MHz, $CDCl_3$): δ = 1.74–2.00 (m, 4H; CH_2), 2.35 (m, 9H; OAc), 2.47 (m, 3H; OAc), 3.22 (m, 2H; CH_2), 3.99 (m, 2H; CH_2), 6.83 (m, 1H; Ar), 7.32 (m, 2H; Ar), 7.95 ppm (m, 2H; H2′, H6′); ^{13}C NMR (62.9 MHz, [D$_6$]DMSO): δ = 8.6 (CH_2I), 20.6 (CH_3), 21.1 (CH_3), 29.7 (CH_2), 30.4 (CH_2), 71.1 (OCH_2), 110.0, 114.2, 114.9, 124.0, 124.3, 127.1, 128.6, 140.4, 142.2, 144.1, 149.6, 153.1, 154.1, 156.3, 168.3 (C=O), 168.4 (C=O), 168.6 (C=O), 169.0 (C=O), 172.5 ppm (C4); ESI-MS (ion trap): *m/z*: 653, $[M+H]^+$; HRMS (ESI-TOF): *m/z*: calcd for $C_{27}H_{26}O_{11}I$: 653.0514 $[M+H]^+$; found: 653.0521.

*3′,4′,5,7-Tetra-acetyl-3-(4-O-triphenylphosphoniumbutyl) quercetin iodide (**7**)*: A mixture of **6** (100 mg, 0.15 mmol) and triphenylphosphine (200 mg, 0.76 mmol, 5 equiv) in toluene (10 mL) was heated at 95 °C under argon. After 6 h, the solvent was eliminated under reduced pressure and the resulting white solid was dissolved in the minimum volume of CH_2Cl_2 (1 mL) and precipitated with diethyl ether (50 mL). The solvent was decanted and the precipitation was repeated five times. Residual solvent was then removed under reduced pressure to afford compound **7** in 72% yield and 96–98% purity. The small amount of impurities consisted of a triacetyl derivative and of an isomer of **7**. ^{1}H NMR (250 MHz, [D$_6$]DMSO): δ = 1.62–1.96 (m, 4H; CH_2), 2.17 (s, 3H; OAc), 3.32 (m, 9H; OAc), 3.68 (t, 2H; CH_2), 4.00 (t, 2H; CH_2), 7.10 (d, J = 2.25 Hz, 1H; Ar), 7.34 (d, J = 9.25 Hz, 1H; H5′), 7.62 (d, J = 2.25 Hz, 1H; Ar), 7.72–8.04 ppm (m, 17H; H2′, H6′); ^{13}C NMR (62.9 MHz, [D$_6$]DMSO): δ = 18.3 (CH_2), 19.6 (CH_2), 20.5 (CH_3), 20.6 (CH_3), 20.9 (CH_3), 21.1 (CH_3), 29.5 (CH_2), 70.3 (OCH_2), 110.1, 114.3, 114.8, 118.6 (Ph, J(^{13}C/^{31}P) = 85.9 Hz), 123.8, 124.1, 127.1, 128.5, 130.5 (Ph, J(^{13}C/^{31}P) = 12.4 Hz), 133.7 (Ph, J(^{13}C/^{31}P) = 10.1 Hz), 135.1 (Ph, J(^{13}C/^{31}P) = 2.8 Hz), 140.2, 142.2, 144.1, 149.5, 153.1, 154.1, 156.2, 168.2 (C=O), 168.4 (C=O), 168.6 (C=O), 168.9 (C=O), 172.7 ppm (C4); ESI-MS (ion trap): *m/z*: 787,

$[M]^+$; HRMS (ESI-TOF): *m/z*: calcd for $C_{45}H_{40}O_{11}P^+$ 787.2303 $[M]^+$; found: 787.2346

*3-(4-O-Iodobutyl) quercetin (**8**)*: Compound **4** (100 mg, 0.25 mmol, 1 equiv) was added to a saturated solution of NaI in dry acetone (10 mL) and heated at reflux for 20 h. After cooling, the resulting mixture was diluted in $CHCl_3$ (30 mL), filtered and washed with H_2O (3×30 mL). The organic layer was dried over $MgSO_4$ and filtered. The solvent was evaporated under reduced pressure to afford the product in 87% yield. ^{1}H NMR (250 MHz, [D$_6$]DMSO): δ = 1.72 (quintet, 2H; CH_2), 1.88 (quintet, 2H; CH_2), 3.29 (t, 2H; CH_2), 3.92 (t, 2H; CH_2), 6.18 (d, J = 1.95 Hz, 1H; Ar,), 6.39 (d, J = 1.95 Hz, 1H; Ar), 6.88 (d, J = 8.3 Hz, 1H; H5′), 7.43 (dd, J = 8.3, 1.95 Hz, 1H; H6′), 7.51 ppm (d, J = 2.0 Hz, 1H; H2′); ^{13}C NMR (62.9 MHz, [D$_6$]DMSO): δ = 8.7 (CH_2I), 29.8 (CH_2), 30.5 (CH_2), 70.9 (OCH_2), 93.8, 98.7, 104.4, 115.6, 115.8, 120.9, 121.0, 136.8, 145.4, 148.8, 156.2, 156.6, 161.5, 164.3, 178.2 ppm (C4); ESI-MS (ion trap): *m/z*: 485, $[M+H]^+$; HRMS (ESI-TOF): *m/z*: calcd for $C_{19}H_{18}O_7I$: 485.0092 $[M+H]^+$; found: 485.0060.

*3-(4-O-Triphenylphosphoniumbutyl) quercetin iodide (**9**)*: A mixture of **8** (100 mg, 0.21 mmol) and triphenylphosphine (275 mg, 1.05 mmol, 5 equiv) in toluene (15 mL) was heated at 95 °C under argon. After 6 h, the solvent was evaporated at reduced pressure, and the resulting yellow solid was dissolved in a minimal volume of CH_2Cl_2 (1 mL) and precipitated with diethyl ether (5×50 mL). The solvents were decanted after each precipitation. Residual solvent was then removed under reduced pressure to afford compound **9** in 73% yield. ^{1}H NMR (250 MHz, [D$_6$]DMSO): δ = 1.65 (quintet, 2H; CH_2), 1.84 (quintet, 2H; CH_2), 3.63 (t, 2H; CH_2), 3.96 (t, 2H; CH_2), 6.18 (d, J = 2.0 Hz, 1H; Ar), 6.39 (d, J = 2.0 Hz, 1H; Ar), 6.74 (d, J = 8.4 Hz, 1H; H5′), 7.33 (dd, J = 8.4, 2.0 Hz, 1H; H6′), 7.44 (d, J = 2.0 Hz, 1H; H2′), 7.50–7.93 ppm (m, 15H; Ar); ^{13}C NMR (62.9 MHz, [D$_6$]DMSO): δ = 18.6 (CH_2), 19.6 (CH_2), 29.7 (CH_2), 70.4 (OCH_2), 93.8, 98.8, 104.3, 115.5, 115.7, 118.6 (Ph, J(^{13}C/^{31}P) = 85.8 Hz), 120.9, 121.0, 130.4 (Ph, J(^{13}C/^{31}P) = 12.4 Hz), 133.7 (Ph, J(^{13}C/^{31}P) = 10.1 Hz), 135.1 (Ph, J(^{13}C/^{31}P) = 2.8 Hz), 136.6, 145.4, 148.8, 156.1, 156.5, 161.4, 164.4, 178.1 ppm (C4); ESI-MS (ion trap): *m/z*: 619 $[M]^+$; HRMS (ESI-TOF): *m/z*: calcd for $C_{37}H_{32}O_7P^+$ 619.1882 $[M]^+$; found: 619.1893.

Solubility in water: Seven standard solutions of **7** within the concentration range 2–6×10^{-5} M were prepared by diluting a 10^{-3} M mother solution, which was in H_2O/CH_3CN (9:1), with water. The absorbance of each solution was measured at 300 nm, which corresponds to a plateau region in the UV absorption spectrum of **7**, and the spectra were plotted against concentration. Linear regression analysis of the data points yielded a slope of (1.244 ± 0.009)×10^4. This curve (Figure S6) was used to interpolate the concentration of an aqueous saturated solution of **7**, which was prepared by vigorously stirring **7** (2 mg) in H_2O (1 mL). After sedimentation, the clear supernatant (200 μL) was added to H_2O (3 mL) and the absorbance of the resulting solution was measured at 300 nm. Three repetitions of this experiment yielded an average value of A = 0.379 ± 0.011, from which a concentration of (3.23 ± 0.06)×10^{-5} M was interpolated by using the calibration curve. By correcting for the dilution factor, a solubility of (4.96 ± 0.21)×10^{-4} mol L^{-1} was obtained.

Chemical stability studies: The chemical stability of compounds **7** and **9** in H_2O and in HBSS buffer at 25 °C was tested by following changes in the UV/Vis spectra between 190 and 500 nm and by HPLC analysis of samples that were withdrawn at different reaction times. The reaction was initiated by adding a freshly prepared CH_3CN solution of the compound of interest (100 μL) to HBSS/CH_3CN (9:1; 3 mL) to give a final concentration in the μM range. The composition of HBSS was: NaCl (136.9 mM), KCl (5.36 mM), $CaCl_2$ (1.26 mM), $MgSO_4$ (0.81 mM), KH_2PO_4 (0.44 mM), Na_2HPO_4 (0.34 mM), glucose (5.55 mM), pH 7.4 (adjusted with NaOH). Spectral changes were followed with a Perkin–Elmer Lambda 5 spectrophotometer (PerkinElmer) equipped with water-thermostated cell holders. Quartz cells with an optical path of 1 cm were used for all measurements. HPLC analyses were performed with the Thermo Separation Products Inc. system by using a reversed-phase column (Gemini C18, 3 μm, 150×4.6 mm i.d.; Phenomenex, (Utrecht, The Netherlands). Solvents A and B were H_2O that contained 0.1% HCOOH and CH_3CN, respectively. The gradient for B was as follows: 10% for 5 min, then from 10 to 100% in 20 min; the flow rate was 0.7 mL min^{-1}. The eluate was preferentially monitored at 300 nm.

Mitochondria: Rat liver mitochondria were isolated by conventional differential centrifugation procedures[55] from fasted male albino Wistar rats that weighed approximately 300 g and had been raised in the local facilities. The standard isolation medium was sucrose (250 mM), HEPES (5 mM, pH 7.4) and EGTA (1 mM); EGTA was omitted in the final resuspension step. The protein content was measured by the biuret method with bovine serum albumin as a standard.[56] The experiments were performed with the permission and supervision of the University of Padova Central Veterinary Service, which acts as Institutional Animal Care and Use Committee and certifies compliance with Italian Law DL 116/92, embodying UE Directive 86/609. No accreditation registry for experimentation on vertebrates exists in Italy.

TPP-selective electrode: The setup used to monitor the concentration of TPP-bearing compounds in solution was built in-house following published procedures.[57,58] A calomel electrode was used as reference and the potentiometric output was directed to a strip chart recorder. The experiments illustrated by Figures 3 and S1 were conducted in a water-jacketed cell at 20 °C. The suspension medium contained sucrose (200 mM), HEPES (10 mM), succinate (5 mM), phosphate (1 mM), rotenone (1.25 μM), pH 7.4 (adjusted with KOH).

Cells: Human colon tumour (HCT116) cells,[59] which were kindly provided by B. Vogelstein, as well as fast- and slow-growing SV-40 immortalised mouse embryo fibroblast (MEF) cells (kindly provided by L. Scorrano and W. J. Craigen, respectively) and mouse colon cancer C-26 cells were grown in Dulbecco's Modified Eagle Medium (DMEM) that contained HEPES buffer (10 mM), foetal calf serum (10%, *v/v*; Invitrogen), penicillin G (100 U mL^{-1}, Sigma), streptomycin (0.1 mg mL^{-1}, Sigma), glutamine (2 mM, GIBCO) and nonessential amino acids (1%, 100× solution; GIBCO), and incubated in a humidified atmosphere of 5% CO_2 at 37 °C.

Metabolism studies: HCT116 cells were seeded onto a 12-well plate, and allowed to grow to about 80% of confluence. They were then washed with warm HBSS, and incubated for the specified periods with 1 mL per well of 20 μM solutions of **7**, **9** or quercetin. The compounds were used as aliquots from 20 mM freshly made stock solutions in DMSO, which were diluted in HBSS just prior to adding the resulting solution to the washed cells. Medium and cells were collected together after 1, 3, 6 and 8 h of incubation. Acetic acid (100 μL, 0.6 M) and fresh ascorbic acid (100 μL, 10 mM) solutions were added, and the samples were immediately stored at −20 °C until treatment and analysis. Treatment consisted of the addition of acetone (1 mL), followed by sonication (2 min), filtration through 0.45 μm PTFE syringe filters (Phenomenex) and concentration under N_2. HPLC analyses were performed with the Agilent Technologies system by using a diode array detector that

operated from 190 to 500 nm (G1315B) and the ion trap mass spectrometer with ESI source. Mass spectra were acquired in positive-ion mode operating in full-scan from *m/z* 100 to 1500. The HPLC protocol was the same as that employed for the chemical stabilities studies.

Fluorescence microscopy: HCT116 cells were sown onto 24 mm round coverslips and allowed to grow for 48 h. The coverslips were then washed with HBSS, mounted into supports, covered with HBSS (1 mL) and placed onto the microscope stage. The imaging apparatus consisted of an Olympus IX71 microscope equipped with an MT20 light source and CellR© software. The excitation wavelength was 380 nm and fluorescence was collected in the 500–550 nm range in the images shown in Figure 4. Sequential images were automatically recorded by following a pre-established protocol. The acquisition and display parameters of all fluorescence images shown were the same, that is, fluorescence intensities can be compared.

ATP hydrolysis assays: The enzymatically coupled NADH oxidation assay was used.[60] Mitochondria (0.25 mg protein mL^{-1}) were incubated for about 1 min in sucrose (250 mM), Tris-HCl (10 mM), EGTA–Tris (20 μM), NaH_2PO_4 (1 mM), $MgCl_2$ (6 mM), rotenone (2 μM), pH 7.6, with phosphoenolpyruvate (PEP; 1 mM), NADH (0.1 mM), alamethicin (20 μM), pyruvate kinase (PK; 20 units), lactate dehydrogenase (LDH; 50 units), all of which were from Sigma, together with the desired compound in a thermostated (25 °C), magnetically stirred cuvette in an Aminco DW-2000 UV/Vis spectrophotometer operating in the dual-wavelength mode. Membrane-permeabilising alamethicin was used to measure ATPase activity without the potential kinetic complications associated with transmembrane transport of the adenine nucleotides.[61] Differential absorbance at 340–372 nm was sampled every 0.6 s. The reaction was started by the addition of ATP (0.5 mM). In this assay, the ADP that was formed by ATP hydrolysis was rephosphorylated by PK to generate pyruvate as the other product. Pyruvate was reduced to lactate by LDH by using NADH, which was oxidised to NAD with a decrease in absorbance, which was the parameter that was monitored. Rates of hydrolysis were determined as the best linear fit of the data.

Cell growth/viability (MTT) assays: C-26 or MEF cells were seeded in standard 96-well plates and allowed to grow in DMEM (200 μL) for 24 h to ensure attachment. In the experiments shown in Figure 6 initial densities were 1000 (C-26, fast MEF) or 2000 (slow MEF) cells per well. The growth medium was then replaced with medium that contained the desired compound from a mother solution in DMSO. The DMSO final concentration was 0.1% in all cases (including controls). Four wells were used for each of the compounds to be tested. The solution was substituted by a fresh aliquot twice, at intervals of 24 h. At the end of the third 24 h period of incubation with the compounds, the medium was removed, cells were washed with PBS, and 100 μL of CellTiter 96® solution (Promega; for details see: http://www.promega.com/tbs) was added. After 1 h colour development at 37 °C, absorbance at 490 nm was measured by using a Packard Spectra Count 96-well plate reader.

Acknowledgements

We thank F. Mancin for useful discussions, P. Bernardi, V. Petronilli and A. Toninello for access to instrumentation, V. Petronilli, A. Angelin, M. E. Soriano and D. Dal Zoppo for operational instructions, B. Vogelstein, L. Scorrano and W. J. Craigen for the cells. This work was supported in part by grants from the Italian Association for Cancer Research (AIRC) and the Italian Foundation for Basic Research (FIRB; M.Z.) and by a fellowship of the Fondazione Cassa di Risparmio di Padova e Rovigo (to L.B.).

Keywords: drug design · mitochondria · natural products · phenols · quercetin

[1] S. Shankar, G. Singh, R. K. Srivastava, *Front. Biosci.* **2007**, *12*, 4839–4854.
[2] J. A. Joseph, B. Shukitt-Hale, F. C. Lau, *Ann. N.Y. Acad. Sci.* **2007**, *1100*, 470–485.
[3] S. Shankar, S. Ganapathy, R. K. Srivastava, *Front. Biosci.* **2007**, *12*, 4881–4899.
[4] N. Labinskyy, A. Csiszar, G. Veress, G. Stef, P. Pacher, G. Oroszi, J. Wu, Ungvari, *Curr. Med. Chem.* **2006**, *13*, 989–996.
[5] N. H. Nam, *Mini-Rev. Med. Chem.* **2006**, *6*, 945–951.
[6] J. A. Baur, D. A. Sinclair, *Nat. Rev. Drug Discov.* **2006**, *5*, 493–506.
[7] D. R. Valenzano, E. Terzibasi, T. Genade, A. Cattaneo, L. Domenici, A. Cellerino, *Curr. Biol.* **2006**, *16*, 296–300.
[8] S. Quideau, *ChemBioChem* **2004**, *5*, 427–430.
[9] W. Bors, C. Michel, *Ann. N.Y. Acad. Sci.* **2002**, *957*, 57–69.
[10] H. E. Seifried, D. E. Anderson, E. I. Fisher, J. A. Milner, *J. Nutr. Biochem.* **2007**, *18*, 567–579.
[11] O. Weinreb, S. Mandel, T. Amit, M. B. Youdim, *J. Nutr. Biochem.* **2004**, *15*, 506–516.
[12] S. Mandel, T. Amit, L. Reznichenko, O. Weinreb, M. B. Youdim, *Mol. Nutr. Food Res.* **2006**, *50*, 229–234.
[13] H. U. Simon, A. Haj-Yehia, F. Levi-Schaffer, *Apoptosis* **2000**, *5*, 415–418.
[14] J. Neuzil, C. Widén, N. Gellert, E. Swettenham, R. Zobalova, L. F. Dong, X. F. Wang, C. Lidebjer, H. Dalen, J. P. Headrick, P. K. Witting, *Redox Rep.* **2007**, *12*, 148–162.
[15] S. Orrenius, *Drug Metab. Rev.* **2007**, *39*, 443–455.
[16] M. Zoratti, I. Szabò, *Biochim. Biophys. Acta* **1995**, *1241*, 139–176.
[17] A. Rasola, P. Bernardi, *Apoptosis* **2007**, *12*, 815–833.
[18] A. P. Halestrap, S. J. Clarke, S. A. Javadov, *Cardiovasc. Res.* **2004**, *61*, 372–385.
[19] F. Di Lisa, P. Bernardi, *Cardiovasc. Res.* **2006**, *70*, 191–199.
[20] K. C. Kregel, H. J. Zhang, *Am. J. Physiol. Regul. Integr. Comp. Physiol.* **2007**, *292*, R18–R36.
[21] D. C. Wallace, *Annu. Rev. Genet.* **2005**, *39*, 359–407.
[22] V. R. Fantin, P. Leder, *Oncogene* **2006**, *25*, 4787–4797.
[23] L. Galluzzi, N. Larochette, N. Zamzami, G. Kroemer, *Oncogene* **2006**, *25*, 4812–4830.
[24] S. S. Sheu, D. Nauduri, M. W. Anders, *Biochim. Biophys. Acta* **2006**, *1762*, 256–265.
[25] M. P. Murphy, R. A. J. Smith, *Annu. Rev. Pharmacol. Toxicol.* **2007**, *47*, 629–656.
[26] H. M. Cochemé, G. F. Kelso, A. M. James, M. F. Ross, J. Trnka, T. Mahendiran, J. Asin-Cayuela, F. H. Blaikie, A.-R. B. Manas, C. M. Porteous, V. J. Adlam, R. A. J. Smith, M. P. Murphy, *Mitochondrion* **2007**, *7*, S94-S102.
[27] C. P. Baines, R. A. Kaiser, N. H. Purcell, N. S. Blair, H. Osinska, M. A. Hambleton, E. W. Brunskill, M. R. Sayen, R. A. Gottlieb, G. W. Dorn, J. Robbins, J. D. Molkentin, *Nature* **2005**, *434*, 658–662.
[28] V. J. Adlam, J. C. Harrison, C. M. Porteous, A. M. James, R. A. Smith, M. P. Murphy, I. A. Sammut, *FASEB J.* **2005**, *19*, 1088–1095.
[29] Q. Wang, J. Xu, G. E. Rottinghaus, A. Simonyi, D. Lubahn, G. Y. Sun, A. Y. Sun, *Brain Res.* **2002**, *958*, 439–447.
[30] M. Shen, G. L. Jia, Y. M. Wang, H. Ma, *Vascul. Pharmacol.* **2006**, *45*, 122–126.
[31] G. Galati, T. Chan, B. Wu, P. J. O'Brien, *Chem. Res. Toxicol.* **1999**, *12*, 521–525.
[32] E. J. Choi, K. M. Chee, B. H. Lee, *Eur. J. Pharmacol.* **2003**, *482*, 281–285.
[33] M. Kanadzu, Y. Lu, K. Morimoto, *Cancer Lett.* **2006**, *241*, 250–255.
[34] H. Raza, A. John, *Toxicol. Appl. Pharmacol.* **2005**, *207*, 212–220.
[35] H. Pelicano, D. Carney, P. Huang, *Drug Resist. Updates* **2004**, *7*, 97–110.
[36] J. Neuzil, X.-F. Wang, L.-F. Dong, P. Low, S. J. Ralph, *FEBS Lett.* **2006**, *580*, 5125–5129.
[37] J. S. Armstrong, *Br. J. Pharmacol.* **2006**, *147*, 239–248.

[38] L. B. Chen, *Annu. Rev. Cell Biol.* **1988**, *4*, 155–181.
[39] B. Kadenbach, *Biochim. Biophys. Acta* **2003**, *1604*, 77–94.
[40] V. R. Fantin, P. Leder, *Cancer Res.* **2004**, *64*, 329–336.
[41] V. R. Fantin, M. J. Berardi, L. Scorrano, S. J. Korsmeyer, P. Leder, *Cancer Cell* **2002**, *2*, 29–42.
[42] K. Ishikawa, K. Takenaga, M. Akimoto, N. Koshikawa, A. Yamaguchi, H. Imanishi, K. Nakada, Y. Honma, J. Hayashi, *Science* **2008**, *320*, 661–664.
[43] S. Günther, C. Ruhe, M. G. Derikito, G. Böse, H. Sauer, M. Wartenberg, *Cancer Lett.* **2007**, *250*, 25–35.
[44] H. M. Rawel, K. Meidtner, J. Kroll, *J. Agric. Food Chem.* **2005**, *53*, 4228–4235.
[45] M. I. Kaldas, U. K. Walle, H. van der Woude, J. M. McMillan, T. Walle, *J. Agric. Food Chem.* **2005**, *53*, 4194–4197.
[46] M. Bouktaib, S. Lebrun, A. Atmani, C. Rolando, *Tetrahedron* **2002**, *58*, 10001–10009.
[47] P. Op de Beck, M.-G. Dijoux, G. Cartier, A.-M. Mariotte, *Phytochemistry* **1998**, *47*, 1171–1173.
[48] I. M. Rietjens, H. M. Awad, M. G. Boersma, M. L. van Iersel, J. Vervoort, P. J. Van Bladeren, *Adv. Exp. Med. Biol.* **2001**, *500*, 11–21.
[49] L. Biasutto, E. Marotta, U. De Marchi, M. Zoratti, C. Paradisi, *J. Med. Chem.* **2007**, *50*, 241–253.
[50] M. P. Murphy, K. S. Echtay, F. H. Blaikie, J. Asin-Cayuela, H. M. Cochemè, K. Green, J. A. Buckingham, E. R. Taylor, F. Hurrell, G. Hughes, S. Miwa, C. E. Cooper, D. A. Svistunenko, R. A. Smith, M. D. Brand, *J. Biol. Chem.* **2003**, *278*, 48534–48545.
[51] J. Zheng, V. D. Ramirez, *Br. J. Pharmacol.* **2000**, *130*, 1115–1123.
[52] J. R. Gledhill, M. G. Montgomery, A. G. Leslie, J. E. Walker, *Proc. Natl. Acad. Sci. USA* **2007**, *104*, 13632–13637.
[53] T. Walle, T. S. Vincent, U. K. Walle, *Biochem. Pharmacol.* **2003**, *65*, 1603–1610.
[54] H. van der Woude, G. M. Alink, B. E. van Rossum, K. Walle, H. van Steeg, T. Walle, I. M. C. M. Rietjens, *Chem. Res. Toxicol.* **2005**, *18*, 1907–1916.
[55] H. G. Hogeboon, W. C. Schneider, *J. Biol. Chem.* **1953**, *204*, 233–238.
[56] A. G. Gornall, C. J. Bardawill, M. M. David, *J. Biol. Chem.* **1949**, *177*, 751–766.
[57] N. Kamo, M. Muratsugu, R. Hongoh, Y. Kobatake, *J. Membr. Biol.* **1979**, *49*, 105–121.
[58] M. Zoratti, M. Favaron, D. Pietrobon, V. Petronilli, *Biochim. Biophys. Acta Bioenerg.* **1984**, *767*, 231–239.
[59] L. Zhang, J. Yu, B. H. Park, K. W. Kinzler, B. Vogelstein, *Science* **2000**, *290*, 989–992.
[60] S. Luvisetto, D. Pietrobon, G. F. Azzone, *Biochemistry* **1987**, *26*, 7332–7338.
[61] See for example: I. S. Gostimskaya, V. G. Grivennikova, T. V. Zharova, L. E. Bakeeva, A. D. Vinogradov, *Anal. Biochem.* **2003**, *313*, 46–52.

Received: March 14, 2008
Published online on October 6, 2008

CHEMBIOCHEM

Supporting Information

for

A Mitochondriotropic Derivative of Quercetin: A Strategy to Increase the Effectiveness of Polyphenols

Andrea Mattarei, Lucia Biasutto, Ester Marotta, Umberto De Marchi, Nicola Sassi, Spiridione Garbisa, Mario Zoratti*, and Cristina Paradisi

Table S1. Chemical shifts (δ) and, enclosed in parenthesis, chemical shift changes (Δδ) of the aromatic protons of quercetin (**1**) and 3-(4-O-chlorobutyl) quercetin (**4**) in [D_6]DMSO for the assignment of the O-alkylation site.

Compound	Chemical shifts (δ) and chemical shifts changes ($\Delta\delta$)				
	δ(H-6)	δ(H-8)	δ(H-5')	δ(H-6')	δ(H-2')
Quercetin (1)	6.194	6.405	6.887	6.544	7.683
Compound 4	6.189 (-0.005)	6.397 (-0.008)	6.893 (+0.006)	7.436 (+0.892)	7.514 (-0.169)

The data in Table S1 show that while the chemical shift of H-6, H-8, H-5' are very similar in **4** and in **1**, those of H-2' and H-6' differ significantly, thus suggesting that O-alkylation has occurred at C-3. Table S2 shows that similar trends are found for pentaacetylquercetin and 3',4',5,7-tetraacetyl-3-(4-O-chlorobutyl) quercetin (**5**) thus supporting the assignment of C-3 as the site of O-alkylation.

Table S2. Chemical shifts (δ) and, enclosed in parenthesis, chemical shift changes ($\Delta\delta$) in $CDCl_3$ of the aromatic protons of pentaacetylquercetin and of compound **5**, for the assignment of the O-alkylation site.

Compound	Chemical shifts (δ) and chemical shifts changes (Δδ)				
	δ(H-6)	δ(H-8)	δ(H-5')	δ(H-6')	δ(H-2')
Pentaacetylquercetin	6.876	7.333	7.351	7.717	7.690
Compound 5	6.822 (-0.054)	7.297 (-0.036)	7.346 (-0.005)	7.975 (+0.258)	7.919 (+0.229)

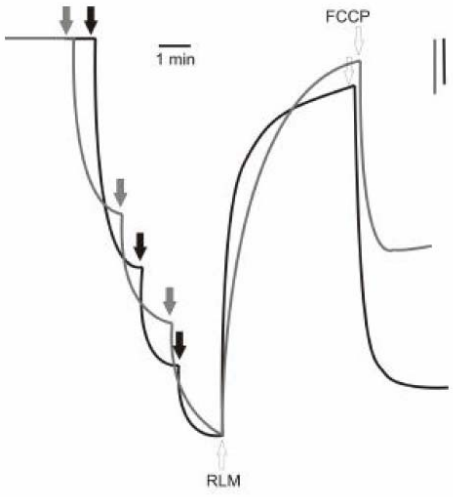

Figure S1. Accumulation of tetraphenylphosphonium (Ph_4P^+) (black) and 3',4',5,7-tetraacetyl-3-(4-O-triphenylphosphoniumbutyl) quercetin iodide (**7**) (gray) by rat liver mitochondria (RLM). Thick arrows indicate the addition of 0.067 µM $Ph_4P^+I^-$ or **7** to the medium (in mM: sucrose 200, HEPES/K^+ 10, succinate/K^+ 5, NaH_2PO_4 1, rotenone $1.25x10^{-3}$; pH 7.4). Addition of RLM (1 mg prot.·mL^{-1}) causes upward deflection of the traces since respiring mitochondria develop a matrix-negative transmembrane potential, and thus take up the positively charged, permeant compounds, which also bind in part to mitochondrial components. Addition of FCCP (in this experiment 0.33 µM), a classic $\Delta\psi_m$-dissipating protonophore (uncoupler), causes extensive release of the compounds. The traces have been normalized to take into account the different response of the electrode in the two cases, which is quantified by the bars in the upper right corner.

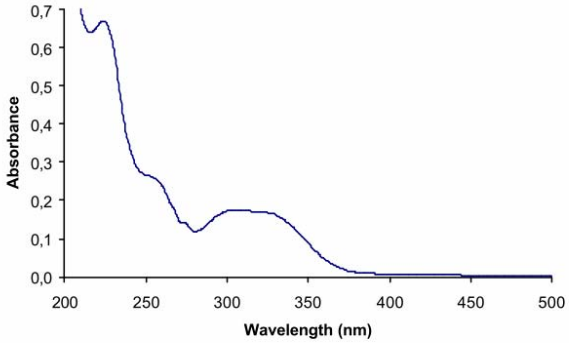

Figure S2. UV/Vis spectrum of **7** (20 µM) in HBSS:CH_3CN 9:1.

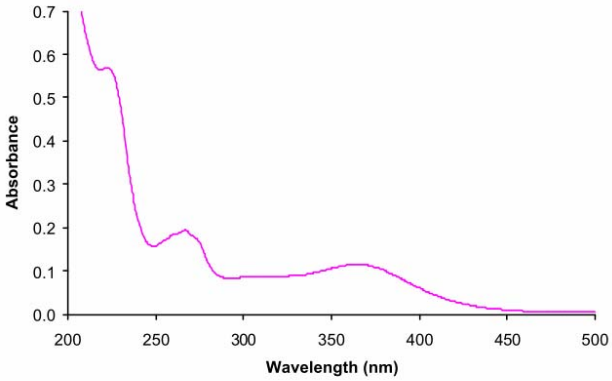

Figure S3. UV/Vis spectrum of 3-(4-O-triphenylphosphoniumbutyl) quercetin iodide (**9**; 10 µM) in HBSS:CH_3CN 9:1.

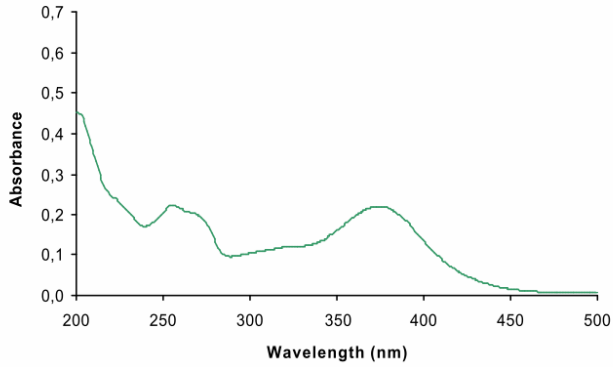

Figure S4. UV-Vis spectrum of quercetin (16 µM) in HBSS:CH_3CN 9:1.

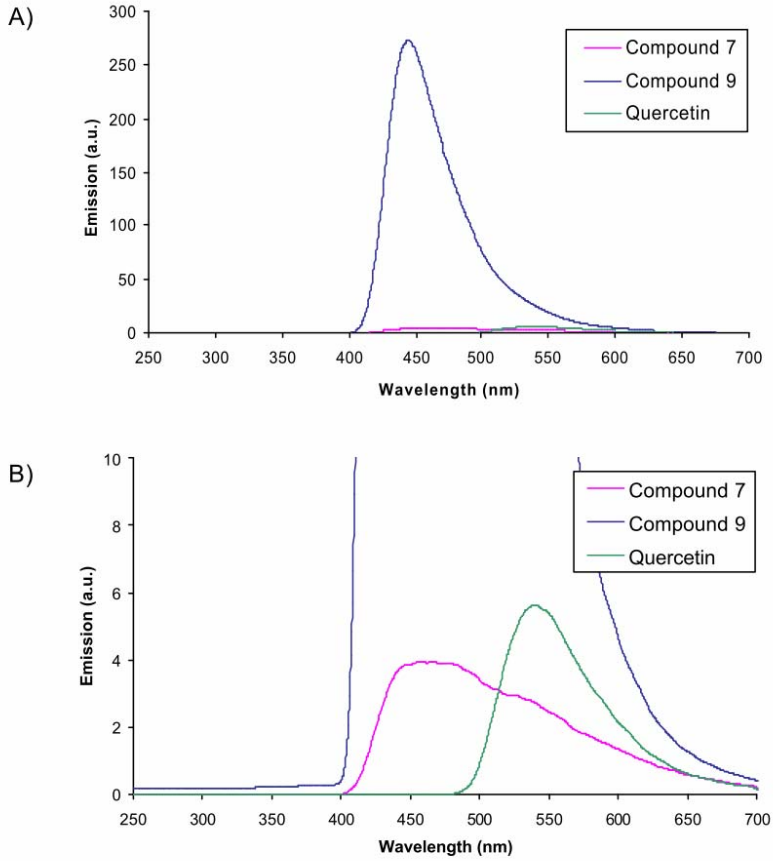

Figure S5. Fluorescence spectra of quercetin, **7** and **9** (2 μM in HBSS containing 0.1% DMSO) at 25°C. The spectra are shown in A and B with different ordinate scales. Compound **7** and quercetin were excited at 380 nm, the wavelength used in microscopy experiments (Figure 4). Compound **9** was excited at 360 nm (its absorption maximum) instead of 380 nm in order to remove a Raman scattering band.

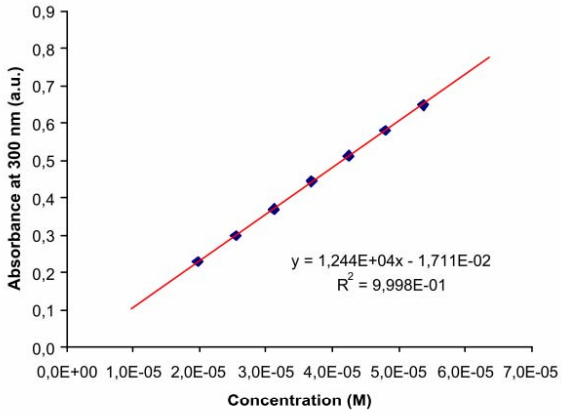

Experimental data	
Concentration (M)	**Absorbance at 300 nm (a.u.)**
$1.97 \cdot 10^{-5}$	0.2291
$2.55 \cdot 10^{-5}$	0.2983
$3.12 \cdot 10^{-5}$	0.3693
$3.68 \cdot 10^{-5}$	0.4453
$4.24 \cdot 10^{-5}$	0.5121
$4.79 \cdot 10^{-5}$	0.5806
$5.37 \cdot 10^{-5}$	0.6485

Figure S6. Calibration curve for the determination of the aqueous solubility of compound **7**.

6. Development of mitochondria-targeted derivatives of resveratrol

Bioorganic & Medicinal Chemistry Letters 18 (2008) 5594–5597

Contents lists available at ScienceDirect

Bioorganic & Medicinal Chemistry Letters

journal homepage: www.elsevier.com/locate/bmcl

Development of mitochondria-targeted derivatives of resveratrol

Lucia Biasutto [a,b,†], Andrea Mattarei [a,†], Ester Marotta [a], Alice Bradaschia [b], Nicola Sassi [b], Spiridione Garbisa [b], Mario Zoratti [b,c,*], Cristina Paradisi [a]

[a] Department of Chemical Sciences, Università di Padova, via Marzolo 1, 35131 Padova, Italy
[b] Department of Biomedical Sciences, Università di Padova, viale G. Colombo 3, 35131 Padova, Italy
[c] CNR Institute of Neuroscience, viale G. Colombo 3, 35131 Padova, Italy

ARTICLE INFO

Article history:
Received 7 August 2008
Revised 27 August 2008
Accepted 28 August 2008
Available online 31 August 2008

Keywords:
Resveratrol
Mitochondria
Triphenylphosphonium
Anti-oxidants
Pro-oxidants
Reactive oxygen species

ABSTRACT

To target natural polyphenols to the subcellular site where their redox properties might be exploited at best, that is, mitochondria, we have synthesised new proof-of-principle derivatives by linking resveratrol (3,4′,5-trihydroxy-*trans*-stilbene) to the membrane-permeable lipophilic triphenylphosphonium cation. The new compounds, (4-triphenylphosphoniumbutyl)-4′-*O*-resveratrol iodide and its bis-acetylated derivative, the latter intended to provide transient protection against metabolic conjugation, accumulate into energized mitochondria as expected and are cytotoxic for fast-growing but not for slower-growing cells. They provide a powerful potential tool to intervene on mitochondrial and cellular redox processes of pathophysiological relevance.

Plant polyphenols are the object of intense interest because they display, at least in vitro, properties and effects of relevance for physiopathological conditions ranging from aging to cancer. These effects are ascribed to their redox properties and to interactions with signaling proteins. Polyphenols can act either as anti- or pro-oxidants, that is, inhibitors or enhancers of oxidative and radical chain processes.[1] Whether an anti- or a pro-oxidant effect predominates depends, besides the redox potential of the polyphenol, on the abundance of metal ions sustaining a redox cycle ($Fe^{2+/3+}$, $Cu^{+/2+}$) and/or of oxidizing enzymes, on the ion-chelating properties of the molecule, on pH, on the concentration of the polyphenol, and on the subcellular compartment. Either pro-oxidant or anti-oxidant activity may lead to useful oncological applications. Reactive Oxygen Species (ROS) are thought to be a major factor in cancerogenesis.[2] In particular, ROS production by mitochondria[3,4] is emerging as a key factor. The metastatic potential of cell lines has been convincingly related to this parameter.[5] Mitochondrial ROS are involved in the activation of Hypoxia Inducible Factor (HIF),[6,7] which influences angiogenesis and other aspects of tumor development.[7,8] Thus, an anti-oxidant action may limit metastasis and tumor growth. Indeed resveratrol, the representative polyphenol selected for this work, inhibits cell shedding from primary tumors.[9] On the other hand, ROS play fundamental roles in apoptosis[10] and can induce the Mitochondrial Permeability Transition (MPT),[11] promoting in both cases cell death. Cancer cells are constitutively under oxidative stress[4] and an intensification of this stress may lead to their selective elimination. Resveratrol, in addition to other important activities,[12] reportedly exerts anti-proliferative and pro-apoptotic effects on various tumor-derived cells[13,14] and antagonizes growth of xenografts and mutagen-induced cancers.[15] It has been recently shown that resveratrol-induced death of cultured colorectal carcinoma cells involves generation of superoxide anion, that is, pro-oxidant action, at mitochondria.[14] The IC_{50} for death induction was found to be in the hundreds of μM range, a concentration which cannot be reached in vivo due to the poor bioavailability of polyphenols.[16]

We are interested in exploiting the potential of polyphenols through chemical modifications designed to serve specific purposes. Thus, an increase in solubility was achieved via esterification with aminoacids.[17] The present work aims at targeting polyphenols to the subcellular compartment where they are expected to best realize their anti-cancer potential (as well as other functions), that is, mitochondria. We report here the synthesis and properties of new mitochondriotropic derivatives of resveratrol obtained by coupling it to the membrane-permeable lipophilic cation triphenylphosphonium (TPP^+)[18] which drives accumulation in compartments held at negative relative voltage, such as the mitochondrial matrix, according to Nernst's law. Since the mitochondria of cancer cells maintain a higher-then-normal transmembrane potential,[19] mitochondria-targeted drugs may be cancer-selective.

The target derivative **4** was synthesised starting from resveratrol (**1**) in three steps as outlined in Scheme 1.[20] Briefly, O-alkyl-

* Corresponding author. Tel.: +39 049 8276054; fax: +39 049 8276049.
E-mail address: zoratti@bio.unipd.it (M. Zoratti).
† The first two authors contributed equally to the work.

0960-894X/$ - see front matter © 2008 Elsevier Ltd. All rights reserved.
doi:10.1016/j.bmcl.2008.08.100

ation introduces a chlorobutyl group which is then converted to the desired TPP^+ derivative via two consecutive nucleophilic substitution steps: –Cl → –I → – TPP^+I^-. Direct substitution of chloride by triphenylphosphine was unsatisfactory because it required high temperatures which led to some decomposition. The assignment of the site of O-alkylation in **2** is based on ^1H NMR data: a unique signal is found for H-2 and H-6 indicating that these protons are equivalent. The acetylated derivative **6** was also prepared (Scheme 1), so as to compare it with **4** and assess the importance of the free hydroxyl groups for the behavior of these new mitochondriotropic molecules.

The solubility in water of the resveratrol derivatives is $(3.12 \pm 0.20) \times 10^{-5}$ mol L^{-1} and $(9.7 \pm 0.6) \times 10^{-5}$ mol L^{-1} for **4** and **6**, respectively. These solubilities are significantly higher (15- and 45-fold, respectively) than that of resveratrol. Both new compounds are essentially stable in aqueous media: **4** for at least one week both in deionised water and in Hank's Balanced Saline Solution (HBSS) with 10% CH_3CN (added to insure solubility of hypothetical reaction products); **6** for at least 24 h in deionised water, while in HBSS acetyl groups were slowly hydrolised (about 7% conversion to the monoacetylated derivative in 6 h). There were no detectable metabolic modifications of either **4** or **6** by cultured Human Colon Tumor (HCT) 116 cells[20] over 6 h (Fig. 1) or whole freshly drawn rat blood over 75 min (not shown), except for the hydrolysis of the acetyl ester groups of **6** in both cases.

Two methods were used to verify accumulation of the new compounds into mitochondria.[21] First, their uptake by isolated, respiring Rat Liver Mitochondria (RLM) was monitored using a TPP^+-sensitive electrode. A representative experiment with **6** is shown in Figure 2. The introduction of mitochondria causes a decrease (upward deflection of the signal) of **6** in the medium, due to uptake into the mitochondrial matrix. After addition of excess Ca^{2+}, which induces the MPT, or of uncouplers (not shown), **6** is partially released. The release is incomplete presumably due to binding of the resveratrol derivative to mitochondrial constituents. Analogous results were obtained with **4** (not shown).

In the second approach we exploited the spectral properties of **6** and **4**, similar to those of resveratrol itself (Supporting Data, Fig. S1 and S2), to follow their accumulation in the mitochondria of cultured cells by monitoring of their fluorescence upon excitation at 340 nm. Images from one such experiment are shown in Figure 3. After addition of **6** to the medium, intracellular structures become progressively fluorescent due to accumulation of the resveratrol derivative (panel B). Addition of a transmembrane potential ($\Delta\psi_m$)-dissipating protonophore (carbonyl cyanide *p*-trifluoromethoxyphenylhydrazone (FCCP)) causes a loss of fluorescence due to efflux of the polyphenol (panel C). Some **6** remains in the cytoplasm of the cells due to the plasma membrane potential maintained by K^+ diffusion. Compound **4** behaved analogously (not shown).

As a first test of potential anti-cancer activity, we verified the effects of **4** and **6**, and of control compounds, on cultured cells (Fig. 4). Controls consisted of the parent polyphenol resveratrol, of the phosphonium salt TriPhenylMethylPhosphonium Iodide (TPMP) and of resveratrol plus this latter compound. We used

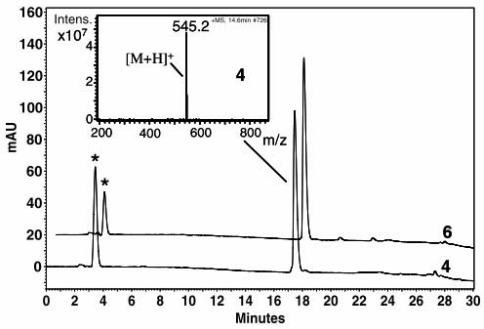

Figure 1. HPLC chromatograms recorded at 320 nm of the extracts obtained after incubation of **4** (lower trace) and **6** (upper trace) with HCT116 cells for 6 h. Inset: positive ESI-MS spectrum of **4**. For clarity, the upper trace was shifted slightly to the right along the time axis: the retention time and the mass spectrum of the major peak in this chromatogram match perfectly those of **4**. Peaks marked with ∗ are due to residual traces of acetone from the sample work-up.

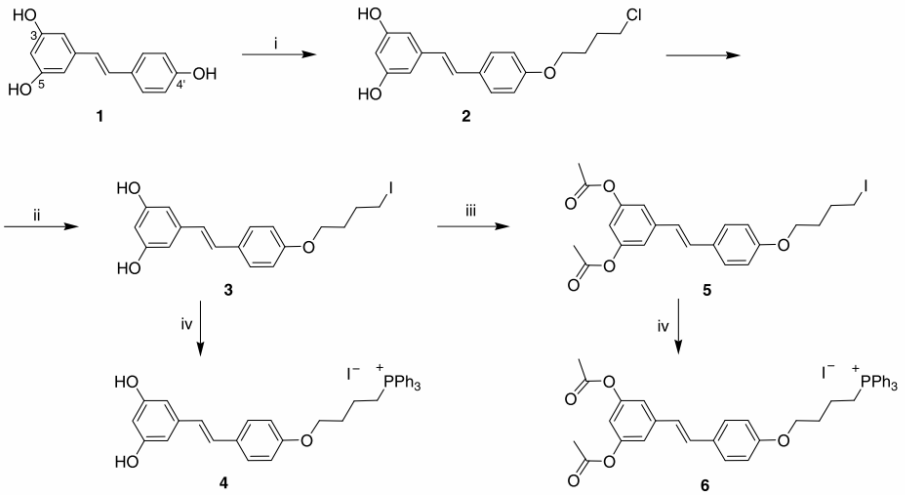

Scheme 1. Synthesis of mitochondriotropic derivatives **4** and **6**. Reagents and conditions: (i) 1-Bromo-4-chlorobutane (1.5 equiv), K_2CO_3 (1.1 equiv), DMF, Ar, rt, 20 h, yield 33%; (ii) NaI, acetone, reflux, 20 h, yield 89%; (iii) $CH_3C(=O)Cl$ (20 equiv), pyr, CH_2Cl_2, yield 73%; (iv) PPh_3 (5 equiv), toluene, 100 °C, 6 h, yield 78%.

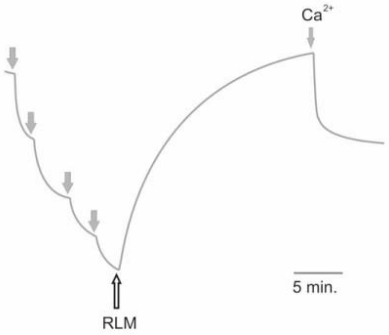

Figure 2. TPP^+-selective electrode response to additions of **6** (thick gray arrows; 0.5 μM each), Rat Liver Mitochondria (RLM) (1 mg prot. mL^{-1}) and $CaCl_2$ (50 μM) at 20 °C.

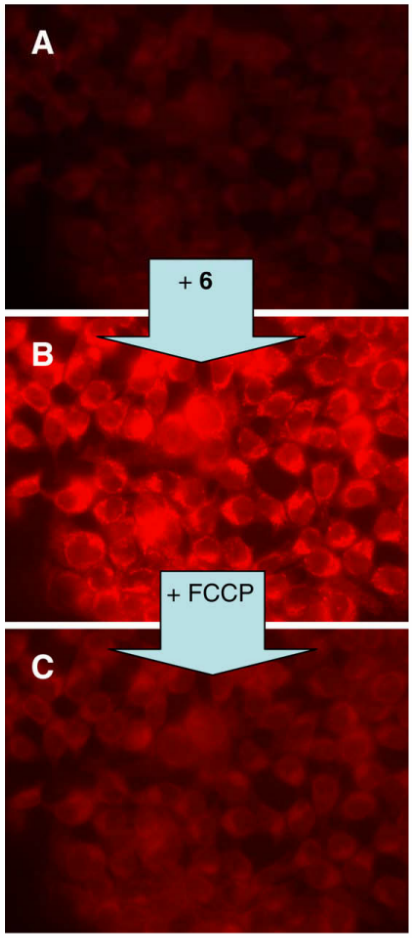

Figure 3. Fluorescence microscope images of cultured HCT116 cells: (A) just before the addition of 10 μM **6**, (B) 25 min after the addition of **6** and just before the addition of 2 μM FCCP, and (C) 10 min after the addition of FCCP.

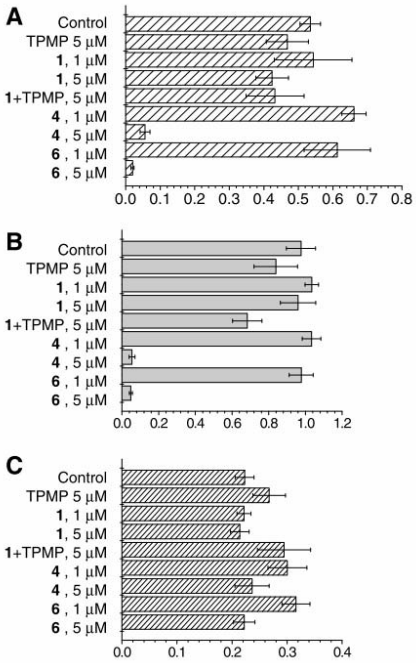

Figure 4. Effect of the mitochondriotropic resveratrol derivatives and control compounds on cell proliferation. Cells were allowed to grow for 3 days in the presence of the specified compounds and assayed using the tetrazolium salt reduction assay (see Supplementary data for details). All measurements were performed in quadruplicate. Averages ± s.d. are given. (A) C-26 mouse colon tumor cells. (B) Fast-growing Mouse Embryonic Fibroblasts (MEF). (C) Slow-growing MEF (note different scale).

the murine colon cancer cell line C-26 and, as controls, fast- and slow-growing non-tumoral mouse embryonic fibroblast (MEF) lines. Cell growth and viability was quantified using the tetrazolium salt reduction (MTT) assay.[21]

The various compounds had little effect on cell proliferation at the 1 μM level. At 5 μM, **4** and **6** displayed a marked cytotoxic effect on the two rapid-growth cell types, that is, C-26 (Fig. 4A) and non-tumoral 'fast' MEFs (Fig. 4B), but not on the slow-growth MEFs (Fig. 4C). Resveratrol, TPMP, and their combination had little effect also at 5 μM and with all three cell types, showing that the activity of the resveratrol-TPP conjugates is not just the sum of the activity of the two components. Selective cytotoxicity for fast-growing cells is characteristic of many chemotherapeutic drugs.

In conclusion we have produced mitochondriotropic resveratrol derivatives with good solubility and stability in aqueous media, which accumulate as expected in regions at negative potential. A class of natural compounds with useful properties can now be targeted to subcellular compartments where they ought to realize their biomedical potential in full. The results of initial cytotoxicity assessments encourage further experimentation in vivo to determine absorption, pharmacokinetics and possible anti-tumoral action.

Acknowledgments

We thank P. Bernardi, V. Petronilli, and A. Toninello for access to instrumentation, V. Petronilli, A. Angelin, M.E. Soriano, and D. Dal

Zoppo for operational instructions, B. Vogelstein, L. Scorrano, and W.J. Craigen for cells. This work was supported in part by grants of the Italian Association for Cancer Research (AIRC) (M.Z. and S.G.) and the Italian Foundation for Basic Research (FIRB) (M.Z.) and by a fellowship of the Fondazione Cassa di Risparmio di Padova e Rovigo (L.B.).

Supplementary data

Supplementary data associated with this article can be found, in the online version, at doi:10.1016/j.bmcl.2008.08.100.

References and notes

1. (a) Cao, G.; Sofic, E.; Prior, R. L. *Free Radic. Biol. Med.* **1997**, *22*, 749; (b) Halliwell, B. *Arch. Biochem. Biophys.* **2008**, *476*, 107.
2. Halliwell, B. *Biochem. J.* **2007**, *401*, 1.
3. Turrens, J. F. *J. Physiol.* **2003**, *552*, 335.
4. Pelicano, H.; Carney, D.; Huang, P. *Drug Resist. Update* **2004**, *7*, 97.
5. Ishikawa, K.; Takenaga, K.; Akimoto, M.; Koshikawa, N.; Yamaguchi, A.; Imanishi, H.; Nakada, K.; Honma, Y.; Hayashi, J. *Science* **2008**, *320*, 661.
6. Qutub, A. A.; Popel, A. S. *Mol. Cell. Biol.* **2008**, *28*, 5106.
7. Patel, S. A.; Simon, M. C. *Cell Death Differ.* **2008**, *15*, 628.
8. Rankin, E. B.; Giaccia, A. J. *Cell Death Differ.* **2008**, *15*, 678.
9. Günther, S.; Ruhe, C.; Derikito, M. G.; Böse, G.; Sauer, H.; Wartenberg, M. *Cancer Lett.* **2007**, *250*, 25.
10. Orrenius, S.; Gogvadze, V.; Zhivotovsky, B. *Annu. Rev. Pharmacol. Toxicol.* **2007**, *47*, 143.
11. Rasola, A.; Bernardi, P. *Apoptosis* **2007**, *12*, 815.
12. (a) Baur, J. A.; Sinclair, D. A. *Nat. Rev. Drug Discov.* **2006**, *5*, 493; (b) Pearson, K. J.; Baur, J. A.; Lewis, K. N.; Peshkin, L.; Price, N. L.; Labinskyy, N.; Swindell, W. R.; Kamara, D.; Minor, R. K.; Perez, E.; Jamieson, H. A.; Zhang, Y.; Dunn, S. R.; Sharma, K.; Pleshko, N.; Woollett, L. A.; Csiszar, A.; Ikeno, Y.; Le Couteur, D.; Elliott, P. J.; Becker, K. G.; Navas, P.; Ingram, D. K.; Wolf, N. S.; Ungvari, Z.; Sinclair, D. A.; de Cabo, R. *Cell Metab.* **2008**, *8*, 157.
13. (a) Fulda, S.; Debatin, K. M. *Cancer Detect. Prev.* **2006**, *30*, 217; (b) Ma, X.; Tian, X.; Huang, X.; Yan, F.; Qiao, D. *Mol. Cell. Biochem.* **2007**, *302*, 99.
14. Juan, M. E.; Wenzel, U.; Daniel, H.; Planas, J. M. *J. Agric. Food Chem.* **2008**, *56*, 4813.
15. (a) Kalra, N.; Roy, P.; Prasad, S.; Shukla, Y. *Life Sci.* **2008**, *82*, 348; (b) Pan, M. H.; Gao, J. H.; Lai, C. S.; Wang, Y. J.; Chen, W. M.; Lo, C. Y.; Wang, M.; Dushenkov, S.; Ho, C. T. *Mol. Carcinog.* **2008**, *47*, 184.
16. Manach, C.; Williamson, G.; Morand, C.; Scalbert, A.; Rémésy, C. *Am. J. Clin. Nutr.* **2005**, *81*, 230S.
17. Biasutto, L.; Marotta, E.; De Marchi, U.; Zoratti, M.; Paradisi, C. *J. Med. Chem.* **2007**, *50*, 241.
18. (a) Murphy, M. P.; Smith, R. A. *Annu. Rev. Pharmacol. Toxicol.* **2007**, *47*, 629; (b) Hoye, A. T.; Davoren, J. E.; Wipf, P.; Fink, M. P.; Kagan, V. E. *Acc. Chem. Res.* **2008**, *41*, 87.
19. (a) Kadenbach, B. *Biochim. Biophys. Acta* **2003**, *1604*, 77; (b) Fantin, V. R.; Leder, P. *Oncogene* **2006**, *25*, 4787.
20. Synthetic procedures and characterization.
4′-(4-O-chlorobutyl) resveratrol (**2**). K_2CO_3 (1.33 g, 9.64 mmol, 1.1 equiv) and 1-bromo-4-chlorobutane (2.25 g, 13.14 mmol, 1.5 equiv) were added under argon to a solution of resveratrol (**1**) (2.00 g, 8.76 mmol) in DMF (10 mL). After stirring overnight, the mixture was diluted in EtOAc (100 mL) and washed with 1 N HCl (3 × 50 mL). The organic layer was dried over $MgSO_4$ and filtered. The solvent was evaporated under reduced pressure and the residue was purified by flash chromatography using CH_2Cl_2/EtOAc 85:15 as eluent to afford 0.930 g of **2** (33%). ^{1}H NMR (250 MHz, DMSO-d_6) δ (ppm): 1.76–1.98 (m, 4H, CH_2), 3.72 (t, 2H, CH_2), 4.02 (t, 2H, CH_2), 6.12 (t, 1H, H-4, J = 2.0 Hz), 6.40 (d, 2H, J = 2.0 Hz, H-2, H-6), 6.82–7.04 (m, 4H, =CH, H-2′, H-6′), 7.50 (d, 2H, H-3′, H-5′, J = 8.75 Hz), 9.21 (s, 2H, 3-OH, 5-OH); ^{13}C NMR (62.9 MHz, DMSO-d_6) δ (ppm): 26.14 (CH_2), 28.90 (CH_2), 45.19 (CH_2Cl), 66.72 (OCH_2), 104.38, 114.62, 126.62, 127.45, 127.76, 129.62, 139.07, 158.16, 158.49; ESI-MS (ion trap): m/z 319, $[M+H]^+$; HRMS (ESI-TOF): m/z 319.1092; Calcd for $C_{18}H_{19}ClO_3{\cdot}H^+$ 319.1095. Anal.: Calcd for $C_{18}H_{19}ClO_3$ C 67.81, H 6.01; found: C 67.78, H 6.02.
4′-(4-O-iodobutyl) resveratrol (**3**). Compound **2** (500 mg, 1.57 mmol, 1 equiv) was added to a saturated solution of NaI in dry acetone (10 mL) and heated at reflux for 20 h. After cooling, the resulting mixture was diluted in EtOAc (100 mL), filtered and washed with water (3× 30 mL). The organic layer was dried over $MgSO_4$ and filtered. The solvent was evaporated under reduced pressure and the residue was purified by flash chromatography using CH_2Cl_2/EtOAc 9:1 as eluent to afford 0.570 g of **3** (89%). ^{1}H NMR (250 MHz, DMSO-d_6) δ (ppm): 1.71–2.00 (m, 4H, CH_2), 3.35 (t, 2H, CH_2), 4.01 (t, 2H, CH_2), 6.12 (t, 1H, H-4, J = 2.0 Hz), 6.40 (d, 2H, H-2, H-6, J = 2.0 Hz), 6.82–7.04 (m, 4H, =CH, H-2′, H-6′), 7.50 (d, 2H, H-3′, H-5′, J = 8.75 Hz), 9.21 (s, 2H, 3-OH, 5-OH); ^{13}C NMR (62.9 MHz, DMSO-d_6) δ (ppm): 8.54 (CH_2I), 29.66 (CH_2), 29.76 (CH_2), 66.39 (OCH_2), 104.38, 114.62, 126.61, 127.45, 127.76, 129.62, 139.07, 158.16, 158.49; ESI-MS (ion trap): m/z 411, $[M+H]^+$. Anal.: Calcd for $C_{18}H_{19}IO_3$ C 52.70, H 4.66; found: C 52.75, H 4.66.
4′-(4-O-triphenylphosphoniumbutyl) resveratrol iodide **(4).** A mixture of **3** (500 mg, 1.22 mmol) and triphenylphosphine (1.60 g, 6.09 mmol, 5 equiv) in toluene (15 mL) was heated at 100 °C under argon. After 6 h, the solvent was eliminated at reduced pressure and the resulting white solid was dissolved in the minimum volume of acetone (3 mL) and precipitated with diethyl ether (100 mL). The solvents were decanted and the procedure repeated 4 more times. The precipitate was then filtered to afford 600 mg of **7** (73%). ^{1}H-NMR (250 MHz, DMSO-d_6) δ (ppm): 1.73 (quintet, 2H, CH_2), 1.92 (quintet, 2H, CH_2), 3.67 (t, 2H, CH_2), 4.06 (t, 2H, CH_2), 6.13 (t, 1H, H-4, J = 1.9 Hz), 6.40 (d, 2H, H-2, H-6, J = 1.75 Hz), 6.83–7.04 (m, 4H, =CH, H-2′, H-6′), 7.50 (d, 2H, H-3′, H-5′, J = 8.75 Hz), 7.71–7.95 (m, 15H, aromatic-H), 9.22 (s, 2H, 3-OH, 5-OH). ^{13}C NMR (62.9 MHz, DMSO-d_6) δ (ppm): 18.48 (CH_2), 20.07 (CH_2), 29.15 (CH_2), 65.93 (OCH_2), 104.38, 114.66, 118.47 (Ph, J(^{13}C/^{31}P) = 85.6 Hz), 126.67, 127.41, 127.73, 129.72, 130.25 (Ph, J(^{13}C/^{31}P) = 12.4 Hz), 133.59 (Ph, J(^{13}C/^{31}P) = 10.1 Hz), 134.93 (Ph, J(^{13}C/^{31}P) = 2.9 Hz), 139.03, 158.00, 158.49; ESI-MS (ion trap): m/z 545, M^+; HRMS (ESI-TOF): m/z 545.2236; Calcd for $C_{36}H_{34}O_3P^+$ 545.2240.
3,5-diacetyl-4′-(4-O-iodobutyl) resveratrol **(5).** A solution of acetyl chloride (1.1 mL, 15 mmol, 20 equiv) in CH_2Cl_2 (20 mL) was added dropwise and under continuous stirring to a mixture of **3** (300 mg, 0.73 mmol, 1 equiv) and anhydrous pyridine (0.85 mL, 10.5 mmol, 15 equiv) in CH_2Cl_2 (20 mL) cooled in dry ice/acetone. The reaction mixture was then allowed to slowly warm up to room temperature. CH_2Cl_2 (50 mL) was added and the organic layer was washed with 1 N HCl (3× 50 mL), dried over $MgSO_4$ and filtered. The solvent was evaporated under reduced pressure and the residue was purified by flash chromatography using CH_2Cl_2:n-hexane 4:1 as eluent to afford 280 mg of **5** (78%). ^{1}H NMR (250 MHz, DMSO-d_6) δ (ppm): 1.73–2.02 (m, 4H, CH_2), 2.29 (s, 6H, OAc), 3.38 (t, 2H, CH_2), 4.02 (t, 2H, CH_2), 6.86 (t, 1H, H-4, J = 1.9 Hz), 6.96 (d, 2H, H-2′, H-6′, J = 8.5 Hz), 7.08 (d, 1H, =CH, J = 16.5 Hz), 7.21–7.33 (m, 3H, H-2, H-6, =CH), 7.53 (d, 2H, H-3′, H-5′, J = 8.75 Hz); ^{13}C NMR (62.9 MHz, DMSO-d_6) δ (ppm): 8.49 (CH_2I), 20.83 (CH_3), 29.62 (CH_2), 29.75 (CH_2), 66.43 (OCH_2), 114.74, 116.79, 124.25, 128.08, 129.10, 130.09, 139.81, 151.15, 158.61, 168.99; ESI-MS (ion trap): m/z 495, $[M+H]^+$; HRMS (ESI-TOF): m/z 495.0664; Calcd for $C_{22}H_{23}O_5I{\cdot}H^+$ 495.0663.
3,5-diacetyl-4′-(4-O-triphenylphosphoniumbutyl) resveratrol iodide **(6)**. A mixture of **5** (200 mg, 0.40 mmol) and triphenylphosphine (525 mg, 2.00 mmol, 5 equiv) in toluene (10 mL) was heated at 100 °C under argon. After 6 h, the solvent was eliminated under reduced pressure and the resulting white solid was dissolved in the minimum volume of acetone (3 mL) and precipitated with diethyl ether (100 mL) five times. The solvents were decanted after each precipitation. The precipitate was than filtered to afford 210 mg of **6** of 96–98% purity (69% yield). ^{1}H NMR (250 MHz, DMSO-d_6) δ (ppm): 1.73 (quintet, 2H, CH_2), 1.93 (quintet, 2H, CH_2), 2.29 (s, 6H, OAc), 3.67 (t, 2H, CH_2), 4.07 (t, 2H, CH_2), 6.86 (t, 1H, H-4, J = 2.2 Hz), 6.91 (d, 2H, H-2′, H-6′, J = 8.75 Hz), 7.08 (d, 1H, =CH, J = 16.25 Hz), 7.21–7.33 (m, 3H, H-2, H-6, =CH), 7.53 (d, 2H, H-3′, H-5′, J = 8.5 Hz), 7.72–7.96 (m, 15H, aromatic-H). ^{13}C NMR (62.9 MHz, DMSO-d_6) δ (ppm): 19.25 (CH_2), 20.84 (CH_2), 29.25 (CH_2), 65.98 (OCH_2), 114.79, 116.81, 118.46 (Ph, J(^{13}C/^{31}P) = 85.9 Hz), 124.31, 128.06, 129.19, 130.05, 130.25 (Ph, J(^{13}C/^{31}P) = 12.4 Hz), 133.59 (Ph, J(^{13}C/^{31}P) = 10.1 Hz), 134.93 (Ph, J(^{13}C/^{31}P) = 2.9 Hz), 139.76, 151.16, 158.46, 169.01; ESI-MS (ion trap): m/z 629, M^+; HRMS (ESI-TOF): m/z 629.2453; Calcd for $C_{40}H_{38}O_5P^+$ 629.2451.
21. For materials, instrumentation, and experimental details please see Supporting Data.

Supporting data

for

Development of mitochondria-targeted derivatives of resveratrol

Lucia Biasutto, Andrea Mattarei, Ester Marotta, Alice Bradaschia, Nicola Sassi,

Spiridione Garbisa, Mario Zoratti, Cristina Paradisi*

Materials and Methods

Materials and instrumentation. Chemicals were purchased from Aldrich, Fluka, Merck-Novabiochem, Riedel de Haen, J.T. Baker, Cambridge Isotope Laboratories Inc., Acros Organics, Carlo Erba and Prolabo, and were used as received. ^{1}H NMR spectra were recorded with a Bruker AC 250F spectrometer operating at 250 MHz. Chemical shifts (δ) are given in ppm relative to the solvent signal (δ 2.49 ppm, DMSO-d_6). LC/MS analyses and mass spectra were performed with a 1100 Series Agilent Technologies system, equipped with MSD SL Trap mass spectrometer with ESI source. HPLC/UV analyses were performed with a Thermo Separation Products Inc. system with a P2000 Spectra System pump and a UV6000LP diode array detector (190-500 nm). Accurate mass measurements were obtained using a Mariner ESI-TOF mass spectrometer (PerSeptive Biosystems). UV-Vis spectra were recorded with a Perkin-Elmer Lambda 5 spectrophotometer. Fluorescence spectra were recorded with a Perkin–Elmer LS-55 spectrofluorimeter equipped with a Hamamatsu R928 photomultiplier. All absorption and fluorescence spectra were recorded at 25°C using thermostated quartz cells with an optical pathlength of 1 cm. Flash chromatographic separations were run on silica gel (Macherey-Nagel 60, 230-400 mesh) under air pressure. Elemental analyses were performed by the Microanalysis Laboratory of the Dept. of Chemical Sciences of the University of Padova.

Solubility of **4** *and* **6** *in water.* Calibration curves were built by plotting absorbance at 320 nm (a plateau in the UV absorption spectrum of both **4** or **6**) *vs* concentration for seven standard solutions in the 10^{-6} - 10^{-4} M range, prepared from a 10^{-3} M mother solution in CH_3CN by dilution with water:CH_3CN/9:1. The concentration of aqueous saturated solutions of **4** and **6** was determined by interpolation (5 repetitions each).

Stability **4** *and* **6** *in water and in HBSS buffer.* At time zero, a 60 μL volume of a freshly prepared 10^{-3} M CH_3CN solution of either **4** or **6** was added to 3 mL of the medium of interest, i.e. water or HBSS:CH_3CN 9:1, at 25°C. The composition of HBSS (Hank's Balanced Saline Solution) was (in mM units): NaCl 136.9, KCl 5.36, $CaCl_2$ 1.26, $MgSO_4$ 0.81, KH_2PO_4 0.44, Na_2HPO_4 0.34, Glucose 5.55, pH 7.4 (with NaOH). Aliquots were withdrawn at desired times and analyzed by HPLC/UV (at 320 nm) and LC/MS on a reversed phase column (Gemini C18, 3 μm, 150 x 4.6 mm i.d.; Phenomenex). Solvents A and B were H_2O containing 0.1% HCOOH and CH_3CN, respectively. The gradient for B was as follows: 30% for 5 min, up to 60% in 15 min, up to 100% in 5 min; the flow rate was 0.7 mL·min^{-1}. For HPLC/UV analyses the 190 - 500 nm range was considered; in the LC/MS analyses mass spectra were acquired in positive ion mode operating in full-scan from 100 to 1500 m/z.

Cells. Human Colon Tumor (HCT116) cells (kindly provided by B. Vogelstein) as well as fast- and slow-growing SV-40 immortalized Mouse Embryo Fibroblast (MEF) cells (kindly provided by L. Scorrano and W.J. Craigen, respectively) and murine colon carcinoma C-26 cells were grown in Dulbecco's Modified Eagle Medium (DMEM), plus 10 mM HEPES buffer, 10% (v/v) fetal calf serum (Invitrogen), 100 U/mL penicillin G (Sigma), 0.1 mg/mL streptomycin (Sigma), 2 mM glutamine (GIBCO) and 1% nonessential amino acids (100X solution; GIBCO), in a humidified atmosphere of 5% CO_2 at 37 °C.

Metabolism studies. HCT116 cells were grown to ~90% of confluence in a 6-well plate, washed with warm HBSS, and incubated with 1 ml/well of 20 μM solution of **4**, **6** or resveratrol. Medium and cells were collected together after 6 hours of incubation. 100 μL of 0.6 M acetic acid and of fresh 10 mM ascorbic acid were added and the samples stored at –20°C until treatment and HPLC and LC/MS

analysis. Treatment consisted in addition of acetone (1 mL), followed by sonication, filtration through 0.45 μm Teflon® syringe filters (Chemtek Analytica) and concentration under N_2. The HPLC protocol was the same used for stability studies.

Mitochondria. Rat liver mitochondria were isolated by conventional differential centrifugation procedures from fasted male albino Wistar rats. The standard isolation medium was 250 mM sucrose, 5 mM HEPES (pH 7.4) and 1 mM EGTA. Protein content was measured by the biuret method with bovine serum albumin as standard.

TPP^+-selective electrode. The setup used to monitor the concentration of TPP^+-bearing compounds was built in-house following published procedures (Zoratti, M.; Favaron, M.; Pietrobon, D.; Petronilli, V. *Biochim. Biophys. Acta* **1984**, *767*, 231-239). A calomel electrode was used as reference. The suspension medium contained 200 mM sucrose, 10 mM Hepes, 5 mM succinate, 1 mM phosphate, 1.25 μM rotenone, pH 7.4 (with KOH).

Fluorescence microscopy. Cells were sown onto 24 mm round coverslips and allowed to grow for 48 hours. The coverslips were then washed with HBSS, mounted into supports, covered with 1 mL of HBSS and placed onto the microscope stage. The imaging apparatus consisted of an Olympus IX71 microscope equipped with an MT20 light source and Cell^R© software. Excitation wavelength was 340 nm and fluorescence was collected in the 450-475 nm range. Sequential images were automatically recorded following a preordained protocol.

Cell growth/viability (MTT) assays. C-26 or MEF cells were seeded in standard 96-well plates and allowed to grow in DMEM (200 μL) for 24 hours to insure attachment. In the experiments of Figure 3 initial densities were 1000 (C-26, fast MEF) or 2500 (slow MEF) cells/well. The growth medium was then replaced with medium containing the desired compound from a mother solution in DMSO. DMSO final concentration was 0.1% in all cases (including controls). Four wells were used for each of the compounds to be tested. The solution was substituted by a fresh aliquot twice, at 24-hour intervals.

At the end of the third 24-hour period of incubation with the drugs the medium was removed and substituted, after a wash with PBS, with 100 µL of CellTiter 96® solution (Promega; for details: www.promega.com/tbs). After a one-hour colour development period at 37°C absorbance at 490 nm was measured using a Packard Spectra Count 96-well plate reader.

7. Impact of mitochondriotropic quercetin derivatives on mitochondria

Biochimica et Biophysica Acta 1797 (2010) 189–196

Contents lists available at ScienceDirect

Biochimica et Biophysica Acta

journal homepage: www.elsevier.com/locate/bbabio

Impact of mitochondriotropic quercetin derivatives on mitochondria

Lucia Biasutto [a,b], Nicola Sassi [a], Andrea Mattarei [b], Ester Marotta [b], Paola Cattelan [c], Antonio Toninello [c], Spiridione Garbisa [a], Mario Zoratti [a,d,*], Cristina Paradisi [b]

[a] Department of Biomedical Sciences, University of Padova, Padova, Italy
[b] Department of Chemical Sciences, University of Padova, Padova, Italy
[c] Department of Biological Chemistry, University of Padova, Padova, Italy
[d] CNR Institute of Neuroscience, Padova, Italy

ARTICLE INFO

Article history:
Received 7 August 2009
Received in revised form 18 September 2009
Accepted 7 October 2009
Available online 14 October 2009

Keywords:
Mitochondrial permeability transition
Mitochondria-targeted polyphenol
Reactive oxygen species
Transmembrane potential
Uncoupling

ABSTRACT

Mitochondria-targeted polyphenols are being developed with the intent to intervene on the levels of reactive oxygen species (ROS) in mitochondria. Polyphenols being more than just anti-oxidants, the interaction of these derivatives with the organelles needs to be characterised. We have studied the effects of two quercetin derivatives, 3-(4-O-triphenylphosphoniumbutyl)quercetin iodide (Q3BTPI) and its tetracetylated analogue (QTA3BTPI), on the inner membrane aspecific permeability, transmembrane voltage difference and respiration of isolated rat liver mitochondria. While the effects of low concentrations were too small to be reliably defined, when used in the 5–20 μM range these compounds acted as inducers of the mitochondrial permeability transition (MPT), an effect due to pro-oxidant activity. Furthermore, Q3BTPI behaved as an uncoupler of isolated mitochondria, causing depolarisation and stimulating oxygen consumption. When applied to tetramethylrhodamine methyl ester (TMRM)-loaded HepG2 or Jurkat cells uptake of the compounds was predictably associated with a loss of TMRM fluorescence, but there was no indication of MPT induction. A production of superoxide could be detected in some cells upon prolonged incubation of MitoSOX®-loaded cells with QTA3BTPI. The overall effects of these model mitochondriotropic polyphenols may thus differ considerably depending on whether their hydroxyls are protected or not and on the experimental system. *In vivo* assays will be needed for a definitive assessment of their bioactivities.

1. Introduction

The production of Reactive Oxygen Species (ROS) in cells, and in particular by mitochondria, is considered to be a major factor in aging and degenerative processes (e.g.: [1–5]) with the implication that undesirable organism deterioration may be slowed down by anti-oxidants. Anti-oxidants, including polyphenols, are thus included in some cosmetics and nutritional supplements. In ischemia/reperfusion (I/R) injury, much of the damage is sustained when circulation is reinstated. A major role in cell death under these circumstances is played by the Mitochondrial Permeability Transition (MPT), a process induced by matrix Ca^{2+} overload and oxidative conditions [6–8]. The involvement of ROS in MPT induction is clearly recognised (e.g.: [2,9,10], and antioxidants may be expected to exert a protective effect. This has led to an ongoing effort to develop "mitochondriotropic" antioxidants [11–18], including polyphenols [19,20], mainly with the goal of counteracting these undesirable redox-mediated effects. However, μM concentrations of mitochondria-targeted quercetin and resveratrol derivatives proved to be cytotoxic for rapidly dividing cultured cells [19,20], suggesting a potential as chemotherapeutic agents. Understanding the reasons for this cytotoxicity ought to help the design of other mitochondria-targeted antioxidants and the utilisation of already available ones.

It is therefore important to characterise the effects of these mitochondria-targeted compounds on isolated mitochondria and on the organelles in cells to gain a sense of what may happen *in vivo*. Here we report our observations with isolated rat liver mitochondria (RLM), cultured HepG2 and Jurkat cells, and two mitochondria-

Abbreviations: BC, Bathocuproinedisulfonic acid; BF, Bathofenanthrolinedisulfonic acid; BHT, 2,5-di-t-Butyl-p-HydroxyToluene; CsA, Cyclosporine A; DTT, Dithiothreitol (1,4-Dimercapto-2,3-butanediol); $\Delta\tilde{\mu}_H$, transmembrane electrochemical proton gradient; $\Delta\Psi$, mitochondrial transmembrane electrical potential difference; FCCP, carbonyl cyanide p-trifluorometoxyphenyl hydrazone; IMM, Inner Mitochondrial Membrane; HE, diHydroEthidine; HBSS, Hank's Balanced Salt Solution; LC/MS, Liquid Chromatography / Mass Spectrometry; MPT, Mitochondrial Permeability Transition; RLM, Rat liver Mitochondria; ROI, Region of Interest; ROS, Reactive Oxygen Species; Q, Quercetin; Q3BTPI, 3-(4-O-triphenylphosphoniumbutyl)quercetin iodide; QTA3BTPI, 3′,4′,5,7-tetra-O-acetyl-3-(4-O-triphenylphosphoniumbutyl)quercetin iodide; TMRM, Tetramethylrhodamine methyl ester; TPP, Triphenylphosphonium

* Corresponding author. CNR Institute of Neuroscience, c/o Department of Biomedical Sciences, Viale G. Colombo 3, 35121 Padova, Italy. Tel.: +39 0498276054; fax: +39 0498276049.
E-mail address: zoratti@bio.unipd.it (M. Zoratti).

0005-2728/$ – see front matter © 2009 Elsevier B.V. All rights reserved.
doi:10.1016/j.bbabio.2009.10.001

targeted quercetin derivatives, 3-(4-O-triphenylphosphoniumbutyl) quercetin iodide (Q3BTPI) and 3′,4′,5,7-tetra-O-acetyl-3-(4-O-triphenylphosphoniumbutyl)quercetin iodide (QTA3BTPI).

2. Materials and methods

2.1. Cells and mitochondria

HepG2 cells were grown in Dulbecco's Modified Eagle Medium (DMEM) (GIBCO) plus 10 mM HEPES buffer, 10% (v/v) fetal calf serum (Invitrogen), 100 U/mL penicillin G (Sigma), 0.1 mg/mL streptomycin (Sigma), 2 mM glutamine (GIBCO) and 1% nonessential amino acids (100× solution; GIBCO), in a humidified atmosphere of 5% CO_2 at 37 °C. Jurkat cells were grown in RPMI-1640 medium supplemented as above plus 50 μM β-mercaptoethanol. Rat liver mitochondria (RLM) were prepared by standard differential centrifugation procedures and obtained as a suspension in 0.25 M sucrose, 5 mM Hepes/K^+, pH 7.4.

2.2. TPP-sensitive electrode

The setup used to monitor the concentration of triphenylphosphonium-bearing compounds in solution was built in-house following published procedures [21,22]. In these electrodes the diffusion of the charged, permeant compound across a permeable polyvinylchloride (PVC) film gives rise to a half-cell potential logarithmically related to the concentration of the compound according to Nernst's law. The film is permeable because doped with tetraphenylborate anion, which acts as a carrier. Such an electrode will respond to all cations capable of diffusing into the PVC film as an ionic couple with tetraphenylborate, i.e., in practice, to triphenylphosphonium-comprising organic molecules. A calomel electrode was used as reference and the potentiometric output was directed to a strip chart recorder. The experiment illustrated in Fig. 1 was conducted at 20 °C.

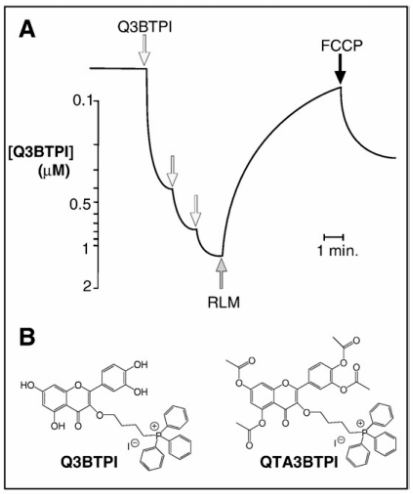

Fig. 1. (A) Accumulation of Q3BTPI by RLM. The response of a TPP-sensitive electrode is shown. Arrows indicate the addition of 0.4 μM Q3BTPI to standard medium. Addition of RLM (1 mg prot.mL^{-1}) causes an upward deflection of the trace since respiring mitochondria take up the positively charged compound, which also bind in part to mitochondrial components. Addition of FCCP causes release. (B) Chemical structures of Q3BTPI and QTA3BTPI.

2.3. Swelling and respiration assays

Preparation of RLM and swelling and respiration assays were carried out as described in [23]. The standard medium contained 250 mM sucrose, 10 mM Hepes/K^+, 5 mM succinate/K^+, 1.25 μM rotenone, 1 mM P_i/K^+, pH 7.4, supplemented with the desired concentration of $CaCl_2$. RLM were used at a concentration of 1 or 0.5 mg.prot.mL^{-1}. Direct determinations of the effects of Q3BTPI on respiration using a Clark electrode could not be carried out because Q3BTPI diffused through the semi-permeable Teflon membrane covering the working surface of the electrode (a cathode at which approximately −0.7 V are applied), and reacted there forming black polymeric products which rapidly gummed up the surface making the electrode unserviceable.

2.4. Fluorimetric assays of mitochondrial potential

Rhodamine 123 (75 nM) fluorescence was used to monitor the transmembrane potential of isolated RLM suspended (0.5 mg.prot. mL^{-1}) in standard medium in a stirred quartz cuvette placed in a Shimadzu RL-5000 spectrofluorimeter at R.T. Excitation was at 503 nm (3 nm slit), and fluorescence was collected at 523 nm (5 nm slit).

Tetramethylrhodamine methyl ester (TMRM; Invitrogen/Molecular Probes) staining of cells was used to monitor mitochondrial transmembrane potential in cultured cells. HepG2 cells were seeded onto 24-mm coverslips in 6-well plates and grown for about two days, avoiding confluence. Coverslips were mounted onto holders, exposed to 20 nM TMRM in DMEM or HBSS (in mM units: NaCl 136.9, KCl 5.36, $CaCl_2$ 1.26, $MgSO_4$ 0.81, KH_2PO_4 0.44, Na_2HPO_4 0.34, glucose 5.55, pH 7.4 with NaOH) for about 20 min, generally in the presence of 4 μM Cyclosporin H or 2 μM Cyclosporin A depending on the details of the experimental protocol, and washed twice. Cells were then covered with 1 mL of the desired medium and observed at room temperature. Images were acquired automatically at 1- or 2-min intervals, using an Olympus Biosystems apparatus comprising an Olympus IX71 microscope and MT20 light source, and processed with Cell$^{R©}$ software. Excitation was at 568 ± 25 nm and fluorescence was collected using a 585-nm longpass filter. Additions were performed by withdrawing 0.5 mL of incubation medium, adding the desired solute to this aliquot, mixing, and adding back the solution into the chamber at a peripheral point.

A Beckton Dickinson Canto II flow cytometer was used to monitor TMRM fluorescence of Jurkat cells. The cells were washed in HBSS, suspended in FACS buffer (135 mM NaCl, 10 mM Hepes, 5 mM $CaCl_2$, pH 7.4) at a density of 1.5×10^6/mL and loaded with 20 nM TMRM (37° C, 20 min). Cells were then diluted 1:5 in FACS buffer and divided into the desired number of identical aliquots. At time zero the desired compound was added, and data collected after the desired incubation times, exciting at 545 nm and measuring fluorescence at 585 nm. Data were analysed using the BD VISTA software. Experiments could be performed only with QTA3BTPI because Q3BTPI significantly altered the scatter parameters of a large fraction of the cells.

2.5. Superoxide production assays

Dihydroethidine (Invitrogen/Molecular Probes) assays were used as described in [23] to detect the production of $O_2^{\cdot-}$ in RLM suspensions. Superoxide generation in cells was followed using the mitochondriotropic probe MitoSOX Red® (Invitrogen/Molecular Probes) used as specified by the producer. Cells were incubated for 15 min with 1 or 2 μM MitoSOX Red® in HBSS, washed twice, covered with 1 mL HBSS, and placed on the microscope stage. Excitation was at 500–520 nm, and fluorescence was collected at λ>570 nm. Images were automatically acquired at 1 or 2 min intervals as above. These experiments could be conducted only with QTA3BTPI and 5 μM Q3BTPI, because 20 μM Q3BTPI apparently interacted with mitoSOX to

produce strongly fluorescent microaggregates giving rise to a "snow-storm" effect which masked any fluorescence increase.

FACS experiments with Jurkat cells were conducted as described for TMRM fluorescence determinations, loading with 1 μM MitoSOX Red®. Also in this case analyses could be performed only with QTA3BTPI.

2.6. QTA3BTPI stability in mitochondrial suspensions

QTA3BTPI was added to a 1 mg.prot.mL^{-1} suspension of RLM in standard medium to give a 20 μM solution. 100 μL samples were withdrawn, stabilised with 1 mM ascorbate and 0.06 M acetic acid, and mixed with an equal volume of acetone. After sonication the solids were separated by centrifugation. The supernatant was concentrated under N_2 and analysed. LC-ESI/MS analyses and mass spectra were performed with a 1100 Series Agilent Technologies system, equipped with binary pump (G1312A) and MSD SL Trap mass spectrometer (G2445D SL) with ESI source. Samples (20 μl) were injected onto a reversed phase column (Gemini C18, 3 μm, 150×4.6 mm i.d.; Phenomenex). Solvents A and B were H_2O containing 0.1% formic acid and CH_3CN, respectively. The gradient for B was as follows: 30% for 5 min, from 30% to 60% in 15 min, from 60% to 100% in 3 min; the flow rate was 0.7 mL/min. The eluate was monitored at 300 nm.

3. Results

To assess the effects of Q3BTPI and QTA3BTPI on isolated rat liver mitochondria we monitored three classical readouts of bioenergetics experiments: mitochondrial volume (as reflected by light scattering), transmembrane potential and oxygen consumption. These parameters, and their variation in response to pharmacological agents, vary to some extent from one preparation to the other. The direct comparisons presented in this paper are based on data obtained with the same preparation.

As an initial step we simply mixed the compounds with RLM suspended in an isotonic sucrose-based medium. Both QTA3BTPI [19] and Q3BTPI (Fig. 1) can be observed to accumulate into isolated mitochondria by monitoring their concentration with a TPP-responsive electrode. Note that Q3BTPI is only partially released upon uncoupling of the organelles indicating that much of the compound is actually bound. Polyphenols are well known to bind avidly to proteins, and the TPP moiety is also understood to participate in interactions with membranes and with macromolecules bearing negative charges (DNA). The group of Smith and Murphy has recently produced a quantitative study of the partition of mitoQ in cells: most of the compound was found to bind to cellular components [24]. Acetylation of the OH groups allows faster redistribution and less extensive binding of QTA3BTPI [19].

Fig. 2A illustrates the results of light-scattering experiments with Q3BTPI under these conditions ($N=3$). In this as well as in the other figures representative experiments are shown, utilising concentrations of the compounds producing a marked change of the readout parameter. Lower concentrations always had similar, but less evident, effects or produced variations too small for a reliable assessment. In the presence of 20 μM Q3BTPI (trace 1) swelling ensued which was not observed when no addition was made (trace 7, with oxygenation) or in the presence of 20 μM tetraphenylphosphonium chloride (trace 6). The latter induced only a much slower and lower-amplitude swelling, presumably due to the energy-driven uptake of the osmotically active solute since it was abolished by FCCP (not shown). The pseudo-absorbance decrease induced by Q3BTPI was in turn more modest than that associated with full-blown Ca^{2+}-induced permeability transition (trace 8), it was partly sensitive to Cyclosporin A (trace 2) and EGTA (trace 9), abolished by FCCP (trace 3) and it was interrupted by a sudden inversion (traces 1, 2). The latter was

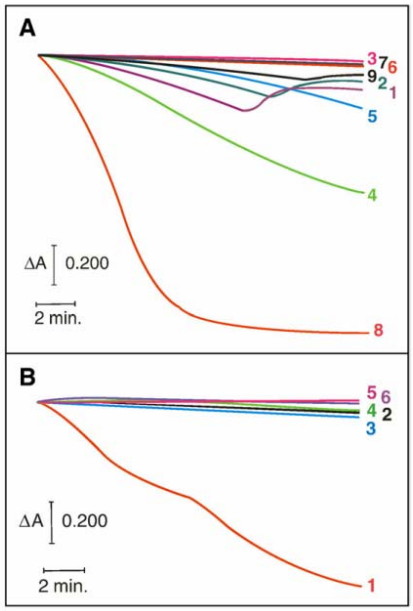

Fig. 2. Effects of Q3BTPI and QTA3BTPI on isolated rat liver mitochondria in the absence of added Ca^{2+}. Parallel light scattering experiments initiated by the addition of 1 mg. prot.mL^{-1} RLM to the cuvettes. Pseudo-absorbance was monitored at 540 nm. The medium contained: (A) traces 1–5 and trace 9: Q3BTPI 20 μM; traces 2,5: CsA 1 μM; trace 3: FCCP 1 μM; trace 6: $Ph_4P^+Cl^-$ 20 μM; trace 8: $CaCl_2$ 80 μM; trace 9: EGTA 100 μM; traces 4, 5, 7, 8: the incubation medium saturated with oxygen; (B) traces 1–3: QTA3BTPI 20 μM; trace 2: CsA 1 μM; trace 3: EGTA 100 μM; traces 4–6: Q 20 μM; trace 5: CsA 1 μM; trace 6: EGTA 100 μM.

associated with the near-exhaustion of the oxygen supply in the spectrophotometer cuvette, since saturating the suspension medium with oxygen beforehand delayed the phenomenon (traces 4, 5). This behaviour indicates that oxygen consumption was strongly enhanced by Q3BTPI. This could not be confirmed directly by measurements with a Clark electrode, because Q3BTPI reacted at the electrode surface producing a tarry substance which rapidly rendered the electrode useless. Oxygenation on the other hand increased the CsA-sensitive portion of the pseudo-absorbance decrease (compare traces 1, 2 vs. 4, 5), i.e., the rate of propagation of the permeability transition in the suspension, confirming that this phenomenon is mediated by oxidative events [23].

The acetylated derivative–QTA3BTPI–and quercetin affected swelling differently, as illustrated in Fig. 2B. In the absence of added Ca^{2+} quercetin in the 10–50 μM range had little effect (cf. trace 4 in Fig. 2B). QTA3BTPI on the other hand induced large amplitude swelling (trace 1) which was essentially abolished by both cyclosporin A and EGTA (traces 2 and 3), and can thus be attributed to the permeability transition taking place in the presence of "contaminating" Ca^{2+}.

These results suggested that both Q3BTPI and QTA3BTPI acted as inducers of the MPT in synergy with any Ca^{2+} present. In this capacity QTA3BTPI seemed to be more efficient than Q3BTPI (in Fig. 2 compare trace 1 minus trace 2 in panel B for QTA3BTPI vs. trace 1 minus trace 2 in panel A for Q3BTPI), which in turn was more efficient than quercetin itself (trace 4 minus trace 5 in panel B). These indications were confirmed by experiments performed in the presence of near-threshold [Ca^{2+}], i.e. of a concentration of Ca^{2+} sufficient for only a slowly-developing MPT-associated swelling in the absence of another

inducing agent (Fig. 3) ($N=31$). QTA3BTPI-induced swelling was always profoundly inhibited by CsA, at variance from that caused by Q3BTPI, which was only partially sensitive (in Fig. 3 compare trace 2 for QTA3BTPI + CsA with trace 4 for Q3BTPI + CsA). Thus, while QTA3BTPI is more efficient at inducing the MPT, Q3BTPI is more efficient at inducing CsA-insensitive swelling. These properties clearly must be related to the presence of free OH groups in Q3BTPI. Quercetin has been shown to induce the MPT via a metal ion-catalyzed oxidative process [23] and the same mechanism may be envisioned for the present compounds. In the presence of metal ions with multiple possible oxidation states (mainly $Fe^{2+/3+}$ and $Cu^{+/2+}$) polyphenols, especially if comprising a catechol moiety, may oxidize in chain reactions producing superoxide and hence H_2O_2. The latter can then undergo Fenton-type reactions producing more aggressive hydroxy and peroxy radicals [25,26]. Oxygen radicals, or, in general, oxidising conditions, are well known to favour the onset of the MPT by acting on key thiol residues [27–29].

MPT induction by QTA3BTPI was somewhat unexpected because the hydroxyls, the sites of oxidation in quercetin, are protected by acetylation. LC/MS analysis revealed that QTA3BTPI undergoes partial deacetylation, producing oxidisable species still capable of electrophoretic accumulation into energised mitochondria (Fig. 4). However over the time course of a swelling experiment essentially no Q3BTPI is produced: the main species found at 15 min still retain two or three of the original four acetyl groups.

The intervention of radicalic/oxidative processes in the onset of QTA3BTPI-induced MPT and, in part, of Q3BTPI-induced swelling was confirmed by the inhibition afforded by BHT + DTT (Fig. 5A) ($N=3$). In the case of quercetin, MPT induction was antagonised by Fe and Cu chelating agents [23], indicating the involvement of Fenton reactions catalysed by metallic species released by or associated with the mitochondria themselves. Selective chelators also affected Q3BTPI and Ca^{2+}-associated swelling (Fig. 5B) ($N=3$), reducing not only the CsA-sensitive component of the swelling curve, but also the CsA-insensitive one (compare traces 6 and 7 in Fig. 5B). This suggests that CsA-insensitive swelling is also largely mediated by ROS produced by metal-catalysed processes, presumably via aspecific membrane permeabilisation by lipoxidation. On the other hand in the case of QTA3BTPI this protective effect was practically absent (compare traces 1 and 2). This would be expected if in this case the relevant redox events took place mostly in the mitochondrial matrix, where QTA3BTPI accumulates. The matrix is inaccessible to BC and BF which are sulfonated (i.e., negatively charged) molecules.

QTA3BTPI is much less reactive than Q3BTPI at the Clark electrode surface, and its effects on respiration can therefore be assessed by

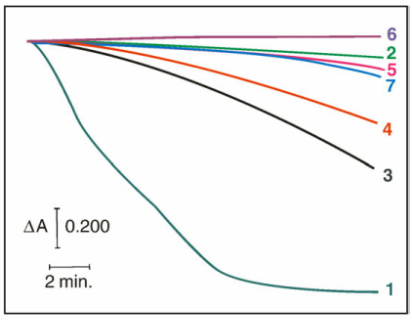

Fig. 3. Effects of Q, Q3BTPI and QTA3BTPI on isolated rat liver mitochondria in the presence of exogenous Ca^{2+}. Light scattering experiments analogous to those of Fig. 2. In all cases the medium was saturated with oxygen and contained $CaCl_2$ 50 μM plus: traces 1,2: QTA3BTPI 10 μM; trace 2: CsA 1 μM; traces 3,4: Q3BTPI 20 μM; trace 4: CsA 1 μM; traces 5, 6: Q 40 μM; trace 6: CsA 1 μM.

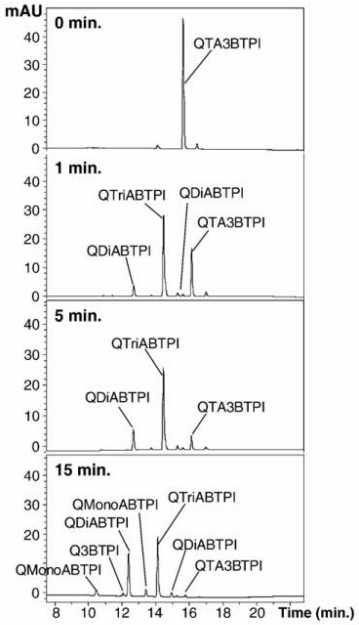

Fig. 4. Deacetylation of QTA3BTPI in the presence of RLM. HPLC chromatograms (300 nm) recorded after different incubation periods of QTA3BTPI with a RLM suspension (1 mg.prot.mL^{-1}). Peak identity was determined by ESI/MS analysis.

polarography. As expected, in the presence of Ca^{2+} its addition caused an acceleration of the rate of oxygen consumption which was blocked by CsA (not shown). An increase in respiratory rate normally implies "uncoupling" of the mitochondrial energy conversion process, which in turn, according to the chemiosmotic model, implies a decrease of the transmembrane electrochemical proton gradient ($\Delta\tilde{\mu}_H$). To verify whether such a decrease was taking place we used the fluorescent transmembrane potential ($\Delta\Psi$) indicator dye Rhodamine 123 (Rh123). In these experiments Rh123 was added to the suspension and equilibrated, so that some was always present outside mitochondria. The high (0.5 mg.prot./mL) density of the latter then insured that any dye released upon depolarisation could be rapidly taken up again upon repolarisation. Q3BTPI indeed induced a sustained recovery of Rh123 fluorescence, corresponding to a decrease of $\Delta\Psi$, when added to a suspension of RLM, also if no Ca^{2+} was added and CsA was present to block the MPT (Fig. 6A) ($N=3$). QTA3BTPI had an analogous depolarising effect (Fig. 6B). In the presence of CsA, however, the increase of Rh123 fluorescence was transient, suggesting a rapid depolarisation due to influx of the permeant cation followed by a slower repolarisation taking place on the time scale of a few minutes (Fig. 6C; $N=4$), as the compound was taken up and an equilibrium distribution was approached. Quercetin itself had little effect under the same conditions (not shown).

We then checked whether our compounds affected mitochondria inside cultured cells (Fig. 7). We followed the mitochondrial potential via TMRM fluorescence. In the experiments of Fig. 7A, representative of 37 separate ones under various conditions, HepG2 cells were loaded with TMRM in the presence of CsH (to inhibit MDR pumps; CsH, contrary to CsA, does not prevent the MPT) and then incubated in HBSS without any pharmacological agent. Under these conditions there was a background loss of TMRM fluorescence (plot "a"), which was hardly affected by the addition of 5 μM Q3BTPI (plot "b"), while

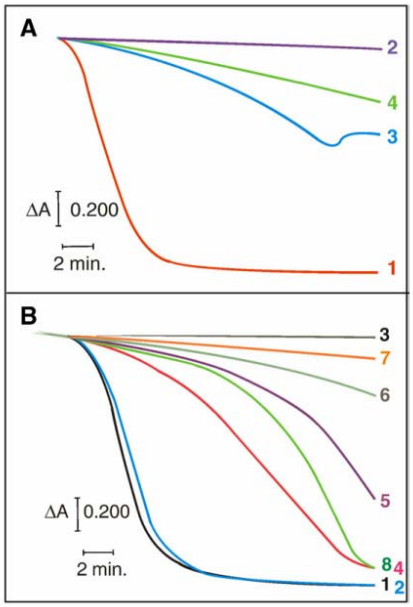

Fig. 5. Contribution of Fe and Cu ions and radical species to the induction of the mitochondrial permeability transition by Q3BTPI and QTA3BTPI. Light scattering experiments analogous to those in Figs 2 and 3. In all cases the medium was saturated with oxygen. (A) All traces: $CaCl_2$ 50 μM. Traces 1, 2: QTA3BTPI 10 μM; trace 2: BHT and DTT, 1 mM each; tracces 3, 4: Q3BTPI 20 μM; tracc 4: BHT and DTT, 1 mM cach. (B) Thc medium contained $CaCl_2$ 40 μM plus: traces 1–3: QTA3BTPI 10 μM; trace 2: BF and BC, 10 μM each; trace 3: CsA 1 μM; traces 4–7: Q3BTPI 20 μM; trace 5: BF and BC, 10 μM each; trace 6: CsA 1 μM; trace 7: BF and BC, 10 μM each, and CsA 1 μM.

20 μM resulted in a modest acceleration (plot "c"). This sluggishness may be explainable in terms of the sequestration of a fraction of this compound by cellular structures.

QTA3BTPI is expected to bind less avidly, since its hydroxyls are capped, and it has been directly observed to accumulate into *in situ* mitochondria [19]. Accordingly, its addition induced a more pronounced but transient acceleration of the fluorescence decrease (plot "d"), which was not affected by either CsA or BHT + DTT (1 mM each) (not shown), ruling out the MPT as its origin. Fluorescence loss proceeded with kinetics comparable to those of QTA3BTPI uptake [19], suggesting that the two phenomena are correlated, i.e., the process may be ascribable to the depolarisation associated with uptake of a permeant cation. A protonophoric cycle by (partially) deacylated species may also intervene. The same type of behaviour by QTA3BTPI was observed when Jurkat cells were analysed by cytofluorimetry (Fig. 7B, C). In the case of Q3BTPI reliable data could not be obtained (see Materials and methods). In experiments with cells loss of TMRM fluorescence does not necessarily indicate an irreversible, permanent depolarisation of the mitochondria. Cells are pre-loaded with TMRM and then washed, so that no dye is present outside cells, a non-equilibrium situation. Indeed, TMRM slowly leaks out of cells under our control conditions. The cells face an extremely larger volume of incubation medium. Under these conditions, any TMRM lost because of a transient depolarisation would not be expected to be regained upon a subsequent recovery of the mitochondrial potential. Thus, fluorescence loss indicates depolarisation, but does not necessarily indicate by itself a *permanent* depolarisation or damage.

Quercetin induces the production of superoxide anion by isolated mitochondria as well as by cultured cells [23]. We could not obtain clear evidence of an analogous effect by Q3BTPI or QTA3BTPI on isolated mitochondria using HE or mitoSOX®. A reliable assessment of the effect of Q3BTPI on the response of MitoSOX® in HepG2 or Jurkat cells was made difficult by technical problems at 20 μM (see Materials and methods) and was not robust enough to reach definite conclusions at the 5 μM level. Addition of QTA3BTPI resulted instead in a fluorescence increase, which took place also in the presence of CsA (Fig. 8). In microscopy experiments an heterogeneity of cell behaviour was evident, as illustrated by the different increases of the fluorescence associated with two cells in the same field shown in Fig. 8A (plots "b" and "c").

4. Discussion

The results presented above plausibly identify the mechanisms responsible for the cytotoxicity of Q3BTPI and QTA3BTPI. They have been obtained *in vitro*, with relatively high concentrations, but we believe they are relevant also for an eventual *in vivo* utilisation of the compounds, since much the same mechanisms and requirements would be expected to apply. Polyphenols *per se* have rather poor bioavailability, and when administered in foods or beverages they are unlikely to reach μM-range concentrations in blood and organs (except as phase II conjugates). Here we are however considering not the natural compounds, but their derivatives, which may be considered as drugs, and administered in various ways. Pharmacological delivery methods can be expected to result in much higher levels, at least locally.

We rationalise the behaviour of Q3BTPI vs. isolated mitochondria in terms of three major concomitant processes: uncoupling of the mitochondria by Q3BTPI acting as a protonophore (Fig. 9), MPT induction–involving Ca^{2+} and ROS in analogy to the process induced by quercetin itself under similar conditions [23]–and CsA-insensitive permeabilisation of the IMM, with consequent swelling, due to the action of ROS on membrane lipids. The uncoupling effect of Q3BTPI

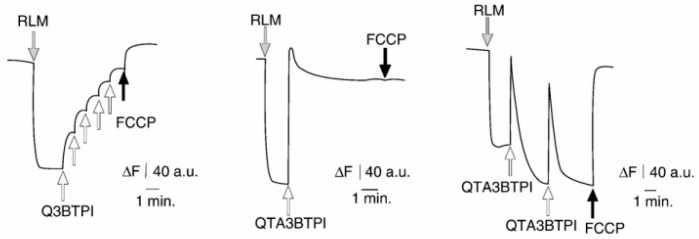

Fig. 6. Effects of Q3BTPI and QTA3BTPI on mitochondrial membrane potential. Variations of Rhodamine 123 fluorescence upon additions of: (A) Q3BTPI (each arrow represents a 10 μM addition); (B, C) QTA3BTPI (each arrow represents a 20 μM addition). In A and C, CsA 1 μM was present during the experiment.

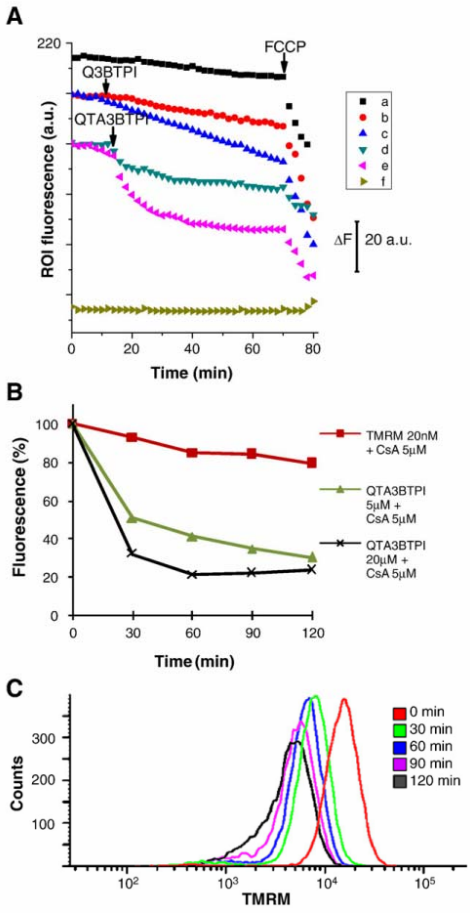

Fig. 7. Mitochondrial membrane potential in cells exposed to Q3BTPI and QTA3BTPI, monitored using TMRM. (A) Representative fluorescence microscopy experiments with TMRM-loaded HepG2 cells. Computer-generated plots of the fluorescence emitted by the field areas (Regions Of Interest, ROI) coinciding with one cell or a portion of background (f). Images were acquired every 60 s. Plot "a" represents a control experiment without addition. Plot "b": Q3BTPI 5 μM; plot "c": Q3BTPI 20 μM; plot "d": QTA3BTPI 5 μM; plot "e": QTA3BTPI 20 μM. Compound additions are indicated by arrows. Plots have been shifted along the ordinate axis for clarity. See Materials and methods for details. (B) Representative FACS experiments with 0 (red; control), 5 (green) or 20 μM (black) QTA3BTPI additions. The experiment was conducted in the presence of 5 μM CsA. Plotted are the normalised median values of histograms such as those shown in panel C. The median of the histogram recorded immediately after the addition of QTA3BTPI was set as 100%. (C) The set of histograms obtained in the experiment with 5 μM QTA3BTPI shown in panel B is shown as an example.

can be explained as follows: Q3BTPI exists in solution as a mixture of instantaneously fully protonated (i.e., positively charged due to the TPP group) and deprotonated species (the first pKa of quercetin is close to 7 [30–32]). The mitochondrial $\Delta\Psi$ will drive the uptake of fully protonated molecules, the chemical gradient between the matrix and the suspension medium will drive the efflux of the unprotonated, zwitterionic specie. A $\Delta\Psi$-decreasing, respiration-stimulating protonophoric futile cycle will thus be generated. Flavonoids have already been identified as potential uncouplers [33], but the presence of the membrane-permeating positive charge enhances this characteristic: quercetin itself is not active as an uncoupler at concentrations below 1 mM [33], while Q3BTPI uncouples in the μM range. Active uptake of Q3BTPI by energised mitochondria is therefore self-limiting.

Direct comparison shows that both QTA3BTPI and Q3BTPI are more efficient MPT co-inducers than quercetin (Fig. 3) in RLM. Since these compounds are accumulated inside suspended mitochondria, this indicates that induction can be mediated by phenomena taking place in the matrix. The higher efficiency is then presumably accounted for by the higher concentration of inducer on the matrix side of the inner mitochondrial membrane (IMM) (in comparison with an analogous experiment with quercetin). While the two mitochondriotropic compounds are better inducers than quercetin,

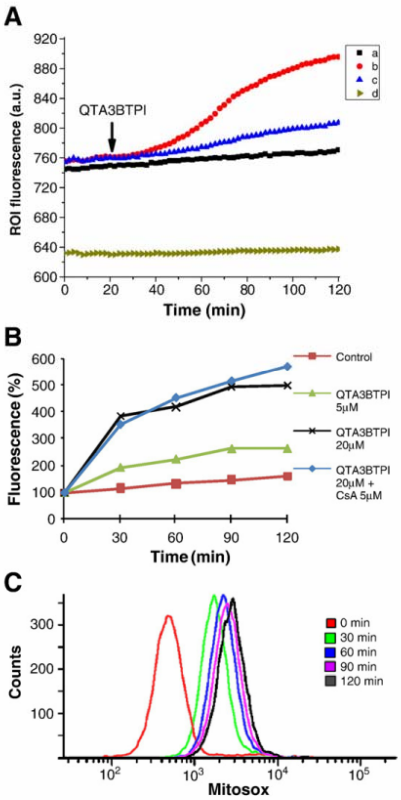

Fig. 8. Superoxide production in cells exposed to QTA3BTPI, monitored using MitoSOX Red®. (A) Representative fluorescence microscopy experiments with MitoSOX Red®-loaded HepG2 cells. A computer-generated plot of the fluorescence emitted by field areas (Regions Of Interest, ROI) coinciding with a cell (a–c) or a portion of background (d). Images were acquired every 2 min. Plot "a" presents the fluorescence associated with a cell in a separate control experiment without additions. 20 μM QTA3BTPI was added, when indicated, in plots "b" and "c", which report the fluorescence associated with two cells in the same field (plot "d" also comes from the same experiment). See Materials and methods for details. (B) Representative FACS experiments with 0 (red; control), 5 (green) or 20 μM (black) QTA3BTPI additions. The graph plotted in blue refer to a parallel experiment with 20 μM QTA3BTPI in the presence of 5 μM CsA. Plotted are the normalised median values of histograms such as those shown in panel C. The median of the histogram recorded immediately after the addition of QTA3BTPI was set as 100%. (C) The set of histograms obtained in the experiment with 20 μM QTA3BTPI in the presence of CsA shown in panel B (blue plot) is shown as an example.

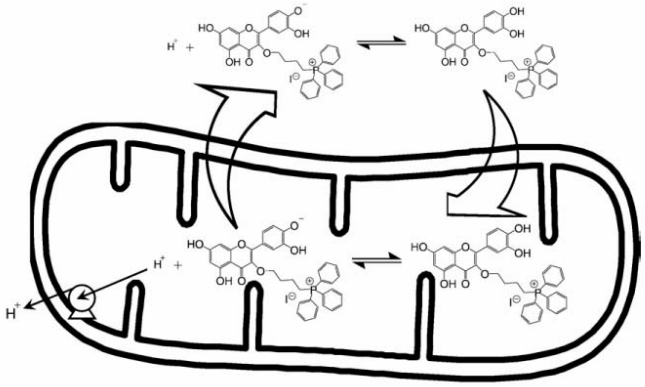

Fig. 9. An illustration of how Q3BTPI may act as a protonophore and uncoupler. See text for details.

the difference is less marked than might have been expected. In the case of Q3BTPI this may be explained by uncoupling, which limits matrix accumulation of both Ca^{2+} and inducer. QTA3BTPI is expected to be less effective than quercetin or Q3BTPI, at parity of concentration, because its hydroxyls are at least initially blocked (see Fig. 4).

The observations on cultured cells differ in some respects from those with isolated mitochondria, indicating that the MPT is much less readily induced in *in situ* mitochondria. This is coherent with the low concentration of Ca^{2+} and of transition metals–the two factors involved in MPT induction with isolated RLM–in the cytoplasm. At least in the case of QTA3BTPI, MPT-independent (because CsA-insensitive) production of superoxide and some loss of $\Delta\Psi$ takes place. Other mitochondriotropic polyphenols may well behave differently, depending on their physico-chemical properties, but compounds of this class are in any case to be studied with care: it is not clear that *in vivo* they would behave only as beneficial antioxidants and ROS quenchers. The results of this investigation may be taken into consideration for the design of other mitochondriotropic compounds: features conferring protonophoric/uncoupling properties will best be avoided if the intention is to produce a cell-saving anti-oxidant molecule, and may conversely be desirable if a candidate for chemotherapeutic applications is desired. Usefulness in oncology may also be maximised by taking into account the findings that cancer cells have elevated levels of copper ions [34] and of oxidative stress [35]. On the other hand mild uncoupling of mitochondria is proposed to have potentially beneficial effects, such as mimicking life-extending caloric restriction (e.g.: [36,37]) and protecting neurons against excitotoxicity (e.g.: [38]). Thus, a less readily oxidisable polyphenol derivative with mild uncoupling activity may also find applications.

Literature reports suggest that concentration, or dosage, may well be an important parameter determining the overall effect of a (mitochondriotropic) polyphenol. For example, EpiGalloCatechin-Gallate (EGCG) may have anti-oxidant and "cell-protective" effects at low dosages (<μM), and pro-oxidant, cytotoxic effects at higher levels [39]. MitoQ, the best studied mitochondriotropic antioxidant, changes from an anti-oxidant to a pro-oxidant behaviour over a relatively small concentration range ([5] and references therein). Low doses of mitochondria-targeted plastoquinone derivatives reportedly exert very beneficial effects *in vivo* [5]. It remains to be seen whether the present compounds may display divergent effects at very low concentration, and whether there may be relatively sharp thresholds for these hypothetical different activities. It also remains to be seen what concentrations may be attained in the organs of laboratory animals, and by what means. Furthermore, as mentioned, the bioactivity of polyphenols is not limited to redox effects. The investigation of the activity of mitochondriotropic polyphenols *in vivo* will need therefore to consider several "readout" parameters, the most important obviously being the impact on physiological or pathological conditions of interest.

Acknowledgments

We thank I. Szabò and V. Petronilli for useful discussions, P. Bernardi's group and F. Zoccarato for access to instrumentation and instructions, U. De Marchi for preliminary experiments, M. Mancon for technical help. This work was supported in part by the Italian Foundation for Basic Research (FIRB), by the Italian Association for Cancer Research (AIRC) and by the University of Padova (Progetto d'Ateneo 2008 to S.G. and a post-doctoral fellowship to L.B.).

References

[1] K.C. Kregel, H.J. Zhang, An integrated view of oxidative stress in aging: basic mechanisms, functional effects, and pathological considerations, Am. J. Physiol. Integr. Comp. Physiol. 292 (2007) R18–R36.
[2] M. Valko, D. Leibfritz, J. Moncol, M.T. Cronin, M. Mazur, J. Telser, Free radicals and antioxidants in normal physiological functions and human disease, Int. J. Biochem. Cell Biol. 39 (2007) 44–84.
[3] A. Carpi, R. Menabò, N. Kaludercic, P. Pelicci, F. Di Lisa, M. Giorgio, The cardioprotective effects elicited by p66(Shc) ablation demonstrate the crucial role of mitochondrial ROS formation in ischemia/reperfusion injury, Biochim. Biophys. Acta 1787 (2009) 774–780.
[4] H. Du, S.S. Yan, Mitochondrial permeability transition pore in Alzheimer's disease: Cyclophilin D and amyloid beta, Biochim. Biophys. Acta 1802 (2010) 198–204.
[5] V.P. Skulachev, V.N. Anisimov, Y.N. Antonenko, L.E. Bakeeva, B.V. Chernyak, V.P. Erichev, O.F. Filenko, N.I. Kalinina, V.I. Kapelko, N.G. Kolosova, B.P. Kopnin, G.A. Korshunova, M.R. Lichinitser, L.A. Obukhova, E.G. Pasyukova, O.I. Pisarenko, V.A. Roginsky, E.K. Ruuge, I.I. Senin, I.I. Severina, M.V. Skulachev, I.M. Spivak, V.N. Tashlitsky, V.A. Tkachuk, M.Y. Vyssokikh, L.S. Yaguzhinsky, D.B. Zorov, An attempt to prevent senescence: a mitochondrial approach, Biochim. Biophys. Acta. 1787 (2009) 437–461.
[6] P. Bernardi, A. Krauskopf, E. Basso, V. Petronilli, E. Blachly-Dyson, F. Di Lisa, M.A. Forte, The mitochondrial permeability transition from *in vitro* artifact to disease target, FEBS J. 273 (2006) 2077–2099.
[7] A. Rasola, P. Bernardi, The mitochondrial permeability transition pore and its involvement in cell death and in disease pathogenesis, Apoptosis 12 (2007) 815–833.
[8] A.P. Halestrap, What is the mitochondrial permeability transition pore? J. Mol. Cell. Cardiol. 46 (2009) 821–831.
[9] J.L. Zweier, M.A. Talukder, The role of oxidants and free radicals in reperfusion injury, Cardiovasc. Res. 70 (2006) 181–190.
[10] V. Petronilli, J. Sileikyte, A. Zulian, F. Dabbeni-Sala, G. Jori, S. Gobbo, G. Tognon, P. Nikolov, P. Bernardi, F. Ricchelli, Switch from inhibition to activation of the mitochondrial permeability transition during hematoporphyrin-mediated photo-oxidative stress. Unmasking pore-regulating external thiols, Biochim Biophys. Acta 1787 (2009) 897–904.
[11] V. Weissig, Targeted drug delivery to mammalian mitochondria in living cells, Expert Opin Drug Deliv. 2 (2005) 89–102.

[12] M.P. Murphy, R.A. Smith, Targeting antioxidants to mitochondria by conjugation to lipophilic cations, Annu. Rev. Pharmacol. Toxicol. 47 (2007) 629–656.
[13] A.T. Hoye, J.E. Davoren, P. Wipf, M.P. Fink, V.E. Kagan, Targeting mitochondria, Acc. Chem. Res. 41 (2008) 87–97.
[14] M.P. Murphy, Targeting lipophilic cations to mitochondria, Biochim. Biophys. Acta 1777 (2008) 1028–1031.
[15] H.H. Szeto, Development of mitochondria-targeted aromatic-cationic peptides for neurodegenerative diseases, Ann. N.Y. Acad. Sci. 1147 (2008) 112–121.
[16] H.H. Szeto, Mitochondria-targeted cytoprotective peptides for ischemia-reperfusion injury, Antiox. Redox Signal. 10 (2008) 601–619.
[17] T.A. Prime, F.H. Blaikie, C. Evans, S.M. Nadtochiy, A.M. James, C.C. Dahm, D.A. Vitturi, R.P. Patel, C.R. Hiley, I. Abakumova, R. Requejo, E.T. Chouchani, T.R. Hurd, J.F. Garvey, C.T. Taylor, P.S. Brookes, R.A. Smith, M.P. Murphy, A mitochondria-targeted S-nitrosothiol modulates respiration, nitrosates thiols, and protects against ischemia-reperfusion injury, Proc. Natl. Acad. Sci. USA 106 (2009) 10764–10769.
[18] J. Ripcke, K. Zarse, M. Ristow, M. Birringer, Small-molecule targeting of the mitochondrial compartment with an endogenously cleaved reversible tag, Chembiochem 10 (2009) 1689–1696.
[19] A. Mattarei, L. Biasutto, E. Marotta, U. De Marchi, N. Sassi, S. Garbisa, M. Zoratti, C. Paradisi, A mitochondriotropic derivative of quercetin: a strategy to increase the effectiveness of polyphenols, Chembiochem 9 (2008) 2633–2642.
[20] L. Biasutto, A. Mattarei, E. Marotta, A. Bradaschia, N. Sassi, S. Garbisa, M. Zoratti, C. Paradisi, Development of mitochondria-targeted derivatives of resveratrol, Bioorg. Med. Chem. Lett. 18 (2008) 5594–5597.
[21] N. Kamo, M. Muratsugu, R. Hongoh, Y. Kobatake, Membrane potential of mitochondria measured with an electrode sensitive to tetraphenyl phosphonium and relationship between proton electrochemical potential and phosphorylation potential in steady state, J. Membr. Biol. 49 (1979) 105–121.
[22] M. Zoratti, M. Favaron, D. Pietrobon, V. Petronilli, Nigericin-induced transient changes in rat-liver mitochondria, Biochim. Biophys. Acta. 767 (1984) 231–239.
[23] U. De Marchi, L. Biasutto, S. Garbisa, A. Toninello, M. Zoratti, Quercetin can act either as an inhibitor or an inducer of the mitochondrial permeability transition pore: A demonstration of the ambivalent redox character of polyphenols, Biochim. Biophys. Acta. 1787 (2009) 1425–1432.
[24] M.F. Ross, T.A. Prime, I. Abakumova, A.M. James, C.M. Porteous, R.A. Smith, M.P. Murphy, Rapid and extensive uptake and activation of hydrophobic triphenylphosphonium cations within cells, Biochem. J. 411 (2008) 633–645.
[25] Y. Sakihama, M.F. Cohen, S.C. Grace, H. Yamasaki, Plant phenolic antioxidant and prooxidant activities: phenolics-induced oxidative damage mediated by metals in plants, Toxicology 177 (2002) 67–80.
[26] U. Shamim, S. Hanif, M.F. Ullah, A.S. Azmi, S.H. Bhat, S.M. Hadi, Plant polyphenols mobilize nuclear copper in human peripheral lymphocytes leading to oxidatively generated DNA breakage: implications for an anticancer mechanism, Free Radic. Res. 42 (2008) 764–772.
[27] V. Petronilli, P. Costantini, L. Scorrano, R. Colonna, S. Passamonti, P. Bernardi, The voltage sensor of the mitochondrial permeability transition pore is tuned by the oxidation-reduction state of vicinal thiols. Increase of the gating potential by oxidants and its reversal by reducing agents, J. Biol. Chem. 269 (1994) 16638–16642.
[28] P. Costantini, B.V. Chernyak, V. Petronilli, P. Bernardi, Modulation of the mitochondrial permeability transition pore by pyridine nucleotides and dithiol oxidation at two separate sites, J. Biol. Chem. 271 (1996) 6746–67451.
[29] P. Costantini, R. Colonna, P. Bernardi, Induction of the mitochondrial permeability transition by N-ethylmaleimide depends on secondary oxidation of critical thiol groups. Potentiation by copper-ortho-phenanthroline without dimerization of the adenine nucleotide translocase, Biochim. Biophys. Acta 1365 (1998) 385–392.
[30] S.V. Jovanovic, S. Steenken, M. Tosic, B. Marjanovic, M.G. Simic, Flavonoids as antioxidants, J. Am. Chem. Soc 116 (1994) 4846–4851.
[31] N. Sauerwald, M. Schwenk, J. Polster, E. Bengsch, Spectrophotometric pK determination of daphnetin, chlorogenic acid and quercetin, Z. Naturforsch. 53b (1998) 315–321.
[32] K. Lemanska, H. Szymusiak, B. Tyrakowska, R. Zielinski, A.E.M.F. Soffers, I.M.C. M. Rietjens, The influence of pH on antioxidant properties and the mechanism of antioxidant action of hydroxyflavones, Free Rad. Biol. Med. 31 (2001) 869–881.
[33] C. van Dijk, A.J. Driessen, K. Recourt, The uncoupling efficiency and affinity of flavonoids for vesicles, Biochem. Pharmacol. 60 (2000) 1593–1600.
[34] A. Gupte, R.J. Mumper, Elevated copper and oxidative stress in cancer cells as a target for cancer treatment, Cancer Treat. Rev. 35 (2009) 32–46.
[35] H. Pelicano, D. Carney, P. Huang, ROS stress in cancer cells and therapeutic implications, Drug Resist. Updat. 7 (2004) 97–110.
[36] C.E. Amara, E.G. Shankland, S.A. Jubrias, D.J. Marcinek, M.J. Kushmerick, K.E. Conley, Mild mitochondrial uncoupling impacts cellular aging in human muscles *in vivo*, Proc. Natl. Acad. Sci. U.S.A. 104 (2007) 1057–1062.
[37] C.C. Caldeira da Silva, F.M. Cerqueira, L.F. Barbosa, M.H. Medeiros, A.J. Kowaltowski, Mild mitochondrial uncoupling in mice affects energy metabolism, redox balance and longevity, Aging Cell 7 (2008) 552–560.
[38] D. Liu, M. Pitta, M.P. Mattson, Preventing NAD(+) depletion protects neurons against excitotoxicity: bioenergetic effects of mild mitochondrial uncoupling and caloric restriction, Ann. N.Y. Acad. Sci. 1147 (2008) 275–282.
[39] S. Mandel, O. Weinreb, T. Amit, M.B. Youdim, Cell signaling pathways in the neuroprotective actions of the green tea polyphenol (-)-epigallocatechin-3-gallate: implications for neurodegenerative diseases, J. Neurochem. 88 (2004) 1555–1569.

8. Toxicology of mitochondriotropic polyphenols

Introduction

Polyphenols are generally seen as anti-oxidants which prevent damages from an excess of ROS production. However many studies demonstrate that they can act also as pro-oxidants, depending on circumstances (Galati et al., 1999; Shakihama et al., 2002; Halliwell, 2008). Their participation in radical/oxidative processes is promoted by conditions such as high concentration, an alkaline pH and the presence of $Fe^{2+/3+}$ and $Cu^{+/2+}$. This production of ROS may be sufficient to result in a "redox catastrophe", leading to oxidation of the GSH pool and to oxidative damage of DNA, proteins and lipids and finally to cell death. The probability of this happening is higher in cancer cells, in which ROS production is more intense (see the introduction of this section for details). Mitochondria, as the major producers of ROS in the cell, may be considered the most relevant site for either an anti-oxidant or a pro-oxidant effect, and this consideration prompted our work on the development of mitochondria-targeted polyphenol derivatives. Furthermore many polyphenols are well-know inhibitors of kinases, the mitochondrial respiratory chain and F_0F_1 ATPase (Dorta et al., 2005; Zheng and Ramirez, 2000; Sarno et al., 2005; Gledhill et al., 2007).

Our group has chosen quercetin and resveratrol to build mitochondrial-targeted compounds. Both these polyphenols are much-studied representatives of the superfamily. Focusing on quercetin, *in vitro* it inhibits different tyrosine and serine-threonine kinases whose activities are linked to survival pathways. It down-regulates the expression of oncogenes (as *H-ras* and *c-myc*) and anti-oncogenes (p53) (Ranelletti et al., 2000), or up-regulates cell-cycle control proteins (Casagrande and Darbon, 2001). In animal models, quercetin seem to inhibit cancer grow and induce apoptosis (Mouria et al., 2002).

Also in the case of resveratrol, several *in vivo* studies (Ulrich et al., 2005) support its efficacy in inhibiting or retarding tumor growth and progression. However, lack of efficacy of resveratrol *in vivo* was reported by others; these discrepancies may be due in part to a low bioavailability and to a limited affinity for some of the targets, which can therefore be engaged at the higher concentrations used in vitro, but not in vivo. *In vitro*, resveratrol is well known to exhibit antiproliferative,

cytotoxic and pro-apoptotic effects in many cell models (Shakibaei et al., 2009; Hail and Lotan, 2009; Pervaiz et al., 2009). The mechanisms include inhibition of ERK1/2-mediated signal transduction pathways, inhibition of kinases such as Cdk1 and Cdk4 (blocking cell-cycle progression) induction of apoptosis by activation of caspases, p53 and Bax or by inhibition of Bcl-2 (Ulrich et al., 2005; Aziz et al., 2003).

One very popular approach to produce mitochondria-targeted compounds takes advantage of the electrical potential difference across the IMM, using membrane-permeable compounds with a net positive charge. Indeed the matrix-side voltage gradient is negative and more so in cancers cells, which makes tumors possible privileged targets for these compounds. Triphenylphosphonium cations are often used to build mitochondriotropic compounds in which they are the “engine” insuring import into the mitochondrial matrix (Murphy and Smith, 2007). Compounds of this type will also concentrate, although to a more limited extent, in the cytosol, due to the plasma membrane potential.

To make quercetin and resveratrol mitochondriotropic, our group synthesized a few derivatives in which a TPP group is linked to one of the hydroxyls on the ring system (Q3BTPI, Q7BTPI, R3BTPI, and R4’BTPI). We have also produced other derivatives which possess not only the TPP group but also acetyl moieties which protect the remaining hydroxyls to avoid unspecific interactions with proteins, to limit formation of negative charges and to hinder metabolism (QTA3BTPI, QTA7BTPI, RDA3BTPI, and RDA4’BTPI). The structures of these compounds are shown in Scheme 1.

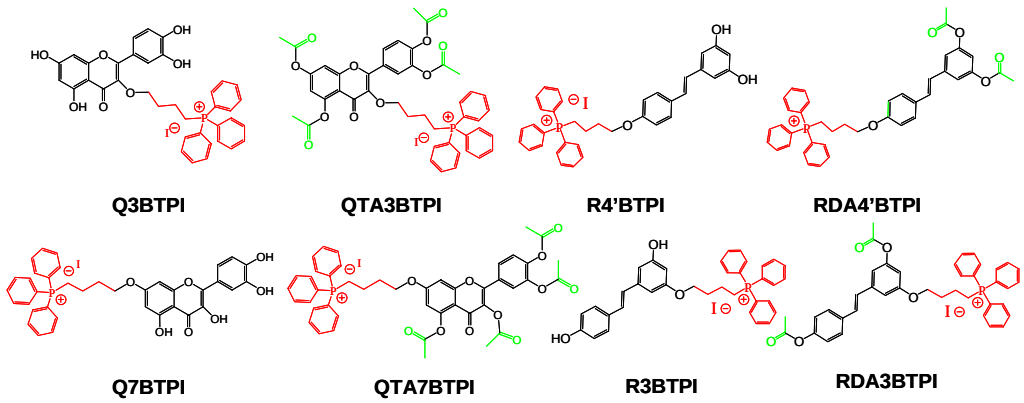

Scheme 1. Structures of the mitochondriotropic compounds used.

The rationale of such an approach calls for the delivery and accumulation in mitochondria of compounds with physico-chemical properties and bioactivities similar to those of the parent compound (quercetin in our case). On the other hand, any modification of the chemical structure will imply a modification of the properties. Thus, e.g., quercetin conjugates produced in metabolism are less oxidation-prone than quercetin itself (Lodi et al., 2008). Isomeric compounds can also differ in their redox properties. Oxidation of flavonoids with a catechol group on the B ring involves this moiety because the resonance stabilization of the resulting radical is maximized (Krishnamachari et al., 2002; Firuzi et al., 2005; Zhou and Sadik, 2008; He et al., 2009) but the rate of the electrochemical process (Hendrickson et al., 1994; Montana et al., 2007) and the identity of the products eventually formed (Jorgensen et al., 1998) have been reported to depend on the presence of a free OH at position 3. A cyclic voltammetry study carried out by Dr. A. Mattarei of our group in collaboration with Prof. A. Gennaro's group at the Dept. of Chemical Sciences has shown that, indeed, Q7BTPI is oxidized at potentials very close to those needed to oxidize quercetin (67 mV vs. SCE in both cases), while the 3-substituted isomer needs a higher anodic potential (132 mV) (A. Mattarei et al., personal communication; note that the absolute values depend to some extent on the experimental conditions chosen). The acetylated derivatives, as expected, are not oxidized at voltages up to 1 V. A similar difference was observed in the case of the resveratrol derivatives. In this case the first oxidation process involves the hydroxyl at position 4', again because of resonance stabilization of the reaction product. Thus, compounds having this oxygen involved in a covalent linkage - and therefore unable either to confer an hydrogen radical or to form the easily oxidizable conjugated base (Resv-O^-) - are expected to require a higher potential than the isomeric, 3-substituted derivative to undergo oxidation. This was confirmed by Dr. Mattarei's experiments, which yielded similar anodic first oxidation potentials for resveratrol and R3BTPI (0.47 vs. 0.49 V, respectively), while R4'BTPI underwent the first oxidation at 0.68 V. These results suggest that Q7BTPI and R3BTPI are the derivatives of choice for experiments intended to cause the accumulation into mitochondria of compounds with redox properties similar to those of the parent polyphenols. If the effects of

these compounds on cells are due, at least in part, to redox processes, we should be able to observe a difference between the isomers. I have therefore assayed their cytotoxic/cytostatic properties as well as mitochondrial depolarization and the production of superoxide elicited from cells.

Materials and methods

Materials. Quercetin was purchased from Sigma, resveratrol from Waseta Int. Trading Co. (Shangai, P.R.China). Q3BTPI, Q7BTPI, 4R4'BTPI and R3BTPI were synthesised by Dr. A. Mattarei of our group. All chemicals for buffer preparations were of laboratory grade, obtained from J. T. Baker, Merck, or Sigma.

Cells. Fast- (doubling time approx. 16 hours) and slow (doubling time approx. 3 days) -growing SV-40 immortalized Mouse Embryo Fibroblast (MEF) cells and mouse colon cancer C-26 cells (doubling time approx. 24 hours) were grown in Dulbecco's Modified Eagle Medium (DMEM) plus 10 mM HEPES buffer, 10% (v/v) fetal calf serum (Invitrogen), 100 U/mL penicillin G (Sigma), 0.1 mg/mL streptomycin (Sigma), 2 mM glutamine (GIBCO) and 1% nonessential amino acids (100X solution; GIBCO), in a humidified atmosphere of 5% CO2 at 37 °C. Jurkats (doubling time approx. 24 hours) were grown in RPMI-1640 supplemented as above.

Cell growth/viability MTT assays. These experiments were intended to compare the effects of our compounds on cells exhibiting different proliferation rates. They pose a problem in that these effects are expected to depend not on the concentration of compound in the growth medium, but rather on the amount accumulated by the cells, which is (presumably) inversely proportional to the number of cells in the assay. This number, equal at the beginning of the experiment, changes during its time course due to the different doubling times of the cultures. Furthermore, in assays with slow-growing cells it was necessary to begin the culture with a more numerous population in order to obtain significant readout values. Results can therefore be of only semi-quantitative significance.

C-26 or MEF cells were seeded in standard 96-well plates and allowed to grow in DMEM (200 µL) for 16-18 hours to ensure attachment. Initial densities were 1000-3000 (C-26, fast-growing MEF) or 2500-3000 (slow-growing MEF)

cells/well in experiments with a 72 h incubation period. After this initial period the growth medium was replaced with medium containing the desired compound from a mother solution in DMSO. Three different concentrations of compounds were used: 1, 3 and 5 μM; DMSO final concentration was 0.1% in all cases (including controls). Experiments were performed in quadruplicate, i.e., four wells were used for each of the compounds to be tested. Cells were incubated with the compounds for 72 hours; the solution was substituted by a fresh aliquot twice, at 24-hour intervals. At the end of the incubation period, the medium was removed and substituted with 90μl of PBS plus 10 μL of CellTiter 96® solution (Promega; for details: www.promega.com/tbs). After a one-hour color development period at 37°C absorbance at 490 nm was measured using a Packard Spectra Count 96-well plate reader.

Mitochondrial potential assay. Tetramethylrhodamine methyl ester (TMRM; Invitrogen/Molecular Probes) staining was used to monitor mitochondrial transmembrane potential by fluorescence microscopy of cultured HepG2 cells and/or by FACS (Fluorescence-Activated Cell Scanning) of Jurkat lymphocytes. The former method was used to study the effect of Q3BTPI and Q7BTPI, while FACS analysis was applied with QTA3BTPI, QTA7BTPI and with the resveratrol-derived compounds.

HepG2 cells were seeded onto 24-mm coverslips in 6-well plates and grown for about two days, avoiding confluence. Coverslips were mounted onto holders, exposed to 20 nM TMRM in DMEM or HBSS for about 20min, generally in the presence of 4 μM Cyclosporin H or 2 μM Cyclosporin A depending on the details of the experimental protocol, and washed twice. Cells were then covered with 1 mL of the desired medium and observed at room temperature. Additions were performed by withdrawing 0.5 mL of incubation medium, adding the desired solute to this aliquot, mixing, and adding back the solution into the chamber at a peripheral point. Images were acquired automatically at 1- or 2-min intervals, using an Olympus Biosystems apparatus comprising an Olympus IX71 microscope and MT20 light source. Excitation was at 568 ± 25 nm and fluorescence was collected using a 585-nm longpass filter. Regions of Interest (ROIs) corresponding to a cell or a group comprising a few cells (or to a background area without cells in it) were identified manually offline, and the

fluorescence emitted in the area was automatically measured and plotted by the CellR© software.

FACS experiments were conducted with Jurkat lymphocytes to avoid cell aggregations and possible membrane potential-altering damage due to trypsinization and other procedures associated with the detachment of adherent cells. Procedures were essentially as described below for superoxide production assays, loading the cells with 20 nM TMRM for approximately 20 min.

Superoxide production assays. Superoxide generation in cells was assessed in FACS experiments using the mitochondriotropic probe MitoSOX Red® (Invitrogen/Molecular Probes). A Beckton Dickinson Canto II flow cytometer was used. Excitation was at 500-520 nm, and fluorescence was collected at wavelengths longer than 570 nm. The cells were washed and resuspended in HBSS (in mM units: NaCl 136.9, KCl 5.36, CaCl2 1.26, MgSO4 0.81, KH2PO4 0.44, Na2HPO4 0.34, glucose 5.55, pH 7.4 with NaOH) at a density of 4 × 10^5/mL and loaded with 1 or 2 μM MitoSOX Red® in HBSS (37°C, 15 min). CsA (5μM), or in some experiments CsH, was included as an inhibitor of MDR pumps, to obtain a higher accumulation ratio for the dye and to limit the rate of efflux during the experiment. The experimental medium was HBSS, rather than the previously used "FACS buffer" (Biasutto et al., 2010- Chapt. 7) to promote cell survival and well-being during the experiment. After loading cells were diluted 1:5 in HBSS (plus 5μM CsA) and divided into the desired number of identical aliquots. At time zero the desired compound was added, and data collected after the desired incubation times, exciting at 545 nm and measuring fluorescence at 585 nm. Data were analyzed using the BD VISTA software.

Results

Cytotoxicity. Mitochondriotropic compounds (Q3BTPI, QTA3BTPI, Q7TBPI, QTA7BTPI, R3BTPI, RDA3BTPI, R4'BTPI, RDA4'BTPI) were tested for their possible cytotoxic/cytostatic action on cultured cells. As controls, we checked also the action of parent polyphenols (quercetin and resveratrol), a phosphonium salt (TPMP) and parent polyphenols plus TPMP. Three cell lines were used for these studies. One is a murine colon cancer line (C-26) with a doubling time approx. of 24 hours, which might be utilized also for planned *in vivo* studies involving the

implantation of tumors in mice. The other two are fast- and slow-growing embryonic murine fibroblasts (MEF), non-tumoral cell lines. To evaluate the cytotoxic/cytostatic action of our compounds, we used the tetrazolium salt reduction (MTT) assay to quantify cell growth and viability. Since the mitochondriotropic compounds accumulate in mitochondria, it is plausible to suppose that their effect depends on the number of cells exposed to them (the greater the number of cells, the lower the amount of compound in each cell and the weaker therefore the effect). Indeed in experiments with higher initial numbers of cells, the effects on cell growth were weaker (data not shown). To minimize this problem and to compare the effects of different compounds on the same cell line we used the various compounds in parallel within the same experiment. In this way the number of viable cells at the beginning of incubation was the same. The results shown are representative of at least three analogous experiments.

Fig. 1 shows representative data for quercetin derivatives. All compounds tested had little or no effect at 1 µM (not shown). The higher effectiveness of Q7BTPI in comparison to Q3BTPI can be appreciated best at the 3 µM level. A cytotoxic/cytostatic effect of the mitochondriotropic quercetins is evident in the case of C-26 cells (Fig. 1A) and, more moderately, on fast-growing MEF cells (Fig. 1B), while the effect on slow-growing MEF cells was insignificant (Fig 1C). The parent polyphenols and TPMP did not have any significant effect on cells vitality.

The results of the MTT assay were confirmed by direct observation of the cell cultures at the microscope (Fig. 2). Whether cell death under these circumstances proceeds by apoptosis or necrosis remains to be investigated.

Fig. 3 illustrates the results of MTT assays with resveratrol-based constructs. The mitochondriotropic isomeric derivatives of this polyphenol are also cytotoxic, but the difference between them is less marked than in the case of the quercetin analogues.

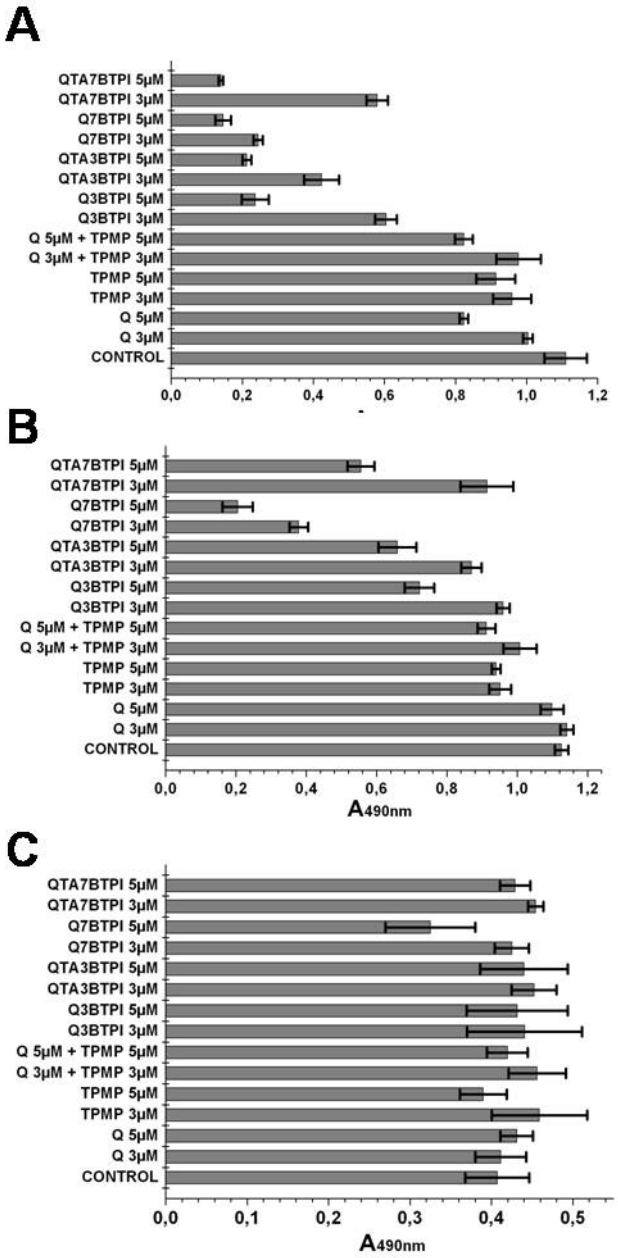

Fig. 1. Effect of quercetin derivatives and control compounds on the readout of tetrazolium reduction assays. Cells were allowed to grow for 3 days in the presence of the specified compounds (see Materials and Methods for details). The panels show the results of individual representative experiments run in parallel with the three cell lines. All measurements were performed in quadruplicate. Averages ± s.d. are given. A) C-26 mouse colon tumor cells. B) Fast-growing Mouse Embryonic Fibroblasts (MEF). C) Slow-growing MEF. Abbreviations: TPMP: methyltriphenylphosphonium; BTPI: n-(4-triphenylphosphonium)butyl iodide; Q: quercetin. In these experiments the number of cells seeded in each well was as follows: A: 3000; B: 1000; C: 2500.

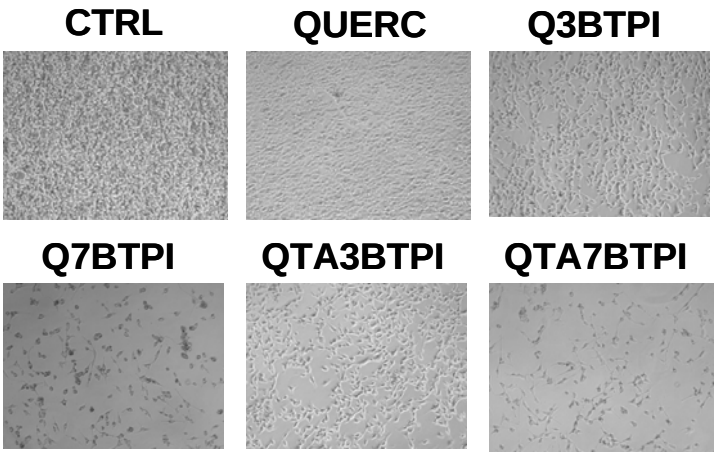

Fig.2. Images of C-26 cell cultures after 72 h of incubation with 5 μM of the indicated compounds.

Effects on cellular parameters. To begin an investigation of the mechanisms of these effects I have monitored mitochondrial potential and superoxide production in cells exposed to these compounds. This part of the study is still in progress. We observed the variation of mitochondrial potential via TMRM fluorescence in microscopy and FACS experiments and the increase of production of ROS via mitoSOX® fluorescence with FACS. CsA was included to block the activity of multi-drugs pumps which can expel the probes. The presence of this MPT inhibitor was intended also to exclude effects due to its onset, allowing the observation of upstream effects, but whether it could indeed block the MPT under the experimental conditions remains to be verified. The cells were treated with quercetin, resveratrol and their derivatives, and photographed every 1 or 2 minutes in microscopy experiments or analyzed after 0 (a few seconds after the addition), 15, 30, 60, 90 and 120 minutes of incubation in FACS experiments.

A set of representative fluorescence microscopy experiments monitoring TMRM fluorescence in HepG2 cells treated Q3BTPI or Q7BTPI is shown in Fig. 4A. Fluorescence loss (depolarization) is visibly faster in the case of Q7BTPI (see also Fig. 7A in Biasutto et al., 2010 – Chapt 7). The acetylated mitochondriotropic derivatives also induced TMRM fluorescence loss in both microscopy (not shown) and FACS experiments (Fig. 4B). In this case there was little difference between the two isomers tested.

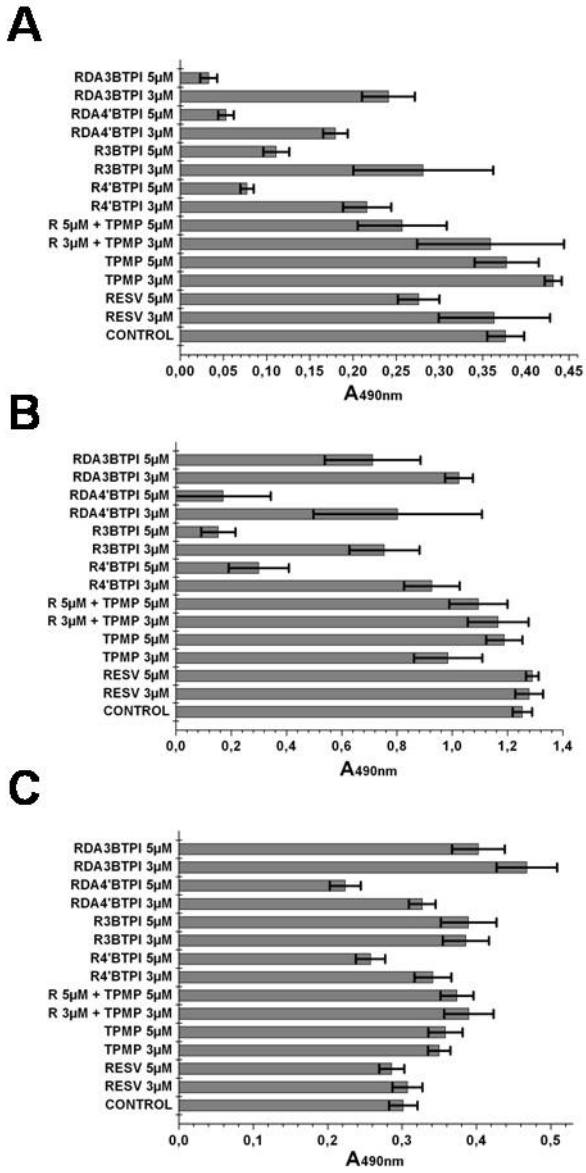

Fig. 3. Effect of resveratrol derivatives and control compounds on the readout of tetrazolium reduction assays. Cells were allowed to grow for 3 days in the presence of the specified compounds (See Materials and Methods for details). The panels show the results of individual representative experiments. All measurements were performed in quadruplicate. Averages ± s.d. are given. A) C-26 mouse colon tumor cells. B) Fast-growing MEF. C) Slow-growing MEF. Abbreviations: TPMP: methyltriphenylphosphonium; BTPI: n-(4-triphenylphosphonium)butyl iodide; RESV: resveratrol. In these experiments the number of cells seeded in each well was as follows: A: 1000; B: 1000; C: 2500.

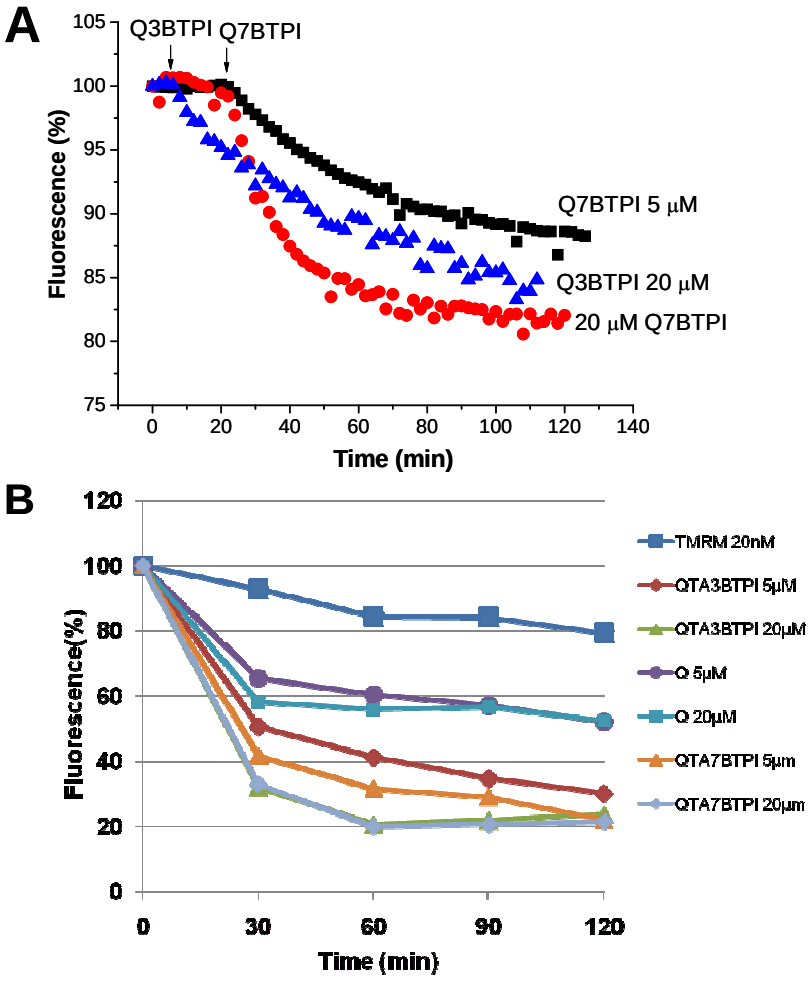

Fig. 4. Mitochondriotropic quercetin derivatives induce loss of TMRM fluorescence from mitochondria. A) Data from three separate representative fluorescence microscopy experiments. Plotted are the normalized fluorescence values of ROIs corresponding to one or a few HepG2 cells (see Materials and Methods for details). 2 µM CsA was present throughout. B) A representative FACS experiment with TMRM-loaded Jurkat cells (see Materials and Methods for details). Plotted are the median values of fluorescence distribution histograms. The specified compounds were added at time 0, and the first set of data was acquired within a few seconds of the addition. The upmost plot (labeled TMRM 20 nM) is the control sample (no additions). 5 µM CsA was present throughout.

QTA3BTPI and QTA7BTPI did not induce appreciable alterations of the forward- and side-scatter FACS parameters of the population at either 5 or 20 µM (not shown). In other cases however important changes of these parameters indicate that the compounds added had an important impact on cell morphology and, presumably, functionality. This is illustrated for Q7BTPI in Fig. 5.

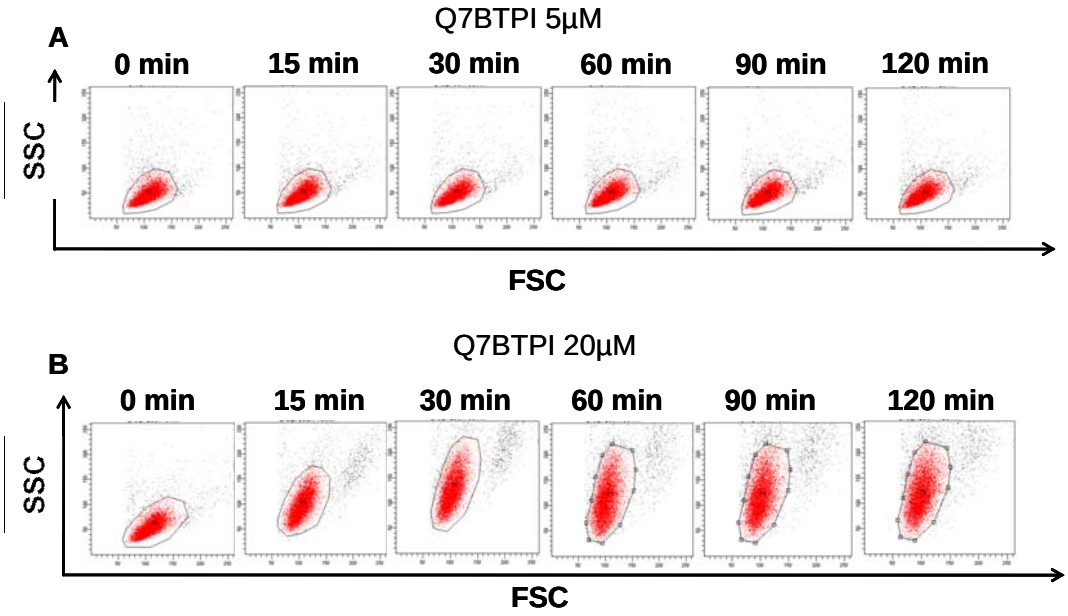

Fig. 5. High concentrations of mitochondriotropic quercetin derivatives cause alterations of the scatter parameters of Jurkat cells. Side- vs. forward scatter plots obtained from suspensions of cells treated with Q7BTPI at the concentrations and for the periods indicated. 10.000 objects were counted in each case.

Q3BTPI had qualitatively similar effects (not shown). With these compounds, at the higher concentration used (20 µM), as the experiment progresses the range of forward scatter of the population remains approximately constant, but side scatter increases progressively, indicating important changes in cell structure for an increasing proportion of cells. Subpopulations cannot be easily distinguished in this case. The data obtained with these compounds in FACS experiments must be interpreted keeping in mind that they originate from a probably rather heterogeneous ensemble.

Some of the mitochondriotropic resveratrol derivatives also cause changes of the scatter parameters. In this case it is the acetylated derivatives, at 20 µM, that induce the appearence and progressive increase of a population of objects with reduced forward scatter and increased side scatter (P2 in Fig. 6B, green), possibly reflecting onset of apoptosis for part of the cells. No such effect was induced at 5 µM (Fig. 6A).

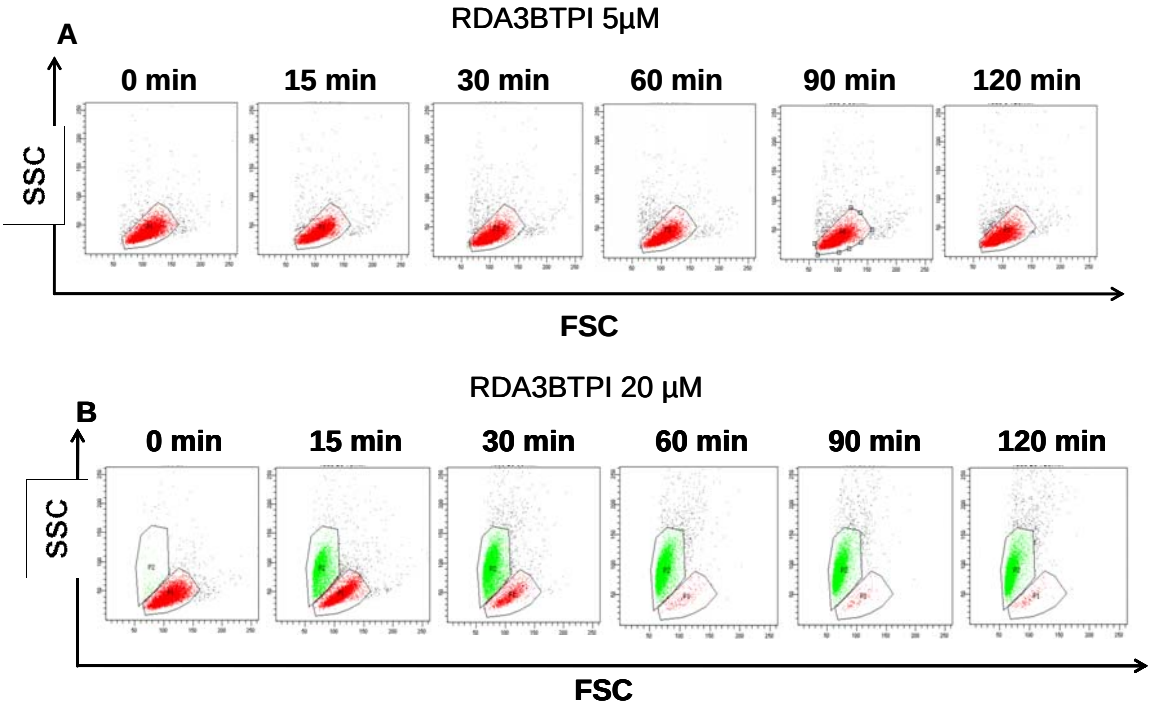

Fig. 6. High concentrations of mitochondriotropic acetylated resveratrol derivatives cause alterations of the scatter parameters of Jurkat cells. Side- vs. forward scatter plots obtained from suspensions of cells treated with RDA3BTPI at the concentrations and for the periods indicated. 10.000 objects were counted in each case. In panel B two populations are marked as red (Population 1) and green (Population 2).

The evolution in time of either TMRM (or MitoSOX®, see below) fluorescence is different for the two populations created by 20 µM compound, as shown in Fig. 7A,B. Population P2 (green) is at all times characterized by a low fluorescence, confirming it represents cells which have already progressed along the path to cell death. Population P1 shows a rapid loss of TMRM fluorescence, which seems to be propedeutic to the transition to population P2. As mentioned, R4'BTPI induces an analogous behaviour, while the non-acetylated resveratrol derivatives, as well as the acetylated ones at 5 µM, do not give rise to split populations. The fluorescence data obtained in these latter cases are therefore presented as the medians of the fluorescence distributions of the whole population (excluding only a low percentage of outliers) in Fig. 7C. With resveratrol derivatives no significant difference was observed between the 3- and 7-BTPI substituted isomers.

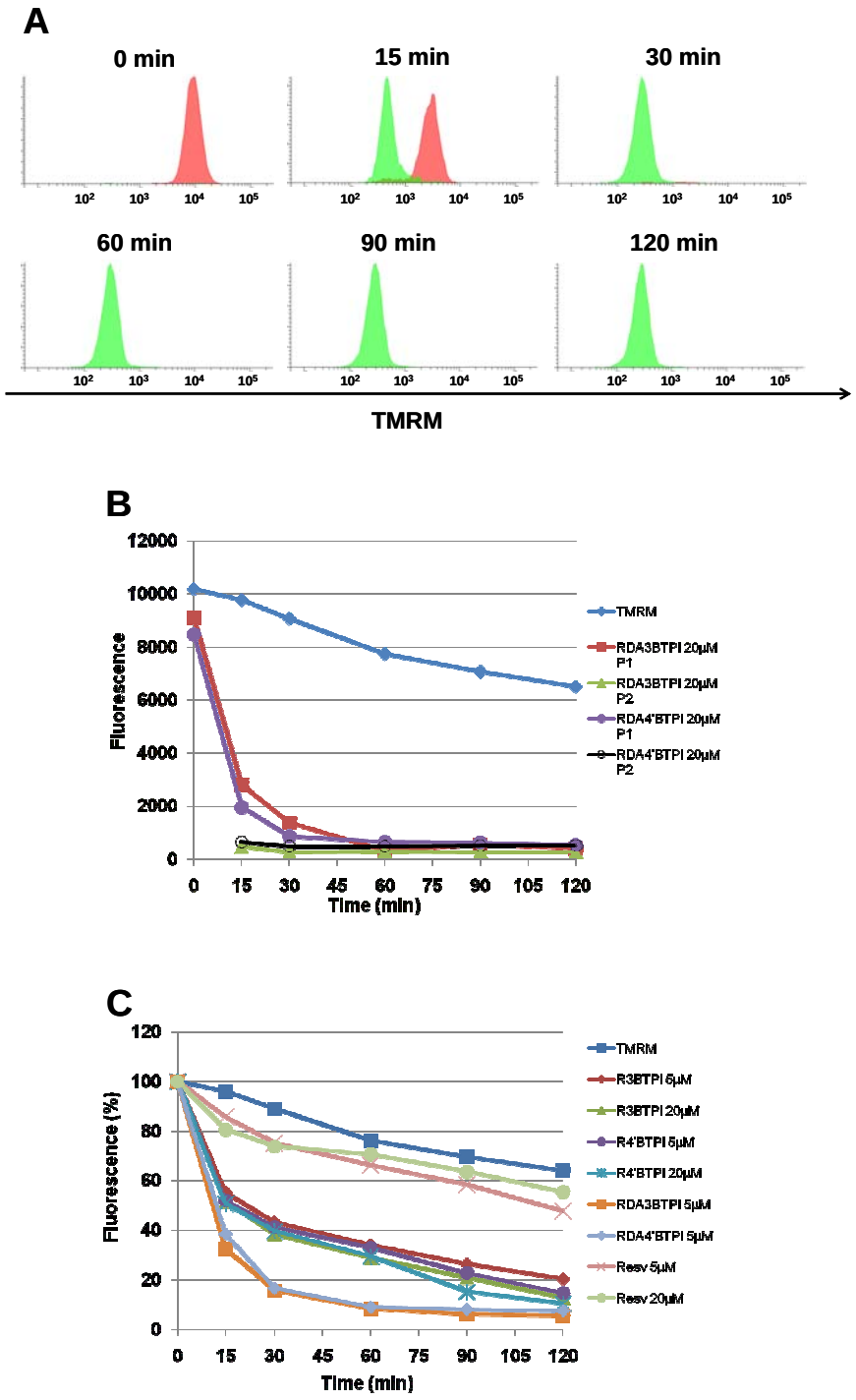

Fig. 7. TMRM fluorescence in Jurkat cells exposed to resveratrol derivatives. A) Fluorescence distribution histograms for cells exposed to 20 µM RDA3BTPI for the indicated times. Two distributions are clearly identifiable, originating from populations analogous to those shown in Fig. 6B. B-C) Plots of the medians of cell fluorescence distribution histograms such as those shown in Fig. 7A for the indicated compounds and concentrations. The label "TMRM" indicates the control sample (no addition). 10.000 cells were detected for each time point. In panel B: P1: Population 1 (red). P2: Population 2 (green).

The results of the MitoSOX® fluorescence assays with the quercetin derivatives appear to reflect the redox properties of the compounds. In keeping with their low oxidation potentials and with their accumulation into mitochondria, where redox activity is most intense, Q3BTPI and Q7BTPI both elicited a strong response, with Q7BTPI easily surpassing Q3BPTI (Fig. 8A,B). All the other compounds tested paled in comparison, although at 20 µM QTA3BTPI and QTA7BTPI did induce a considerable response, possibly because they can be partly deacetylated by the cells (Biasutto et al., 2010 – Chapt. 7) (Fig. 8C).

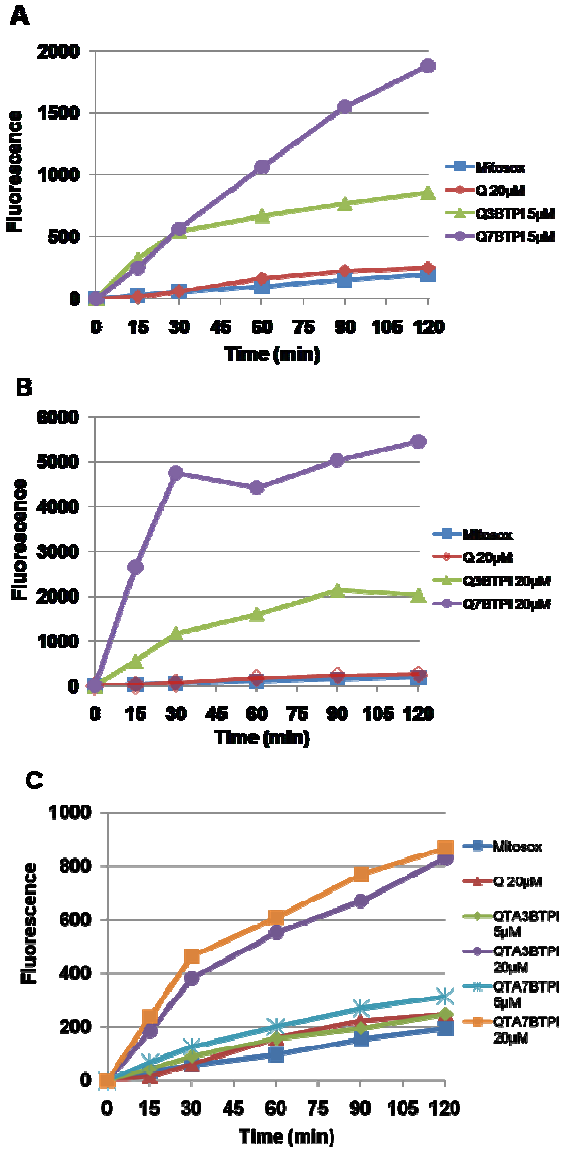

Fig. 8. MitoSOX® fluorescence response elicited by quercetin derivatives in Jurkat cells (FACS experiments). Plots of the medians of cell fluorescence distribution histograms analogous to those shown in Fig. 7A for the indicated compounds and concentrations. The label "MitoSOX" indicates the control sample (no addition). 10.000 cells were detected for each time point.

Fluorescence microscopy determinations on the other hand showed only a modest increase of MitoSOX fluorescence at 5 µM Q3BTPI (Biasutto et al., 2010- Chapt. 7) or Q7BTPI (Fig. 9).

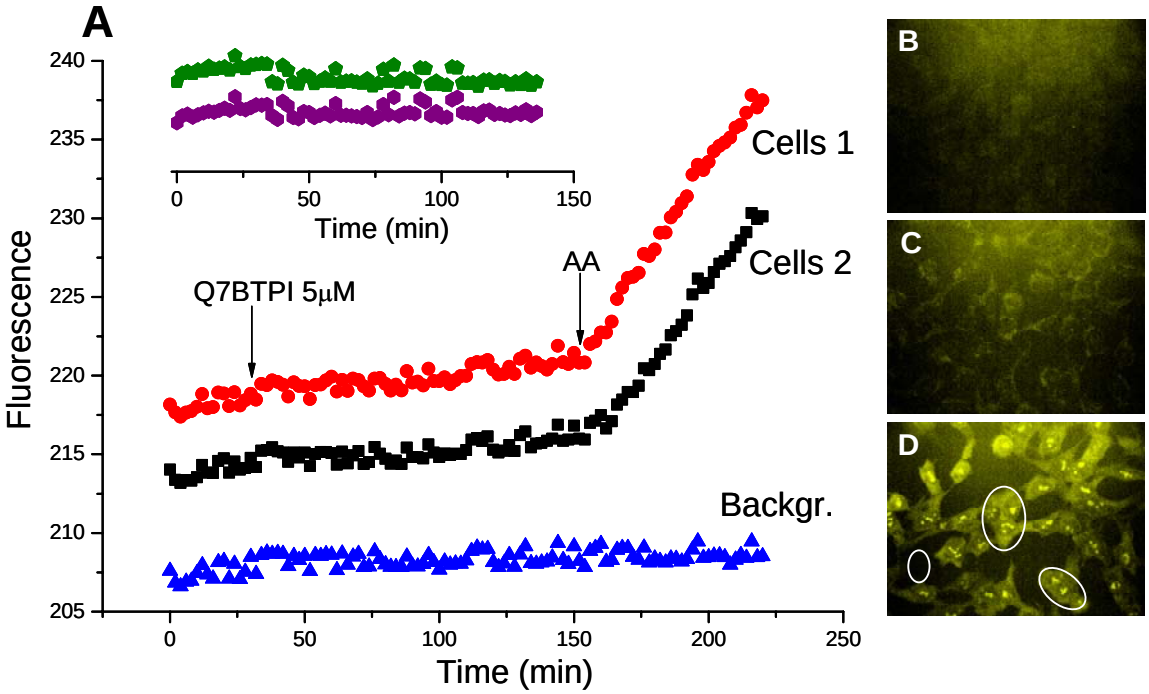

Fig. 9. MitoSOX® fluorescence in HepG2 cells treated with Q7BTPI. A representative experiment is shown. 5 µM Q7BTPI was added after 30 min of incubation, 2 µg/mL Antimycin A after 150 min. A) Plotted are the fluorescence values recorded from the ROIs outlined in panel D. The inset shows, with the same scaling, an analogous plot from a different experiment with no addition (control). B-D) Representative images acquired at time 0, 150 (after 120 min of incubation with with Q7BTPI) and 220 min (after 70 min of incubation with Antimycin). AA: Antimycin A.

In analogy to the behavior observed in experiments monitoring TMRM fluorescence, in the case of 20 µM RDA3BTPI and RDA4'BTPI MitoSOX® fluorescence also reflected the presence of two populations (see Fig. 6B). Fig. 10A shows the MitoSOX® fluorescence distributions obtained in the same experiment presented in Fig. 6B. Population P1, presumably representing still relatively healthy cells, shows little fluorescence increase. Population P2 is characterized by high and increasing fluorescence, which is therefore likely to be secondary to a primary death-inducing chain of events started by the drugs (Fig. 10B). Fluorescence increase is relatively modest in all other case (Fig. 10C).

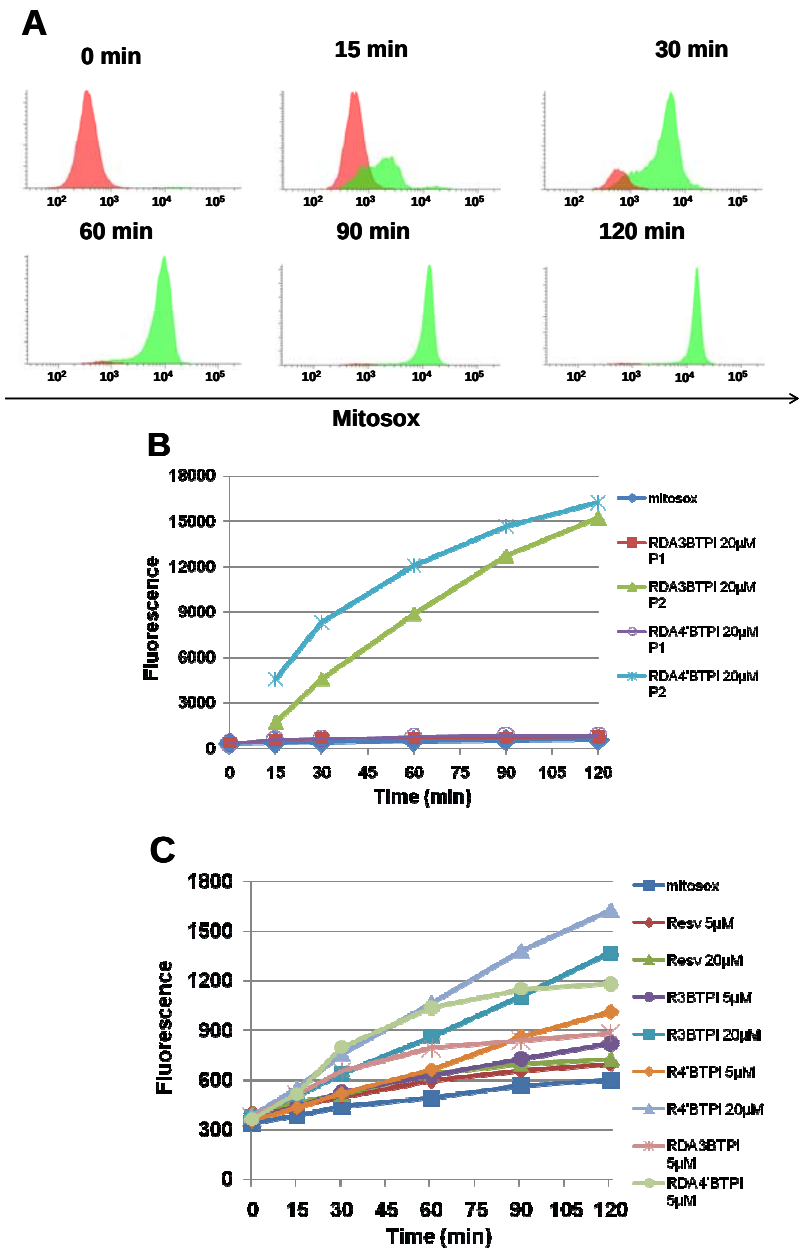

Fig. 10. MitoSOX® fluorescence in Jurkat cells exposed to resveratrol derivatives. A) Fluorescence distribution histograms for cells exposed to 20 µM RDA3BTPI for the indicated times. Two distributions are clearly identifiable, originating from the populations shown in Fig. 6B (same experiment). B-C) Plots of the medians of cell fluorescence distribution histograms for the indicated compounds and concentrations. The label "MitoSOX" indicates the control sample (no addition). 10.000 cells were measured for each time point. In panel B: P1: Population 1 (red). P2: Population 2 (green).

Conclusions

In MTT assays with adherent cells, mitochondriotropic derivatives showed a cytotoxic/cytostatic action on tumoral and fast-growing cells, while with slow-growing cells the effect was much milder. The controls involving exposure to quercetin or resveratrol, phosphonium salts and their combination did not produce similar effects. The combination of the polyphenol kernel and the mitochondriotropic phosphonium moiety is thus a key feature of these molecules. Q7BTPI turned out to be a more effective death inducer than its isomer Q3BTPI. This correlates with the ease of oxidation of these compounds, and it is tempting to associate death induction with pro-oxidant behavior. Both compounds induced only a very modest production of superoxide, visualized as MitoSOX® fluorescence in microscopy experiments with adherent cells maintaining their morphological characteristics throughout the experiment. A strong MitoSOX® fluorescence response was observed instead in FACS experiments, with Q7BTPI being more effective than Q3BTPI. The SSC-FSC plots at 5 µM show little alteration with respect to the control, while at 20 µM a definite change takes place, indicating an impact on cell morphology and, possibly, functionality. An even more drastic effect can be observed with the acetylated resveratrol compounds (Fig.s 6 and 10). These molecules are very reluctant to undergo oxidation *per se*, and the superoxide production they induce is confined to the cells that have undergone the changes associated with variation of the scatter parameters. Thus, superoxide production seems to be downstream of alterations induced via still unknown mechanisms by the compounds. The doubt that this may be the case also for Q3BTPI and Q7BTPI is legitimate and will need to be resolved.

A toxic effect of these compounds is that they induce loss of TMRM fluorescence, i.e., mitochondrial depolarization. We have previously concluded that at least quercetin derivatives can act as uncouplers by setting up a futile protonophoric cycle (Biasutto et al., 2010 – Chapt. 7). Other phenomena may also help account for depolarization: quercetin (Dorta et al., 2005) and at least Q3BTPI (Biasutto, L., Cattelan, P., et al., unpublished results) inhibit the respiratory chain; both quercetin and resveratrol and their derivatives inhibit the mitochondrial ATP

synthase (Zheng and Ramirez, 2000; Gledhill et al., 2007; Datiles et al., 2008; Mattarei et al., 2008 – Chapt 5). Inhibition of the respiratory chain may provide the initial input for a self-amplifying cycle of ROS production, which may lead to cell disruption via aspecific oxidative processes and/or the MPT (despite the presence of CsA in our experiments, since this inhibitor is not always efficacious (Zoratti et al., 2005)).

It should be pointed out that the experiments reported here were performed in *in vitro* model systems, and that measurable effects were observed only at what may be considered high concentrations (3 µM or higher) and, more relevantly, at high compound/cell ratios. What the effects of these compounds may turn out to be *in vivo* remains an open question, and much may well depend on the attainable levels. Considerably lower dosages may have little effect or an hormetic action, inducing cytoprotective anti-oxidant responses. If high concentrations can be achieved, at least locally, they are likely to have a cytotoxic effect which may be put to use to fight established cancer. Selectivity vs. cancer cells may be expected in this case latter case to be achievable by topologically restricted delivery as well as because of the higher mitochondrial potential maintained by most cancer cells (e.g.: Modica-Napolitano and Aprille, 2001). In turn achievable levels *in vivo* are expected to depend on the mode of administration, efficiency of adsorption, metabolism, binding, rate of transport and excretion. All these aspects as well as toxicology need to be explored before the usefulness of compounds of this type in real life can be assessed.

References

Annis MG, Soucie EL, Dlugosz PJ, Cruz-Aguado JA, Penn LZ, Leber B, Andrews DW (**2005**) Bax forms multispanning monomers that oligomerize to permeabilize membranes during apoptosis. EMBO J. 24:2096-103.

Aon MA, Cortassa S, Akar FG, Brown DA, Zhou L, O'Rourke B (**2009**) From mitochondrial dynamics to arrhythmias. Int J Biochem Cell Biol. 41:1940-8.

Arcangeli A, Crociani O, Lastraioli E, Masi A, Pillozzi S, Becchetti A (**2009**) Targeting ion channels in cancer: a novel frontier in antineoplastic therapy. Curr Med Chem.16:66-93.

Azad N, Rojanasakul Y, Vallyathan V (**2008**) Inflammation and lung cancer: roles of reactive oxygen/nitrogen species. J Toxicol Environ Health B Crit. 11:1-15.

Aziz MH, Kumar R, Ahmad N (**2003**) Cancer chemoprevention by resveratrol: in vitro and in vivo studies and the underlying mechanisms. Int J Oncol. 23:17–28.

Beavis AD, Garlid KD (**1990**) Evidence for the allosteric regulation of the mitochondrial K^+/H^+ antiporter by matrix protons. J Biol Chem. 265:2538– 2545.

Behrend, L, Henderson G, Zwacka RM (**2003**) Reactive oxygen species in oncogenic transformation. Biochem Soc Trans. 31:1441–1444.

Bernardi P (**1999**) Mitochondrial transport of cations: channels, exchangers, and permeability transition. Physiol Rev. 79:1127-1155.

Brahimi-Horn MC, Chiche J, Pouyssegur J (**2007**) Hypoxia signaling controls metabolic demand. Curr. Opin. Cell. Biol. 19:223–229.

Brierley GP, Baysal K, Jung DW (**1994**) Cation transport systems in mitochondria: Na^+ and K^+ uniports and exchangers. J Bioenerg Biomembr. 26:519–526.

Brierley GP, Jung DW (**1988**) K^+/H^+ antiport in mitochondria. J Bioenerg Biomembranes 20:193– 209.

Cahalan MD, Wulff H, Chandy KG (**2001**) Molecular properties and physiological roles of ion channels in the immune system. J Clin Immunol. 21:235-252.

Casagrande F, Darbon JM (**2001**) Effects of structurally related flavonoids on cell cycle progression of human melanoma cells: regulation of cyclin-dependent kinases CDK2 and CDK1. Biochem Pharmacol. 61:1205-15.

Chan T, Galati G, O'Brien PJ (**1999**) Oxygen activation during peroxidase catalyzed metabolism of flavones or flavanones. Chem Biol Interact. 122:15-25.

Chandy KG, Wulff H, Beeton C, Pennington M, Gutman GA, Cahalan MD (**2004**) K^+ channels as targets for specific immunomodulation. Trends Pharmacol Sci. 25:280-289.

Chen EI, Hewel J, Krueger JS, Tiraby C, Weber MR, Kralli A, Becker K, Yates JR 3rd, Felding-Habermann B (**2007**) Adaptation of energy metabolism in breast cancer brain metastases. Cancer Res. 67:1472–1486.

Circu ML, Aw TY (**2010**) Reactive oxygen species, cellular redox systems, and apoptosis. Free Radic Biol Med. [Epub ahead of print]

Cook, JA, Gius D, Wink DA, Krishna MC, Russo A, Mitchell JB (**2004**) Oxidative stress, redox, and the tumor microenvironment. Semin Radiat Oncol. 14:259-266.

D'Alessio M, De Nicola M, Coppola S, Gualandi G, Pugliese L, Cerella C, Cristofanon S, Civitareale P, Ciriolo MR, Bergamaschi A, Magrini A, Ghibelli L (**2005**) Oxidative Bax dimerization promotes its translocation to mitochondria independently of apoptosis. FASEB J. 19:1504 –1506.

Datiles MJ, Johnson EA, McCarty RE (**2008**) Inhibition of the ATPase activity of the catalytic portion of ATP synthases by cationic amphiphiles. Biochim Biophys Acta. 1777:362-8.

De Marchi U, Biasutto L, Garbisa S, Toninello A, Zoratti M (**2009**) Quercetin can act either as an inhibitor or an inducer of the mitochondrial permeability transition pore: A demonstration of the ambivalent redox character of polyphenols. Biochim Biophys Acta. 1787:1425-32.

Dorta DJ, Pigoso AA, Mingatto FE, Rodrigues T, Prado IM, Helena AF, Uyemura SA, Santos AC, Curti C (**2005**) The interaction of flavonoids with mitochondria: effects on energetic processes. Chem Biol Interact. 152:67-78.

Firuzi O, Lacanna A, Petrucci R, Marrosu G, Saso L (**2005**) Evaluation of the antioxidant activity of flavonoids by "ferric reducing antioxidant power" assay and cyclic voltammetry. Biochim Biophys Acta. 1721:174-84.

Galati G, Chan T, Wu B, O'Brien PJ (**1999**) Glutathione-dependent generation of reactive oxygen species by the peroxidase-catalyzed redox cycling of flavonoids. Chem Res Toxicol. 12:521-525.

Garcia-Calvo M, Leonard RJ, Novick J, Stevens SP, Schmalhofer W, Kaczorowski GJ, Garcia ML (**1993**) Purification, characterization, and biosynthesis of margatoxin, a component of Centruroides margaritatus venom that selectively inhibits voltage-dependent potassium channels. J Biol Chem. 268:18866-74.

Garlid KD, Dos Santos P, Xie ZJ, Costa AD, Paucek P (**2003**) Mitochondrial potassium transport: the role of the mitochondrial ATP-sensitive K+ channel in cardiac function and cardioprotection. Biochim Biophys Acta. 1606:1-21.

Garlid KD, Paucek P, Yarov-Yarovoy V, Sun X, Schindler PA (**1996**) The mitochondrial K_{ATP} channel as a receptor for potassium channel openers. J Biol Chem. 271:8796-8799.

Gledhill JR, Montgomery MG, Leslie AG, Walker JE (**2007**) Mechanism of inhibition of bovine F1-ATPase by resveratrol and related polyphenols. Proc Natl Acad Sci U S A. 104:13632-7.

Gogvadze V, Norberg E, Orrenius S, Zhivotovsky B (**2010**) Involvement of Ca^{2+} and ROS in alpha-tocopheryl succinate-induced mitochondrial permeabilization. Int J Cancer. [Epub ahead of print]

Green DR, Kroemer G (**2004**) The pathophysiology of mitochondrial cell death. Science. 305:626-9.

Grover GJ, McCullough JR, Henry DE, Conder ML, Sleph PG (**1989**) Anti-ischemic effects of the potassium channel activators pinacidil and cromakalim and the reversal of these effects with the potassium channel blocker glyburide. J Pharmacol Exp Ther. 251:98-104.

Hail N Jr, Lotan R (**2009**) Cancer chemoprevention and mitochondria: targeting apoptosis in transformed cells via the disruption of mitochondrial bioenergetics/redox state. Nutr Food Res. 53:49-67.

Halestrap AP (**1989**) The regulation of the matrix volume of mammalian mitochondria in vivo and in vitro, and its role in the control of mitochondrial metabolism. Biochim Biophys Acta. 973:355–382.

Halestrap AP (**2009**) What is the mitochondrial permeability transition pore? Journal of Molecular and Cellular Cardiology. 46:821–831.

Halestrap AP, Clarke SJ, Javadov SA (**2004**) Mitochondrial permeability transition pore opening during myocardial reperfusion--a target for cardioprotection. Cardiovasc Res. 61:372-85.

Halliwell B (**2008**) Are polyphenols antioxidants or pro-oxidants? What do we learn from cell culture and in vivo studies? Arch Biochem Biophys. 476:107-112.

Halliwell B (**2009**) The wanderings of a free radical. Free Radic Biol Med. Mar 46:531-42.

Halliwell B, Gutteridge J (**1999**) Free Radicals in Biology and Medicine, 3rd ed. Oxford University Press Inc., New York, NY, U.S.A.

He JB, Yu CL, Duan TL, Deng N (**2009**) In situ spectroelectrochemical analysis of quercetin in acidic medium. Anal Sci. 25:373-7.

Hendrickson HP, Kaufman AD, Lunte CE (**1994**) Electrochemistry of catechol-containing flavonoids. J Pharm Biomed Anal. 12:325-34.

Hengartner MO. (**2000**) The biochemistry of apoptosis. Nature. 407:770-6.

Hileman EO, Liu J, Albitar M, Keating MJ, Huang P (**2003**) Intrinsic oxidative stress in cancer cells: a biochemical basis for therapeutic selectivity. Cancer Chemother Pharmacol. 53:209-19.

Indran IR, Pervaiz S (**2009**) Tumor cell redox state and mitochondria at the center of the non-canonical activity of telomerase reverse transcriptase. Mol Aspects Med. [Epub ahead of print]

Iyanagi T (**2007**) Molecular mechanism of phase I and phase II drug-metabolizing enzymes: implications for detoxification. Int Rev Cytol. 260:35-112.

Jänicke RU, Sprengart ML, Wati MR, Porter AG (**1998**) Caspase-3 is required for DNA fragmentation and morphological changes associated with apoptosis. J Biol Chem. 273:9357-60.

Jørgensen LV, Cornett C, Justesen U, Skibsted LH, Dragsted LO (**1998**) Two-electron electrochemical oxidation of quercetin and kaempferol changes only the flavonoid C-ring. Free Radic Res. 29:339-50.

Kagan VE, Bayir HA, Belikova NA, Kapralov O, Tyurina YY, Tyurin VA, Jiang J, Stoyanovsky DA, Wipf P, Kochanek PM, Greenberger JS, Pitt B, Shvedova AA, Borisenko G (**2009**) Cytochrome c/cardiolipin relations in mitochondria: a kiss of death. Free Radic Biol Med. 46:1439-53.

Kasibhatla S, Amarante-Mendes GP, Finucane D, Brunner T, Bossy-Wetzel E, Green DR (**1998**) Analysis of DNA Fragmentation Using Propidium Iodide (PI) Staining After Ethanol Fixation. This protocol was adapted

from "Apoptosis Assays," Chapter 15, in Cells (eds. Spector et al.). Cold Spring Harbor Laboratory Press, Cold Spring Harbor, NY, USA, 1998. Cold Spring Harb. Protoc.; 2006; doi:10.1101/pdb.prot4431

Knowles, HJ, Harris AL (**2001**) Hypoxia and oxidative stress in breast cancer. Hypoxia and tumourigenesis. Breast Cancer Res. 3:318 –322.

Koopman WJ, Nijtmans LG, Dieteren CE, Roestenberg P, Valsecchi F, Smeitink JA, Willems PH (**2009**) Mammalian mitochondrial complex I: Biogenesis, Regulation and Reactive Oxygen Species generation. Antioxid Redox Signal. [Epub ahead of print]

Koukourakis, MI, Giatromanolaki A, Simopoulos C, Polychronidis A, Sivridis E (**2005**) Lactate dehydrogenase 5 (LDH5) relates to up-regulated hypoxia inducible factor pathway and metastasis in colorectal cancer. Clin. Exp. Metastasis 22:25–30.

Krishnamachari V, Levine LH, Paré PW (**2002**) Flavonoid oxidation by the radical generator AIBN: a unified mechanism for quercetin radical scavenging. J Agric Food Chem. 50:4357-63.

Kumarswamy R, Chandna S (**2009**) Putative partners in Bax mediated cytochrome-c release: ANT, CypD, VDAC or none of them? Mitochondrion. 9:1-8.

Lewis RS, Cahalan MD (**1995**) Potassium and calcium channels in lymphocytes. Annu Rev Immunol. 13:623–653.

Li XQ, Heazy MG, Mahdi F, Jezek P, Lane RD, Garlid KD (**1990**) Purification of a reconstitutively active K^+/H^+ antiporter from rat liver mitochondria. J Biol Chem. 265:15316– 15322.

Liberman EA, Topaly VP, Tsofina LM, Jasaitis AA, Skulachev VP (**1969**) Mechanism of coupling of oxidative phosphorylation and the membrane potential of mitochondria. Nature. 222:1076-8.

Lodi F, Jiménez R, Menendez C, Needs PW, Duarte J, Perez-Vizcaino F (**2008**) Glucuronidated metabolites of the flavonoid quercetin do not auto-oxidise, do not generate free radicals and do not decrease nitric oxide bioavailability. Planta Med. 74:741-6.

Manach C, Williamson G, Morand C, Scalbert A, Rémésy C (**2005**) Bioavailability and bioefficacy of polyphenols in humans. I. Review of 97 bioavailability studies. Am J Clin Nutr. 81:230S-242S.

Mathupala SP, Ko YH, Pedersen PL (**2006**) Hexokinase II: Cancer's double-edged sword acting as both facilitator and gatekeeper of malignancy when bound to mitochondria. Oncogene 25:4777–4786.

Mironova GD, Negoda AE, Marinov BS, Paucek P, Costa AD, Grigoriev SM, Skarga YY, Garlid KD (**2004**) Functional distinctions between the mitochondrial ATP-dependent K channel ($mitoK_{ATP}$) and its inward rectifier subunit (mitoKIR). J Biol Chem. 279:32562-8.

Modica-Napolitano JS, Aprille JR (**2001**) Delocalized lipophilic cations selectively target the mitochondria of carcinoma cells. Adv Drug Deliv Rev. 49:63-70.

Montaña MP, Pappano N, Giordano SO, Molina P, Debattista NB, García NA (**2007**) On the antioxidant properties of three synthetic flavonols. Pharmazie. 62:72-6.

Mouria M, Gukovskaya AS, Jung Y, Buechler P, Hines OJ, Reber HA, Pandol SJ (**2002**) Food-derived polyphenols inhibit pancreatic cancer growth through mitochondrial cytochrome C release and apoptosis. Int J Cancer 98:761-9.

Mullauer FB, Kessler JH, Medema JP (**2009**) Betulinic acid induces cytochrome c release and apoptosis in a Bax/Bak-independent, permeability transition pore dependent fashion. Apoptosis. 14:191-202.

Murphy MP (**2008**) Targeting lipophilic cations to mitochondria. Biochim Biophys Acta. 1777(7-8):1028-31.

Murphy MP (**2009**) How mitochondria produce reactive oxygen species. Biochem J. 417:1-13.

Murphy MP, Smith RA (**2007**) Targeting antioxidants to mitochondria by conjugation to lipophilic cations. Annu Rev Pharmacol Toxicol. 47:629-56.

Murry CE, Jennings RB, Reimer KA (**1986**) Preconditioning with ischemia: a delay of lethal cell injury in ischemic myocardium. Circulation. 74:1124-1136.

Nichols CG (**2006**) K_{ATP} channels as molecular sensors of cellular metabolism. Nature. 440:470-476.

Nie C, Tian C, Zhao L, Petit PX, Mehrpour M, Chen Q (**2008**) Cysteine 62 of Bax is critical for its conformational activation and its proapoptotic activity in response to H2O2-induced apoptosis. J Biol Chem. 283:15359-69.

Nowikovsky K, Schweyen RJ, Bernardi P (**2009**) Pathophysiology of mitochondrial volume homeostasis: potassium transport and permeability transition. Biochim Biophys Acta. 1787:345-50.

O'Rourke B (**2007**) Mitochondrial ion channels. Annu Rev Physiol. 69:19-49.

O'Rourke B, Cortassa S, Aon MA (**2005**) Mitochondrial ion channels: gatekeepers of life and death. Physiology 20:303-315.

Panyi G, Possani LD, Rodríguez de la Vega RC, Gáspár R, Varga Z (**2006**) K^+ channel blockers: novel tools to inhibit T cell activation leading to specific immunosuppression. Curr Pharm Des. 12:2199-2220.

Park WS, Kang SH, Son YK, Kim N, Ko JH, Kim HK, Ko EA, Kim CD, Han J (**2007**) The mitochondrial Ca^{2+}-activated K^+ channel activator, NS 1619 inhibits L-type Ca^{2+} channels in rat ventricular myocytes. Biochem Biophys Res Commun. 362:31-36.

Pelicano H, Carney D, Huang, P (**2004**) ROS stress in cancer cells and therapeutic implications. Drug Resist Updat. **7**:97–110.

Perron NR, Brumaghim JL (**2009**) A review of the antioxidant mechanisms of polyphenol compounds related to iron binding. Cell Biochem Biophys. 53:75-100.

Perry G, Raina AK, Nunomura A, Wataya T, Sayre LM, Smith MA (**2000**) How important is oxidative damage? Lessons from Alzheimer's disease. Free Radic Biol. Med. 28:831–834.

Pervaiz S, Holme AL, Aggarwal BB, Anekonda TS, Baur JA, Gojkovic-Bukarica L, Ragione FD, Kim AL, Pirola L, Saiko P (**2009**) Resveratrol: its biologic targets and functional activity. Antioxid Redox Signal. 11:2851-97.

Petrosillo G, Moro N, Ruggiero FM, Paradies G (**2009**) Melatonin inhibits cardiolipin peroxidation in mitochondria and prevents the mitochondrial permeability transition and cytochrome c release. Free Radic Biol Med. 47:969-74.

Piwońska M, Wilczek E, Szewczyk A, Wilczynski GM (**2008**) Differential distribution of Ca^{2+}-activated potassium channel beta4 subunit in rat brain: immunolocalization in neuronal mitochondria. Neuroscience 153:446-460.

Ramos S (**2007**) Effects of dietary flavonoids on apoptotic pathways related to cancer chemoprevention. J Nutr Biochem. 18:427-42.

Ranelletti FO, Maggiano N, Serra FG, Ricci R, Larocca LM, Lanza P, Scambia G, Fattorossi A, Capelli A, Piantelli M (**2000**) Quercetin inhibits p21-RAS expression in human colon cancer cell lines and in primary colorectal tumors. Int J Cancer. 85:438-45.

Ralph SJ, Neuzil J (**2009**) Mitochondria as targets for cancer therapy. Mol Nutr Food Res. 53:9-28.

Rasola A, Bernardi P (**2007**) The mitochondrial permeability transition pore and its involvement in cell death and in disease pathogenesis. Apoptosis. 12:815-33.

Redel A, Lange M, Jazbutyte V, Lotz C, Smul TM, Roewer N, Kehl F (**2008**) Activation of mitochondrial large-conductance calcium-activated K^+ channels via protein kinase A mediates desflurane-induced preconditioning. Anesth Analg. 106:384-391.

Richter C, Gogvadze V, Laffranchi R, Schlapbach R, Schweizer M, Suter M, Walter P, Yaffee M (**1995**) Oxidants in mitochondria: from physiology to diseases. Biochim Biophys Acta 1271:67–74.

Roche TE, Hiromasa Y (**2007**) Pyruvate dehydrogenase kinase regulatory mechanisms and inhibition in treating diabetes, heart ischemia, and cancer. Cell Mol Life Sci. 64:830–849.

Ross MF, Prime TA, Abakumova I, James AM, Porteous CM, Smith RA, Murphy MP (**2008**) Rapid and extensive uptake and activation of hydrophobic triphenylphosphonium cations within cells. Biochem J. 411:633-45.

Rusznák Z, Bakondi G, Kosztka L, Pocsai K, Dienes B, Fodor J, Telek A, Gönczi M, Szucs G, Csernoch L (**2008**) Mitochondrial expression of the two-pore domain TASK-3 channels in malignantly transformed and non-malignant human cells. Virchows Arch. 452:415-26.

Sablina AA, Budanov AV, Ilyinskaya GV, Agapova LS, Kravchenko JE, Chumakov PM (**2005**) The antioxidant function of the p53 tumor suppressor. Nat Med. 11:1306-13.

Sakamoto K, Ohya S, Muraki K, Imaizumi Y (**2008**) A Novel Opener of Large-Conductance Ca^{2+}-Activated K^+ (BK) Channel Reduces Ischemic Injury in Rat Cardiac Myocytes by Activating Mitochondrial K_{Ca} Channel. J Pharmacol Sci. 108:135-139.

Sakihama Y, Cohen MF, Grace SC, Yamasaki H (**2002**) Plant phenolic antioxidant and prooxidant activities: phenolics-induced oxidative damage mediated by metals in plants. Toxicology 177: 67-80.

Sands Z, Grottesi A, Sansom MS (**2005**) Voltage-gated ion channels. Curr Biol. 15, R44-R47.

Sarno S, Moro S, Meggio F, Zagotto G, Dal Ben D, Ghisellini P, Battistutta R, Zanotti G, Pinna LA (**2002**) Toward the rational design of protein kinase casein kinase-2 inhibitors. Pharmacol Ther. 93:159-168.

Shakibaei M, Harikumar KB, Aggarwal BB (**2009**) Resveratrol addiction: to die or not to die. Mol Nutr Food Res. 53:115-28.

Siemen D, Loupatatzis C, Borecky J, Gulbins E, Lang F (**1999**) Ca^{2+}-activated K^+ channel of the BK-type in the inner mitochondrial membrane of a human glioma cell line. Biochem Biophys Res Commun. 257:549-554.

Skalska J, Piwońska M, Wyroba E, Surmacz L, Wieczorek R, Koszela-Piotrowska I, Zielińska J, Bednarczyk P, Dołowy K, Wilczynski GM, Szewczyk A, Kunz WS (**2008**) A novel potassium channel in skeletal muscle mitochondria. Biochim Biophys Acta 1777:651-659.

Skulachev VP, Anisimov VN, Antonenko YN, Bakeeva LE, Chernyak BV, Erichev VP, Filenko OF, Kalinina NI, Kapelko VI, Kolosova NG, Kopnin BP, Korshunova GA, Lichinitser MR, Obukhova LA, Pasyukova EG, Pisarenko OI, Roginsky VA, Ruuge EK, Senin II, Severina II, Skulachev MV, Spivak IM, Tashlitsky VN, Tkachuk VA, Vyssokikh MY, Yaguzhinsky LS, Zorov DB (**2009**) An attempt to prevent senescence: a mitochondrial approach. Biochim Biophys Acta. 1787:437-61.

Subramanian S, Kalyanaraman B, Migrino RQ (**2009**)Mitochondrially Targeted Antioxidants for the Treatment of Cardiovascular Diseases. Recent Pat Cardiovasc Drug Discov. [Epub ahead of print]

Szabò I, Bock J, Jekle A, Soddemann M, Adams C, Lang F, Zoratti M, Gulbins E (**2005**) A novel potassium channel in lymphocyte mitochondria. J Biol Chem. 280:12790-12798.

Szabó I, Bock J, Grassmé H, Soddemann M, Wilker B, Lang F, Zoratti M, Gulbins E (**2008**) Mitochondrial potassium channel Kv1.3 mediates Bax-induced apoptosis in lymphocytes. Proc Natl Acad Sci USA. 105:14861-14866.

Szabò I, Zoratti M, Gulbins E **(2010)** Contribution of voltage-gated potassium channels to the regulation of apoptosis. FEBS Lett. Jan 23. [Epub ahead of print]

Szewczyk A, Skalska J, Glab M, Kulawiak B, Malinska D, Koszela-Piotrowska I, Kunz WS (**2006**) Mitochondrial potassium channels: frompharmacology to function. Biochim Biophys Acta. 1757:715–720.

Tiligada E (**2006**) Chemotherapy: induction of stress responses. Endocr. Relat. Cancer 13 (Suppl. 1):S115–S124.

Tomiyama A, Serizawa S, Tachibana K, Sakurada K, Samejima H, Kuchino Y, Kitanaka C (**2006**) Critical role for mitochondrial oxidative phosphorylation in the activation of tumor suppressors Bax and Bak. J Natl Cancer Inst. 98:1462-73.

Torres YP, Morera FJ, Carvacho I, Latorre R **(2007)** A marriage of convenience: β-subunits and voltage-dependent K^+ channels. J Biol Chem. 282:24485-24489.

Trachootham D, Lu W, Ogasawara MA, Nilsa RD, Huang P (**2008**) Redox regulation of cell survival. Antioxid Redox Signal. 10:1343–1374.

Ulrich S, Wolter F, Stein JM (**2005**) Molecular mechanisms of the chemopreventive effects of resveratrol and its analogs in carcinogenesis. Mol Nutr Food Res. 49:452-61.

Vafa O, Wade M, Kern S, Beeche M, Pandita TK, Hampton GM, Wahl GM (**2002**) c-Myc can induce DNA damage, increase reactive oxygen species, and mitigate p53 function: a mechanism for oncogeneinduced genetic instability. Mol Cell. 9:1031–1044.

Vennekamp J, Wulff H, Beeton C, Calabresi PA, Grissmer S, Hänsel W, Chandy KG (**2004**) Kv1.3-blocking 5-phenylalkoxypsoralens: a new class of immunomodulators. Mol Pharmacol. 65:1364-74.

Wellman GC, Nelson MT (**2003**) Signaling between SR and plasmalemma in smooth muscle: sparks and the activation of Ca2+-sensitive ion channels. Cell Calcium. 34:211-29.

Zhang DX, Chen YF, Campbell WB,. Zou AP, Gross GJ, Li PL (**2001**) Characteristics and superoxide-induced activation of reconstituted myocardial mitochondrial ATP-sensitive potassium channels. Circ Res. 89:1177-1183.

Zheng J, Ramirez VD (**2000**) Inhibition of mitochondrial proton F0F1-ATPase/ATP synthase by polyphenolic phytochemicals. Br J Pharmacol. 130:1115-1123.

Zhou A, Sadik OA (**2008**) Comparative analysis of quercetin oxidation by electrochemical, enzymatic, autoxidation, and free radical generation techniques: a mechanistic study. J Agric Food Chem. 56:12081-91.

Zoratti M, De Marchi U, Biasutto L, Szabò I (**2010**) Electrophysiology clarifies the megariddles of the mitochondrial permeability transition pore. FEBS Lett. Jan 16. [Epub ahead of print]

Zoratti M, De Marchi U, Gulbins E, Szabò I (**2009**) Novel channels of the inner mitochondrial membrane. Biochim Biophys Acta. 1787:351-63.

Zoratti M, Szabò I (**1995**) The mitochondrial permeability transition. Biochim Biophys Acta. 1241:139-76.

Zoratti M, Szabò I, De Marchi U (**2005**) Mitochondrial permeability transitions: how many doors to the house? Biochim Biophys Acta. 1706:40-52.

Abbreviations (please see also lists in some individual chapters)

ABC: ATP-Binding Cassette

BCRP: Breast Cancer Resistance Protein

BTPI: (n-Butyl-4-TriphenylPhosphonium) Iodide

BK_{Ca}: Big Ca-dependent K^+ channel

Cdk: Cyclin-dependent kinase

CFTR: Cystic Fibrosis Transmembrane conductance Regulator

ChTx: Charybdotoxin

CsA: Cyclosporin A

CsH: Cyclosporin H

$\Delta\psi_{m,i}$: mitochondrial transmembrane potential

DCCD: *N*,*N'*-Dicyclohexylcarbodiimide

DMEM: Dulbecco's Modified Eagle Medium

FACS: Fluorescence-Activated Cell Scanning

GSH: Glutathione

GST: Glutathione-S-Transferase

HCT116: Human Colon Tumor 116

HBSS: Hank's balanced saline solution

HEPES: N-(2-idroxyethyl)-piperazin-N'-2-ethansolfonic acid

HIF-1: Hypoxia-Inducible Factor-1

HK: HexoKinase

IK_{Ca}: intermediate conductance Ca-dependent channel

IMM: Inner Mitochondrial Membrane

IP: Ischemic Preconditioning

K_{ATP}: ATP-sensitive K^+ channel

KHE: K^+/H^+ exchanger

Kir: K^+-selective inward-rectifying channel

LDH: Lactate DeHydrogenase

MEF: Mouse Embryonic Fibroblast

MDR: Multiple Drug Resistance

MgTx: Margatoxin

MPTP: Mitochondrial Permeability Transition Pore

MRP: Multiple Resistance Protein

MTT: 3-(4,5-Dimethylthiazol-2-yl)-2,5-Diphenyltetrazolium Bromide

OMM: Outer Mitochondrial Membrane

PAGE: PolyAcrylamide Gel Electrophoresis

PBS: Phosphate-Buffered Saline

PDK: Pyruvate Dehydrogenase Kinase

P-gp: P-glycoprotein

Pipes: Piperazine-1,4-bis(2-ethanesulfonic acid)

PM: Plasma Membrane

Psora-4: 5-(4-Phenylbutoxy)psoralen

Q: Quercetin

QBTPI: (n-butyl-4-triphenylphosphonium)-quercetin-iodide

QTA: Tetraacetyl-quercetin

QTABTPI: (n-butyl-4-triphenylphosphonium)-tetraacetyl-quercetin iodide

R: Resveratrol

RDA: Diacetyl-resveratrol

RDABTPI: (n-butyl-4-triphenylphosphonium)-diacetyl-resveratrol iodide

ROI: Region of Interest

ROS: Reactive Oxygen Species

RPMI: Roswell Park Memorial Institute

R.T.: Room Temperature

SCE: Standard Calomel Electrode

SDS: Sodium Dodecyl Sulphate

SOD: SuperOxide Dismutase

SUR: SulfonylUrea Receptor

TASK-3: TWIK (Two-pore Weakly Inward rectifying) acid-sensitive K^+ channel

TES: N-[tris(hydroxymethyl)methyl]-2-aminoethanesulfonic acid

TMRM: TetraMethylRhodamine Methyl ester

TPMP: TriPhenylMethylPhosphonium

TPP: TriPhenylPhosphonium

VacA: *Helicobacter pylori* Vacuolating toxin A

VDAC: Voltage-Dependent Anion Channel (porin)

VEGF: Vascular Endothelial Frowth Factor